Disease Dynamics and Its Optimal Control

Thesis submitted for the award
of the degree of

Doctor of Philosophy

by

Chittaranjan Mondal

Under the supervision of

Prof. Nandadulal Bairagi

Center for Mathematical Biology and Ecology
Department of Mathematics
Jadavpur University
Kolkata-700032, India
October 2022

Declaration

I, Chittaranjan Mondal, solemnly declare that this thesis represents my own work which has been done after registration for the degree of PhD at Jadavpur University and has not been previously included in any thesis or dissertation for the purpose of earning a degree, diploma, or any other credential.

Chittaranjan Mondal

DEPARTMENT OF MATHEMATICS
FACULTY OF SCIENCE
JADAVPUR UNIVERSITY
Kolkata – 700032, India
Telephone: 91 (33) 2414 6717

Dr. Nandadulal Bairagi
Professor and Coordinator
CENTRE FOR MATHEMATICAL BIOLOGY AND ECOLOGY
Mail: nbairagi.math@jadavpuruniversity.in

Date: 28/10/2022

CERTIFICATE FROM THE SUPERVISOR

This is to certify that the thesis entitled "**Disease Dynamics and Its Optimal Control**" submitted by **Sri Chittaranjan Mondal**, who got his name registered **(Ref. No.: S-21/80/18 and Index No.: 28/18/Maths./25)** on 07/02/18 for the award of Ph.D. (Science) degree of Jadavpur University, is absolutely based upon his own work under the supervision of myself, and that neither this thesis nor any part of it has been submitted for either any degree / diploma or any other academic award anywhere before.

28/10/22

Nandadulal Bairagi

Nandadulal Bairagi (Ph. D.)
Professor, Dept. of Mathematics
Jadavpur University
Kolkata-700032

This thesis is dedicated to

the memory of my father

Late Jadab Mondal

Acknowledgement

First and foremost, I would like to express my sincere gratitude to my supervisor, Prof. Nandadulal Bairagi, Department of Mathematics, Jadavpur University, Kolkata, for allowing me to study and learn under his guidance. His dedication to mathematics, work ethic, uncompromising behavior, and discipline became my inspiration from the day one I started my research. He guided my Ph.D work, gave practical advice, and spent a lot of time discussing and reviewing complex aspects of this work. Without his close companionship, invaluable help, and constant support and cooperation, not only in mathematics but also in life, it would not have been possible for me to complete the preparation of this thesis on time.

I am grateful for the wholehearted help and encouragement of the Center for Mathematical Biology and Ecology, Department of Mathematics, Jadavpur University, Bio-Mathematical Society of India, and all my teachers at the Department of Mathematics, Jadavpur University.

I am grateful to the Council of Scientific & Industrial Research (CSIR), Govt. of India for supporting me financially through a Research Fellowship.

I thank Dr. Debadatta Adak, Dr. Phonindra Nath Das, Dr. Suman Saha, Dr. Ankur Gupta, Dr. Santu Ghorai, Mr. Chandan Maji, and Dr. Milan Biswas for their kind help.

I thank my fellow researchers and coworkers Dr. Bhaskar Chakraborty, Dr. Shuvojit Mondal, Dr. Ritwika Mondal, Mr. Abhijit Majumder, Ms. Priyanka Saha, Mr. Santanu Bhattacharya, Mr. Ayanava Basak, Mr. Sounov Marick, Mr. Chirodeep Mondal and Mr. Debjit Pal who have been a constant source of encouragement and help.

Finally, I thank my wife Rupa Mandal, for supporting me in every aspect of life and bearing my wishes with a smile. Only because of her now I am here, from nowhere.

Abstract

Human immunodeficiency virus type-1 (HIV-1) is a deadly pathogen that infects $CD4^+$T cells, one type of immune cell. A gradual decline of $CD4^+$T cells in blood plasma is a signature of HIV-1 infection. HIV infection causes AIDS (Acquired Immunodeficiency Syndrome) when the $CD4^+$T cells count drops to 200 cells per μl from its normal value of 1000 cells per μl. The immune system cannot function properly in a reduced level of $CD4^+$T cells. As a result, an HIV-infected individual becomes susceptible to various opportunistic infections. Basic HIV-1 in-host models consider dissemination of infection through cell-free mode, where the free plasma virus infects the healthy $CD4^+$T cells. Recent in vitro studies, however, show that infection can spread from one infected cell to another uninfected cell. This cell-to-cell viral spread through virological synapses is the predominant mode of HIV-1 infection. Antiretroviral therapy significantly reduces the viral load and increases the $CD4^+$T cell count, thus preventing the onset of AIDS and increasing the life span of HIV-1 infected patients.

Previous studies on HIV-1 infection with mono or multi-blockers consider the mode of infection through a single pathway, which is the cell-free mode. So, the question is, what would be the control strategy in cell-to-cell transmission mode? To the best of our knowledge, no work has considered such controls in a multi-pathways HIV-1 infection model. Therefore, the main objective of this thesis is to gain insights into the effect of single and multi-blockers drugs on the dynamics of an HIV-1 infection model in the presence of both cell-to-cell and cell-free infection modes.

Most models of HIV-1 infection assume that the transmission process follows a mass action

or bilinear law. This law says that the infection rate at any time is proportional to the product of viral and host cell numbers. But, the mass action law has some unrealistic properties, e.g., the number of newly infected $CD4^+T$ cells produced by a single virus may be unbounded. Some authors have used a saturated infection rate to prevent this unboundedness of the contact rate. In the case of HIV, the process between the first effective contact of a virus/ infected cell with a healthy $CD4^+T$ cell and the latter becoming productively infectious is not instantaneous. After entering a virus into the healthy cell, many intracellular mechanisms occur to make the cell productively infectious. The time required for transforming a healthy cell into an infectious cell is known as the intercellular delay. We considered a multi-pathways in-host HIV-1 infection model with saturated infection rates and intracellular delay using three controls to explore the viremia.

HIV-1 mathematical models usually consider the interaction between the host cells (i.e., $CD4^+T$) and plasma free-virus. However, the activated $CD8^+T$ of CTL cells can kill the infected host cells and thus reduce the production of the free virus through the infected cell lysis. It is to be mentioned that the activation of CTL is not instantaneous. It takes some time for stimulation by our immune cells. It is of utmost importance to know how far different antiretroviral therapies can control viremia in the presence of delay. We, therefore, studied a multi-pathways HIV-1 infection model with CTL delay in the presence of treatments. The main objective is to explore how immune response delay affects the plasma viral load in the presence and absence of the blockers and to determine the optimal dose.

We analyzed our considered models in all cases under two cases: (i) the controls are constant or (ii) the controls are time-dependent. We prove that the proposed model's unique solutions exist and are bounded. We demonstrate the local and global stabilities of the disease-free and infected steady states in the constant control case. It is shown for the delay-induced model that there exists some critical value (τ^*) of the delay parameter below which the system is stable and above which it is unstable. The stability switching occurs through a Hopf bifurcation. In the time-dependent control, we define a suitable optimal control problem. An objective function is characterized based on maximizing the healthy $CD4^+T$ cell counts and minimizing the count of infected $CD4^+T$ cells along with other systemic costs of drug therapy. We derived the

necessary conditions for optimal infection control by applying Pontryagin's minimum principle. It is analytically shown that an optimal control triplet exists that maximizes the objective functional. Using extensive simulation results, we have demonstrated the effect of different control measures with mono-drug and multi-drug therapies with different delays. It is shown that removing the infection is not possible, and the infected cells persist in all three mono-drug protocols using any mono-drug treatment. However, virus counts go below the detection level of a protease inhibitor but infected $CD4^+T$ cells persist. This, however, does not happen in the case of an RTI inhibitor or synapse-forming inhibitor. Infected $CD4^+T$ cells persist, but the non-zero virus count may be possible due to cell-to-cell infection dissemination and protease inhibitor use. Such a result has not been shown in any previous study. In the case of a multi-drug therapy, we observed that infection could be removed in all options which contain the protease inhibitor. Our study deciphers that immune response delay significantly affects the system dynamics. If CTL's response is quicker, then $CD4^+T$ cell count may remain stable but fails to do so if response time increases.

The Covid-19 pandemic has put the world under immeasurable stress. Initially, no specific drug or vaccine was used to prevent the coronavirus infection. Therefore, in the absence of a vaccine or specific drug, we proposed a mathematical Covid-19 epidemic control model using the repurposing drugs and non-pharmaceutical interventions. A case study with the Indian Covid-19 epidemic data is presented to visualize and illustrate the effects of lockdown, maintaining personal hygiene & safe distancing, and repurposing drugs. It is shown that India significantly improved the overall Covid-19 epidemic burden through the combined use of NPIs and repurposing drugs.

Contents

1 Introduction

1.1 Disease

According to Oxford English Dictionary, the disease is "any particular abnormality which affects the structure or function of all or parts of an organism negatively, and that is not due to any immediate external injury". Diseases are often referred to as medical conditions that are associated with specific signs and symptoms. Disease can affect people not only physically but also mentally as being diagnosed and living with a disease can change the outlook of the affected person. The study of disease is called pathology, which includes the study of etiology. Diseases are of two types: infectious or communicable or transmissible disease and non-communicable or non-transmissible disease. A non-communicable disease is a medical condition or disease which is not transmissible. It cannot spread directly from one person to person. In humans, the examples of non-communicable disease are heart disease and cancer.

An infection can be defined as the invasion of the body tissues of an organism by disease-causing agents, their multiplication, and the host tissue's response to the infectious agents and the toxins they produce. It is an illness (i.e., characteristic medical signs and/or symptoms of diseases) originating from an infection, presence and growth of pathogenic biological agents in an individual host organism. A wide range of pathogens, specifically bacteria and viruses cause infections. The agents of infectious diseases are:

- Viruses and related agents such as viroids (e.g. HIV, Rhinovirus, Lyssaviruses such as Rabies virus, Ebolavirus and Severe acute respiratory syndrome coronavirus 2 etc.),

- Bacteria (e.g. Mycobacterium tuberculosis, Staphylococcus aureus, Escherichia coli, Clostridium botulinum, and Salmonella spp. etc.),
- Fungi (e.g. candida, aspergillus, Cryptococcus etc.),
- Prions,
- Parasites (e.g. malaria, toxoplasma, babesia etc.),
- Arthropods (e.g. ticks, mites, fleas, and lice etc.).

1.2 Epidemiology

Epidemiology is the study and analysis of the distribution and determinants of health and disease states in specific populations. Epidemiology means "the study of what is in people" and is derived from the Greek words 'epi' meaning on or upon, 'demo' meaning people, and 'logos' meaning study. It deals with design, collection, statistical analysis and interpretation of data. Epidemiology has helped develop methodology that is applied to disease prevention, clinical research, health promotion and health service researches. Hence, epidemiology is described as the basic science of public health. The objective of epidemiology is (i) to identify the cause and risk factors in disease, (ii) to seek the disease community where they occur, (iii) to study the natural history of the disease, (iv) to evaluate the existing and new preventive methods, and (v) to develop public health policy.

1.3 Disease Dynamics

In the modern era, epidemiology has become an important subject. The relationship between mathematics and epidemiology is rising day after day. Epidemiology provides an innovative and excellent branch for mathematicians, while for epidemiologists, mathematical modeling provides a momentous research tool in studying disease evolution. In other words, mathematical models can project how diseases progress to show the probable outcome of an epidemic and help inform public health interventions. Using basic assumptions or aggregated statistics along with mathematics, the models try to find parameters of various diseases and use those parameters to calculate the effects of different interventions. The modeling can provide information on which intervention(s) to avoid and which to try or may predict future growth patterns, etc. John Graunt was the first scientist to study the infectious model to quantify the causes of death in his book "Natural and Political Observations made upon the Bills of Mortality" in 1662. Daniel Bernoulli proposed a smallpox model to understand the dynamics in 1760, and many authors consider it the first epidemiological mathematical model. In the early 20th century, William Hamer and Ronald Ross applied the law of mass action to explain epidemic behavior.

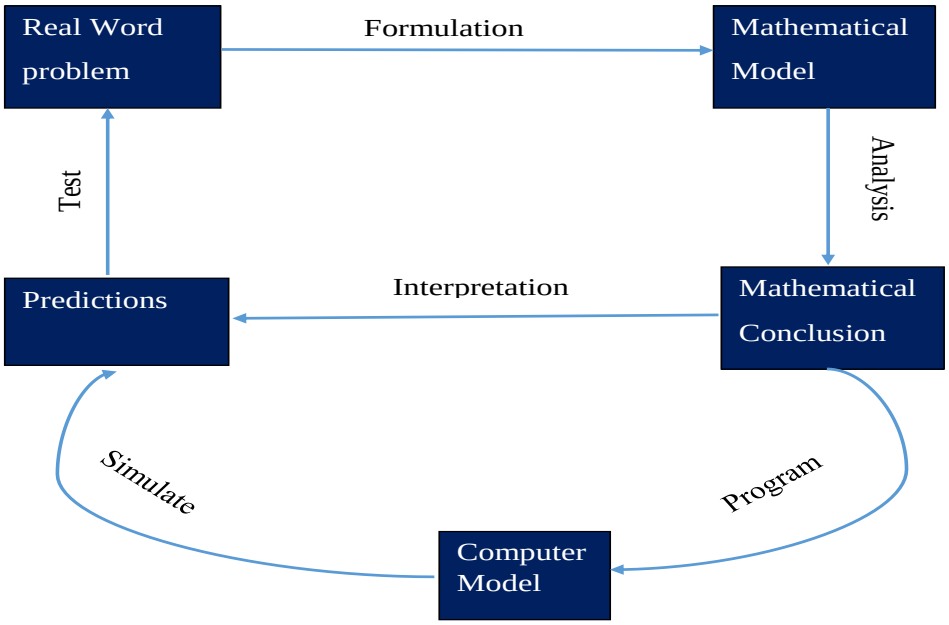

Figure 1.1: Scientific process to connect real world problem with mathematics.

Between 1927 and 1933, Kermack and McKendrick had a major influence on the development of mathematical epidemiology models through the theoretical paperwork of their infectious disease models. Most basic theories were developed at that time, but theoretical progress has been steady since then. To expatiate the transmission of several diseases, mathematical models are increasingly being used. These models are compartmental and may be quite simple, but they are really important to study and gain knowledge about the underlying aspects of infectious diseases and to assess the potential impact of control programs on reducing morbidity and mortality.

1.4 Mathematical Modelling

Mathematical modeling is a process by which a real-world problem can be described in the language of mathematics. The concept of modeling is used in all fields such as engineering, physics, chemistry, etc. Mathematical modeling helps us to (i) understand the transmission of disease dynamics, (ii) predict the near future disease status, and (iii) determine the effective control strategies. In general, the mathematical models applied to the epidemiology of infectious diseases can be classified into two types: (1) The deterministic models considering nonrandom rate flows in a population stratified in compartments; and (2) The stochastic models that consider probabilities in the movements between the compartments of the model, such as the probability of a susceptible individual being infected and the probability of transmitting the

disease in the population addressed by a mathematical system [1].

1.5 Brief Notes on AIDS and Its Etiologic Agent HIV

The history of the HIV and AIDS epidemic began with illness, fear, and death as the world faced new and unknown viruses at that time. But, technological advances have made it possible for people living with HIV to live longer and healthier lives with treatment. It is believed that HIV originated in Kinshasa (Democratic Republic of Congo) around 1920 when HIV crossed species from chimpanzees to humans. Until the 1980s, no one knew how many people were infected with HIV or AIDS. At that time HIV was unknown and transmission was not followed by noticeable signs or symptoms. By 1980, HIV may have already spread to five continents (North America, South America, Europe, Africa, and Australia). In this period, between 100,000 and 300,000 people could have already been infected [2]. In September 1981, the CDC (Center for Disease Control) used the term AIDS (acquired immune deficiency syndrome) for the first time [3] and the very next year, AIDS was defined as "a disease at least moderately predictive of a defect in cell-mediated immunity occurring in a person with no known cause for diminished resistance to that disease". In 1981, cases of a rare lung infection called Pneumocystis carinii pneumonia (PCP) were found in five young, previously healthy gay men in Los Angeles [4]. At the same time, there were reports of a group of men in New York and California with an unusually aggressive cancer named Kaposi's Sarcoma [5]. Both of these diseases were seen only in patients with severe impairment of their immune system [6] which was caused due to the reduction of the helper T lymphocytes or CD4+T lymphocytes. CD4 (cluster of differentiation 4) is a glycoprotein found on the surface of immune cells such as T helper cells, monocytes, macrophages, and dendritic cells. In December 1981, the first cases of PCP were reported in people who inject drugs [7]. By the end of the year, there were 270 reported cases of severe immune deficiency among gay men and 121 of them had died [8]. In June 1982, a group of cases among gay men in Southern California suggested that the cause of the immune deficiency was sexual and the syndrome was initially called gay-related immune deficiency (or GRID) [9]. Later that month, the disease was reported in hemophiliacs and Haitians leading many to believe it had originated in Haiti [3, 10]. AIDS cases were also being reported in several European countries [11]. In January 1983, AIDS was reported among the female partners of men who had the disease suggesting it could be passed on via heterosexual sex [3]. By the end of the year, the number of AIDS cases in the USA had risen to 3,064 and 1,292 people among them had died [9].

In 1986, the International Committee on Taxonomy of Viruses gave the AIDS virus a separate name, Human Immunodeficiency Virus or HIV [12]. There are two types of HIV: HIV-1 and HIV-2. HIV-1 is more virulent and more infective than HIV-2 [13], and is the cause of the majority of HIV infections globally. The lower infectivity of HIV-2, compared to HIV-1, implies that fewer of those exposed to HIV-2 will be infected per exposure. Due to its relatively

poor capacity for transmission, HIV-2 is largely confined to West Africa [14].

1.5.1 Structure of HIV

Human Immunodeficiency Virus (HIV-1, HIV-2) are the member of the genus Lentivirus, part of the family Retroviridae on the basis of their genetic, biological and morphological characteristics [15]. The structure of HIV virion roughly spherical with a diameter about 120 nanometre [16]. A schematic diagram of HIV virus is given in Fig. 1.2. The virus is surrounded by the viral envelope, that is composed of the lipid bilayer taken from the membrane of a human host cell when the newly formed virus particle buds from the cell. The viral envelope is made up of 72 knobs containing trimers or tetramers of the envelope glycoproteins gp41, gp120 and gp140 [17]. A matrix composed of the viral protein p17 surrounds the capsid ensuring the integrity of the virion particle [18]. Capsid is formed by 2,000 copies of the viral protein, named p24. The viral capsid contains two identical copies of positive single-stranded RNA along with viral enzymes (Reverse Transcriptase, Integrase, ribonuclease and Protease) and the nucleocapsid proteins p7 [18]. The RNA genome consists of at least seven structural landmarks (LTR, TAR, RRE, PE, SLIP, CRS, and INS), and nine genes (gag, pol, and env, tat, rev, nef, vif, vpr, vpu, and sometimes a tenth tev, which is a fusion of tat, env and rev), encoding 19 proteins. Three of these genes, gag, pol, and env, contain information needed to make the structural proteins for new virus particles [18]. For example, env codes for a protein called gp160 that is cut in two by a cellular protease to form gp120 and gp41. The six remaining genes, tat, rev, nef, vif, vpr, and vpu (or vpx in the case of HIV-2), are regulatory genes for proteins that control the ability of HIV to infect cells, produce new copies of virus (replicate), or cause disease [18].

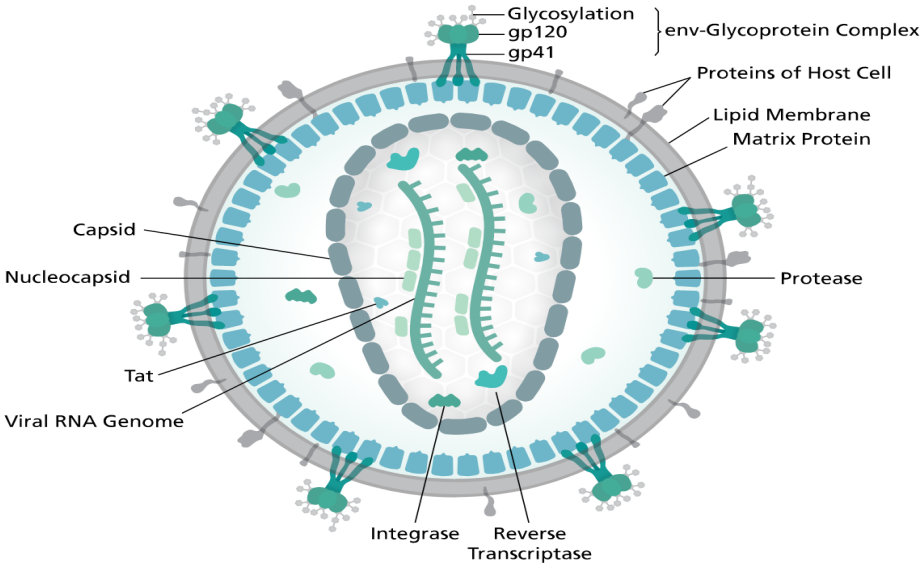

Figure 1.2: Structure of HIV virus. Picture courtesy: https://en.wikipedia.org/wiki/HIV

1.5.2 Replication Cycle of HIV in Human Body

HIV virus has no independent existence without infecting and replicating in human living cells. HIV especially infects varieties of immune cells such as macrophages, dendritic cells and $CD4^{+}$T lymphocytes, which constitute a quarter of the white blood cell count and also microglial cells, a type of neuroglia located in the brain and spinal cord. After entering the cells, HIV goes through several steps to replicate itself and create new virus particles and it is the so-called HIV life cycle. It is important to know the steps of the HIV life cycle so that the drugs used to control HIV infection can interrupt this replication cycle. A schematic diagram of HIV replication cycle is given in Fig. 1.3.

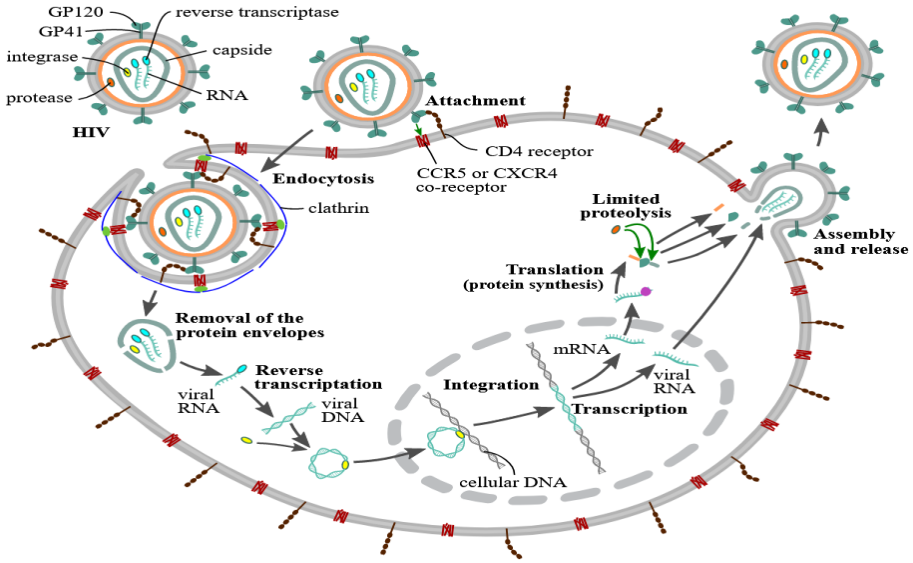

Figure 1.3: The HIV replication cycle. Picture courtesy: https://en.wikipedia.org/wiki/HIV

Step I: Entry to the cell is initiated by the interaction of the trimeric envelope complex (gp160 spike) on the HIV viral envelope and both CD4 receptor and a chemokine co-receptor (usually CCR5 or CXCR4) on the target cell surface [19, 20]. The gp160 spike contains HIV viral envelope glycoprotein (gp120) binding domains for both CD4 and chemokine receptors [19, 20]. Now, there are three important processes. In the first two processes, HIV viral envelope glycoprotein (gp120) binds to the CD4 receptor and chemokine co-receptor (usually CCR5 or CXCR4) by virological synapses, facilitating efficient cell-to-cell spreading of HIV-1 [21]. The third and final process in this step is fusion. In fusion, the HIV RNA and various enzymes, including reverse transcriptase, integrase and protease enter the cell [19].

Step II: Replication and transcription. HIV is a single-stranded RNA virus. This RNA genome needs to be converted into double stranded DNA in order to be integrated into the host

cell DNA. After the viral capsid enters the cell, an enzyme called reverse transcriptase releases the positive-sense single-stranded RNA genome from the attached viral proteins and copies it into a complementary DNA (cDNA) molecule [22] and the precess is termed as reverse transcription. Without reverse transcription, the viral genome cannot be incorporated into the host cell and thus cannot be replicated to form new copies of virions [23]. The reverse transcription process is extremely error-prone, and the resulting mutations may cause drug resistance or allow the virus to evade the body's immune system. Then, the cDNA and its complement together form a double-stranded viral DNA that is then transported into the cell nucleus. Subsequently, through the viral enzyme integrase, the viral DNA is integrated into the host cell's genome [22] and this process is called an integration. The integrated DNA is also called provirus. Once the integration process begins, the host cell is known as an infected cell because the proviral DNA remains permanently within the target cell in either a productive or latent state. After integration, cell may turn to an activated state which brings transcription of integrated proviral DNA into messenger RNA (mRNA). After the transcription process, the viral mRNA is migrated from the cell nucleus to the cell cytoplasm, where building blocks for a new virus are synthesized. In the cytoplasm, viral mRNA is translated to produce viral proteins by viral protease enzyme. The structural proteins required for new mature viral particles which are produced during this translation process.

Step III: Assembly and release. This is the final step of viral cycle and is accomplished by two processes, namely, assembly and release. In the first process, assembly functional viral proteins and viral RNA (mRNA) at the host cell's plasma membrane. Then by budding the viral RNA (mRNA) together with related proteins forms new HIV-1 virions in the host cell's plasma membrane and hence new HIV-1 virions are released from the cell surface so that can proceed to infect other healthy cells.

1.5.3 The Stages of HIV Infection

There are three main stages of HIV infection are (i) acute HIV infection, (ii) chronic HIV infection, and (iii) acquired immunodeficiency syndrome (AIDS). A schematic diagram of stages of HIV infection in human body is given in Fig. 1.4.

Stage I: Acute HIV infection or primary HIV infection is the first stage of HIV infection and usually develops within 2 to 4 weeks after HIV infection. During the acute stage of infection, HIV grows rapidly and spreads throughout the body. The virus attacks and destroys the infection-fighting CD4 cells ($CD4^+$ T lymphocytes) of the immune system. At this stage, the level of HIV in the blood is very high. Within 2 to 4 weeks after HIV infection, many individuals develop a flu-like or mononucleosis-like illness, while others have no significant symptoms [24]. The most common symptoms that occur in 40–90% of cases include fever, large tender

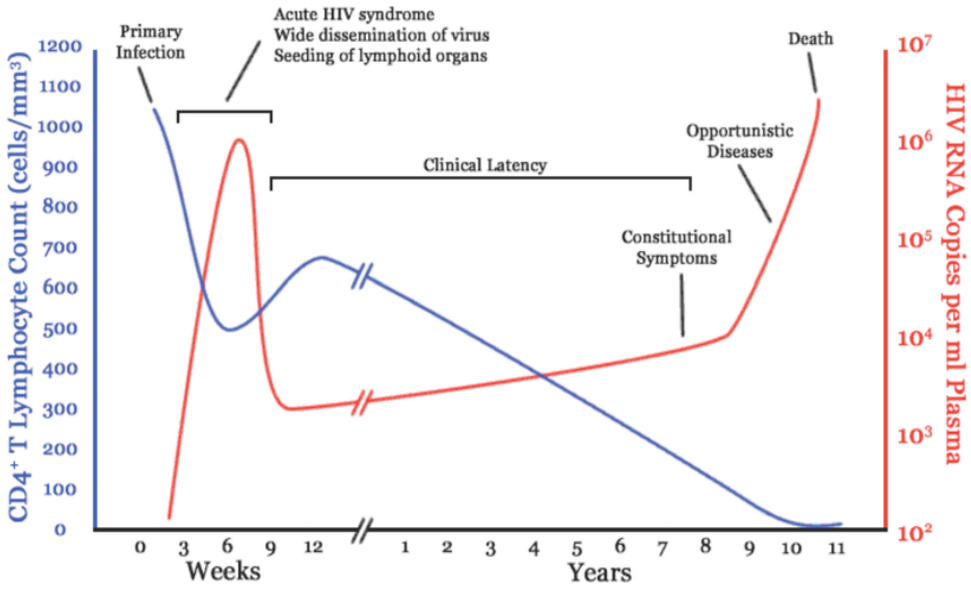

Figure 1.4: Clinical course of HIV infection. Picture courtesy: https://en.wikipedia.org/wiki/HIV

lymph nodes, throat inflammation, a rash, headache, tiredness, and/or sores of the mouth and genitals. The duration of the symptoms varies but is usually one or two weeks [25], though, for the nonspecific character, these symptoms are not often recognized as signs of HIV infection.

Stage II: Chronic HIV infection. The initial symptoms are followed by a stage called clinical latency or asymptomatic HIV, or chronic HIV. Without treatment, this second stage of HIV infection can last from about three years to over 20 years (on average, about eight years) [26]. While typically there are few or no symptoms at first, near the end of this stage many people experience fever, weight loss, gastrointestinal problems, and muscle pain [27]. Between 50% and 70% of people also develop persistent generalized lymphadenopathy, characterized by unexplained, non-painful enlargement of more than one group of lymph nodes (other than in the groin) for over three to six months [28]. Most HIV-1 infected individuals have a detectable viral load and in the absence of treatment will eventually progress to AIDS.

Stage III: Acquired immunodeficiency syndrome (AIDS). AIDS is the final, most severe stage of HIV infection. Because HIV has severely damaged the immune system, the body cannot fight off opportunistic infections. Opportunistic infections are infections and infection-related cancers that occur more frequently or are more severe in people with weakened immune systems than in people with healthy immune systems. AIDS condition can be characterized by HIV infection with either a $CD4^{+}T$ cell count below 200 cells per μl or the occurrence of specific diseases associated with HIV infection [28]. The people with AIDS frequently have systemic symptoms such as prolonged fevers, sweats (particularly at night), swollen lymph nodes, chills, weakness, and unintended weight loss. Diarrhea is another common symptom,

present in about 90% of people with AIDS [29]. People with AIDS have an increased risk of developing various viral-induced cancers, including Kaposi's sarcoma, Burkitt's lymphoma, primary central nervous system lymphoma, and cervical cancer [30]. People can also be affected by diverse psychiatric and neurological symptoms independent of opportunistic infections and cancers [31].

1.5.4 Growth of Worldwide HIV/AIDS Epidemic

After initiation in 1981, HIV/AIDS has become one of the world's most serious health and development challenges. Various organization have been built up to monitor and prevent the spread of HIV/AIDS worldwide. Over the past twenty years, UNICEF (United Nations International Children's Emergency Fund) has been the leading voice for children in the global AIDS response. The WHO Department of HIV/AIDS is another organization, monitoring the HIV/AIDS epidemic efficiently on a global scale. However, The Joint United Nations Programme on HIV and AIDS, or UNAIDS is the main advocate for accelerated, comprehensive and coordinated global action on the HIV/AIDS epidemic.

According to UNAIDS global report [32] in 2021, 38.4 million [33.9 million–43.8 million] people globally were living with HIV. There are 1.5 million [1.1 million–2.0 million] people became newly infected with HIV and 650000 [510000–860000] people died from AIDS-related illnesses in 2021. Since the start of the epidemic, there are 84.2 million [64.0 million–113.0 million] people have become infected with HIV and 40.1 million [33.6 million–48.6million] people have died from AIDS-related illnesses. The prime aim of UNAIDS is ending the HIV/AIDS epidemic by 2030.

1.5.4.1 HIV/AIDS Epidemic in India

In 1986, the first known cases of HIV in India was diagnosed amongst six female sex workers in Chennai, Tamil Nadu [33]. In 1992, the India government set up the National AIDS Control Organisation (NACO) to oversee policies and prevention and control programmes relating to HIV and AIDS and the National AIDS Control Programme (NACP) for HIV prevention.

According to NACO annual report published in 2019 [34], there were an estimated 23.49 lakh (17.98 lakh – 30.98 lakh) people living with HIV/AIDS in 2019, with an adult (15–49 years) HIV prevalence of 0.22% (0.17–0.29%). This includes around 79 thousand children living with HIV accounting for 3.4% of the total people living with HIV/AIDS estimates. There were 9.94 lakh women living with HIV (15+ years) constituting around 44% of the total estimated 15+ years of people living with HIV/AIDS. There were 69.22 thousand (37.03 thousand – 121.50 thousand) new HIV infections in 2019, which has declined by 37% since 2010 and by 86% since attaining the peak in 1997. There were 58.96 thousand (33.61 thousand – 102.16 thousand) AIDS-related deaths in the year 2019, which has declined by 66% since 2010 and by 78% since attaining its peak in 2005. HIV incidence was estimated at 0.05 per 1,000 uninfected

populations in 2019. Around 20.52 thousand pregnant women were estimated to be in need of Prevention of Mother-to-Child Transmission of HIV.

1.5.5 Treatment of HIV/AIDS

There is currently no cure, nor an effective HIV vaccine for treating of HIV/AIDS infection. There are several classes of antiretroviral agents that act on different stages of the HIV life-cycle. The use of multiple drugs that act on different viral targets is known as highly active antiretroviral therapy (HAART). HAART decreases the patient's total burden of HIV, maintains function of the immune system, and prevents opportunistic infections that often lead to death [35]. The World Health Organization (WHO) recommend offering antiretroviral treatment to all patients with HIV [36]. Because of the complexity of selecting and following a regimen, the potential for side effects, and the importance of taking medications regularly to prevent viral resistance.

There are six classes of drugs, which are usually used in combination, to treat HIV infection. Antiretroviral (ARV) drugs are broadly classified by the phase of the HIV life-cycle that the drug inhibits.

• **Entry inhibitors or fusion inhibitors** interfere with binding, fusion and entry of HIV-1 to the host cell by blocking one of several targets. Maraviroc and enfuvirtide are the two available agents in this class.

• **Nucleoside reverse-transcriptase inhibitors (NRTI)** and **nucleotide reverse-transcriptase inhibitors (NtRTI)** are nucleoside and nucleotide analogues which inhibit reverse transcription. Examples of NRTIs include zidovudine, abacavir, lamivudine, emtricitabine, and of NtRTIs – tenofovir and adefovir.

• **Non-nucleoside reverse-transcriptase inhibitors (NNRTI)** inhibit reverse transcriptase by binding to an allosteric site of the enzyme; NNRTIs act as non-competitive inhibitors of reverse transcriptase. Nevirapine and efavirenz, etravirine, rilpivirine are the examples of NNRTIs drugs.

• **Integrase inhibitors** (also known as integrase nuclear strand transfer inhibitors or INSTIs) inhibit the viral enzyme integrase, which is responsible for integration of viral DNA into the DNA of the infected cell. The clinically approved integrase inhibitors are raltegravir, elvitegravir, dolutegravir, bictegravir, and cabotegravir.

• **Protease inhibitors** block the viral protease enzyme necessary to produce mature virions upon budding from the host membrane. Particularly, these drugs prevent the cleavage of gag and gag/pol precursor proteins. Virus particles produced in the presence of protease inhibitors are defective and mostly non-infectious. Examples of HIV protease inhibitors are lopinavir, indinavir, nelfinavir, amprenavir and ritonavir. Darunavir and atazanavir are recommended as first line therapy choices.

• **Highly active antiretroviral therapy (HAART)** include two nucleoside reverse-transcriptase

inhibitors (NRTI) as a "backbone" along with one non-nucleoside reverse-transcriptase inhibitor (NNRTI), protease inhibitor (PI) or integrase inhibitors (also known as integrase nuclear strand transfer inhibitors or INSTIs) as a "base" [36].

1.6 A Brief Introduction to COVID-19 Pandemic

The novel virus was first identified from an ongoing outbreak in Wuhan, China, in December 2019 [37]. Attempts to contain it there failed, allowing the virus to spread to other areas of China and later worldwide. During the initial outbreak in Wuhan, the virus and disease were commonly referred to as coronavirus, Wuhan coronavirus [38, 39]. In January 2020, the World Health Organization (WHO) recommended "2019 novel coronavirus" (2019-nCoV) [40] as the provisional name for the virus and also declared the outbreak a public health emergency of international concern, and a pandemic on 11 March 2020. On 11 February 2020, the International Committee on Taxonomy of Viruses adopted the official name "severe acute respiratory syndrome coronavirus 2" (SARS-CoV-2) [41].

1.6.1 Structure of SARS-CoV-2 Virion

Severe acute respiratory syndrome coronavirus 2 (SARS-CoV-2) virus is a strain of coronavirus, a member of genus betacoronavirus, part of the family coronaviridae on the basis of genetic and biological characteristics [42]. A schematic diagram of SARS-CoV-2 virion is given in Fig. 1.5. SARS-CoV-2 virion is 60–140 nanometres ($2.4 \times 10^{-6} - 5.5 \times 10^{-6}$) in diameter [43, 44]. SARS-CoV-2 is composed of four structural proteins, known as the S (spike), E (envelope), M (membrane), and N (nucleocapsid) proteins. Since, SARS-CoV-2 is a linear, positive-sense, single-stranded RNA genome [45], the N protein holds the RNA genome, and the S, E, and M proteins together create the viral envelope [46]. S proteins are glycoproteins, and type I membrane proteins [47] and also have two functional parts, says, S1 and S2 [45]. The function of spike proteins is to attach and fuse with the membrane of a host cell [46]; specifically, its S1 subunit catalyzes attachment, the S2 subunit fusion [48].

1.6.2 Transmission and Symptoms of COVID-19

COVID-19 is mainly transmitted when people breathe in air contaminated by droplets/aerosols and small airborne particles containing the virus. Infected people release these particles when they breathe, talk, cough, sneeze, or sing [49, 50]. The more physically close people are the greater chance of infection. However, the infection can occur over longer distances, particularly indoors [49, 51].

Symptoms of COVID-19 are variable, ranging from mild symptoms to severe illness [52]. Common symptoms include headache, loss of smell and taste, nasal congestion and runny nose,

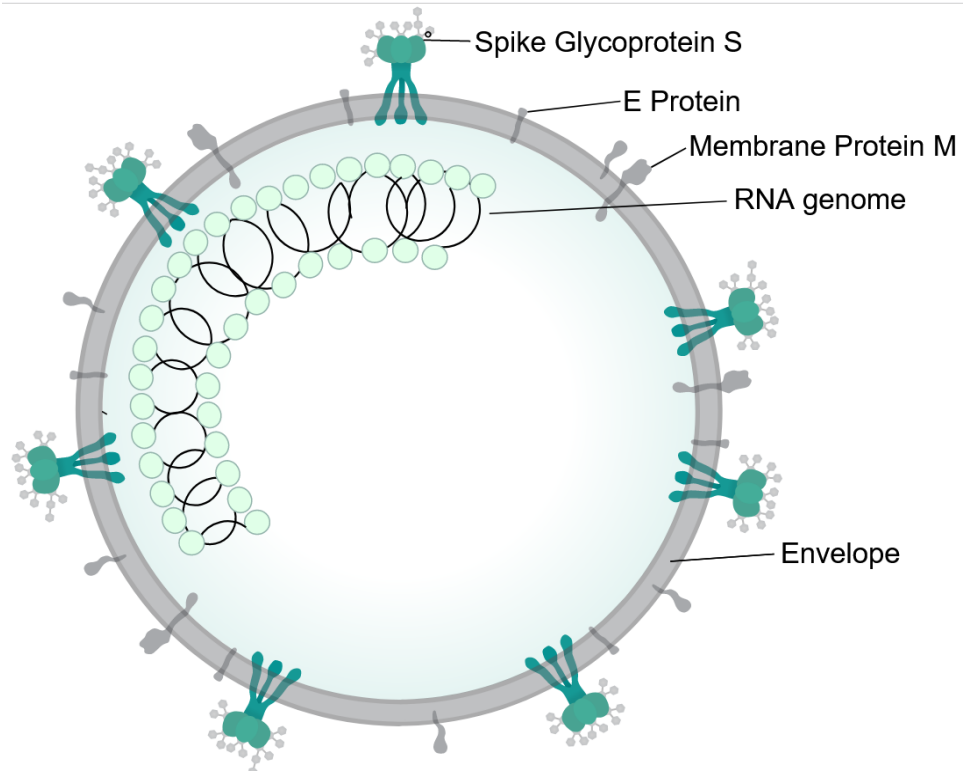

Figure 1.5: Structure of SARS-CoV-2 virion. Picture courtesy: https://en.wikipedia.org/wiki/COVID-19

cough, muscle pain, sore throat, fever, diarrhea, and breathing difficulties [53]. People with the same infection may have different symptoms, and their symptoms may change over time. There are three types of common clusters of symptoms have been identified: (i) respiratory symptom cluster with cough, sputum, shortness of breath, and fever, (ii) a musculoskeletal symptom cluster with muscle and joint pain, headache, and fatigue, and (iii) a cluster of digestive symptoms with abdominal pain, vomiting, and diarrhea [54]. Symptoms of COVID-19 are depicted in Fig. 1.6.

1.6.3 Diagnosis and Treatment of COVID-19

On the basis of COVID-19 symptoms, provisionally diagnosed to confirm using reverse transcription polymerase chain reaction (RT-PCR) or other nucleic acid (NAT) testing of infected secretions and both tests detect the presence of viral RNA fragments [55].

COVID-19 is transmitted by breathing and infected people release these virus when they breathe, talk, cough, sneeze, or sing. This virus is remarkable because our immune system is unable to fight it and it has amazing human-to-human transmission capacity. So, to prevent COVID-19, Centers for Disease Control and Prevention (CDC) and World Health Organization (WHO) advise to use face-mask, keep social distancing, avoid crowded indoor spaces, hand-washing and hygiene, surface cleaning, healthy diet and lifestyle etc. These primary interventions are called non-pharmaceutical interventions. And also, almost all governments

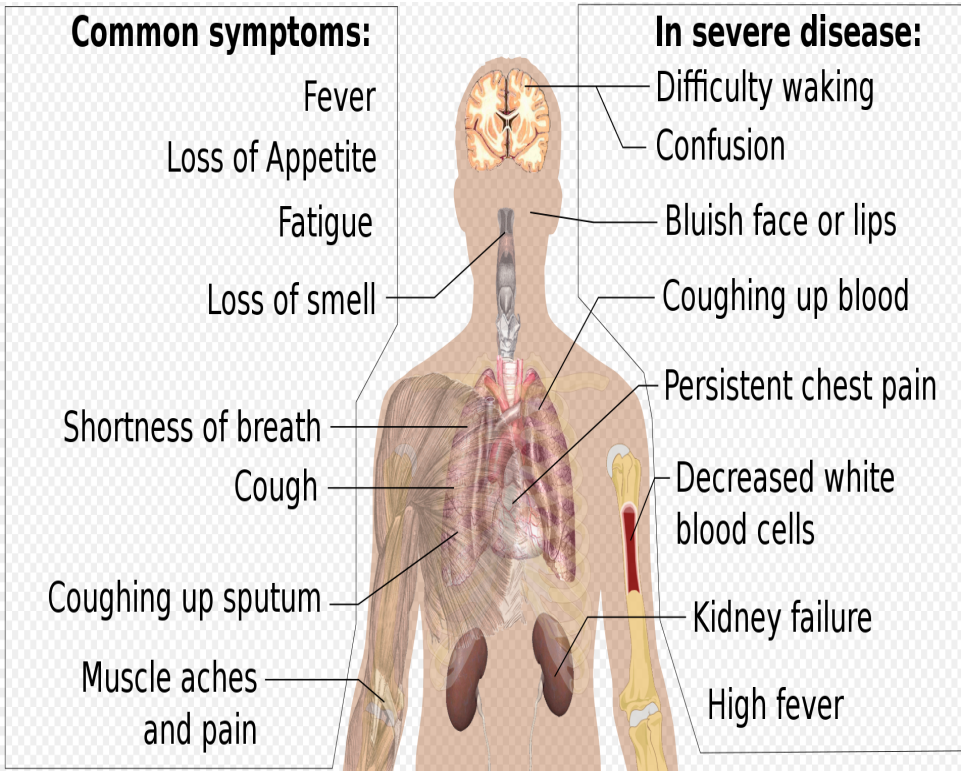

Figure 1.6: Symptoms of COVID-19. Picture courtesy: https://en.wikipedia.org/wiki/COVID-19

worldwide have implemented lockdown to reduce covid-19 infection.

For the first two years of the pandemic, no specific and effective pharmaceutical treatment or cure was available [56]. In 2021, the European Medicines Agency's (EMA) Committee for Medicinal Products for Human Use (CHMP) approved the oral antiviral protease inhibitor, nirmatrelvir/ritonavir (marketed as Paxlovid) or remdesivir, to treat adult patients [57]. But, these drugs have also failed to reduce covid-19 infection. In 2020, the first COVID-19 vaccines were developed and made available to the public with emergency use approval [58]. Initially, most COVID-19 vaccines were two-dose vaccines, with the sole exception being the single-dose Janssen COVID-19 vaccine [58]. However, immunity from the vaccines has been found to wane over time, requiring people to get booster doses of the vaccine to maintain immunity against COVID-19 [58]. The COVID-19 vaccines are widely credited for their role in reducing the spread of COVID-19 and reducing the severity and death caused by COVID-19, although some people have still managed to get the virus even after vaccination [58–60]. Now the current CoronaVac, Covaxin, Convidecia, Janssen, Medigen, Moderna, Novavax, Oxford–AstraZeneca, Pfizer–BioNTech, Sinopharm BIBP, Sputnik V COVID-19 vaccines are available over the worldwide. However, we can see that COVID-19 vaccines are not sufficient to eradicate the pandemic. So we must follow non-pharmaceutical interventions as well as take a booster dose.

1.6.4 Impact of The COVID-19 Pandemic

The pandemic has disrupted the world in many ways and continues to do so. We do not know when or how many years it will take to overcome that obstacle. This pandemic has especially disrupted the social and economic system around the world and resulted in the largest global recession since the Great Depression. So, many well-reputed-small industries or companies have closed down and as a result, many workers have become jobless. Not only that, existing many industries or companies have laid off their employees. So most of the people are financially exhausted in one way or another, in the world. During the lockdown, the disruption of the supply chain led to widespread supply shortages, including food shortages. Most importantly, the pandemic has affected our education. For lockdown, in many geographic locations, educational institutions were partially or fully closed. Although, few institutions have taken online classes. However, due to the closure of most of the educational institutions, the education of students has suffered greatly and will continue to do so in the future. The public areas were partially or fully closed, and many events were canceled or postponed for lockdown. The pandemic also raised very important issues of racial and geographic discrimination, health equity, and the balance between public health needs and individual rights. Social media and mass media circulate the misinformation and that intensifies political tensions. Pollution has dropped unprecedentedly due to the global lockdown.

1.6.5 The Global Prevalence of The COVID-19 Pandemic

COVID-19 pandemic is an ongoing outbreak. It has spread worldwide. According to WHO on 26 August 2022, there have been 59,68,73,121 confirmed cases of COVID-19 worldwide, including 64,59,684 deaths since the start of the pandemic. And till 23 August 2022, a total of 12,44,94,43,718 vaccine doses have been administered worldwide. The United States of America has the highest number of infections and deaths from Covid-19. India is next in line for Covid-19 infections.

1.6.6 COVID-19 Pandemic in India

The first case of COVID-19 infection was found in Kerala, India [61]. Now, according to the Ministry of Health and Family Welfare (MoHFW), Government of India on 26 August 2022, the number of confirmed cases of COVID-19 turns to 4,43,89,176 including 5,27,556 deaths since the start of the pandemic. As of 15 August 2022, a total of 2,08,53,87,344 vaccine doses have been administered. So far, the Indian Government is advising people to wear face masks, maintain social distancing, and follow a healthy lifestyle and hygiene rules.

1.7 Basic Mathematical Tools

In this section, we present some basic definitions, theorems and mathematical tools that have been used throughout this thesis.

Definition 1.1 ***(Dynamical System)*** *Dynamical system is an evolution rule that defines a trajectory as a function of a single parameter (time) on a set of states (the phase space).*

Definition 1.2 ***(Deterministic System)*** *A dynamical system is called deterministic if for each state in the phase space there is a unique consequent, i.e., the evolution rule of deterministic dynamical system is a function taking a given state to a unique subsequent state.*

In deterministic systems, for each time t, the evolution rule is a mapping from the phase space to the phase space given by

$$\phi(p,t) \equiv \phi_t(p) : M \longrightarrow M,$$

where $t \in \mathbb{R}$ is the continuous time variable, M is the phase space, $p(t) = \phi_t(p_0)$ denotes the position of the system at time t that started at p_0. Moreover, we assume that $t \geq 0$ and at $t = 0$, $\phi_t(x_0) = p_0$.

Definition 1.3 ***(Orbits or Trajectories)*** *The sequence of states that follow from or lead to a given initial state is called an orbit or a trajectory. The positive or forward orbit is defined as the following set of subsequent states*

$$\Gamma_p^+ \equiv \{\phi_t(p) \ : \ t \geq 0\}.$$

Similarly, the negative or backward orbit is the set of sequences of states that lead, according to the evolution rule, to the initial state. If the function ϕ_t is injective then the negative orbit is given by the set

$$\Gamma_p^- \equiv \{\phi_t(p) \ : \ t \leq 0\}.$$

Otherwise, it is possible that several prior points could lead to the same p.

Summing up, the full orbit of a point p is given by $\Gamma_p = \Gamma_p^+ \cup \Gamma_p^-$.

Definition 1.4 ***(Invariant Set)*** *A set Λ is said to be invariant under an evolution rule ϕ_t if*

$$\phi_t(\Lambda) = \Lambda, \textit{ for all } t.$$

Thus, for each $p \in \Lambda$, $\phi_t(p) \in \Lambda$, for any t. Therefore, for each point p in an invariant set Λ, the entire orbit of p will be contained in Λ. Moreover, a set Λ is said to be forward invariant if $\phi_t(\Lambda) \subset \Lambda$ for all $t > 0$.

Definition 1.5 ***(Autonomous System of Differential Equations)*** *A system of differential equations of the form*

$$\dot{p} = f(p)$$

where $p \in \mathbb{R}^n$ and vector field $f : E(\subset \mathbb{R}^n) \longrightarrow \mathbb{R}^n$ is said to be autonomous if f does not depend on t explicitly. Unless stated otherwise, we will assume

$$f \in C^1(E) = \{\text{Set of all continuously differentiable functions on } E\}.$$

Definition 1.6 ***(Initial Value Problem)*** *An autonomous system of differential equations is called an initial value problem if it satisfies the initial condition*

$$p(t_0) = p_0.$$

Therefore, an initial value problem for an autonomous system of differential equations is expressed by

$$\begin{cases} \dot{p} = f(p), \\ p(t_0) = p_0. \end{cases} \tag{1.1}$$

Definition 1.7 ***(Lipschitz Function)*** *Let E be an open subset of $\mathbb{R}^n$. A function $f : E \to \mathbb{R}^n$ is Lipschitz if for all $p,\ q \in E$ there is a real constant $K > 0$ such that*

$$|f(p) - f(q)| \leq K|p - q|.$$

Theorem 1.8 ***(Picard-Lindelöf Existence and Uniqueness [62])*** *Suppose that for $p_0 \in \mathbb{R}^n$ there is real number $b > 0$ such that there is a closed ball $B_b(p_0)$ and $f : B_b(p_0) \to \mathbb{R}^n$ is Lipschitz with constant K. Then the initial value problem (1.1) has a unique solution $p(t)$ for $t \in [t_0 - a, t_0 + a]$ provided that*

$$a = \frac{b}{M} \text{ where } M = \max_{p \in B_b(p_0)} |f(p)|.$$

Definition 1.9 ***(Equilibrium Solutions)*** *An equilibrium solution (steady state solution or fixed point or critical point) of the system (1.1) is a constant solution $\bar{p}$ satisfying*

$$f(\bar{p}) = 0.$$

Definition 1.10 ***(Linearization)*** *For the system (1.1), we assume $f \in C^1(E)$ and $\bar{p}$ is an equilibrium point. Then the linearization of $\dot{p} = f(p)$ at the equilibrium $\bar{p} \in E$ is the system of differential equations*

$$\dot{q} = Df(\bar{p})q,$$

where

$$q(t) = p(t) - \bar{p} \text{ and } Df(\bar{p}) = \begin{pmatrix} \frac{\partial f_1}{\partial p_1} & \frac{\partial f_1}{\partial p_2} & \cdots & \frac{\partial f_1}{\partial p_n} \\ \frac{\partial f_2}{\partial p_1} & \frac{\partial f_2}{\partial p_2} & \cdots & \frac{\partial f_2}{\partial p_n} \\ . & . & . & . \\ . & . & . & . \\ . & . & . & . \\ \frac{\partial f_n}{\partial p_1} & \frac{\partial f_n}{\partial p_2} & \cdots & \frac{\partial f_n}{\partial p_n} \end{pmatrix}_{p=\bar{p}}.$$

The matrix $Df(p)$ is called the Jacobian matrix or variational matrix of f at $\bar{p}$.

Definition 1.11 ***(Generalized Eigenspaces)*** *The equilibrium solutions of system (1.1) are classified by their generalized eigenspaces according to the sign of the real part of the eigenvalues of the variational matrix $Df(p)$ evaluated at the equilibrium solution. Let, σ_n, $n \in \mathbb{N}$ be the eigenvalues associated with the equilibrium $\bar{p}$ of the system (1.1). Then*

- *E^u = Unstable eigenspace spanned by the eigenvectors of the eigenvalues σ_n with $Re(\sigma_n) > 0$.*
- *E^c = Center eigenspace spanned by the eigenvectors of the eigenvalues σ_n with $Re(\sigma_n) = 0$.*
- *E^s = Stable eigenspace spanned by the eigenvectors of the eigenvalues σ_n with $Re(\sigma_n) < 0$.*

Therefore, the complete eigenspace E with respect to the equilibrium $\bar{p}$ is given by the following direct sum:

$$E = E^u \oplus E^c \oplus E^s.$$

Definition 1.12 ***(Hyperbolic Equilibrium)*** *An equilibrium $\bar{p}$ of system (1.1) is hyperbolic if none of the eigenvalues of $Df(\bar{p})$ is zero or purely imaginary. In this case E^c is empty. Hyperbolic equilibrium can be categorized into following three classes.*

1. ***Sink.*** *An equilibrium $\bar{p}$ of system (1.1) is a sink if all of the eigenvalues of $Df(\bar{p})$ have negative real parts. In this case, $E = E^s$ and the equilibrium is called stable. Sink can be classified as stable node or stable focus.*
    - ***Stable Node:*** *If the eigenvalues are negative real then the sink is called a stable node.*
    - ***Stable Focus:*** *If the eigenvalues are complex conjugates with negative real part then it is called a stable focus.*
2. ***Source.*** *An equilibrium $\bar{p}$ of system (1.1) is a source if all of the eigenvalues of $Df(\bar{p})$ have positive real parts. In this case, $E = E^u$ and the equilibrium is called unstable. Source can be classified as unstable node or unstable focus.*

- ***Unstable Node:*** *If the eigenvalues are real and positive then a source is called an unstable node.*
- ***Unstable Focus:*** *If the eigenvalues are complex conjugates with positive real part then it is called an unstable focus.*

3. ***Saddle****: An equilibrium $\bar{p}$ of system (1.1) is saddle if it is hyperbolic but not a sink or a source. Here, $E = E^s \oplus E^u$. A saddle point is also an unstable equilibrium.*

Definition 1.13 ***(Non hyperbolic Equilibrium)*** *An equilibrium $\bar{p}$ of system (1.1) is non hyperbolic or degenerate if at least one of the eigenvalues of $Df(\bar{p})$ have zero real part. In this case E^c is non empty.*

- ***Center:*** *It is a non hyperbolic equilibrium where eigenvalues are complex conjugates with zero real part.*

Definition 1.14 ***(Local Stability)*** *An equilibrium solution $\bar{p}$ of (1.1) is said to be locally stable if for each $\varepsilon > 0$ there exists a $\delta > 0$ such that every solution $p(t)$ of (1.1) with initial condition $p(t_0) = p_0$ and $||p_0 - \bar{p}|| < \delta \ \Rightarrow \ ||p(t) - \bar{p}|| < \varepsilon$ for all $t \geq t_0$, where $||.||$ is the Euclidean norm. If the equilibrium solution is not locally stable it is said to be unstable.*

Definition 1.15 ***(Local Asymptotic Stability)*** *An equilibrium solution $\bar{p}$ of (1.1) is said to be locally asymptotically stable if it is locally stable and if there exists a $\sigma > 0$ such that $||p_0 - \bar{p}|| < \sigma \ \Rightarrow \ \lim_{t\to\infty} ||p(t) - \bar{p}|| = 0$.*

Definition 1.16 ***(Instability)*** *An equilibrium solution $\bar{p}$ of (1.1) is called unstable if it is not stable.*

Theorem 1.17 ***(Hartman-Grobman Theorem [63])*** *If $\bar{p}$ is a hyperbolic equilibrium point of the system (1.1), then there is a homeomorphism h (i.e., h is a continuous, injective mapping with a continuous inverse) defined on some neighborhood $\Omega_{\bar{p}}$ in $\mathbb{R}^n$, locally taking orbits of the nonlinear system $\dot{p} = f(p),\ p \in \mathbb{R}^n$ to those of the linear system $\dot{q} = Df(\bar{p})q,\ q \in \mathbb{R}^n$, where $q = p - \bar{p}$. The mapping h preserves the sense of orbits and can also be chosen so as to preserve parameterization by time.*

If the mapping h is a homeomorphism, then stability (or lack of it) for the linear system implies local asymptotic stability of the nonlinear system (or lack of it).

Theorem 1.18 ***(Routh-Hurwitz Criteria [64])*** *Given the polynomial,*

$$P(\sigma) = \sigma^n + a_1\sigma^{n-1} + ... + a_{n-1}\sigma + a_n, \tag{1.2}$$

where the coefficients a_i are real constants, $i = 1, 2, ..., n$. n Hurwitz matrices are defined by using the coefficients of $P(\sigma)$ as

$$H_k = \begin{pmatrix} a_1 & 1 & 0 & 0 & ... & 0 \\ a_3 & a_2 & a_1 & 1 & ... & 0 \\ a_5 & a_4 & a_3 & a_2 & ... & 0 \\ . & . & . & . & ... & . \\ . & . & . & . & ... & . \\ . & . & . & . & ... & . \\ 0 & 0 & 0 & 0 & ... & a_k \end{pmatrix}, \; k = 1,2,...,n,$$

where $a_k = 0$ if $k > n$. All the roots of the polynomial $P(\sigma)$ will have negative real part if and only if the determinants of all k Hurwitz matrices are positive, i.e., $det(H_k) > 0,\ k = 1,2,...,n$. Following are the Routh-Hurwitz criteria for $n = 2$ and 3.

- $n = 2\ :\ a_1 > 0,\ a_2 > 0.$
- $n = 3\ :\ a_1 > 0,\ a_3 > 0,\ a_1 a_2 - a_3 > 0.$

Theorem 1.19 ***(Local Stability Using Routh-Hurwitz Criteria)*** *Let $\bar{p}$ be an equilibrium of the system (1.1) and the characteristic equation of the variational matrix $Df(\bar{p})$, given by (1.2), satisfies the Routh-Hurwith criteria, i.e., $det(H_k) > 0,\ k = 1,2,...,n$. Then the equilibrium $\bar{p}$ is locally asymptotically stable.*

Definition 1.20 ***(Global Asymptotic Stability)*** *An equilibrium solution $\bar{p}$ of (1.1) is said to be globally asymptotically stable if it is locally asymptotically stable and if $||p_0 - \bar{p}|| < \infty$ implies $\lim_{t\to\infty} ||p(t) - \bar{p}|| = 0$.*

Definition 1.21 ***(Positive Definite Function)*** *Let E be an open subset of $\mathbb{R}^n$ containing the equilibrium $\bar{p}$ of system (1.1). A real-valued $C^1(E)$ function V, $V : E \to \mathbb{R}$, is said to be positive definite [64] on the set E if the following two conditions hold:*

$$(i)\ V(\bar{p}) = 0,$$
$$(ii)\ V(p) > 0 \text{ for all } p \in E \text{ with } p \neq \bar{p}.$$

The function V is said to be negative definite if $-V$ is positive definite.

Theorem 1.22 ***(Lyapunov Stability Theorem [64])*** *Let $\bar{p}$ be an equilibrium of the system (1.1) and V be a positive definite C^1 function given by $V : E \to \mathbb{R}$, where E is an open subset of $\mathbb{R}^n$ containing the equilibrium $\bar{p}$.*

1. *If $\frac{dV}{dt} \leq 0$ for all $p \in E \setminus \{\bar{p}\}$ then $\bar{p}$ is said to be locally stable. V, in this case, is called a 'weak Lyapunov function'.*
2. *If $\frac{dV}{dt} < 0$ for all $p \in E \setminus \{\bar{p}\}$ then $\bar{p}$ is said to be locally asymptotically stable. In this case, V is called a 'strict Lyapunov function'.*

3. *If* $\frac{dV}{dt} > 0$ *for all* $p \in E \setminus \{\bar{p}\}$ *then* $\bar{p}$ *is unstable.*

Theorem 1.23 ***(LaSalle's Invariance Principle [65])*** *Let* $\bar{p}$ *be an equilibrium of system (1.1) and L be a weak Lyapunov function given by* $L : E \to \mathbb{R}$*, where E is an open, forward invariant subset of* $\mathbb{R}^n$ *containing the equilibrium* $\bar{p}$*. Let* $Z = \left\{ p \in E \ : \ \frac{dL}{dt} = 0 \right\}$ *be the set where L is not decreasing. If* $\bar{p}$ *is the largest forward invariant subset of Z then it attracts every point in E and eventually becomes globally stable in E.*

Definition 1.24 ***(Periodic Solution)*** *A solution* $\psi(p,t)$ *of (1.1) is called a periodic solution if there exists a positive number T such that*

$$\psi(p_0, t+T) = \psi(p_0,t) \text{ for all } t \text{ and}$$
$$\psi(p_0, t+s) \neq \psi(p_0,t) \text{ for all } 0 < s < T.$$

It is obvious that if $\psi(p_0,t)$ *has a period T then such solutions has period* $2T,\ 3T,\ \ldots$ *If T is the smallest, we call this solution* $\psi(p,t)$ *as* $T-$ *periodic.*

Theorem 1.25 ***(Bendixson's Criteria [64])*** *Consider the system (1.1) in* $\mathbb{R}^2$*. Suppose D is a simply connected open subset of* $\mathbb{R}^2$*. If divergence of f,* $\nabla.f = \Sigma_{n=1}^{2} \frac{\partial f_n}{\partial p_n}$ *is not identically zero and does not change sign in D, then there are no periodic orbits of the autonomous system (1.1) in D.*

Theorem 1.26 ***(Dulac's Criteria [64])*** *Consider the system (1.1) in* $\mathbb{R}^2$*. Suppose D is a simply connected open subset of* $\mathbb{R}^2$ *and* $B(p,q)$ *is a real valued* C^1 *function in D. If divergence of* Bf*,* $\nabla.(Bf) = \Sigma_{n=1}^{2} \frac{\partial (Bf_n)}{\partial p_n}$ *is not identically zero and does not change sign in D then there is no periodic orbit of the autonomous system (1.1) in D.*

Theorem 1.27 ***(Hopf Bifurcation Theorem [64])*** *Consider an autonomous system of ordinary differential equations*

$$\dot{p} = f(p,\xi),\ p \in \mathbb{R}^n,\ \xi \in \mathbb{R}, \text{ and } f \text{ is continuously differentiable.} \tag{1.3}$$

Suppose, the system (1.3) has an equilibrium $\bar{p}(\xi)$*. Moreover, the Jacobian matrix* $Df(\bar{p}(\xi),\xi)$ *has one pair of complex eigenvalues*

$$\sigma_{1,2}(\xi) = A(\xi) \pm iB(\xi)$$

such that for some $\xi = \xi^*$ *it becomes purely imaginary, i.e.,*

$$A(\xi^*) = 0 \text{ and } B(\xi^*) \neq 0.$$

Then the eigenvalues will cross the imaginary axis with nonzero speed if (transversality condition)

$$\left.\frac{dA(\xi)}{d\xi}\right|_{\xi=\xi^*} \neq 0.$$

The system of differential equations (1.3) will undergo a Hopf bifurcation around $\bar{p}(\xi)$ *for* $\xi = \xi^*$ *and will possess a periodic solution with approximate period* $T = \frac{2\pi}{B(\xi^*)}$ *as* ξ *crosses* ξ^*.

1.8 A Brief Notes on Optimal Control Theory

Optimal control (OC) is the process of determining control and state trajectories for a dynamic system over a period of time in order to optimize an objective functional or a cost functional or a performance index [66]. For example, the dynamical system might be a spacecraft with controls corresponding to rocket thrusters, and the objective might be to reach the moon with minimum fuel expenditure or the dynamical system could be a nation's economy, with the objective to minimize unemployment; the controls, in this case, could be fiscal and monetary policy or what percentage of the population should be vaccinated as time evolves in a given epidemic model to minimize the number infected and the cost implementing the vaccination strategy.

Historically, OC is an extension of the calculus of variations. In the seventeenth century, the first formal results of the calculus of variations were obtained. Johann Bernoulli challenged other famous contemporary mathematicians - such as Newton, Leibniz, Jacob Bernoulli, L'Hôpital, and von Tschirnhaus - with the Brachistochrone problem: "Given two points A and B in a vertical plane, what is the curve traced out by a point acted on only by gravity, which starts at A and reaches B in the shortest time?"

The generalization of the calculus of variations to optimal control theory was strongly inspired by military applications and has developed rapidly since 1950. The Russian mathematician Lev S. Pontryagin (1908-1988) and his co-workers (V. G. Boltyanskii, R. V. Gamkrelidz, and E. F. Misshchenko) achieved the ultimate breakthrough with the formulation and demonstration of the Pontryagin Maximum Principle [67]. Now, this principle plays an important role in research with suitable conditions for optimization problems with differential equations as constraints.

Today, the OC theory is extensive and with several approaches. One can adjust controls in a system to achieve a goal, where the underlying system can include: ordinary differential equations, partial differential equations, discrete equations, stochastic differential equations, integro-difference equations, and a combination of discrete and continuous systems. In this work, we apply the OC theory to ordinary differential equations with a fixed time.

1.9 Basic Mathematical Tools for Optimal Control Problem

A typical optimal control problem requires a objective functional or cost functional or performance index $J(x(t),u(t))$, a set of state variables $(x(t) \in X)$, a set of control variables $(u(t) \in U)$ in a time t, with $t_0 \leq t \leq t_f$. The main goal is finding a piecewise continuous control $u(t)$ and the associated piecewise differentiable state variable $x(t)$ to maximize a given objective function. Before defining the basic optimal control problem, we first state some definitions.

Definition 1.28 ***(Piecewise Continuous)*** *let $I \subseteq \mathbb{R}$ be an interval (finite or infinite). A finite-valued function $k : I \to \mathbb{R}$ is said to be piecewise continuous if it is continuous at each $t \in I$, with the possible exception of at most a finite number of t, and if k is equal to either its left or right limit at every $t \in I$.*

Definition 1.29 ***(Piecewise Differentiable)*** *let $I \subseteq \mathbb{R}$ be an interval (finite or infinite). Let a finite-valued function $k : I \to \mathbb{R}$ be continuous on I and differentiable at all but some finite points of I. Further, if k' is continuous wherever it is defined. Then, k is a piecewise differentiable function.*

Definition 1.30 ***(Continuously Differentiable)*** *let $I \subseteq \mathbb{R}$ be an interval (finite or infinite). A finite-valued function $k : I \to \mathbb{R}$ is said to be continuously differentiable if k' exists and is continuous on I.*

Definition 1.31 ***(Concave)*** *let $I = [a,b] \subseteq \mathbb{R}$ be an finite interval. A finite-valued function $k : I \to \mathbb{R}$ is said to be concave on I if*

$$\alpha k(t_1) + (1-\alpha)k(t_2) \leq k(\alpha t_1 + (1-\alpha)t_2)$$

for all $0 \leq \alpha \leq 1$ and for any $a \leq t_1, t_2 \leq b$.

A function k is said to be convex on $[a,b]$ if it satisfies the reverse inequality, or equivalently, if $-k$ is concave.

Definition 1.32 ***(Basic optimal control problem in Lagrangian form)*** *An optimal control problem is in the form*

$$\max_u \; J(x(t),u(t)) = \int_{t_0}^{t_f} f(t,x(t),u(t))dt \tag{1.4}$$

subject to

$$\begin{aligned} \dot{x}(t) &= g(t,x(t),u(t)), \\ x(t_0) &= x_0, \end{aligned}$$

and $x(t_f)$ could be free, which means that the value of $x(t_f)$ is unrestricted.

For our purpose, f and g will always be continuously differentiable functions in all three arguments. We assume that the control set U is Lebesgue measurable function. Thus, as the control(s) will always be piecewise continuous, the associated states will always be piecewise continuous.

We focus on finding the maximum of a function. However, we can switch back and fourth between maximization and minimization by simply negating the cost functional:

$$min\{J\} = -max\{-J\}.$$

1.9.1 Pontryagin's Maximum Principle

The necessary first-order conditions to find the optimal control were developed by Pontryagin and his co-workers. This result is considered one of the most important results of Mathematics in the 20th century.

Pontryagin introduced the idea of adjoint functions to append the differential equation to the objective functional. Adjoint functions have a similar purpose as Lagrange multipliers in multivariate calculus, which append constraints to the function of several variables to be maximized or minimized.

Definition 1.33 ***(Hamiltonion)*** *Let us consider the optimal control problem defined in* (1.4)*. The function*

$$H(t,x(t),u(t),\lambda(t)) = f(t,x(t),u(t)) + \lambda(t)g(t,x(t),u(t)) \tag{1.5}$$

is called Hamiltonian function and λ is the adjoint variable.

Now we state Pontryagin Maximum Principle Theorem:

Theorem 1.34 ***Pontryagin Maximum Principle*** *If $u^*(t)$ and $x^*(t)$ are optimal for problem* (1.4)*, then there exists a piecewise differentiable adjoint variable $\lambda(t)$ such that*

$$H(t,x^*(t),u(t),\lambda(t)) \leq H(t,x^*(t),u^*(t),\lambda(t))$$

for all controls u at each time, where H is the Hamiltonian previously defined and

$$\lambda'(t) = -\frac{\partial H(t,x^*(t),u^*(t),\lambda(t))}{\partial x}$$
$$\lambda(t_f) = 0.$$

Proof The proof of this theorem is quite technical and we opted to omit it. The original Pontryagin's text [67] or Clarke's book [68] are good references to find the proof.

Remark 1.35 *The last condition $\lambda(t_f) = 0$, called the transversality condition, is only used when the optimal control problem does not have terminal value in the state variable, i.e., $x(t_f)$ is free.*

This principle converted the problem of finding a control which maximizes the objective functional subject to the state ODE and initial condition into the problem of optimizing the Hamiltonian pointwise. As consequence, with this adjoint equation and Hamiltonion, we have

$$\frac{\partial H}{\partial u} = 0 \text{ at } u = u^* \tag{1.6}$$

for each t. Therefore, the Hamiltonian has a critical point: usually this condition is called *optimality condition*. Thus, to find the necessary conditions, we do not need to calculate the integral in the objective functional, but only use the Hamiltonian.

The following is an outline of how this principle can be applied to solve the simplest problems:

i. Form the Hamiltonian for the problem.

ii. Write the adjoint differential equation, transversality boundary condition, and the optimality condition. Observe that there are three unknowns: u^*, x^* and λ.

iii. Try to eliminate u^* by using optimality equation $\frac{\partial H}{\partial u} = 0$, i.e., solve for u^* in terms of x^* and λ.

iv. Solve the two differential equations for x^* and λ with two boundary conditions, substituting u^* in the differential equations with the expression for the optimal control from the previous step.

v. After finding the optimal state and adjoint, solve for the optimal control.

Here we present a simple example to illustrate this principle.

Example 1.36 *[69]*
Consider the optimal control problem:

$$\min_{x,u} \; J(x(t),u(t)) = \int_0^2 (x + \frac{1}{2}u^2)dt$$

subject to

$$\begin{aligned} \dot{x}(t) &= x + u, \\ x(0) &= \frac{1}{2}e^2 - 1, \\ x(2) &\text{ is free.} \end{aligned}$$

The Hamiltonian can be written as:

$$H(t,x,u,\lambda) = x + \frac{1}{2}u^2 + \lambda(x+u) \tag{1.7}$$

Using Theorem 1.34, the equation of adjoint λ is given by the negative with partial derivative of H (1.7) with respect to x, i.e.,

$$\lambda'(t) = -\frac{\partial H}{\partial x} \Leftrightarrow \lambda'(t) = -1-\lambda.$$

Since $x(2)$ is free, transversality condition of adjoint variable λ is $\lambda(2) = 0$. Now we solve the equation

$$\lambda'(t) = -1-\lambda \implies \lambda'(t)+\lambda = -1.$$

Therefore integrating factor is $I.F. = e^{\int 1dt} = e^t$. Now multiplying I.F. both side and integrating, we get

$$\lambda(t)e^t = -e^t + C \implies \lambda(t) = -1 + Ce^{-t},$$

where C is a arbitrary intrigating constant. Now applying transversality condition $\lambda(2) = 0$, we have

$$\lambda(2) = -1 + Ce^{-2} \implies 0 = -1 + Ce^{-2} \implies C = e^2.$$

Therefore

$$\lambda(t) = -1 + e^{2-t}.$$

We differentiate hamiltonian H (1.7) partially with respect to u and find the critical value $u = u^*$ for which H is minimized. Mathematically,

$$\frac{\partial H}{\partial u} = 0 \Leftrightarrow u + \lambda = 0.$$

It is called an optimality condition and the critical value of u is given by

$$u^* = -\lambda.$$

Substituting the solution of λ, the optimality condition leads to

$$u^* = -\lambda \Leftrightarrow u^* = 1 - e^{2-t}.$$

One can solve the state variable x with the same way of λ, and the associated state is

$$x^* = \frac{1}{2}e^{2-t} - 1.$$

Remark 1.37 *If the Hamiltonian is linear in the control variable u, it can be difficult to calculate u^* from the optimality equation, since $\frac{\partial H}{\partial u}$ would not contain u. Specific ways of solving these kind of problems can be found in [70].*

Up to this we have showed only the necessary conditions to solve basic optimal control problems. Now, it is important to study some conditions that can guarantee the existence of a finite objective functional value at the optimal control and state variables, based on [70–73]. The following theorem is for sufficient condition:

Theorem 1.38 *Consider the optimal control problem:*

$$\max_u \; J(x(t),u(t)) = \int_{t_0}^{t_f} f(t,x(t),u(t))dt$$

subject to

$$\begin{aligned} \dot{x}(t) &= g(t,x(t),u(t)), \\ x(t_0) &= x_0. \end{aligned}$$

Suppose that $f(t,x,u)$ and $g(t,x,u)$ are both continuously differentiable functions in their three arguments and concave in x and u. Suppose u^* is a control with associated state x^*, and λ a piecewise differentiable function, such that u^*, x^* and λ together are satisfied on $t_0 \le t \le t_f$:

$$\begin{aligned} &f_u + \lambda g_u = 0, \\ &\lambda' = -(f_x + \lambda g_x), \\ &\lambda(t_f) = 0, \\ &\lambda(t) \ge 0. \end{aligned}$$

Then for all controls u, we have

$$J(u^*) \ge J(u).$$

Proof The proof of this theorem is available in [70]. This theorem is not strong enough to guarantee that $J(u^*)$ is finite. Such results require some conditions on f and/or g. Here is an example of an existence result from [71].

Theorem 1.39 *Let the set of controls for the system* (1.4) *be Lebesgue integrable functions (instead of just piecewise continuous functions) on $t_0 \le t \le t_f$ in $\mathbb{R}$. Suppose that $f(t,x,u)$ is*

convex in u, and there exists constants C_4 *and* $C_1, C_2, C_3 > 0$ *and* $\beta > 1$ *such that*

$$\begin{aligned} &g(t,x,u) = \alpha(t,x) + \beta(t,x)u, \\ &|g(t,x,u)| \leq C_1(1+|x|+|u|), \\ &|g(t,x_1,u) - g(t,x,u)| \leq C_2|x_1 - x|(1+|u|), \\ &f(t,x,u) \geq C_3|u|^{\beta} - C_4, \end{aligned}$$

for all t with $t_0 \leq t \leq t_f$, x, x_1, u *in* $\mathbb{R}$. *Then there exists an optimal control* u^* *maximizing* $J(u)$, *with* $J(u^*)$ *finite.*

Proof The proof of this theorem is available on [71]. For a minimization problem, g would have a concave property and the inequality on f would be reverse.

Note that the necessary conditions developed to this point deal with piecewise continuous optimal controls, while this existence theorem guarantees an optimal control which is only Lebesgue integrable. This disconnection can be improved by extending the necessary conditions to Lebesgue integrable functions [70, 73], but we did not set forth this idea in the thesis. See the existence of optimal control results in [74].

1.9.2 Optimal Control with Bounded Controls

Definition 1.40 *(optimal control with bounded control) An optimal control with bounded control can be written in the form*

$$\max_{u} \; J(x(t),u(t)) = \int_{t_0}^{t_f} f(t,x(t),u(t))dt \tag{1.8}$$

subject to

$$\begin{aligned} \dot{x}(t) &= g(t,x(t),u(t)), \\ x(t_0) &= x_0, \\ a \leq &u(t) \leq b, \end{aligned}$$

where a, b *are real fixed constants and* $a < b$.

To solve the optimal control problems with bounds on the control, we must develop alternative necessary conditions.

Proposition 1.41 *(necessary conditions). If* u^* *and* x^* *are optimal for problem* (1.8)*, then there exists a piecewise differentiable adjoint variable* $\lambda(t)$ *such that*

$$H(t,x^*(t),u(t),\lambda(t)) \leq H(t,x^*(t),u^*(t),\lambda(t))$$

for all controls u at each time t, where H is the Hamiltonian previously defined and

$$\lambda'(t) = -\frac{\partial H(t, x^*(t), u^*(t), \lambda(t))}{\partial x} \quad \textit{(adjoint condition)},$$
$$\lambda(t_f) = 0 \qquad\qquad\qquad\qquad \textit{(transversality condition)}.$$

By an adaptation of the Pontryagin Maximum Principle, the optimal control must satisfy (optimality condition):

$$u^* = \begin{cases} a & \text{if } \dfrac{\partial H}{\partial u} < 0, \\ a \leq \tilde{u} \leq b & \text{if } \dfrac{\partial H}{\partial u} = 0, \\ b & \text{if } \dfrac{\partial H}{\partial u} > 0, \end{cases} \tag{1.9}$$

i.e., the maximization is over all admissible controls, and $\tilde{u}$ is obtained by the expression $\frac{\partial H}{\partial u} = 0$. In particular, the optimal control u^* maximizes H pointwise with respect to $a \leq u(t) \leq b$.

Proof The proof of this result can be found in [72]. If we have a minimization problem, then u^* is instead chosen to minimize H pointwise. This has the effect of reversing < and > in the first and third lines of optimality condition (1.9).

Remark 1.42 *In order to numerically solve a problem with the addition of bounds of the control, we can write in a compact way the optimal control $\tilde{u}$ obtained without truncation, bounded by a and b:*

$$u^*(t) = min(a, max(b, \tilde{u})).$$

Not all optimal control problems can be solved analytically. Most epidemiological issues are complicated to solve analytically, so it is necessary to employ numerical methods. There are many numerical methods to solve optimal control problems, some of which are the Shooting method and Multiple shooting method (can be found in [75]). In addition, a very well-known method, the forward-backwards sweep method, can be found in the book by Lenhart and Workman [70].

1.10 Literature review and motivation

Human immunodeficiency virus type-1 (HIV-1) is a deadly pathogen which infects $CD4^+$T cells, one type of immune cells. The gradual depletion of $CD4^+$T cells in blood plasma is the signature of HIV-1 infection. AIDS (Acquired Immunodeficiency Syndrome) develops when the $CD4^+$T cells count drops to 200 cells/μl from its average value of 1000 cells/μl [76]. In reduced levels of $CD4^+$T cells, the immune system cannot act appropriately. As a result, an HIV-infected individual becomes susceptible to different opportunistic infections.

Perelson [77] first proposed a simple mathematical model for the interactions between the human immune system and HIV in 1989. In this paper, the author formulated a general model

of a large number of ordinary differential equations and many parameters that could potentially be responsible for many of the immunological consequences of HIV infection. For simplicity, the author modified the general model into a four-compartmental model consisting of free HIV, uninfected, latently infected, and productively infected $CD4^+$T cells. The author exhibits some surprising features of AIDS: the long latent period, the almost complete absence of free virus particles, the low frequency of infected $CD4^+$T cells, and the gradual decline of $CD4^+$T cells during the disease. In 1993, Perelson et al. [78] extended the model of Perelson's model [77] and proved some of the model's behaviour mathematically. In the last decade of the 20th century, several models (for example, [79–96]) of HIV infection have been developed using Perelson et al. [78] model concept to understand HIV dynamics, disease progression, diversity of viral load, and the interaction of the human immune system with HIV.

Transmission of HIV-1 within a host may be possible through two modes, viz. cell-free mode and cell-to-cell mode [97–99]. In cell-free transmission mode, free plasma virus infect the healthy $CD4^+$T cells, whereas infection spreads from one infected cell to another uninfected cell in case of cell-to-cell transmission mode. Several models (for example, [77–96]) incorporated only cell-free transmission mode. In the case of cell-to-cell transmission mode, the infection spreads from one infected cell to another uninfected cell [97–100]. Here transfer of virus particles may occur through different mechanisms, viz. virological synapses, filopodia and nanotubes. However, more than 90% dissemination of infection in cell-to-cell transmission mode occurs through virological synapse formation [97]. In this mechanism, the virus can evade some biophysical processes, and barriers compare to cell-free mode [101]. A tight junction (virological synapse) is created between an infected cell and an uninfected cell, and the virus material is directly transferred to an uninfected host. Neutralizing antibodies have limited effect in this binding process [100]. After entering into the uninfected cell, the basic steps of the virus life cycle are followed [102].

Cell-free infection may be a favourable way of virus dissemination at the initial stage of infection [103] or when antibody-mediated immune responses are less active or in the absence of antiviral drug therapy. In contrast, cell-to-cell infection mode may be a more competent way of viral transmission at a relatively later stage of infection when antibody-mediated immune responses are significantly strong or in the presence of antiviral drug therapy [104]. Recent experimental results show that cell-to-cell viral spread through virological synapses is significantly more efficient and faster than cell-free mode [97, 98, 100]. In vitro experiments demonstrate that cell-to-cell dissemination of infection may be 100-fold more efficient than the cell-free infection mode [101, 104–106]. It is, therefore, essential to incorporate both the dissemination modes of viral infection while discussing the mathematical model of HIV-1 infection within a host body.

Antiretroviral therapy has significantly reduced the viral load and increased the $CD4^+$T cell count, thus preventing the onset of AIDS and increasing the life span of HIV-1 infected patients. Although significant improvement in managing viremia using antiretroviral drug

therapies is possible, complete resolution of HIV-1 infection from the host body is yet to be achieved. Mainly two types of drugs are used to suppress HIV-1 infection in a host [95]. Reverse transcriptase inhibitors (RTI) block the synthesis of viral DNA from HIV-1 RNA and thereby reduces viral infectivity. On the other hand, protease inhibitors (PI) are used to inhibit the proper cleavage of viral polyprotein inside the infected cell and thereby reduce the number of functionally effective viral production. Different models have been proposed and studied, taking into the effect of drug therapies [88, 90, 107–113]. These models consider the spread of infection through a single pathway, the cell-free mode. In a recent study, Ahmed et al. [114] applied two controls RTIs and PIs on a four-dimensional HIV model incorporating cell-free mode only. Numerically, they observed that early initiation of treatment had a profound impact on improving the quality of life. Danane and Allali [115] studied a five-dimensional HIV model incorporating cell-free mode with RTIs and PIs controls. They demonstrated that with the two optimal treatments, the number of healthy $CD4^+T$ cells increased remarkably while the number of latently infected $CD4^+T$ cells and infected $CD4^+T$ cells decreased significantly. Moreover, it has also been observed that with the control strategy, the viral load is reduced considerably compared to the model without control which can improve the patient's quality of life. Also, they observed that the drug therapy should be administrated without any stops during the infection. Ngina et al. [116] applied three controls, viz. RTIs, PIs, and FIs (fusion inhibitors) on a seven-dimensional HIV model considering cell-free mode. It is shown that multi-drug therapy is always more beneficial in controlling disease progression compared to mono-drug therapy. It is also suggested, so far as mono-drug treatment is concerned, that PI is possibly the best drug and FI is the worst drug to control viral load and infected $CD4^+T$ cells. In another study, Rahmoun et al. [117] studied a three-dimensional HIV model taking cell-free mode with three controls, viz., RTIs, PIs, and IL-2 (interleukin-2). It is shown that combination therapy is essential for keeping the virus count under a detectable level and healthy cell counts at an acceptable level. It is also demonstrated that IL-2 treatment is not an efficient controller even when it significantly boosts healthy cell proliferation.

Previous studies [88, 90, 107–113, 116–119] on HIV-1 infection control models with mono or multi-blockers consider the mode of infection through a single pathway, which is the cell-free mode. So the question is, what would be the control strategy in the presence of cell-to-cell transmission mode also? To the best of our knowledge, no work has considered such controls in a multi-pathways HIV-1 infection model. Therefore, one of the objectives of this thesis is to gain insights into the effect of the single and multi-blockers drugs on the dynamics of an HIV-1 infection model in the presence of both cell-to-cell and cell-free infection modes.

It is reported that cell-to-cell spread allows HIV-1 to overcome barriers to infection [101, 102, 120]. There is evidence that antiretroviral drugs like tenofovir (TFV), efavirenz (EFV) and zidovudine (AZT) show reduced effectiveness in inhibiting cell-to-cell transmission [102, 121, 122]. Sigal et al. [123] demonstrated that the cell-to-cell spread of HIV permits ongoing replication despite antiretroviral therapy. Akbari and Asheghi [124] applied two controls, viz. RTIs

and PIs on a five-dimensional HIV model considering both transmission modes. They numerically demonstrated that the density of infected cells increased before treatment and decreased after treatment. It is also suggested that the optimal dosage of drugs effectively controls AIDS better and minimizes the side effects of the drugs. Liu et al. [125] studied a four-dimensional HIV model incorporating cell-free and cell-to-cell mode with two control RTIs and PIs. They have used PIs to prevent producing new viruses from infected $CD4^+T$ cells and applied PIs with some constant multiplication to inhibit cell-to-cell transmission. They have defined two types of objective functionals according to linear and quadratic control. Their numerical results exhibited that the control effects are similar for both objective functionals, and both can increase the uninfected $CD4^+T$ cell counts and reduce the concentration of free virus particles. Qin et al. [127] applied RTIs inhibitor in both transmission modes in a four-dimensional HIV model. Their numerical result showed a decrement in the viral load and an increment in the level of uninfected $CD4^+T$ cells. Furthermore, Guo and Qiu [128] applied a combination of RTIs and PIs inhibitors in a cell-free transmission mode only in a four-dimensional HIV model considering CTL immune response. In this model, they assume drug efficacy as a constant. Their theoretical and numerical results exhibit that CTL immune response is an important factor and should not be ignored in HIV infection. Observations of these studies suggest that existing antiretroviral drugs may be efficient in controlling cell-free transmission but unable to inhibit the dissemination of infection through cell-to-cell mode. A recent study by Hubner et al. [97] suggests that future control strategies through drug therapy and vaccination should focus on blocking cell-to-cell dissemination of infection.

HIV-1 mathematical models usually consider the interaction between the host cells (i.e., $CD4^+T$) and plasma free-virus. However, the activated $CD8^+T$ of CTL cells can kill the infected host cells and thus reduce the production of the free virus through the infected cell lysis. Some studies have considered the role of CTL on the HIV models with multi-mode dissemination of infection [129–132]. It is to be mentioned that the activation of CTL is not instantaneous. It takes some time for stimulation by our immune cells. Xu and Zhou [133] studied a delay-induced HIV model with two modes of infection transmission. It is of utmost importance to know how far different antiretroviral therapies can control viremia in the presence of delay. We, therefore, want to study a multi-pathways HIV-1 infection model with CTL delay in the presence of treatments. The main objective is to explore how immune response delay affects the plasma viral load in the presence and absence of the blockers and to determine the optimal dose.

The world has been passing through an extraordinary crisis period since late December 2019 due to an extraordinary pathogen Covid-19 [134]. The coronavirus spreads when an individual inhales the droplets containing virus [135]. Such contaminated droplets are produced during sneezing and coughing by an infected individual. Study shows that these droplets usually cannot travel more than 2 meters from its source and it is therefore advised to maintain a distance of six feet between two individuals to avoid an infection [136]. The number of suspended

droplets, however, can be reduced through practice of good cough and sneeze etiquette, which reduces the transmission probability of infection from an infective to a susceptible. Using of face musk is one of the most effective nonpharmaceutical measures that protect individuals from inhaling of virus-carrying droplets and restricts transmission [137, 138]. An individual may also be infected if one touches a contaminated surface and then touches his/her mouth, nose and eyes [139]. However, the most effective way to reduce large-scale contamination and community transmission is the lockdown [140]. To prevent human-to-human transmission of the coronavirus through contact, many countries have implemented nationwide or region-wide lockdown by closing academic institutions, offices, restaurants, community halls, social gathering and all modes of transportation. This mechanism has been proved to be effective in containing the transmission but unable to eradicate the disease in the absence of a vaccine [141].

In the absence of specific drugs and vaccines, some repurposing drugs were effectively used to save the lives of many severely infected covid patients [142]. Existing drugs like dexamethasone, favipiravir and remdesivir are some of such drugs which have been proven to be useful in treating covid-19 patients. Dexamethasone is a corticosteroid used for multiple problems like arthritis, asthma, intestinal disorder etc. The WHO and the NIH (National Institute of Health) have recently approved its use for the treatment of acute Covid-19 patients. It has been shown through randomized clinical trials that the immunosuppressant dexamethasone can save the lives of critically ill (on ventilation) Covid-19 patients and can reduce the mortality rate by one-third [143, 144]. An RNA polymerase inhibitor remdesivir, a drug used for Ebola virus infection, has shown the prophylactic and therapeutic efficacy for patients with severe Covid-19 [145, 146]. In vitro and in vivo experiments confirmed the efficacy of the nucleotide prodrug remdesivir against coronaviruses [147]. Both the European Union [148] and the USA [149] governments have approved its use in the treatment of COVID-19. Another important treatment study that can give life to many seriously ill Covid-19 patients is convalescent plasma or immunoglobulins therapy [150]. This passive immunization therapy has the potentiality to improve the survival rate of covid patients [151]. Use of such repurposing drugs along with the non-pharmaceutical intervention strategies may be the best possible way for fighting against the ongoing pandemic in the absence of any vaccine and specific drug for this novel coronavirus.

Numerous mathematical models on the Covid-19 pandemic have appeared to forecast the epidemic's future. These models reasonably address the epidemic burden of an affected country to guide the policymakers and the healthcare providers on preparedness. Fitting the data of China, Italy and France with a SIRD model, Fanelli and Piazza [152] showed that the kinetic parameter representing the recovery rate remains the same for many countries. Still, the death rates of the respective countries are different. A higher dimensional transmission model was proposed in [153] to study the Covid-19 epidemic in Wuhan. In Chatterjee et al. [154], a simple SEIR compartmental model was simulated with Monte Carlo (MC) simulation technique to measure the effect of NPIs. An epidemic model was used to investigate the dynamics of SARS-

CoV-2 with multiple transmission pathways by Yang and Wang [155]. They infer from the analytical and numerical results that the infection will remain endemic for a long time. A regression model for Covid-19 was used to estimate the final size and its peak time for China, South Korea, and the rest of the World [156]. In [157], a simple SIR model was used to estimate various epidemic parameters by fitting the epidemic data of the Republic of Korea. Nonlinear incidence was used in an epidemic model to show that lockdown can cause significant delay to attain the epidemic peak but is unable to eradicate the disease [158]. A simple iteration model, which uses only daily values of confirmed cases, was considered to forecast the covid positive cases for the United States, Slovenia, Iran, and Germany [159]. Pal et al. [160] explained the Covid-19 transmission dynamics during the unlock phase and the significance of testing with the help of a mathematical model. By simulating an SEIR model, Fang et al. [161] studied the impact of different control measures in spreading coronavirus. A computational model was used in [162] to assess the effect of face musk in the disease spreading of Covid-19. It is shown that the universal use of face masks and other non-pharmaceutical practices can significantly inhibit disease progression. None of these studies has considered the effect of repurposing drugs for fighting SARS-CoV-2 in the absence of a vaccine or specific drug. One of the objectives of this thesis is to demonstrate through mathematical modelling and analysis how and to what extent the NPIs and repurposing drugs can improve the overall Covid-19 epidemic burden.

1.11 Overview

Basic HIV-1 in-host models consider dissemination of infection through cell-free mode, where the infection spreads from free plasma virus to an uninfected $CD4^+T$ cell. Recent in vitro studies, however, demonstrate that cell-to-cell viral spread through virological synapses is the predominant mode of HIV-1 infection. The gradual depletion of $CD4^+T$ cells in the blood plasma is the signature of HIV-1 disease. Different blockers are used to prevent the lack of $CD4^+T$ cells by blocking the spread of infection and virus replication.

In **Chapter 2**, we study the effect of three blockers on a hypothetical HIV-1 infected subject when administered individually or in combination. For this, an HIV model that considers both the cell-free and cell-to-cell modes of spread of infection is analyzed with three controls. In the first phase of this study, we consider all three controls as constant and prove the local as well as global stabilities of the disease-free and infected steady states. We consider the controls time-dependent in the second phase and define a suitable optimal control problem. An objective function is characterized based on maximizing the healthy $CD4^+T$ cell counts and minimizing the count of infected $CD4^+T$ cells along with other systemic costs of drug therapy. Using Pontryagin's Maximum Principle, we give the necessary conditions for optimal control. We investigate and compare the effect of different mono- and multi-drug therapies through numerical simulations. In the case of mono blockers, the results show that the drug

which blocks cell-to-cell dissemination of infection is a better option for treating an HIV-1 infected individual. In the case of multi-blockers, a combined medicine that contains cell-to-cell blockers and protease inhibitors controls the infection efficiently.

In **Chapter 3**, we study optimal control in a multi-pathways in-host HIV-1 infection model with saturated infection rates and intracellular delay using three controls. The controls may be constant or time-dependent. In the case of constant controls, we proved that the infection-free equilibrium of the system is locally and globally asymptotically stable with some parametric condition. The stability of the infected equilibrium may be lost through Hopf bifurcation if the intracellular delay is longer. We define a suitable objective function in the time-dependent controls to maximize the cell counts of healthy $CD4^+T$ cells minimizing unhealthy $CD4^+T$ cells. We then derive the optimality conditions of our delay-induced control problem. Numerically we observe and compare the results of different type of time dependent control therapies. In the case of mono-drug therapy, no blocker can remove the infection for any delay, as infected $CD4^+$ T cells always persist. In the case of multi-drug therapy, the infection can remove by multi-drug therapies for all delays, except the combination of RTI and PI inhibitors. The result shows that a multi-drug therapy scheme that contains u_2 and u_1 blockers is a better option for treating HIV-1 infection. The result shows that a multi-drug therapy scheme that contains u_2 and u_3 blockers is a better option for treating HIV-1 infection. The result also indicates that the treatment duration depends on delay, i.e., if the delay is shorter, then the treatment period is also shorter.

In **Chapter 4**, we study a multi-pathways in-host HIV-1 infection model in the presence of immune response delay and three controls. The controls may be constant or time-dependent. In the case of constant controls, it is shown that the infection-free equilibrium of the system is locally and globally asymptotically stable when the basic reproduction number is less than unity. The stability of the infected equilibrium may be lost through Hopf bifurcation if the immune response delay is longer. We define a suitable objective function in the time-dependent controls to maximize the cell counts of healthy $CD4^+T$ cells and CTLs. We then derive the optimality conditions of our delay-induced control problem. We examine and compare the effect of mono and multi-drug therapies through numerical simulations. We demonstrate that removing infection is not possible using any mono-drug treatment. It is demonstrated that the blocker that inhibits synapse formation during cell-to-cell disease transmission should be used while using multi-drug therapy to clear the infection. However, this control is not an efficient blocker in the mono-drug treatment protocol. Our study reveals that if CTL's response is quicker, $CD4^+T$ cell count may remain stable but becomes unstable if response time increases.

The Covid-19 pandemic has put the world under immeasurable stress. There is no specific drug or vaccine that can cure the infection or protect people from the infection of coronavirus. Therefore, it is prudent to use the existing resources and control strategies optimally to contain the virus spread and provide the best possible treatments to the infected individuals. Repurposing drugs and non-pharmaceutical intervention strategies may be the right way to fight against

the ongoing pandemic. This work aims to demonstrate through mathematical modelling and analysis how and to what extent such control strategies can improve the overall Covid-19 epidemic burden. For this, in **Chapter 5**, we have proposed a simplified but realistic epidemic model considering five disjoint classes through which a covid-infected individual has to be passed. We have also considered three control parameters to incorporate the effect of lockdown, maintaining personal hygiene & safe distancing, and using repurposing drugs. The criteria for disease elimination & persistence were established through the basic reproduction number. A case study with the Indian Covid-19 epidemic data is presented to visualize and illustrate the effects of lockdown, maintaining personal hygiene & safe distancing, and repurposing drugs. It is shown that India can significantly improve the overall Covid-19 epidemic burden through the combined use of NPIs and repurposing drugs. However, containment of spreading is difficult without serious community participation.

The thesis ends with the future direction.

2

Optimal control in a multi-pathways HIV-1 infection model: A comparison between mono-drug and multi-drug therapies[1]

2.1 The model

HIV-1 infection can be transmitted through cell-free mode, where a free plasma virus infects a susceptible $CD4^+$T cell, or through cell-to-cell transmission mode, where the infection spreads from one infected cell to another cell [97–99]. Basic HIV-1 within-host infection model considers only the cell-free transmission mode [78, 80, 81, 83–86, 89, 90, 92–96]). At the initial stage of infection or when antibody-mediated immune responses are less active or in the absence of antiviral drug therapy, spreading of infection mostly occurs through the cell-free mode [103]. On the other hand, cell-to-cell infection spreading occurs at the later stage of infection when the antibody-mediated immune responses are significantly strong or in the presence of antiviral drug therapy [104]. Different experimental observations support that cell-to-cell dissemination of infection may be more efficient than cell-free mode [101, 104–106]. So, to better understand the disease dynamics, both the dissemination modes of viral infection should be incorporated in the model formulation of HIV-1 infection.

If $x(t)$ be the density (number of cells per cubic millimeter) of uninfected $CD4^+$T cells in

[1] *The bulk of this chapter has been published in International Journal of Control, DOI:10.1080/00207179.2019.1690694, (2019).*

the blood plasma at an arbitrary time t then its demography can be represented by

$$\dot{x} = f_1(x),$$

where f_1 is a C^1 function such that $f_1(x) > 0$ for $0 < x < \tilde{x}$, $f_1(\tilde{x}) = 0$, $f_1^{'}(\tilde{x}) < 0$ and $f_1(x) < 0$ when $x > \tilde{x}$. If $y(t)$ and $v(t)$ be the concentrations of productively infected CD4$^+$T cells and virus particles in the peripheral blood at time t then the infection rate at time t through cell-free mode and cell-to-cell mode can be expressed by $f_2(x,v)$ and $f_3(x,y)$, respectively. If α is the lysis rate of infected cells, μ is the natural death rate of CD4$^+$T cells, c is the production rate of new virus particles per cell lysis and γ be the virus clearance rate, then the rate equations for $x,\ y$ and v can be represented by the following coupled nonlinear differential equations:

$$\begin{aligned} \dot{x} &= f_1(x) - f_2(x,v) - f_3(x,y), \\ \dot{y} &= f_2(x,v) + f_3(x,y) - (\alpha+\mu)y, \\ \dot{v} &= c\alpha y - \gamma v, \end{aligned} \tag{2.1}$$

where $f_2,\ f_3$ are C^1 functions.

Here we introduce three controls to the multi pathways HIV-1 infection model (2.1). One control $u_1(t)$ is introduced to reduce the transmission of infection through cell-free mode. This control is mainly reverse transcriptase inhibitors (RTIs). A second control $u_2(t)$ is introduced to block cell-to-cell infection that targets the factors required for synapse formation, a predominant mode of transmission of infection through cell-to-cell mode, under the assumption that such a drug exists. The third control $u_3(t)$ is applied to prevent HIV-1 protease from cleaving the HIV-1 polyprotein into functional units (PIs). With these three controls, the multi-pathways HIV-1 infection model (2.1) reads

$$\begin{aligned} \dot{x}(t) &= f_1(x) - (1-u_1(t))f_2(x,v) - (1-u_2(t))f_3(x,y), \\ \dot{y}(t) &= (1-u_1(t))f_2(x,v) + (1-u_2(t))f_3(x,y) - (\alpha+\mu)y(t), \\ \dot{v}(t) &= (1-u_3(t))c\alpha y(t) - \gamma v(t). \end{aligned} \tag{2.2}$$

A typical form of the function f_1 is $f_1(x) = s - \mu x$ [163, 164], where s is the constant input of CD4$^+$T cells from thymus, μ is its natural death rate. Sometimes additional proliferation of CD4$^+$T cells is considered due to antigenic infection and f_1 is represented as $f_1(x) = s - \mu x + rx(1-x/K)$, where r and K are, respectively, the proliferation rate of CD4$^+$T cells and its maximum attainable value [93, 94]. Here we consider the form $f_1 = s - \mu x$ because additional cell proliferation is unlikely to occur in presence of drug therapies. Different forms of incidence functions f_2 and f_3 have been considered in the literatures. For example, saturated infection rate of the form $f_2(x,v) = \frac{\beta_1 xv}{1+v}$ has been considered in [165] and [166] to prevent the unboundedness of the contact rate. On the other hand, [89] considered the saturation effect on x population as

$f_2(x,v) = \frac{\beta_1 xv}{a+x}$ and a generalized Hill-type function $f_2(x,v) = \frac{\beta_1 x^n v}{a^n+x^n}$ was considered in [130, 167, 168]. We here consider the frequently used mass action form for both the incidence functions f_2 and f_3. According to this law, the incidence or disease transmission functions have the forms $f_2(x,v) = \beta_1 xv$ [82, 87, 163, 164, 169–171] and $f_3(x,y) = \beta_2 xy$ [99, 131, 133, 172, 173], where β_1 and β_2 are, respectively, the cell-free and cell-to-cell transmission coefficients. Under these assumptions, also considering $f_1(x) = s - \mu x$, and the model (2.2) takes the form

$$\begin{aligned} \dot{x}(t) &= s - \mu x(t) - (1-u_1(t))\beta_1 x(t)v(t) - (1-u_2(t))\beta_2 x(t)y(t), \\ \dot{y}(t) &= (1-u_1(t))\beta_1 x(t)v(t) + (1-u_2(t))\beta_2 x(t)y(t) - (\alpha+\mu)y(t), \\ \dot{v}(t) &= (1-u_3(t))c\alpha y(t) - \gamma v(t). \end{aligned} \tag{2.3}$$

with initial conditions

$$x(0) = x_0 > 0,\ y(0) = y_0 \geq 0,\ v(0) = v_0 \geq 0. \tag{2.4}$$

All parameters are nonnegative. Table 2.1 describes the system parameters and their reported range. System (2.3) will be optimized with respect to the control parameters u_1, u_2 and u_3. To the best of our knowledge, no work has been done earlier by considering the effect of drug therapy in a multi-pathways HIV-1 infection model.

Table 2.1: Parameter description and their values with references.

Parameter	Description	Reported range	References	Default value
s	Constant production rate of CD4$^+$T cells	0-10 cells mm^{-3}	[93, 174]	10
μ	Death rate of susceptible CD4$^+$T cells	0.0014-0.03 day^{-1}	[175, 176]	0.01
β_1	Cell-free disease transmission coefficient	0.000025-0.5 mm^{-3} virion day^{-1}	[91, 93]	0.0001
β_2	Cell-to-cell disease transmission coefficient	0.00001-0.7 mm^{-3} infected cells day^{-1}	[99]	0.0003
α	Lysis death rate of infected CD4$^+$T cells	0.2-0.5 day^{-1}	[84, 91]	0.29
c	Virus production rate of infected CD4$^+$T cells	10-2500 virions cell^{-1}	[93, 174]	variable
γ	Removal rate of virus	2-3 day^{-1}	[82, 91, 175]	3

A large class of in-host HIV-1 infection models [92, 177] and the references therein) can be deduced from (2.3) for $u_1(t) = u_3(t) = 0$ and $\beta_2 = 0$. In fact, all basic target cell-limited models, where lack of CD4$^+$T cells is assumed to be responsible for the decrement of virus cell count after its initial blip, assume cell-free dissemination of infection via mass-action law.

The model (2.3) was analyzed by [131] when $u_1(t) = u_2(t) = u_3(t) = 0$ and $\mu = 0$. Effect of drug therapy when $\beta_2 = 0$ in model (2.3) was considered in [109]. This work is therefore a generalization of many previous works.

The rest of this chapter is arranged in the following sequence. In Section 2.2, we present some basic results. Section 2.3 is devoted to analyze the dynamics when controls are constant. We also perform here sensitivity analysis of system parameters. Some simulation results are also presented to validate the analytical findings. Section 2.4 deals with the optimal control of the system when controls are time dependent. We give the existence and uniqueness of the optimal control triplet. Extensive numerical computations of the model with time dependent controls are also presented. Comparison of different control schemes are presented here. The chapter ends with a discussion in Section 2.5.

2.2 Basic results

2.2.1 Positivity and boundedness of the solutions

Lemma 2.1 *For the initial condition (2.4), solutions of system (2.3) are positively invariant provided* $u_1(t) = 1$ *and* $u_2(t) = 1$ *do not hold simultaneously and* $u_3(t) \in [0,1)$. *Moreover, all solutions are uniformly bounded in* Γ, *where*

$$\Gamma = \left\{ (x(t), y(t), v(t)) \in \mathbb{R}^3_+ \mid 0 < x(t) \leq \tilde{x},\ 0 \leq y(t) \leq \frac{s}{\vartheta},\ 0 \leq v(t) \leq \frac{2c\alpha s}{(\alpha+\mu)\vartheta} \right\},$$

and $\vartheta = \min\left\{\mu, \frac{(\alpha+\mu)}{2}, \gamma\right\}$, $\tilde{x} = s/\mu$.

Proof First we show that $x(t)$ is positive $\forall\ t \geq 0$. If not, let $t_1 > 0$ be the first time when $x(t_1) = 0$. From (2.4), we have $x(t) > 0$ when $t = 0$. Therefore, $x(t) > 0$ for all $t \in [0, t_1)$. Putting $t = t_1$ in the first equation of (2.3), we get $\dot{x}(t_1) = s > 0$. It means that $x(t)$ is increasing at $t = t_1$. So there exists $\psi > 0$, sufficiently small, such that $\forall t \in (t_1 - \psi, t_1)$, $x(t) < 0$. This contradicts our assumption. Hence $x(t) > 0$ for all t and

$$x(t) = x_0 e^{-\int_0^t (\alpha+\mu)(\rho_1) d\rho_1} + \int_0^t s e^{-\int_{\rho_1}^t (\alpha+\mu)(\theta) d\theta} d\rho_1,$$

where $(\alpha+\mu)(t) = \mu + (1-u_1(t))\beta_1 v(t) + (1-u_2(t))\beta_2 y(t)$.

To show the positivity of $y(t)$ and $v(t)$ for all $t > 0$, we assume that there exists $t_2 > 0$ such that $\min\{y(t_2), v(t_2)\} = 0$ for the first time. If $y(t_2) = 0$, then $y(t) > 0$ for all $0 \leq t < t_2$, whereas $v(t) > 0$ for all $0 \leq t \leq t_2$. At $t = t_2$, we have $\dot{y}(t_2) = (1-u_1(t_2))\beta_1 x(t_2) v(t_2) > 0$ $\Rightarrow$ $y(t)$ is increasing at $t = t_2$. Following the positivity of $x(t)$, we again lead to a contradiction.

Therefore, $y(t) > 0$ for all t and

$$\begin{aligned} y(t) =& y_0 e^{-(\alpha+\mu)t} + \int_0^t [(1-u_1(\rho_2))\beta_1 x(\rho_2)v(\rho_2) \\ &+ (1-u_2(\rho_2))\beta_2 x(\rho_2)y(\rho_2)]e^{-(\alpha+\mu)(t-\rho_2)}d\rho_2. \end{aligned}$$

Following similar arguments, we can prove that $v(t) > 0$ for all t and

$$v(t) = v_0 e^{-\gamma t} + \int_0^t [(1-u_3(\rho_3))c\alpha y(\rho_3)e^{-\gamma(t-\rho_3)}d\rho_3.$$

Hence, all solutions of (2.3) are positively invariant.

Now we show that all solutions of (2.3) are bounded. From the first equation of (2.3), by standard comparison theorem [178], one gets

$$\dot{x}(t) \leq s - \mu x(t) \Rightarrow \lim_{t\to\infty} x(t) \leq \frac{s}{\mu} = \tilde{x}. \tag{2.5}$$

Thus, $x(t)$ is bounded for all $t \geq 0$.

Define

$$W(t) = x(t) + y(t) + \frac{(\alpha+\mu)}{2c\alpha}v(t).$$

Differentiating $W(t)$ along the solutions of (2.3), one obtains

$$\begin{aligned} \dot{W}(t) &= \dot{x}(t) + \dot{y}(t) + \frac{(\alpha+\mu)}{2c\alpha}\dot{v}(t) \\ &= s - \mu x(t) - (\alpha+\mu)y(t) + (1-u_3(t))\frac{(\alpha+\mu)}{2}y(t) - \frac{\gamma(\alpha+\mu)}{2c\alpha}v(t) \\ &\leq s - \mu x(t) - \frac{(\alpha+\mu)}{2}y(t) - \frac{\gamma(\alpha+\mu)}{2c\alpha}v(t) \leq s - \vartheta W(t), \end{aligned}$$

where $\vartheta = \min\left\{\mu, \frac{(\alpha+\mu)}{2}, \gamma\right\}$. Therefore, following a standard comparison theorem [178],

$$\lim_{t\to\infty} W(t) \leq \frac{s}{\vartheta}.$$

Hence, $\lim_{t\to\infty} y(t) \leq \frac{s}{\vartheta}$ and $\lim_{t\to\infty} v(t) \leq \frac{2c\alpha s}{(\alpha+\mu)\vartheta}$. Therefore, all solutions of (2.3) are uniformly bounded in $\Gamma = \Bigg\{(x(t), y(t), v(t)) \in \mathbb{R}^3_+ \mid 0 < x(t) \leq \tilde{x},\ 0 \leq y(t) \leq \frac{s}{\vartheta},$
$0 \leq v(t) \leq \frac{2c\alpha s}{(\alpha+\mu)\vartheta}\Bigg\}$.

2.3 Analysis of the model with fixed controls

Control parameters u_i, $i = 1,2,3$ may be constant or time dependent. We, therefore, analyze the model in two steps. Here we first consider that the control parameters are constant.

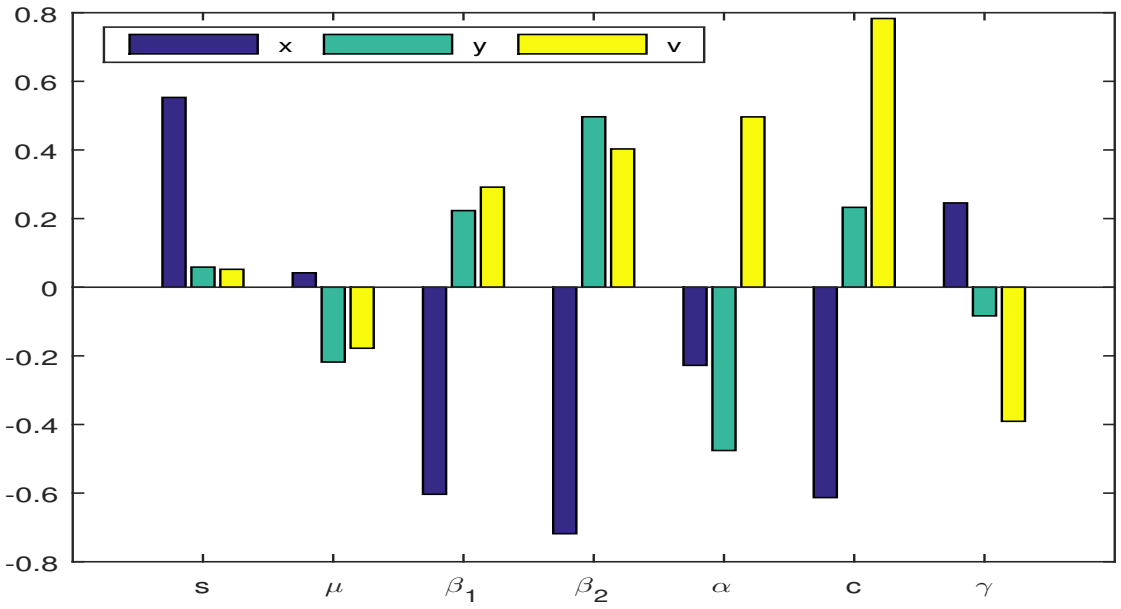

Figure 2.1: Latin Hypercube Sampling-Partial Ranked Correlation Coefficients sensitivity analysis for system (2.3) with $p < 0.00001$. Parameters are varied in their reported range (see Table 2.1 without control.

2.3.1 Sensitivity analysis of parameters

Parameters play an important role in model dynamics and some parameters may be very sensitive compare to other. We apply Latin Hypercube Sampling Method (LHS) [179] to find most sensitive parameters of our system, which are monotonically related to the system output. There are seven parameters in our model and these parameters are used for Partial Ranked Correlation Coefficients (PRCC) analysis (see Fig. 2.1). Length of the bar against a parameter shows its effect on the system. Fig. 2.1 indicates that the parameters c, β_2, β_1, α are most sensitive and have strong effects in the growth of system population with PRCCs significant to 0.00001 level (p-values < 0.00001). Among these parameters, c is the most sensitive parameter and we therefore analyze our system with respect to c.

2.3.2 Basic reproduction number

We first define two basic reproduction numbers corresponding to two modes of infection. This basic reproduction number plays significant role and considered to be an important threshold quantity for the elimination of infection. In the absence of infection, the equilibrium level of $CD4^+T$ cells is given by $\tilde{x} = \frac{s}{\mu}$. One can evaluate the basic reproduction number by calculating the next generation matrix [180]. The Jacobian matrix of the system (2.3) in absence of cell-to-cell transmission (when $\beta_2 = 0$) at $(\tilde{x}, 0, 0)$, where $\tilde{x} = \frac{s}{\mu}$ is the equilibrium density of healthy

$CD4^+T$ cells in absence of infection, is represented by

$$J_{11} = \begin{pmatrix} -\mu & 0 & -(1-u_1)\beta_1\tilde{x} \\ 0 & -(\alpha+\mu) & (1-u_1)\beta_1\tilde{x} \\ 0 & (1-u_3)c\alpha & -\gamma \end{pmatrix}.$$

The submatrix of J_{11} associated with the infectious compartments can be split as

$$\begin{aligned} J_{12} &= \begin{pmatrix} -(\alpha+\mu) & (1-u_1)\beta_1\tilde{x} \\ (1-u_3)c\alpha & -\gamma \end{pmatrix} = \begin{pmatrix} 0 & (1-u_1)\beta_1\tilde{x} \\ 0 & 0 \end{pmatrix} - \begin{pmatrix} (\alpha+\mu) & 0 \\ -(1-u_3)c\alpha & \gamma \end{pmatrix} \\ &= F_1 - V_1. \end{aligned}$$

The next generation matrix is then given by

$$F_1V_1^{-1} = \frac{1}{\gamma(\alpha+\mu)} \begin{pmatrix} (1-u_1)(1-u_3)c\alpha\beta_1\tilde{x} & (1-u_1)\beta_1\tilde{x}(\alpha+\mu) \\ 0 & 0 \end{pmatrix}.$$

The basic reproduction number for virus-to-cell transmission, R_{01}, is the spectral radius of the matrix $F_1V_1^{-1}$ [180] and is defined by

$$R_{01} = \frac{\beta_1(1-u_1)\tilde{x}c\alpha(1-u_3)}{(\alpha+\mu)\gamma}.$$

Note that $\beta_1(1-u_1)$ is the effective infection rate corresponding to cell-free infection mode; $\tilde{x}$ is the equilibrium value of $CD4^+T$ cells in the absence of all kinds of infection; $\frac{1}{(\alpha+\mu)}$ is the average life span of the infected $CD4^+T$ cells; $c\alpha(1-u_3)$ is the number of virus produced from the cell lysis of an infected cell and $\frac{1}{\gamma}$ is the average life span of virus. Therefore, the total number of newly infected $CD4^+T$ cells produced by one infected cell in its life period through cell-free infection mode is R_{01}.

Similarly, one can define the corresponding basic reproduction number for cell-to-cell infection mode by

$$R_{02} = \frac{\beta_2(1-u_2)\tilde{x}}{(\alpha+\mu)}.$$

The Jacobian matrix in the case of both modes of transmission evaluated at the infection-free equilibrium $\tilde{x} = (\frac{s}{\mu}, 0, 0)$ is

$$J_{21} = \begin{pmatrix} -\mu & -(1-u_2)\beta_2\tilde{x} & -(1-u_1)\beta_1\tilde{x} \\ 0 & (1-u_2)\beta_2\tilde{x} - (\alpha+\mu) & (1-u_1)\beta_1\tilde{x} \\ 0 & (1-u_3)c\alpha & -\gamma \end{pmatrix}. \tag{2.6}$$

The submatrix of J_{21} associated with the infectious compartments can be split as

$$J_{22} = \begin{pmatrix} (1-u_2)\beta_2\tilde{x} - (\alpha+\mu) & (1-u_1)\beta_1\tilde{x} \\ (1-u_3)c\alpha & -\gamma \end{pmatrix} = \begin{pmatrix} (1-u_2)\beta_2\tilde{x} & (1-u_1)\beta_1\tilde{x} \\ 0 & 0 \end{pmatrix} - \begin{pmatrix} (\alpha+\mu) & 0 \\ -(1-u_3)c\alpha & \gamma \end{pmatrix} = F - V.$$

The next generation matrix is then given by

$$FV^{-1} = \frac{1}{\gamma(\alpha+\mu)} \begin{pmatrix} [(1-u_2)\beta_2\gamma + (1-u_1)(1-u_3)c\alpha\beta_1]\tilde{x} & (1-u_1)\beta_1\tilde{x}(\alpha+\mu) \\ 0 & 0 \end{pmatrix}.$$

The ensemble basic reproductive number, R_0, is the spectral radius of FV^{-1} and is determined by

$$R_0 = \frac{[(1-u_2)\beta_2\gamma + (1-u_1)(1-u_3)c\alpha\beta_1]\tilde{x}}{\gamma(\alpha+\mu)} = R_{01} + R_{02}.$$

Thus, the basic reproduction number of the system is the sum of the basic reproduction number of two modes of infection process.

2.3.3 Existence and stability of the equilibria

Equilibrium points are the biologically feasible solutions of the following simultaneous equations:

$$\begin{aligned} s - \mu x(t) - (1-u_1)\beta_1 x(t)v(t) - (1-u_2)\beta_2 x(t)y(t) &= 0, \\ (1-u_1)\beta_1 x(t)v(t) + (1-u_2)\beta_2 x(t)y(t) - (\alpha+\mu)y(t) &= 0, \\ (1-u_3)c\alpha y(t) - \gamma v(t) &= 0. \end{aligned}$$

The equilibrium density $\tilde{x}$ of the infection-free equilibrium $E_1(\tilde{x},0,0)$ is determined to be $\tilde{x} = \frac{s}{\mu}$. Note that it always exists. The infected equilibrium E^* is (x^*, y^*, v^*), where $x^* = \frac{\tilde{x}}{R_0}$, $y^* = \frac{\mu x^*}{(\alpha+\mu)}(R_0 - 1)$ and $v^* = \frac{(1-u_3)c\alpha y^*}{\gamma}$. This equilibrium exists if $R_0 > 1$, $u_1 = u_2 = 1$ do not hold simultaneously and $u_3 \in [0,1)$. Because, if $u_1 = u_2 = 1$ then $y(t) \to 0$ as $t \to \infty$; and if $u_3 = 1$ then $v(t) \to 0$ as $t \to \infty$. In both the cases, E^* does not exist. Note that

$$\begin{aligned} R_0 > 1 &\rightleftharpoons [(1-u_2)\beta_2\gamma + (1-u_1)(1-u_3)c\alpha\beta_1]\tilde{x} > \gamma(\alpha+\mu) \\ &\rightleftharpoons (1-u_1)(1-u_3)c\alpha\beta_1\tilde{x} > \gamma[(\alpha+\mu) - (1-u_2)\beta_2\tilde{x}] \\ &\rightleftharpoons c > \frac{\gamma[(\alpha+\mu) - (1-u_2)\beta_2\tilde{x}]}{(1-u_1)(1-u_3)\alpha\beta_1\tilde{x}} = c^*, \end{aligned} \tag{2.7}$$

where c^* is the critical value of c at $R_0 = 1$. Therefore, all populations exist when $c > c^*$, $u_1 = 1$ & $u_2 = 1$ do not hold simultaneously and $u_3 \in [0,1)$. We then have the following lemma.

Lemma 2.2 *The system (2.3) has two equilibrium points.*

(I) The infection-free equilibrium $E_1 = (\tilde{x}, 0, 0)$ *always exists with* $\tilde{x} = \frac{s}{\mu}$.

(II) The infected equilibrium $E^* = (x^*, y^*, v^*)$ *exists when*

(i) $c > c^*$,
(ii) $u_1 = 1$ *and* $u_2 = 1$ *does not hold simultaneously, and*
(iii) $u_3 \in [0,1)$,

with equilibrium densities $x^* = \frac{\tilde{x}}{R_0}$, $y^* = \frac{\mu x^*}{(\alpha+\mu)}(R_0 - 1)$, $v^* = \frac{(1-u_3)c\alpha y^*}{\gamma}$.

We now prove the stability of two equilibrium points with respect to the virus replication factor c.

Theorem 2.3 *The infection-free steady state* E_1 *is locally and globally asymptotically stable if* $c < c^*$.

Proof The variational matrix at E_1 reads as

$$V(E_1) = \begin{pmatrix} m_{11} & m_{12} & m_{13} \\ 0 & m_{22} & m_{23} \\ 0 & m_{32} & m_{33} \end{pmatrix},$$

where $m_{11} = -\mu$, $m_{12} = -(1-u_2)\beta_2\tilde{x}$, $m_{13} = -(1-u_1)\beta_1\tilde{x}$, $m_{22} = (1-u_2)\beta_2\tilde{x} - (\alpha + \mu)$, $m_{23} = (1-u_1)\beta_1\tilde{x}$, $m_{32} = (1-u_3)c\alpha$, $m_{33} = -\gamma$. It is to be recalled that $V(E_1)$ is the matrix described in (2.6).
The characteristic equation associated with this matrix is

$$(\xi - m_{11})[\xi^2 - (m_{22} + m_{33})\xi + (m_{22}m_{33} - m_{23}m_{32})] = 0. \tag{2.8}$$

Clearly, one characteristic root is $\xi_1 = m_{11} = -\mu(< 0)$. Other two roots will have negative real parts if and only if $(m_{22} + m_{33})$ is negative and $(m_{22}m_{33} - m_{23}m_{32})$ is positive. Observe that $m_{22} + m_{33} = (1-u_2)\beta_2\tilde{x} - (\alpha+\mu) - \gamma$. Following (2.7),

$$\begin{aligned} c < c^* &\Rightarrow \frac{(1-u_1)(1-u_3)c\alpha\beta_1\tilde{x}}{\gamma} < (\alpha+\mu) - (1-u_2)\beta_2\tilde{x} \\ &\Rightarrow (1-u_2)\beta_2\tilde{x} - \gamma - (\alpha+\mu) < -\left[\frac{(1-u_1)(1-u_3)c\alpha\beta_1\tilde{x}}{\gamma} + \gamma\right] < 0. \end{aligned}$$

This proves that $m_{22}+m_{33}<0$ if $c<c^*$. Moreover,

$$\begin{aligned} m_{22}m_{33}-m_{23}m_{32} &= (\alpha+\mu)\gamma-\tilde{x}[(1-u_1)(1-u_3)c\alpha\beta_1+(1-u_2)\beta_2\gamma] \\ &= (1-u_1)(1-u_3)\alpha\beta_1\tilde{x}[c^*-c]. \end{aligned}$$

This shows that $m_{22}m_{33}-m_{23}m_{32}>0$ if and only if $c<c^*$. Thus, all roots of Eqn. (2.8) will have negative real parts if $R_0<1$, implying that the infection-free equilibrium E_1 is locally asymptotically stable. It is to be noted that if E_1 is locally asymptotically stable then E^* fails to exist.

To prove the global stability, we define a Lyapunov function as

$$U_1(t)=x(t)-\tilde{x}-\tilde{x}\ln\left(\frac{x(t)}{\tilde{x}}\right)+y(t)+\frac{\tilde{x}\beta_1(1-u_1)}{\gamma}v(t).$$

So, $U_1(t)>0$ for all positive values of $x(t),\ y(t),\ v(t)$, and $U_1(t)=0$ only at E_1. Differentiating $U_1(t)$ along the solutions of (2.3), and using $s=\mu\tilde{x}$, we have

$$\begin{aligned} \dot{U}_1(t) &= \left(1-\frac{\tilde{x}}{x(t)}\right)\dot{x}(t)+\dot{y}(t)+\frac{\tilde{x}\beta_1(1-u_1)}{\gamma}\dot{v}(t) \\ &= \left(1-\frac{\tilde{x}}{x(t)}\right)[s-\mu x(t)-(1-u_1)\beta_1x(t)v(t)-(1-u_2)\beta_2x(t)y(t)] \\ &\quad +[(1-u_1)\beta_1x(t)v(t)+(1-u_2)\beta_2x(t)y(t)-(\alpha+\mu)y(t)] \\ &\quad +\frac{\tilde{x}\beta_1(1-u_1)}{\gamma}[(1-u_3)c\alpha y(t)-\gamma v(t)] \\ &= \mu\ \tilde{x}\ \left(2-\frac{\tilde{x}}{x(t)}-\frac{x(t)}{\tilde{x}}\right)-\frac{(1-u_1)(1-u_3)\alpha\beta_1\tilde{x}y(t)}{\gamma}\ [c^*-c]. \end{aligned}$$

As A.M (Arithmetic mean) $\geq$ G.M (Geometric mean), we get $\dot{U}_1(t)\leq 0$ if $c<c^*$. Let $G_1=\{(x(t),y(t),v(t))\in\mathbb{R}^3_+:\ \dot{U}_1=0\}$ and S_1 be the largest invariant set in G_1. Then by LaSalle's invariance principle [65], all non-negative solutions converge to S_1. Moreover, $\dot{U}_1=0$ if and only if $x(t)=\tilde{x}$ and $y(t)=0$. Therefore, invariance of S_1 yields $S_1=\{E_1\}$ and every solution in Γ tends to E_1 when $c<c^*$. Thus, E_1 is globally asymptotically stable if $c<c^*$.

Theorem 2.4 *The infected steady state E^* is locally and globally asymptotically stable whenever it exists.*

Proof The variational matrix at E^* is computed as

$$V(E^*)=\begin{pmatrix} n_{11} & n_{12} & n_{13} \\ n_{21} & n_{22} & n_{23} \\ 0 & n_{32} & n_{33} \end{pmatrix},$$

where

$$\begin{aligned} &n_{11} = -\mu - (1-u_1)\beta_1 v^* - (1-u_2)\beta_2 y^* = -\tfrac{s}{x^*},\ n_{12} = -(1-u_2)\beta_2 x^*,\\ &n_{13} = -(1-u_1)\beta_1 x^*,\ n_{21} = (1-u_1)\beta_1 v^* + (1-u_2)\beta_2 y^* = \tfrac{(\alpha+\mu)y^*}{x^*},\\ &n_{22} = (1-u_2)\beta_2 x^* - (\alpha+\mu) = -\tfrac{(1-u_1)\beta_1 x^* v^*}{y^*},\ n_{23} = (1-u_1)\beta_1 x^*,\\ &n_{32} = (1-u_3)c\alpha,\ n_{33} = -\gamma. \end{aligned} \tag{2.9}$$

The characteristic equation is given by

$$\xi^3 + X_1\xi^2 + X_2\xi + X_3 = 0,$$

where

$$\begin{aligned} X_1 &= -(n_{11}+n_{22}+n_{33}),\\ X_2 &= n_{11}(n_{22}+n_{33}) + (n_{22}n_{33} - n_{23}n_{32}) - n_{12}n_{21},\\ X_3 &= -[n_{11}(n_{22}n_{33} - n_{23}n_{32}) - n_{12}n_{21}n_{33} + n_{13}n_{21}n_{32}]. \end{aligned}$$

Noting that $n_{22}n_{33} - n_{23}n_{32} = (\alpha+\mu)\gamma - [(1-u_1)(1-u_3)c\alpha\beta_1 + (1-u_2)\beta_2\gamma]x^* = (\alpha+\mu)\gamma - (\alpha+\mu)\gamma = 0$, the quantities X_2 and X_3 simplifies to $X_2 = n_{11}(n_{22}+n_{33}) - n_{12}n_{21}$, $X_3 = n_{12}n_{21}n_{33} - n_{13}n_{21}n_{32}$. According to Routh-Hurwitz criteria, E^* will be locally asymptotically stable if and only if $X_1 > 0$, $X_3 > 0$ and $X_1X_2 - X_3 > 0$. From (2.9), one can easily see that $X_1 > 0$ and $X_3 > 0$. Simple computation gives

$$\begin{aligned} X_1X_2 - X_3 = \ &(-n_{11}^2 n_{22} - n_{11}^2 n_{33} - n_{22}^2 n_{11} - n_{33}^2 n_{11} + n_{11}n_{12}n_{21} + n_{22}n_{12}n_{21}\\ &- n_{11}n_{22}n_{33}) + [n_{13}n_{21}n_{32} - n_{11}n_{22}n_{33}]. \end{aligned} \tag{2.10}$$

One can easily verify that all terms of (2.10) in the first bracket are positive. Also,

$$\begin{aligned} n_{13}n_{21}n_{32} - n_{11}n_{22}n_{33} &= -(1-u_1)(1-u_3)\beta_1 c\alpha(\alpha+\mu)y^*\\ &\quad - \left(s(1-u_2)\beta_2 - \frac{s(\alpha+\mu)}{x^*}\right)\gamma\\ &= \frac{s(\alpha+\mu)\gamma}{x^*} - s(1-u_2)\beta_2\gamma\\ &\quad - (1-u_1)(1-u_3)\beta_1 c\alpha(\alpha+\mu)\left(\frac{s-\mu x^*}{(\alpha+\mu)}\right)\\ &= \frac{s(\alpha+\mu)\gamma}{x^*} - s[(1-u_2)\beta_2\gamma + (1-u_1)(1-u_3)\beta_1 c\alpha]\\ &\quad + (1-u_1)(1-u_3)\beta_1 c\alpha\mu x^* = (1-u_1)(1-u_3)\beta_1 c\alpha\mu x^* (> 0). \end{aligned}$$

Thus, following Routh-Hurwitz criterion, E^* is locally asymptotically stable whenever it exists.

For global stability, Lyapunov function is defined as

$$U_2(t) = \int_{x^*}^{x} \left(1 - \frac{x^*}{x(t)}\right) dx + \int_{y^*}^{y} \left(1 - \frac{y^*}{y(t)}\right) dy + \frac{\beta_1(1-u_1)x^*}{\gamma} \int_{v^*}^{v} \left(1 - \frac{v^*}{v(t)}\right) dv.$$

Note that $U_2(t) > 0$ for all positive values of $x(t),\ y(t),\ v(t)$ and $U_2(t) = 0$ only when $x = x^*, y = y^*, v = v^*$. The derivative of $U_2(t)$ along the solutions of (2.3) is

$$\begin{aligned}\dot{U}_2(t) &= \left(1 - \frac{x^*}{x(t)}\right)\dot{x}(t) + \left(1 - \frac{y^*}{y(t)}\right)\dot{y}(t) + \frac{\beta_1(1-u_1)x^*}{\gamma}\left(1 - \frac{v^*}{v(t)}\right)\dot{v}(t),\\ &= W_1(t) + W_2(t) + W_3(t).\end{aligned}$$

Define $N(x(t)) = s - \mu x(t)$. Then

$$\begin{aligned}W_1(t) &= \left(1 - \frac{x^*}{x(t)}\right)\dot{x}(t)\\ &= \left(1 - \frac{x^*}{x(t)}\right)[N(x(t)) - \beta_1(1-u_1)x(t)v(t) - \beta_2(1-u_2)x(t)y(t)]\\ &= \left(1 - \frac{x^*}{x(t)}\right)[N(x(t)) - N(x^*)] + \left(1 - \frac{x^*}{x(t)}\right)N(x^*) - x(t)[\beta_1(1-u_1)v(t)\\ &\quad + \beta_2(1-u_2)y(t)] + x^*[\beta_1(1-u_1)v(t) + \beta_2(1-u_2)y(t)]\\ &= \left(1 - \frac{x^*}{x(t)}\right)[N(x(t)) - N(x^*)] + x^*[\beta_1(1-u_1)v^* + \beta_2(1-u_2)y^*]\\ &\quad - \frac{x^{*2}}{x(t)}[\beta_1(1-u_1)v^* + \beta_2(1-u_2)y^*] - x(t)[\beta_1(1-u_1)v(t)\\ &\quad + \beta_2(1-u_2)y(t)] + x^*[\beta_1(1-u_1)v(t) + \beta_2(1-u_2)y(t)],\end{aligned}$$

$$\begin{aligned}W_2(t) &= \left(1 - \frac{y^*}{y(t)}\right)\dot{y}(t)\\ &= \left(1 - \frac{y^*}{y(t)}\right)[\beta_1(1-u_1)x(t)v(t) + \beta_2(1-u_2)x(t)y(t) - (\alpha+\mu)y(t)]\\ &= (1-u_1)\beta_1 x(t)v(t) + (1-u_2)\beta_2 x(t)y(t) - (\alpha+\mu)y(t)\\ &\quad - \beta_1(1-u_1)\frac{x(t)v(t)y^*}{y(t)} - (1-u_2)\beta_2 x(t)y^* + \beta_1(1-u_1)x^*v^* + \beta_2(1-u_2)x^*y^*,\end{aligned}$$

$$\begin{aligned}
W_3(t) =& \frac{\beta_1(1-u_1)x^*}{\gamma}\left(1-\frac{v^*}{v(t)}\right)\dot{v}(t)\\
=& \frac{\beta_1(1-u_1)x^*}{\gamma}\left(1-\frac{v^*}{v(t)}\right)[(1-u_3)c\alpha y(t)-\gamma v(t)]\\
=& \frac{\beta_1(1-u_1)(1-u_3)c\alpha x^* y(t)}{\gamma} - \frac{\beta_1(1-u_1)(1-u_3)c\alpha x^* y(t)v^*}{\gamma v(t)}\\
&+\beta_1(1-u_1)v^*x^* - \beta_1(1-u_1)v(t)x^*\\
=& \beta_1(1-u_1)v^*x^* - \beta_1(1-u_1)v(t)x^* - (1-u_2)\beta_2 x^* y(t)\\
&-[\beta_1(1-u_1)x^*v^*]\frac{c\alpha(1-u_3)y(t)}{\gamma v(t)} + (\alpha+\mu)y(t)\\
=& \beta_1(1-u_1)v^*x^* - \beta_1(1-u_1)v(t)x^* - (1-u_2)\beta_2 x^* y(t)\\
&-(1-u_1)\beta_1\frac{x^*v^{*2}y(t)}{v(t)y^*} + (\alpha+\mu)y(t).
\end{aligned}$$

Summing up, we have

$$\begin{aligned}
\dot{U}_2(t) =& \left(1-\frac{x^*}{x(t)}\right)[N(x(t))-N(x^*)] + \beta_2(1-u_2)\left(2-\frac{x^*}{x(t)}-\frac{x(t)}{x^*}\right)x^*y^*\\
&+\beta_1(1-u_1)x^*v^*\left(3-\frac{x^*}{x(t)}-\frac{x(t)v(t)y^*}{x^*v^*y(t)}-\frac{y(t)v^*}{y^*v(t)}\right).
\end{aligned}$$

Observe that $\left(1-\frac{x^*}{x(t)}\right)[N(x(t))-N(x^*)] = -\frac{\mu\ (x(t)-x^*)^2}{x(t)} < 0$ and $\left(2-\frac{x^*}{x(t)}-\frac{x(t)}{x^*}\right) < 0$ and $\left(3-\frac{x^*}{x(t)}-\frac{x(t)v(t)y^*}{x^*v^*y(t)}-\frac{y(t)v^*}{y^*v(t)}\right) < 0$ follows readily from the inequality A.M $\geq$ G.M. Therefore, $\dot{U}_2(t) \leq 0$. Let $G_2 = \{(x(t),y(t),v(t)) \in \mathbb{R}^3_+ : \dot{U}_2(t) = 0\}$ and S_2 be the largest invariant set in G_2. Then by LaSalle's invariance principle [65], all non-negative solutions converge to S_2. Moreover, $\dot{U}_2(t) = 0$ if and only if $x(t) = x^*$ and $y(t)v^* = y^*v(t)$. Therefore, invariance of S_2 yields $S_2 = \{(x(t),y(t),v(t)) \in \mathbb{R}^3_+ : x = x^*, y(t)v^* = y^*v(t)\}$. Now any such point of S_2 must satisfy $\dot{x}(t) = 0 \ \Rightarrow [s-\mu x^*] - \frac{x^*v(t)}{v^*}(\beta_1(1-u_1)v^* + \beta_2(1-u_2)y^*) = (s-\mu x^*)\left(1-\frac{v(t)}{v^*}\right) = 0 \Rightarrow v(t) = v^*$. This gives $y(t) = y^*$ and $S_2 = \{E^*\}$. Thus the largest invariant set in G_2 is $\{E^*\}$ and E^* is globally asymptotically stable. This completes the proof.

Remark 2.5 *We have proved the stability of the two equilibrium points E_1 and E^* with respect to the virus replication factor c, which measures the number of new virus produced by a single infected CD4$^+$T cell due to lysis. Thus, for the existence and stability of the interior equilibrium E^*, the production of new virus due to cell lysis must exceed some lower threshold value c^*, otherwise the system will be stable with respect to infection-free equilibrium.*

2.3.4 Numerical simulations

Here we present simulation results to substantiate our analytical findings considering the parameter values of Table 2.1 . We fix the values of control parameters as $u_1 = u_2 = u_3 = 0.5$. In vitro experiments claim that cell-to-cell dissemination of infection may be 100 times higher

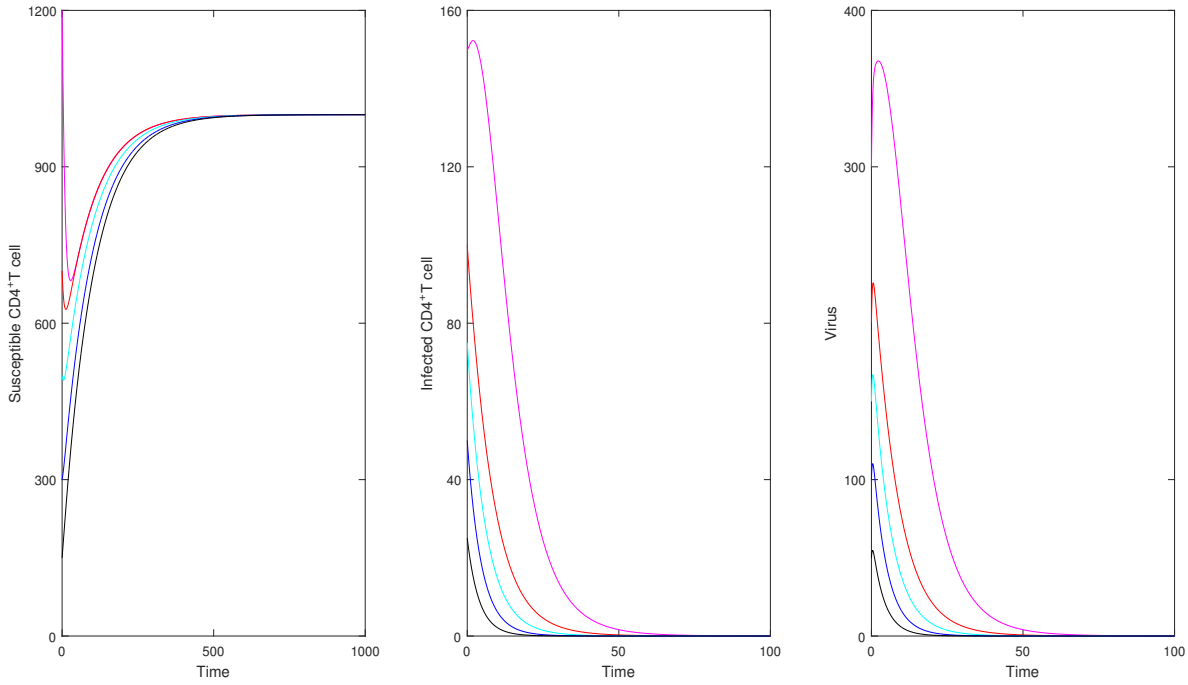

Figure 2.2: Time evolution of system (2.3) with fixed controls and different initial points. Here $u_1 = u_2 = u_3 = 0.5$, $c = 50$ and other parameters are as in the Table 2.1. These figures show that the disease-free equilibrium is globally asymptotically stable.

than that of the cell-free mode [101, 104, 105]. We, however, consider β_2 is only three times higher than β_1. For these parameter values, the critical value of c is computed as $c^* = 62.069$. For $c = 50$ $(< c^*)$, we note that $R_0 = 0.9028$ (< 1) and the infection-free equilibrium E_1 becomes globally asymptotically stable (Fig.2.2), following Theorem 2.3. On the other hand, following Theorem 2.4, E^* is globally asymptotically stable (Fig.2.3) for $c = 75 > c^*$, where $R_0 = 1.1042$ (> 1).

In Fig. 2.4, we represent the contour plot of the basic reproduction number R_0 as a function of two controls u_1 and u_3 for different fixed values of the third control u_2. The area below each curve represents the stability region of E^*, while the area above each curve represents the stability region of E_1 for some given value of u_2. Fig. 2.4 shows that any non-zero value of u_2 may remove infection by using suitable control regimens of u_1 and u_3. For example, if we select $u_1 = 0.5$ and $u_2 = 0.4$ then to remove infection, value of the other control u_3 should be more than 0.669.

2.4 Analysis of the model with time-dependent controls

In the previous section, we have presented analysis of multi-pathways HIV-1 infection model with constant controls. The study will be more worthy if the controls are considered to be

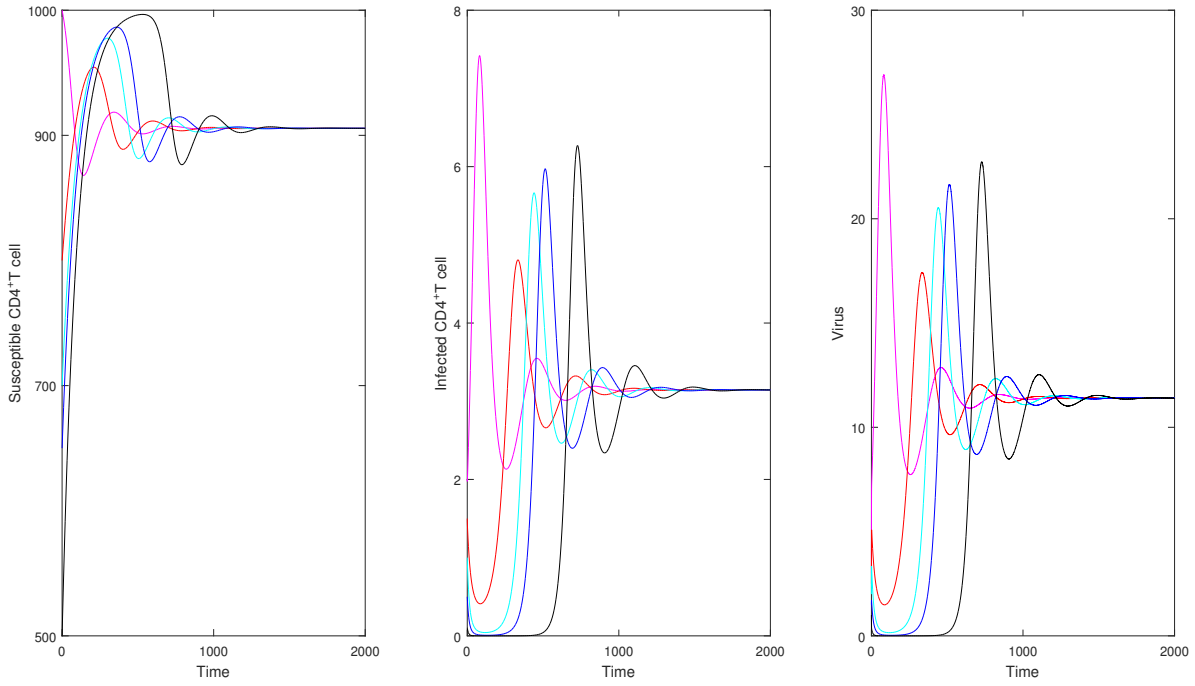

Figure 2.3: Solutions starting with different initial values converge to the infected equilibrium E^*, indicating its global stability. Here $c = 75$ and other parameters are as in Fig. 2.2.

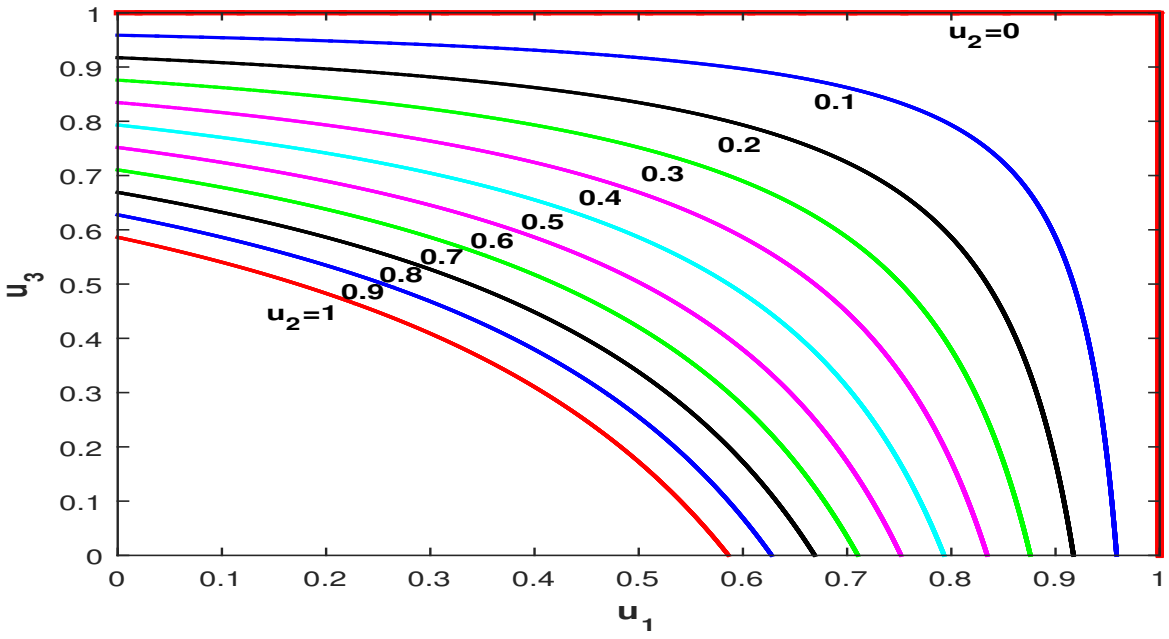

Figure 2.4: Contour plot of R_0 as a function of two controls u_1 and u_3 for different fixed values of u_2. Parameters are as in Table 2.1 with $c = 75$.

time-dependent. We assume here that all three controls vary with time. We also consider the cost of antiretroviral drugs and their side effects. $CD4^+T$ cells count decreases as the HIV-1 infection progresses. We, therefore, seek to maximize the number of uninfected $CD4^+T$ cells through controls and at the same time minimize the number of infected $CD4^+T$ cells because cell-to-cell infection increases with the number of infected cells. Also, the number of cell-free virus (released by bursting of infected cell) increases with the number of infected cells, thereby increasing the cell-free infection.

We define our objective functional subject to the state equations (2.3) as

$$J(u_1,u_2,u_3)=\int_0^{t_f}[K_1x(t)-\{K_2y(t)+A_1u_1^2(t)+A_2u_2^2(t)+A_3u_3^2(t)\}]\,dt. \tag{2.11}$$

The first term on the right side of (2.11) represents the benefit of susceptible $CD4^+T$ cells and other terms contributes deleterious effects. For instance, the second term signifies the harmful effect of infected $CD4^+T$ cells. It is well known that the antiretroviral drugs have significant side effects. This deleterious effects of drugs are reflected by u_1^2, u_2^2 and u_3^2. Here K_1, K_2 are the weight constants associated with susceptible and infected $CD4^+T$ cells [181]. A_1, A_2, A_3 are positive weight constants used to balance the size of the terms [88, 112, 182, 183]. Our target is to find the optimal treatment regimens that maximizes the healthy $CD4^+T$ cells, minimizes the infected $CD4^+T$ cells and deleterious effect of three inhibitory drugs. Thus our objective is to find a triplet of optimal controls $(\hat{u}_1,\hat{u}_2,\hat{u}_3)$ such that

$$J(\hat{u}_1,\hat{u}_2,\hat{u}_3)=\max_{(u_1,u_2,u_3)\in\Omega} J(u_1,u_2,u_3),$$

where $\Omega=\{(u_1(t),u_2(t),u_3(t)) : u_i(t), i=1,2,3,$ is measurable and $0\le u_i(t)\le 1,\ \forall t\in[0,t_f]\}$ is the control set and t_f is the final time where control stops.

2.4.1 Existence of an optimal control triplet

Theorem 2.6 *There exists an optimal control triplet $(\hat{u}_1,\hat{u}_2,\hat{u}_3)$ in Ω associated with the time-dependent control problem (2.3) that maximizes the objective functional $J(u_1,u_2,u_3)$.*

Proof To prove this theorem, we use an existence result from [71]. To apply this result, one has to satisfy the following hypothesis:

(H_1) The set of controls and the corresponding state variables is nonempty.

(H_2) The control set Ω is convex and closed.

(H_3) The right hand side of the state system is continuous, bounded above by a sum of the bounded control and state, and can be written as a linear function of u_i with coefficients depending on the state and time.

(H_4) The integrand of the objective functional is concave on Ω.

(H_5) There exist constants $C_1,\ C_2 > 0$ and $B > 1$ such that the integrand of the objective functional is bounded above by $C_2 - C_1(|u_1(t)|^2 + |u_2(t)|^2 + |u_3(t)|^2)^{B/2}$.

Following [184], (H_1) is satisfied for the control system (2.3) for bounded coefficients. (H_2) holds readily from the definition of the control set Ω. As the controlled system is linear in $u_1,\ u_2$ and u_3, the right hand side of (2.3) satisfies (H_3) as the solutions are bounded. The integrand of the objective functional is concave on the admissible control set Ω. Hence (H_4) is satisfied. Again,

$$\begin{aligned} &K_1x(t) - [K_2y(t) + A_1u_1^2(t) + A_2u_2^2(t) + A_3u_3^2(t)] \\ &\leq K_1x(t) - [A_1u_1^2(t) + A_2u_2^2(t) + A_3u_3^2(t)] \\ &\leq C_2 - C_1(|u_1(t)|^2 + |u_2(t)|^2 + |u_3(t)|^2)^{B/2}, \end{aligned}$$

where C_2 depends on the upper bound of $x(t)$ given in (2.5), $B > 1$ and $C_1 > 0$ as $A_1,\ A_2,\ A_3 > 0$. Summing up all these results, we conclude that there exists an optimal control triplate. Hence the theorem.

2.4.2 Optimality system

To derive the necessary conditions for the optimal control triplet $(\hat{u}_1, \hat{u}_2, \hat{u}_3)$, we use Pontryagin's Maximum principle [185]. We first define the Lagrangian of the optimal control problem (2.11) subject to the system of differential equations (2.3) as follows:

$$L = K_1x(t) - [K_2y(t) + A_1u_1^2(t) + A_2u_2^2(t) + A_3u_3^2(t)].$$

To maximize the Lagrangian, we construct the Hamiltonian

$$\begin{aligned} H(x,y,v;u_1,u_2,u_3;\lambda_1,\lambda_2,\lambda_3) =\ & L + \lambda_1(t)\dot{x} + \lambda_2(t)\dot{y} + \lambda_3(t)\dot{v} \\ =\ & \Big(K_1x(t) - [K_2y(t) + A_1u_1^2(t) + A_2u_2^2(t) + A_3u_3^2(t)]\Big) \\ & + \lambda_1(t)\Big(s - \mu x(t) - (1-u_1(t))\beta_1x(t)v(t) - (1-u_2(t))\beta_2x(t)y(t)\Big) \\ & + \lambda_2(t)\Big((1-u_1(t))\beta_1x(t)v(t) + (1-u_2(t))\beta_2x(t)y(t) - (\alpha+\mu)y(t)\Big) \\ & + \lambda_3(t)\Big((1-u_3(t))c\alpha y(t) - \gamma v(t)\Big), \end{aligned}$$

where λ_i $(i = 1,2,3)$ are co-state or adjoint variables satisfies the following canonical equations:

$$\dot{\lambda_1}(t) = -\frac{\partial H}{\partial x},\ \dot{\lambda_2}(t) = -\frac{\partial H}{\partial y},\ \dot{\lambda_3}(t) = -\frac{\partial H}{\partial v}.$$

Following Pontryagin's Maximum principle [185], we have the following theorem.

Theorem 2.7 *If $\hat{u}_1, \hat{u}_2, \hat{u}_3$ are optimal controls of (2.11) subject to the system of differential equations (2.3) and $\hat{x}$, $\hat{y}$, $\hat{v}$ are the corresponding optimal state variables, then there exists co-state or adjoint variables λ_i $(i = 1,2,3)$ such that the following conditions are satisfied along with the control system (2.3):*
***(i)** Co-state equations:*

$$\begin{aligned}
\dot{\lambda_1}(t) &= \lambda_1(t)\Big[\mu + (1-u_1(t))\beta_1 v(t) + (1-u_2(t))\beta_2 y(t)\Big] \\
&\quad - \lambda_2(t)\Big[(1-u_1(t))\beta_1 v(t) + (1-u_2(t))\beta_2 y(t)\Big] - K_1, \\
\dot{\lambda_2}(t) &= \lambda_1(t)\Big[(1-u_2(t))\beta_2 x(t)\Big] - \lambda_2(t)\Big[(1-u_2(t))\beta_2 x(t) - (\alpha+\mu)\Big] \\
&\quad - \lambda_3(t)\Big[1-u_3(t)\Big]c\alpha + K_2, \\
\dot{\lambda_3}(t) &= \lambda_1(t)\Big[(1-u_1(t))\beta_1 x(t)\Big] - \lambda_2(t)\Big[(1-u_1(t))\beta_1 x(t)\Big] + \gamma\lambda_3(t);
\end{aligned} \tag{2.12}$$

***(ii)** Optimality conditions:*

$$H(\hat{x},\hat{y},\hat{v};\hat{u}_1,\hat{u}_2,\hat{u}_3;\lambda_1,\lambda_2,\lambda_3) = \max_{0\le u_i\le 1\ ,\ i=1,2,3} H(\hat{x},\hat{y},\hat{v};u_1,u_2,u_3;\lambda_1,\lambda_2,\lambda_3),$$

which implies

$$\begin{aligned}
\frac{\partial H}{\partial u_1}\Big|_{u_1=\hat{u}_1} = 0 \Rightarrow \hat{u}_1 &= \frac{(\lambda_1-\lambda_2)\beta_1\hat{x}\hat{v}}{2A_1}, \\
\frac{\partial H}{\partial u_2}\Big|_{u_2=\hat{u}_2} = 0 \Rightarrow \hat{u}_2 &= \frac{(\lambda_1-\lambda_2)\beta_2\hat{x}\hat{y}}{2A_2}, \\
\frac{\partial H}{\partial u_3}\Big|_{u_3=\hat{u}_3} = 0 \Rightarrow \hat{u}_3 &= \frac{-\lambda_3 c\alpha\hat{y}}{2A_3};
\end{aligned} \tag{2.13}$$

***(iii)** Transversality conditions:*

$$\lambda_i(t_f) = 0,\ i = 1,2,3. \tag{2.14}$$

The optimal system consists of the control system (2.3) coupled with the co-state equations given by (2.12) with initial conditions (2.4) and transversality conditions (2.14) together with the optimal control triplet given by (2.13).

Hence we obtain the following optimal system:

$$
\begin{cases}
\dot{x}(t) = s - \mu x(t) - (1-u_1(t))\beta_1 x(t)v(t) - (1-u_2(t))\beta_2 x(t)y(t),\\
\dot{y}(t) = (1-u_1(t))\beta_1 x(t)v(t) + (1-u_2(t))\beta_2 x(t)y(t) - (\alpha+\mu)y(t),\\
\dot{v}(t) = (1-u_3(t))c\alpha y(t) - \gamma v(t),\\
\\
\dot{\lambda_1}(t) = \lambda_1(t)\Big[\mu + (1-u_1(t))\beta_1 v(t) + (1-u_2(t))\beta_2 y(t)\Big]\\
\qquad - \lambda_2(t)\Big[(1-u_1(t))\beta_1 v(t) + (1-u_2(t))\beta_2 y(t)\Big] - K_1,\\
\dot{\lambda_2}(t) = \lambda_1(t)\Big[(1-u_2(t))\beta_2 x(t)\Big] - \lambda_2(t)\Big[(1-u_2(t))\beta_2 x(t) - (\alpha+\mu)\Big]\\
\qquad - \lambda_3(t)\Big[1-u_3(t)\Big]c\alpha + K_2,\\
\dot{\lambda_3}(t) = \lambda_1(t)\Big[(1-u_1(t))\beta_1 x(t)\Big] - \lambda_2(t)\Big[(1-u_1(t))\beta_1 x(t)\Big] + \gamma\lambda_3(t),\\
\\
x(0) = x_0 > 0,\ y(0) = y_0 \geq 0,\ v(0) = v_0 \geq 0,\\
\lambda_i(t_f) = 0,\ i = 1,2,3,\\
\\
\text{where}\\
u_1 = \min\left\{1, \max\left\{\frac{(\lambda_1-\lambda_2)\beta_1 xv}{2A_1}, 0\right\}\right\},\\
u_2 = \min\left\{1, \max\left\{\frac{(\lambda_1-\lambda_2)\beta_2 xy}{2A_2}, 0\right\}\right\},\\
u_3 = \min\left\{1, \max\left\{-\frac{\lambda_3 c\alpha y}{2A_3}, 0\right\}\right\}.
\end{cases}
\tag{2.15}
$$

2.4.3 Uniqueness of optimal system

Theorem 2.8 *Solution of the optimal system (2.15) is unique for sufficiently small t_f.*

Proof If possible, let $(x,y,v,\lambda_1,\lambda_2,\lambda_3)$ and $(\bar{x},\bar{y},\bar{v},\bar{\lambda_1},\bar{\lambda_2},\bar{\lambda_3})$ be two solutions of the optimality system (2.15). Let $\psi = e^{-\lambda t}\theta$ and $\psi' = e^{-\lambda t}\theta'$, where

$$
\psi = \Big(x(t),y(t),v(t),\lambda_1(t),\lambda_2(t),\lambda_3(t)\Big)^T,\ \theta = \Big(X(t),Y(t),V(t),a_1(t),a_2(t),a_3(t)\Big)^T,
$$
$$
\psi' = \Big(\bar{x}(t),\bar{y}(t),\bar{v}(t),\bar{\lambda_1}(t),\bar{\lambda_2}(t),\bar{\lambda_3}(t)\Big)^T,\ \theta' = \Big(\bar{X}(t),\bar{Y}(t),\bar{V}(t),\bar{a_1}(t),\bar{a_2}(t),\bar{a_3}(t)\Big)^T,
$$

and λ has to be chosen suitably. Moreover, we have

$$
u_1 = \min\left\{1, \max\left\{\frac{(a_1-a_2)\beta_1 XVe^{\lambda t}}{2A_1}, 0\right\}\right\},\ \ \bar{u}_1 = \min\left\{1, \max\left\{\frac{(\bar{a}_1-\bar{a}_2)\beta_1 \bar{X}\bar{V}e^{\lambda t}}{2A_1}, 0\right\}\right\},
$$
$$
u_2 = \min\left\{1, \max\left\{\frac{(a_1-a_2)\beta_2 XYe^{\lambda t}}{2A_2}, 0\right\}\right\},\ \ \bar{u}_2 = \min\left\{1, \max\left\{\frac{(\bar{a}_1-\bar{a}_2)\beta_2 \bar{X}\bar{Y}e^{\lambda t}}{2A_2}, 0\right\}\right\},
$$
$$
u_3 = \min\left\{1, \max\left\{-\frac{a_3 c\alpha Y}{2A_3}, 0\right\}\right\},\ \ \bar{u}_3 = \min\left\{1, \max\left\{-\frac{\bar{a}_3 c\alpha \bar{Y}}{2A_3}, 0\right\}\right\}.
$$

From the first equation of (2.15), we obtain

$$\dot{X}(t)+\lambda X(t)=se^{-\lambda t}-\mu X(t)-(1-u_1(t))\beta_1 X(t)V(t)e^{\lambda t}-(1-u_2(t))\beta_2 X(t)Y(t)e^{\lambda t},$$
$$\dot{\bar{X}}(t)+\lambda \bar{X}(t)=se^{-\lambda t}-\mu \bar{X}(t)-(1-\bar{u}_1(t))\beta_1 \bar{X}(t)\bar{V}(t)e^{\lambda t}-(1-\bar{u}_2(t))\beta_2 \bar{X}(t)\bar{Y}(t)e^{\lambda t}.$$

Subtracting and integrating for $t=0$ to $t=t_f$, we have

$$\begin{aligned}&\frac{[X(t_f)-\bar{X}(t_f)]^2}{2}+(\lambda+\mu)\int_0^{t_f}[X(t)-\bar{X}(t)]^2dt\\ =&-\beta_1\int_0^{t_f}e^{\lambda t}[(1-u_1(t))X(t)V(t)-(1-\bar{u}_1)\bar{X}(t)\bar{V}(t)](X(t)-\bar{X}(t))\,dt\\ &-\beta_2\int_0^{t_f}e^{\lambda t}[(1-u_2(t))X(t)Y(t)-(1-\bar{u}_2)\bar{X}(t)\bar{Y}(t)](X(t)-\bar{X}(t))\,dt.\end{aligned}\tag{2.16}$$

Observe that

$$\begin{aligned}&\int_0^{t_f}[(1-u_1(t))X(t)V(t)-(1-\bar{u}_1(t))\bar{X}(t)\bar{V}(t)](X(t)-\bar{X}(t))dt\\ &=\int_0^{t_f}[(\bar{u}_1(t)-u_1(t))(X(t)-\bar{X}(t))X(t)V(t)+(1-\bar{u}_1(t))[(X(t)\\ &\qquad-\bar{X}(t))^2V(t)+\bar{X}(t)(V(t)-\bar{V}(t))(X(t)-\bar{X}(t))]]dt\\ &\le Q_1\int_0^{t_f}[(u_1(t)-\bar{u}_1(t))^2+(X(t)-\bar{X}(t))^2+(V(t)-\bar{V}(t))^2]dt,\end{aligned}\tag{2.17}$$

where Q_1 is determined from the bounds of $u_1(t),\bar{u}_1(t),X(t),\bar{X}(t),V(t),\bar{V}(t)$.
Similarly,

$$\begin{aligned}&\int_0^{t_f}[(1-u_2(t))X(t)Y(t)-(1-\bar{u}_2(t))\bar{X}(t)\bar{Y}(t)](X(t)-\bar{X}(t))dt\\ &\le Q_2\int_0^{t_f}[(u_2(t)-\bar{u}_2(t))^2+(X(t)-\bar{X}(t))^2+(Y(t)-\bar{Y}(t))^2]dt,\end{aligned}\tag{2.18}$$

where Q_2 is determined from the bounds of $u_2(t),\bar{u}_2(t),X(t),\bar{X}(t),Y(t),\bar{Y}(t)$.
Again,

$$\begin{aligned}&\int_0^{t_f}(u_1(t)-\bar{u}_1(t))^2dt\le Q_3\frac{\beta_1^2e^{2\lambda t_f}}{4A_1^2}\int_0^{t_f}[(a_1(t)-a_2(t))X(t)V(t)\\ &-(\bar{a}_1(t)-\bar{a}_2(t))\bar{X}(t)\bar{V}(t)]^2dt\le Q_3\frac{\beta_1^2e^{2\lambda t_f}}{4A_1^2}\int_0^{t_f}[(X(t)-\bar{X}(t))^2\\ &+(V(t)-\bar{V}(t))^2+(a_1(t)-\bar{a}_1(t))^2+(a_2(t)-\bar{a}_2(t))^2]dt,\end{aligned}\tag{2.19}$$

where Q_3 depends on the bounds of $a_1(t),\bar{a}_1(t),a_2(t),\bar{a}_2(t),X(t),\bar{X}(t),V(t),\bar{V}(t)$.

Similarly,

$$\begin{aligned}\int_0^{t_f}(u_2(t)-\bar{u}_2(t))^2dt &\leq Q_4\frac{\beta_2^2e^{2\lambda t_f}}{4A_2^2}\int_0^{t_f}[(X(t)-\bar{X}(t))^2+(Y(t)-\bar{Y}(t))^2\\ &+(a_1(t)-\bar{a}_1(t))^2+(a_2(t)-\bar{a}_2(t))^2]dt,\end{aligned} \tag{2.20}$$

where Q_4 depends on the bounds of $a_1(t),\bar{a}_1(t),a_2(t),\bar{a}_2(t),X(t),\bar{X}(t),Y(t),\bar{Y}(t)$ and

$$\begin{aligned}\int_0^{t_f}(u_3(t)-\bar{u}_3(t))^2dt &\leq Q_5\frac{c^2\alpha^2}{4A_3^2}\int_0^{t_f}[a_3(t)Y(t)-\bar{a}_3(t)\bar{Y}(t)]^2dt\\ &\leq Q_5\frac{c^2\alpha^2}{4A_3^2}\int_0^{t_f}[(Y(t)-\bar{Y}(t))^2+(a_3(t)-\bar{a}_3(t))^2]dt,\end{aligned} \tag{2.21}$$

where Q_5 depends on the bounds of $Y(t),\bar{Y}(t),a_3(t),\bar{a}_3(t)$.
Using (2.17), (2.18), (2.19), (2.20) in (2.16), one can obtain

$$\begin{aligned}&\frac{[X(t_f)-\bar{X}(t_f)]^2}{2}+(\lambda+\mu)\int_0^{t_f}[X(t)-\bar{X}(t)]^2dt\\ &\leq R_1e^{3\lambda t_f}\int_0^{t_f}[(X(t)-\bar{X}(t))^2+(Y(t)-\bar{Y}(t))^2+(V(t)-\bar{V}(t))^2\\ &\quad+(a_1(t)-\bar{a}_1(t))^2+(a_2(t)-\bar{a}_2(t))^2]dt,\end{aligned} \tag{2.22}$$

where R_1 depends on $Q_1,\ Q_2,\ Q_3,\ Q_4,\ \frac{\beta_1^2}{4A_1^2}$ and $\frac{\beta_2^2}{4A_2^2}$.
By a similar process, we obtain

$$\begin{aligned}&\frac{[Y(t_f)-\bar{Y}(t_f)]^2}{2}+(\lambda+(\alpha+\mu))\int_0^{t_f}[Y(t)-\bar{Y}(t)]^2dt\\ &\leq R_2e^{3\lambda t_f}\int_0^{t_f}[(X(t)-\bar{X}(t))^2+(Y(t)-\bar{Y}(t))^2+(V(t)-\bar{V}(t))^2\\ &\quad+(a_1(t)-\bar{a}_1(t))^2+(a_2(t)-\bar{a}_2(t))^2]dt.\end{aligned} \tag{2.23}$$

$$\begin{aligned}&\frac{[V(t_f)-\bar{V}(t_f)]^2}{2}+(\lambda+\gamma)\int_0^{t_f}[V(t)-\bar{V}(t)]^2dt\\ &\leq R_3\int_0^{t_f}[(Y(t)-\bar{Y}(t))^2+(V(t)-\bar{V}(t))^2+(a_3(t)-\bar{a}_3(t))^2]dt.\end{aligned} \tag{2.24}$$

$$\begin{aligned}&\frac{[a_1(0)-\bar{a}_1(0)]^2}{2}+(\lambda+\mu)\int_0^{t_f}[a_1(t)-\bar{a_1}(t)]^2dt\\ &\leq R_4e^{3\lambda t_f}\int_0^{t_f}[(X(t)-\bar{X}(t))^2+(Y(t)-\bar{Y}(t))^2+(V(t)-\bar{V}(t))^2\\ &\quad+(a_1(t)-\bar{a}_1(t))^2+(a_2(t)-\bar{a}_2(t))^2]dt.\end{aligned} \tag{2.25}$$

$$\begin{aligned}
&\frac{[a_2(0)-\bar{a}_2(0)]^2}{2}+(\lambda+(\alpha+\mu))\int_0^{t_f}[a_2(t)-\bar{a_2}(t)]^2dt\\
&\leq R_5e^{3\lambda t_f}\int_0^{t_f}[(X(t)-\bar{X}(t))^2+(Y(t)-\bar{Y}(t))^2+(a_1(t)-\bar{a}_1(t))^2\\
&\quad+(a_2(t)-\bar{a}_2(t))^2+(a_3(t)-\bar{a}_3(t))^2]dt.
\end{aligned}\tag{2.26}$$

$$\begin{aligned}
&\frac{[a_3(0)-\bar{a}_3(0)]^2}{2}+(\lambda+\gamma)\int_0^{t_f}[a_3(t)-\bar{a_3}(t)]^2dt\\
&\leq R_6e^{3\lambda t_f}\int_0^{t_f}[(X(t)-\bar{X}(t))^2+(a_1(t)-\bar{a}_1(t))^2\\
&\quad+(a_2(t)-\bar{a}_2(t))^2+(a_3(t)-\bar{a}_3(t))^2]dt.
\end{aligned}\tag{2.27}$$

Here R_i $(i=1,2,3,4,5,6)$ depends on the coefficients and bounds of the state variables as well as co-state variables. From (2.22) $-$ (2.27), we get

$$\begin{aligned}
&\left[(\lambda+\mu)-\sum_{i=1,\ i\neq3}^{6}R_ie^{3\lambda t_f}\right]\int_0^{t_f}[X(t)-\bar{X}(t)]^2dt+\left[(\lambda+(\alpha+\mu))\right.\\
&\left.-\sum_{i=1,\ i\neq3}^{5}R_ie^{3\lambda t_f}-R_3\right]\int_0^{t_f}[Y(t)-\bar{Y}(t)]^2dt+\left[(\lambda+\gamma)-\sum_{i=1,\ i\neq3}^{4}R_ie^{3\lambda t_f}\right.\\
&\left.-R_3\right]\int_0^{t_f}[V(t)-\bar{V}(t)]^2dt+\left[(\lambda+\mu)-\sum_{i=1,\ i\neq3}^{6}R_ie^{3\lambda t_f}\right]\int_0^{t_f}[a_1(t)-\bar{a}_1(t)]^2dt\\
&+\left[(\lambda+(\alpha+\mu))-\sum_{i=1,\ i\neq3}^{6}R_ie^{3\lambda t_f}\right]\int_0^{t_f}[a_2(t)-\bar{a}_2(t)]^2dt\\
&+\left[(\lambda+\gamma)-(R_3+R_5e^{3\lambda t_f}+R_6e^{3\lambda t_f}\right]\int_0^{t_f}[a_3(t)-\bar{a}_3(t)]^2dt\leq0.
\end{aligned}\tag{2.28}$$

It can be easily seen that the coefficients of the integrals on the left hand side of (2.28) can be made non-negative by selecting λ sufficiently large and t_f sufficiently small. For instance, if we set $\lambda>\sum_{i=1,\ i\neq3}^{6}R_i-\mu$ and select $t_f<\frac{1}{3\lambda}\ ln\frac{\lambda+\mu}{\sum_{i=1,\ i\neq3}^{6}R_i}$, then the coefficient $\lambda+\mu-\sum_{i=1,\ \neq3}^{6}R_ie^{3\lambda t_f}$ of the integral $\int_0^{t_f}[X(t)-\bar{X}(t)]^2dt$ becomes non-negative. We can choose λ and t_f for each of the rest integrals in a similar manner. We then select maximum value of different λ and minimum value of different t_f. Corresponding to this maximum λ and minimum t_f, coefficients of all integrals of (2.28) will be non-negative. This gives $X(t)=\bar{X}(t)$, $Y(t)=\bar{Y}(t)$, $V(t)=\bar{V}(t)$, $a_1(t)=\bar{a}_1(t)$, $a_2(t)=\bar{a}_2(t)$, $a_3(t)=\bar{a}_3(t)$. Therefore, $x(t)=\bar{x}(t)$, $y(t)=\bar{y}(t)$, $v(t)=\bar{v}(t)$ and $\lambda_1(t)=\bar{\lambda}_1(t)$, $\lambda_2(t)=\bar{\lambda}_2(t)$, $\lambda_3(t)=\bar{\lambda}_3(t)$ and thus two solutions of (2.15) are identical. Hence, for sufficiently small t_f, solution of (2.15) is unique. Thus the theorem is proven.

2.4.4 Numerical simulations

In this section, we numerically solve the optimal systems (2.3) and (2.11) with the same set of parameters given in Table 2.1. State equations are solved with the help of fourth order Runge-

Kutta forward method and adjoint equations (co-state variables) are solved by fourth order Runge-Kutta backward method. For the uniqueness of the optimal solution, length of the time interval $[0,t_f]$ should be small [70, 112]. Here we consider treatment period for 50 days and therefore t_f is set 50 in each simulation. As the weight parameters K_1, K_2 are associated with $CD4^+T$ cells, we assign same weight value to them. Assuming the same deleterious effects of all three inhibitors, the same weights for A_1, A_2, A_3 are considered unless stated otherwise. The initial value of the state variables are chosen as $x(0) = 500,\ y(0) = 100,\ v(0) = 100$ [116]. To observe the efficacy of different inhibitors with mono-drug or multi-drug therapy protocols, we examine the following control settings:

A) Mono-drug therapy

(i) Only the blocker which reduces cell-free infection is administered, i.e. $u_1 \neq 0,\ u_2 = 0 = u_3$.

(ii) Only the blocker which reduces cell-to-cell infection is administered, i.e. $u_1 = 0,\ u_2 \neq 0,\ u_3 = 0$.

(iii) Only the blocker which reduces production of new virus particles is administered, i.e. $u_1 = 0 = u_2,\ u_3 \neq 0$.

B) Multi-drug therapy

(i) One blocker is administered to reduce the cell-free infection and the second blocker is administered to reduce cell-to-cell infection, i.e. $u_1 \neq 0, u_2 \neq 0, u_3 = 0$.

(ii) One blocker is administered to reduce the cell-to-cell infection and the other blocker is administered to reduce the production of new virus particles, i.e. $u_1 = 0, u_2 \neq 0, u_3 \neq 0$.

(iii) One blocker is administered to reduce the cell-free infection and another blocker is administered to reduce the production of new virus particles, i.e. $u_1 \neq 0, u_2 = 0, u_3 \neq 0$.

(iv) All three blockers are administered simultaneously, i.e. $u_1 \neq 0, u_2 \neq 0, u_3 \neq 0$.

In each case, we compare the effect of different control measures with the result of no control. A comparison among the strategies $A(i)$, $A(ii)$ and $A(iii)$ is presented in Fig. 2.5. It shows that when we apply PI drug only (the case $u_1 = u_2 = 0,\ u_3 \neq 0$) to block the production of new virus particles, a significant increase in susceptible $CD4^+T$ cells population and a decrease in infected $CD4^+T$ cells as well as in virus population is observed (see third column of Fig. 2.5). Note that PI drug is in its upper bound up to 39 days and then sharply drops to zero at the end of treatment period. It is noticeable that the virus load goes to an undetectable level immediately after applying the control but revert sharply after 40 days of treatment point. In the case of no control, all cell counts decrease slowly. Note that the changing rates of susceptible and infected $CD4^+T$ become significantly slower through out the stipulated time in

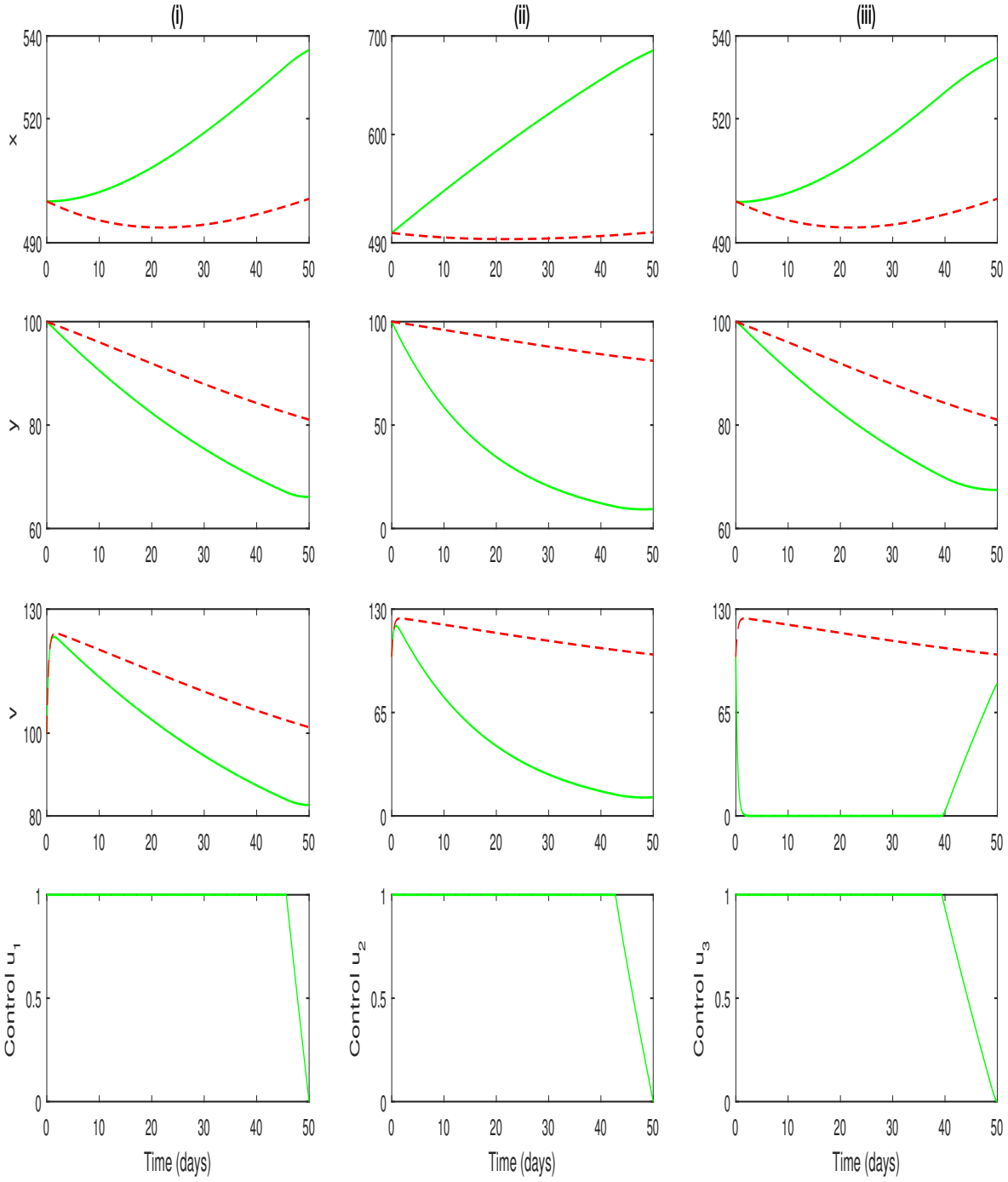

Figure 2.5: Comparison of different mono-drug therapies under case (A) with no therapy. First row shows the variation in susceptible CD4$^+$T cell population for cases $A(i)$ to $A(iii)$. Second and third rows show the same for infected CD4$^+$T cell and virus count, respectively. Here solid line indicates the case of single control only and dotted line represents the case of no control. Fourth row represents the optimal controls under cases $A(i)$ to $A(iii)$. Parameters are as in Table 2.1 with $c = 75$. Here $K_1 = 1 = K_2$ and $A_1 = A_2 = A_3 = 5$.

the presence of other two mono-drug therapies, though the overall trend remains unaltered. In mono-drug therapy, controls u_1 and u_2 are at its maximal value until they drop to zero at 42 and 45 days, respectively (see Figs. 2.5 i,ii in the last row). It says that all mono-blockers should be administered for a longer time with high dose. Out of these three mono-drug therapy protocols, the blocker which reduces cell-to-cell dissemination of infection gives better control (Fig. 2.5 ii) compare to other two. Here increment in the susceptible CD4$^+$T cells count is very high and reduction of infected CD4$^+$T cells and virus count is significantly low compare to other two mono-drug therapies.

When two blockers are used then it is observed that both the multi-drug therapy protocols $B(i)$ and $B(ii)$, which contain the blocker that inhibits cell-to-cell spread of infection, perform equally good (Figs. 2.6 (i), 2.7 (ii)). In both cases, susceptible CD4$^+$T cells count is significantly high, but infected CD4$^+$T cells & virus count remain low, indicating better control by these inhibitors. However, the drug protocol $B(iii)$ is relatively less effective in controlling HIV infection. A multi-drug that contains all three blockers shows slightly better control compare to the controls $B(i)$ and $B(ii)$ (Fig. 2.7). Considering the cost and other deleterious effects of antiretroviral drugs, the multi-drug therapy protocols $B(i)$ and $B(ii)$ would be a better option to treat HIV infected patients compare to the protocol $B(iv)$. If we look at the control variables of corresponding protocols $B(i)$ and $B(ii)$ presented in the fourth row of Fig. 2.6, one can easily notice that the multi-drug therapy protocol $B(ii)$ is better than $B(i)$. This is because the drug PI (corresponding to control u_3) is gradually reduced from day 19th of its application, whereas in the former case, the drug RTI (corresponding to control u_1) is gradually reduced from 30th day of its application to achieve similar blood profile.

Weight constants play important role in optimal control dynamics [186]. With this view, we demonstrated the effect of weight constants on the system dynamics in case of multi-drug therapy $B(iv)$. Since the weight constants K_1, K_2 are associated with the same cells, we vary them simultaneously with same weights, keeping other parameters fixed. Fig. 2.8 shows that healthy CD4$^+$T cells count increases with the increasing weight constant but both the counts for infected CD4$^+$T cells and virus decrease with the increasing value of weight constant. Thus, plasma profiles of host cells and virus particles become better as the weight increases. In Fig. 2.9, we show the effect of other weight parameters A_1, A_2, A_3 on the system while K_1, K_2 remain fixed. It shows that healthy CD4$^+$T cells count decreases with increasing weight constants. On the other hand, cells count of infected CD4$^+$T cells and virus increase with increasing value of weight constants. So, plasma profiles become worsen with increasing value of the weight constants.

2.5 Discussion

We first proved that the solutions of our system remain positive for all future time when started with positive initial value and are uniformly bounded. Using next generation matrix, we have

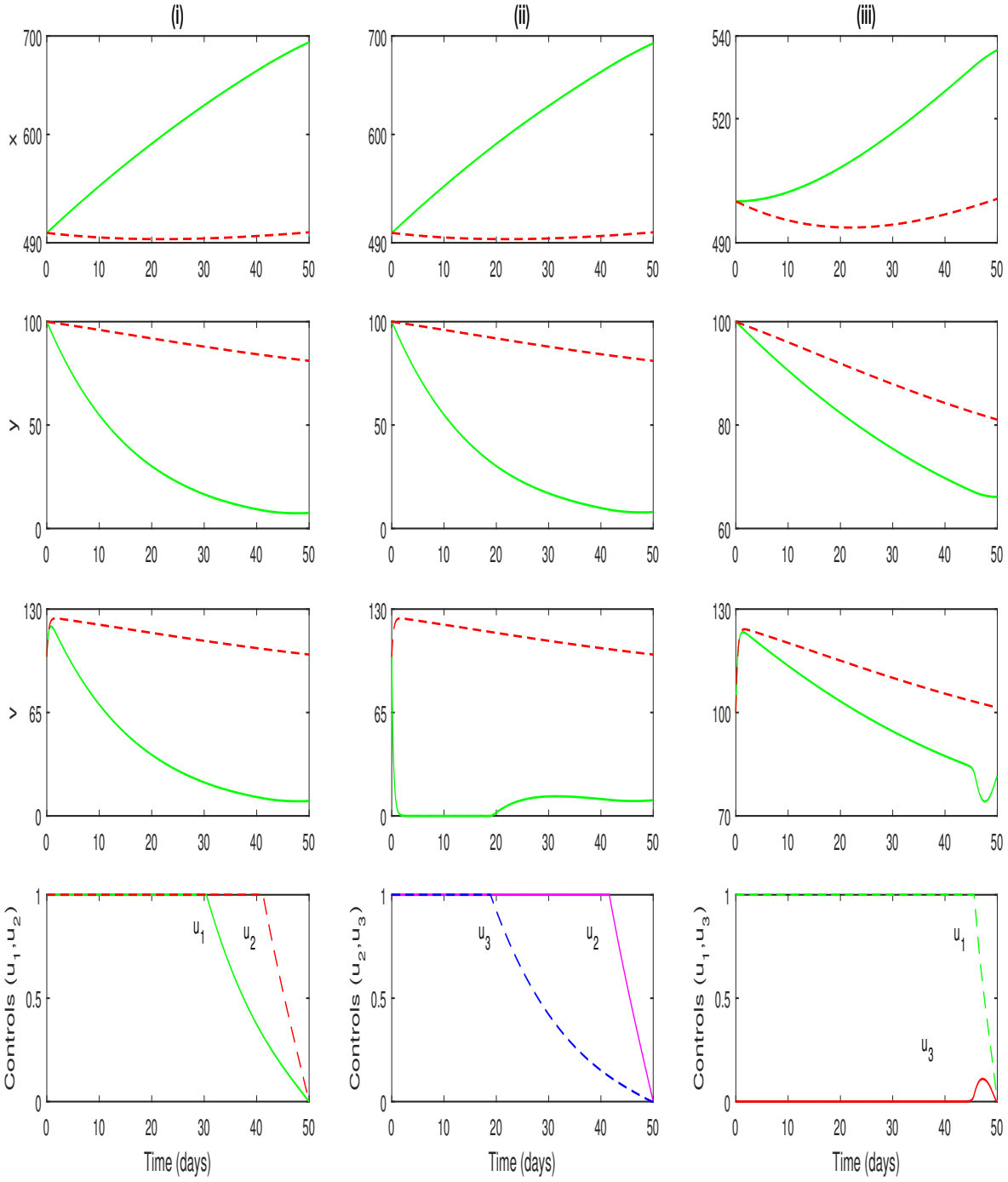

Figure 2.6: Comparison of different multi-drug therapies under case (B) with no therapy. First row shows the variation in susceptible CD4$^+$T cell population for cases $B(i)$ to $B(iii)$. Second and third rows show the same for infected CD4$^+$T cell population and virus count, respectively. Solid line represents the case of two controls and dotted line indicates the case of no control. Fourth row represents the corresponding optimal controls under cases $B(i)$ to $B(iii)$. Parameters are as in Fig. 2.5.

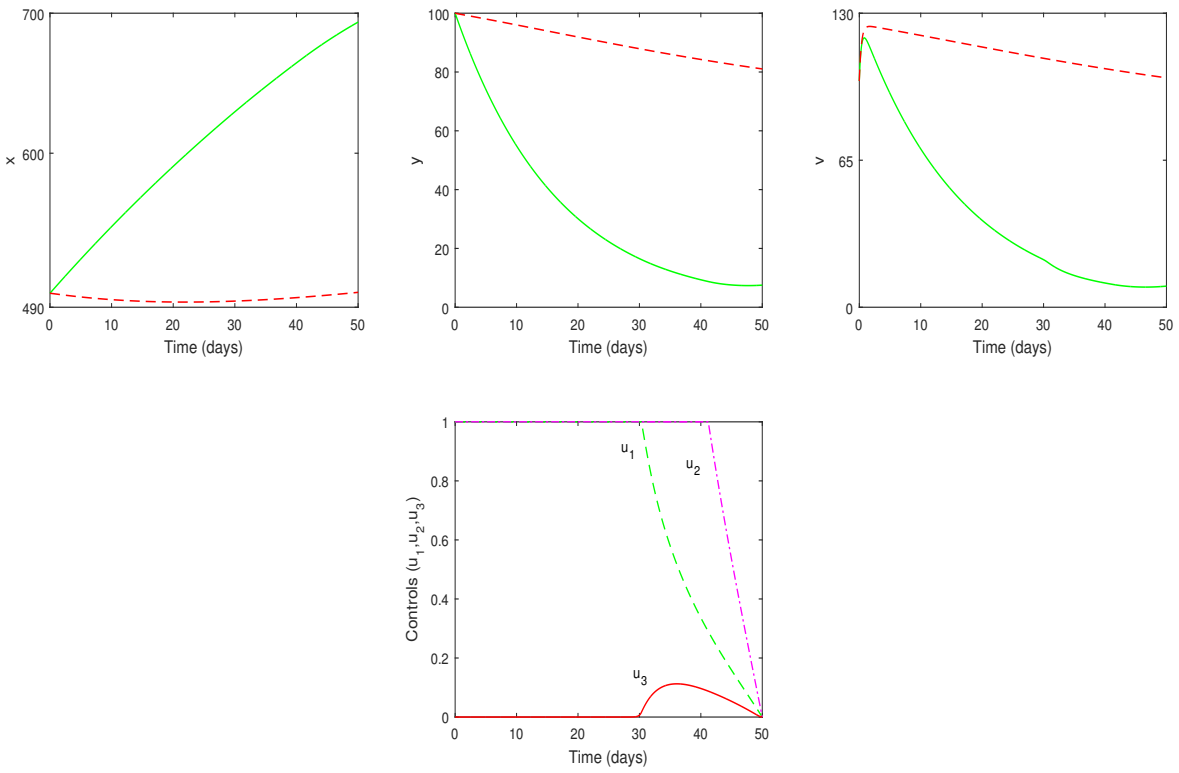

Figure 2.7: This figure shows the variation in susceptible CD4$^+$T cell, infected CD4$^+$T cell and virus population in the presence of all three inhibitors (case $B(iv)$). Here solid line represents the case of three controls and dotted line indicates the case of no control. Second row represents the control profile under the case $B(iv)$. Parameters are in Fig. 2.5.

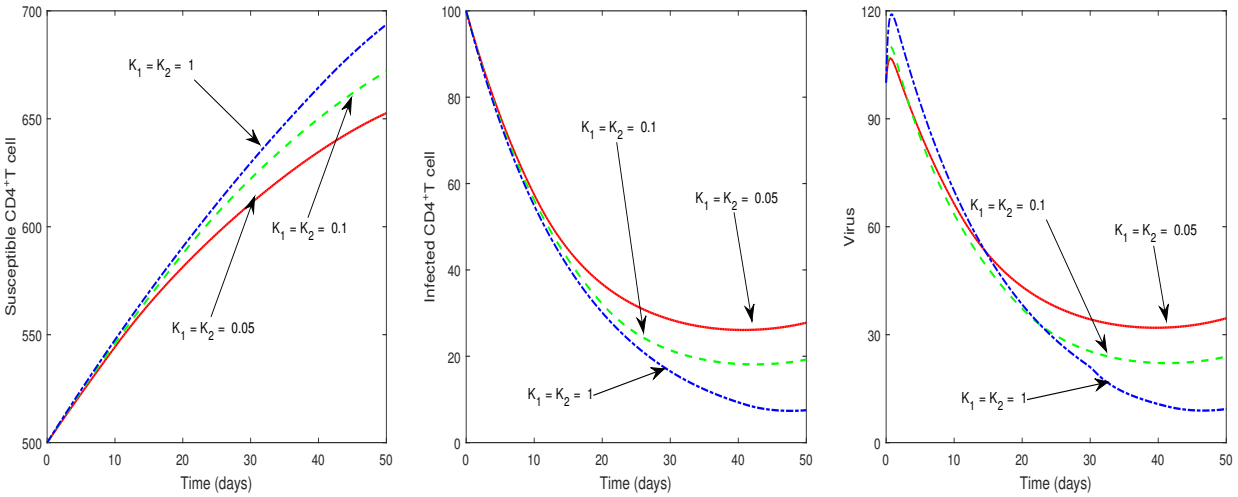

Figure 2.8: Effect of weight parameters K_1, K_2 on the system populations with control scheme $B(iv)$. These figures shows that susceptible CD4$^+$T cells increase with increasing weight constant. However, infected CD4$^+$T cells and virus counts decrease with increasing weight constant. Parameters are as in Fig. 2.5 and $A_1 = A_2 = A_3 = 5$.

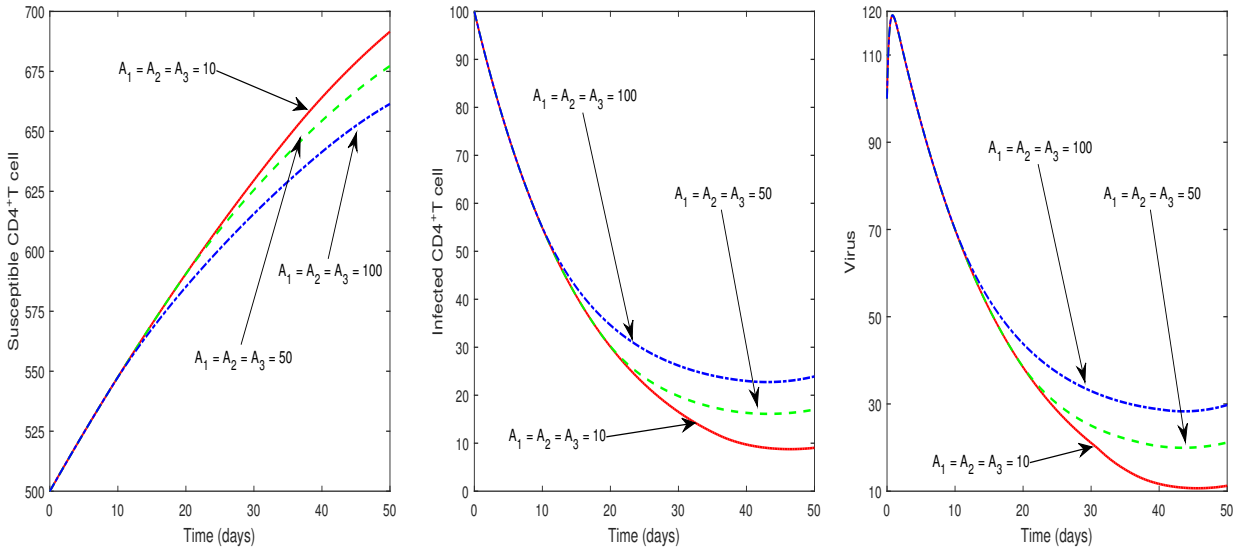

Figure 2.9: Effect of weight parameters A_1, A_2, A_3 on the system populations with control scheme $B(iv)$. These figures shows that healthy CD4$^+$T cells decreases, while infected CD4$^+$T cells and virus counts increase with increasing values of th weight parameters. Rest of the parameters are as in Fig. 2.5 with $K_1 = K_2 = 1$.

determined two basic reproduction numbers, one for virus-to-cell transmission and the other for cell-to-cell transmission, when the controls are constant. The basic reproduction number (of the entire system) in presence of both transmission modes is found to be the sum of these two. Basic reproduction number is an important parameter in disease models and determines whether a disease will be established or eliminated from the system. We have proved that the infection-free steady state is locally and globally asymptotically stable when the basic reproduction number of the system is less than unity, or alternatively, when the virus replication factor is not too high $(c < c^*)$. The infected steady state, on the other hand, is locally and globally asymptotically stable if the basic reproduction number is greater than unity, alternatively, the virus replication factor is sufficiently high $(c > c^*)$. When the controls are not constant but time-dependent then the infection-free equilibrium does not arise, but we derive a set of necessary conditions for optimal control of the infection by applying Pontryagin's Maximum Principle. Our objective in such a case was to find the optimal treatment regimens that maximizes the uninfected CD4$^+$T cells count but minimizes infected CD4$^+$T cells count and the deleterious effect of antiretroviral drugs. We analytically show that there exists an optimal control triplet associated with the time-dependent controls that maximize the objective function. Numerically we investigated and compared the CD4$^+$T cells count and virus load under mono- or multi-drugs therapy protocols. Though the drug therapy for HIV is for life, we have presented here a 50-days treatment schedule to check the efficacy of the new possible drug that blocks the cell-to-cell spread of infection. The treatment regime, however, can be extended as per the requirement. The results show that cell-to-cell mono blocker gives better control than

the other two mono blocker controls. In case of multi blockers, any combined drug that blocks cell-to-cell infection may be a better option for treating HIV infection. It is observed that the multi-drug therapy protocols $B(i)$ and $B(ii)$ are equally good to increase healthy $CD4^+$T cells count and to keep low virus load. Interestingly, both of these control profiles contain cell-to-cell blocker. However, looking at the optimal control profiles of $B(i)$ and $B(ii)$ and keeping in mind the cost of antiviral drugs along with its deleterious effects, the multi-drug therapy protocols $B(ii)$ that contains PI and cell-to-cell inhibitors is better than $B(i)$ because PI (u_3 control) has to be applied at higher dose for lesser period compare to RTI (u_1 control) to achieve optimality. Thus, our study reveals that a drug which blocks cell-to-cell dissemination of infection could be a novel therapeutic target in controlling HIV-1 infection and supports the observation that future control strategies of in-host HIV-1 infection through drug therapy should focus on blocking cell-to-cell dissemination of infection [97]. Obviously, there are avenues for further improvement in the model. One can modify this multi-pathways and multi-drugs model by incorporating the effect of cytotoxic T lyphocytes (CTL). Delay is an integral part of different physiological activities. For example, response of our immune system is not instantaneous rather involves immune response delay. One can consider such delay-induced system and then study the effect of different drug therapies.

3

Optimal control in a multi-pathways in-host HIV infection model with saturated incidence, intracellular delay and self-proliferation of the host cells

3.1 Introduction

In developing mathematical models for disease dynamics, it is imperative to express the disease transmission term mathematically. Most models of HIV-1 infection assume that the transmission process follows a mass action or bilinear law [91, 131, 172, 176, 187]. This law says that the infection rate at any time is proportional to the product of viral and host cell numbers [188]. In our previous model (2.3), we assumed the transmission process in both modes of infection follows a mass action law. In particular, we expressed the cell-free mode and cell-to-cell mode of transmissions as $f_2(x,v) = \beta_1 x(t)v(t)$ and $f_3(x,y) = \beta_2 x(t)y(t)$, where β_1 and β_2 are the respective transmission coefficients, and $x(t), y(t)$, $v(t)$ are the concentrations of susceptible $CD4^+T$ cells, productively infective $CD4^+T$ cells and virus particles at any time t. But, the mass action law has some unrealistic properties, e.g., the number of newly infected $CD4^+T$ cells produced by a single virus depends on x and becomes very high when x is large [189]. To prevent this unboundedness of the contact rate, some authors [165, 166] used saturated infec-

tion rate $f_2(x,v)=\frac{\beta_1 xv}{1+v}$. On the other hand, [89] considered the saturation effect on x population as $f_2(x,v)=\frac{\beta_1 xv}{a+x}$ with a as the half-saturation constant to understand the failure of CD8$^+$T cells vaccination against Simian/Human Immunodeficiency Virus. A generalized Hill-type function $f_2(x,v)=\frac{\beta_1 x^n v}{a^n+x^n}$ was considered in [130, 167, 168] to observe the dynamics of HIV-1 infection models. Most authors [99, 131, 133, 172, 173] used the mass action form to represent the of cell-to-cell incidence function $f_3(x,y)=\beta_2 xy$.

Time delay is crucial for realistic representation of biological phenomena [190]. In the epidemic model, the intracellular delay is an obvious event to be considered to make the epidemic model more realistic. In the case of HIV, the process between the first effective contact of a virus/ infected cell with a healthy CD4$^+$T cell and the latter becoming productively infectious is not instantaneous. After entering a virus into the healthy cell, many intracellular mechanisms occur to make the cell productively infectious. The time required for transforming a healthy cell into an infectious cell is known as the intercellular delay. Various HIV-1 infection models have been studied considering such an intracellular delay [91, 94, 130–132, 165–167, 170–172, 191, 192].

CD4$^+$T cell is the main target of HIV. The cell count gradually decreases due to the infection. In the presence of HIV antigen, CD4$^+$T cells proliferate and try to maintain homeostasis. Such proliferation was not considered in the in-host HIV model studied in the previous chapter. In this chapter, we modify our previously studied model from three points of view. First, we consider saturated type incidence functions $f_2(x,v)=\frac{\beta_1 xv}{a+v}$, $f_3(x,y)=\frac{\beta_1 xy}{b+y}$, where a and b are respective half-saturation constants. Secondly, we consider the proliferation of susceptible CD4$^+$T cells in its rate equation. Third, the intracellular delay is considered in the infection transmission terms. With these modifications, the model system (2.3) becomes

$$\begin{aligned}
\dot{x}(t) &= s-\mu x(t)+rx(t)\Big(1-\frac{x(t)+y(t)}{K}\Big)-(1-u_1(t))\frac{\beta_1 x(t)v(t)}{a+v(t)}\\
&\quad -(1-u_2(t))\frac{\beta_2 x(t)y(t)}{b+y(t)},\\
\dot{y}(t) &= (1-u_1(t))\frac{\beta_1 x(t-\tau)v(t-\tau)}{a+v(t-\tau)}+(1-u_2(t))\frac{\beta_2 x(t-\tau)y(t-\tau)}{b+y(t-\tau)}\\
&\quad -(\alpha+\mu)y(t),\\
\dot{v}(t) &= (1-u_3(t))c\alpha y(t)-\gamma v(t).
\end{aligned} \tag{3.1}$$

with initial conditions

$$\begin{aligned}
&x(\theta)=\phi_1(\theta)>0, y(\theta)=\phi_2(\theta)>0, v(\theta)=\phi_3(\theta)>0, \theta\in[-\tau,0], \text{where}\\
&\phi=(\phi_1,\phi_2,\phi_3)\in\mathbb{R}^3_+ \text{with } \phi_i(\theta)\geq 0\ (\theta\in[-\tau,0], i=1,2,3)\\
&\text{and } \phi_2(0)>0, \phi_3(0)>0.
\end{aligned} \tag{3.2}$$

Here r is the intrinsic growth rate of the susceptible CD4$^+$T cell, and K is the carrying capacity.

The three controls u_1, u_2 and u_3 bear the same meaning as before. All parameters are positive due to the biological demands. The objective is to find the effect of saturated incidence and intracellular delay in the dynamics of the in-host HIV model with controls.

This chapter is arranged in the following sequence. In Section 3.2, we present some preliminary results. In section 3.3, we analyze the dynamics when controls are constant. Some simulation results are also presented here to validate the analytical findings. Section 3.4 deals with the optimal control of the system when controls are time-dependent. We give the existence and uniqueness of the optimal control triplet. A comparison of different control schemes is presented in numerical simulations. The chapter ends with a discussion in Section 3.5.

3.2 Preliminaries

Let $M = C([-\tau,0],\mathbb{R}^3_+)$ be the Banach Space of continuous real-valued functions mapping from $[-\tau,0]$ to $\mathbb{R}^3_+$ with sup-norm $\|\phi\| = sup_{-\tau\le\theta\le 0}\{|\phi(\theta)|\}$, where $\phi = (\phi_1,\phi_2,\phi_3) \in \mathbb{R}^3_+$. Following fundamental theory of functional differential equations [193], for any $\phi \in C([-\tau,0],\mathbb{R}^3_+)$, there exists a unique solution

$$\Omega(t,\phi) = (x(t,\phi), y(t,\phi), v(t,\phi))$$

of the system (3.1) with initial conditions (3.2).

Lemma 3.1 *Let $\Omega(t,\phi) = (x(t),y(t),v(t))$ be solutions of system (3.1) with initial conditions (3.2). Then the solutions are positively invariant provided $u_1 = 1, u_2 = 1$ do not hold simultaneously and $u_3 \in [0,1)$. The solutions are uniformly bounded on the region*

$$\Sigma = \left\{ \begin{array}{c} \Omega(t,\phi) \in \mathbb{R}^3_+ \mid 0 < x(t) \le x_0, 0 \le y(t) \le \frac{2(s+rx_0)}{\mu}, \\ 0 \le v(t) \le \frac{2c\alpha(s+rx_0)}{\gamma\mu} \end{array} \right\} \tag{3.3}$$

with $x_0 = \frac{K}{2r}[(r-\mu) + \sqrt{(r-\mu)^2 + \frac{4rs}{K}}]$, $\mu K > s$ and $r > \mu$.

Proof First we show that $x(t)$ is positive for all $t \ge 0$. If not, there exists a time $t_1 > 0$ such that $x(t) > 0$ for all $t \in [0,t_1)$ and $x(t_1) = 0$. Now put $t = t_1$ in the first equation of (3.1), then we get $\dot{x}(t_1) = s$. This implies that $x(t)$ is increasing at $t = t_1$. Therefore, there exists $\tilde{t} > 0$, sufficiently small, such that for all $t \in (t_1 - \tilde{t}, t_1) \subset [0,t_1)$, $x(t) < 0$, which is a contradiction. Hence $x(t) > 0$, for all $t \ge 0$. From the second equation of (3.1), we get

$$\begin{aligned} &\dot{y}(t) \ge (1-u_2(t))\frac{\beta_2 x(t-\tau)y(t-\tau)}{b+y(t-\tau)} - (\alpha+\mu)y(t) \\ &\implies y(t) \ge y(0)e^{-(\alpha+\mu)t} + \int_0^t (1-u_2(m))\frac{\beta_2 x(m-\tau)y(m-\tau)}{b+y(m-\tau)} e^{-(\alpha+\mu)(t-m)} dm. \end{aligned}$$

From the third equation of (3.1), one obtains

$$v(t) = v(0)e^{-\gamma t} + \int_0^t (1-u_3(m))c\alpha y(m)e^{-\gamma(t-m)}dm.$$

Applying (3.2), we have $y(t) \geq 0$ and $v(t) \geq 0$, for all $t \geq 0$. Therefore, all solutions of(3.1) are positively invariant.

Now, we show that all solutions of (3.1) are bounded. First equation of (3.1) can be expressed as

$$\dot{x} \leq -\frac{1}{K}[rx^2 - K(r-\mu)x - sK]. \tag{3.4}$$

Assuming the condition $r > \mu$, we define a function $f(x) = rx^2 - K(r-\mu)x - sK$. Therefore, the equation $f(x) = 0$ has two roots, say, x_0 and $\tilde{x}$, where $x_0 = \frac{K}{2r}[(r-\mu) + \sqrt{(r-\mu)^2 + \frac{4rs}{K}}] > 0$ and $\tilde{x} = \frac{K}{2r}[(r-\mu) - \sqrt{(r-\mu)^2 + \frac{4rs}{K}}] < 0$. We also assume that $\mu K > s$, so that $CD4^+T$ cells count decreases if it ever reaches K [194]. Hence, (3.4) can be written as

$$\dot{x} \leq -\frac{r}{K}(x-x_0)(x-\tilde{x})$$
$$x(t) \leq \frac{x_0 - \tilde{x}e^{-\frac{x_0-\tilde{x}}{K}t+c_1}}{1-e^{-\frac{x_0-\tilde{x}}{K}t+c_1}},$$

where the constant c_1 can be determined by the initial conditions (3.2) and hence

$$\lim_{t\to\infty} sup\, x(t) \leq x_0. \tag{3.5}$$

To find the upper boundary region, we define

$$D(t) = x(t) + x(t-\tau) + y(t).$$

At $t = 0$, $D(0) = x(0) + x(-\tau) + y(0)$ and from the initial conditions (3.2), we have $D(0) = \phi_1(\theta) + \phi_1(\theta) + \phi_2(\theta) > 0$, where $\theta \in [-\tau, 0]$. Hence, $D(t) > 0$ for all $t \geq 0$. Differentiating $D(t)$ with respect to t, we get

$$\begin{aligned}
\dot{D}(t) =& \dot{x}(t) + \dot{x}(t-\tau) + \dot{y}(t) \\
=& s - \mu x(t) + rx(t)\Big(1 - \frac{x(t)+y(t)}{K}\Big) - (1-u_1(t))\frac{\beta_1 x(t)v(t)}{a+v(t)} - (1-u_2(t))\frac{\beta_2 x(t)y(t)}{b+y(t)} \\
&+ s - \mu x(t-\tau) + rx(t-\tau)\Big(1 - \frac{x(t-\tau)+y(t-\tau)}{K}\Big) - (1-u_1(t-\tau)) \\
&\frac{\beta_1 x(t-\tau)v(t-\tau)}{a+v(t-\tau)} - (1-u_2(t-\tau))\frac{\beta_2 x(t-\tau)y(t-\tau)}{b+y(t-\tau)} + (1-u_1(t)) \\
&\frac{\beta_1 x(t-\tau)v(t-\tau)}{a+v(t-\tau)} + (1-u_2(t))\frac{\beta_2 x(t-\tau)y(t-\tau)}{b+y(t-\tau)} - (\alpha+\mu)y(t) \\
&\leq 2s - \mu[x(t) + x(t-\tau) + y(t)] + r[x(t) + x(t-\tau)].
\end{aligned}$$

From (3.5), one then have

$$\dot{D}(t) \leq 2(s+rx_0) - \mu D(t).$$

Therefore,

$$\lim_{t\to\infty} supD(t) \leq \frac{2(s+rx_0)}{\mu}.$$

We then immediately have $\limsup_{t\to\infty} y(t) \leq \frac{2(s+rx_0)}{\mu}$ and from the third equation of (3.1), we then obtain $\limsup_{t\to\infty} v(t) \leq \frac{2c\alpha(s+rx_0)}{\gamma\mu}$. Hence the lemma is proven.

3.3 Model analysis for fixed controls

Controls parameters $u_i,\ i = 1,2,3$, may be either constant or time-dependent. To analyze the model, we first consider u_i as constant and in the subsequent section, we consider u_i as time-dependent.

Lemma 3.2 *The system (3.1) has two equilibrium points.*
1. The infection-free equilibrium point $E_1 = (x_0, 0, 0)$ always exists with $x_0 = \frac{K}{2r}\Big[(r-\mu) + \sqrt{(r-\mu)^2 + \frac{4rs}{K}}\Big]$.
2. The infected equilibrium point $E^* = (x^*, y^*, v^*)$ exists if

(i) either $\beta_2 < \beta_2^*$ with $c > c^*(\beta_2)$, or $\beta_2 > \beta_2^*$ with $c > 0$,

(ii) $u_1 = 1$ and $u_2 = 1$ do not hold simultaneously and $u_3 \in [0,1)$.

Here $\beta_2^* = \frac{b(\alpha+\mu)}{(1-u_2)x_0}$, $c^*(\beta_2) = \frac{(1-u_2)}{(1-u_1)(1-u_3)}\frac{a\gamma}{b\alpha\beta_1}(\beta_2^* - \beta_2)$, $v^* = Ay^*$, $y^* = \frac{s-\mu x^* + rx^*(1-\frac{x^*}{K})}{\frac{rx^*}{K}+(\alpha+\mu)}$ and x^* is the positive real root of the quartic equation

$$f(x) = M_1x^4 + M_2x^3 + M_3x^2 + M_4x + M_5 = 0, \tag{3.6}$$

where

$$\begin{cases} A = (1-u_3)\frac{c\alpha}{\gamma},\ B = A[(1-u_1)\beta_1 + (1-u_2)\beta_2],\ C = (\alpha+\mu)(a+bA), \\ D = \frac{1}{ab\gamma(\alpha+\mu)}\Big((1-u_1)(1-u_3)\beta_1 bc\alpha + (1-u_2)a\beta_2\gamma\Big)x_0, M_1 = -\frac{r^2}{K^2}\Big(B + (\alpha+\mu)A\Big), \\ M_2 = \frac{ab(\alpha+\mu)r^2D}{x_0K^2} + \frac{2Ar(\alpha+\mu)(r-\mu)}{K} + \frac{Br}{K}(r-\alpha-2\mu) + \frac{Cr^2}{K^2},\ M_3 = \frac{ab(\alpha+\mu)r}{K}\big(\frac{2(\alpha+\mu)D}{x_0} - \frac{r}{K}\big) \\ \qquad + B\big(\frac{rs}{K} + (\alpha+\mu)(r-\mu)\big) - \frac{Cr}{K}(r-\alpha-2\mu) - A(\alpha+\mu)\big((r-\mu)^2 - \frac{2rs}{K}\big), \\ M_4 = ab(\alpha+\mu)^2\big(\frac{2(\alpha+\mu)D}{x_0} - \frac{2r}{K}\big) + Bs(\alpha+\mu) - C\big(\frac{rs}{K} + (\alpha+\mu)(r-\mu)\big) \\ \qquad - 2As(\alpha+\mu)(r-\mu), M_5 = -\Big(ab(\alpha+\mu)^3 + s(\alpha+\mu)(C+As^2)\Big). \end{cases}$$

Proof The equilibrium points are the biologically feasible solutions of

$$\begin{aligned} s-\mu x(t)+rx(t)\Big(1-\frac{x(t)+y(t)}{K}\Big)-(1-u_1(t))\frac{\beta_1 x(t)v(t)}{a+v(t)}-(1-u_2(t))\frac{\beta_2 x(t)y(t)}{b+y(t)} &= 0,\\ (1-u_1(t))\frac{\beta_1 x(t-\tau)v(t-\tau)}{a+v(t-\tau)}+(1-u_2(t))\frac{\beta_2 x(t-\tau)y(t-\tau)}{b+y(t-\tau)}-(\alpha+\mu)y(t) &= 0,\\ (1-u_3(t))c\alpha y(t)-\gamma v(t) &= 0. \end{aligned}$$

The equilibrium density of the infection-free equilibrium point E_1 is $x_0=\frac{K}{2r}\Big[(r-\mu)+\sqrt{(r-\mu)^2+\frac{4rs}{K}}\Big]$, which is the positive root of

$$s-\mu x(t)+rx(t)\Big(1-\frac{x(t)}{K}\Big)=0.$$

It always exists without any conditions. The infected equilibrium point $E^*=(x^*,y^*,v^*)$, where $v^*=(1-u_3)\frac{c\alpha}{\gamma}y^*$, $y^*=\frac{s-\mu x^*+rx^*(1-\frac{x^*}{K})}{\frac{rx^*}{K}+(\alpha+\mu)}$ and x^* is the positive real root of the quartic equation (3.6). Observe that, if $u_1=1$ and $u_2=1$ are both simultaneously hold, then $y\to 0$ as $t\to\infty$; also if $u_3=1$ then $v\to 0$ as $t\to\infty$. Therefore, infected equilibrium E^* does not exists for condition (ii) of the Lemma 3.2. Let the equation (3.6) has at least one positive real root, say, x^*, then E^* exists if $y^*>0$. In this case, $y^*>0$ if $s-\mu x^*+rx^*(1-\frac{x^*}{K})>0\Rightarrow r/Kx^{*2}-(r-\mu)x^*-s<0$. Since $x_0>0$ and $\tilde{x}<0$ be two roots of the equation $r/Kx^{*2}-(r-\mu)x^*-s=0$, then

$$r/Kx^{*2}-(r-\mu)x^*-s<0\Rightarrow\quad (x^*-x_0)(x^*-\tilde{x})<0\Rightarrow\quad x^*<x_0\ as\ x^*-\tilde{x}>0.$$

Therefore, y^* exists if and only if $x^*<x_0$ and hence, E^* exists if $0<x^*<x_0$. Again, from the second equation of the system (3.1), we have

$$(1-u_1)(1-u_3)\frac{\beta_1 c\alpha}{\gamma}\frac{x^*}{a+v^*}+(1-u_2)\beta_2\frac{x^*}{b+y^*}-(\alpha+\mu)=0.$$

It is obvious that $\frac{1}{a+v^*}\le\frac{1}{a}$ and $\frac{1}{b+y^*}\le\frac{1}{b}$, where $a,b\neq 0$. As $x^*<x_0$, the above expression becomes

$$(1-u_1)(1-u_3)\frac{\beta_1 c\alpha}{\gamma a}x_0+(1-u_2)\frac{\beta_2}{b}x_0-(\alpha+\mu)>0.$$

It gives

$$c>c^*(\beta_2),$$

where

$$c^*(\beta_2)=\frac{(1-u_2)\gamma a}{(1-u_1)(1-u_3)\beta_1 b\alpha}(\beta_2^*-\beta_2)$$

and

$$\beta_2^*=\frac{b(\alpha+\mu)}{(1-u_2)x_0}.$$

Thus, whenever $\beta_2 < \beta_2^*$ hold then E^* exists if $c > c^*(\beta_2)$. However, if $\beta_2 > \beta_2^*$ then E^* exists for any $c > 0$. This completes the proof.

3.3.1 Stability analysis

We linearize the system (3.1) about an arbitrary equilibrium point $\bar{E}(\bar{x},\bar{y},\bar{z})$ and the linearized system can be represented in the matrix form

$$\frac{dX}{dt} = YX(t) + ZX(t-\tau), \tag{3.7}$$

where

$$Y = \begin{pmatrix} m_{11} & m_{12} & m_{13} \\ 0 & m_{22} & 0 \\ 0 & m_{32} & m_{33} \end{pmatrix}, Z = \begin{pmatrix} 0 & 0 & 0 \\ n_{21} & n_{22} & n_{23} \\ 0 & 0 & 0 \end{pmatrix}, X(t) = \begin{pmatrix} x(t) & y(t) & v(t) \end{pmatrix}^T$$

and

$$\begin{cases} m_{11} = -\mu + r(1-(2\bar{x}+\bar{y})/K) - (1-u_1)\frac{\beta_1\bar{v}}{(a+\bar{v})} - (1-u_2)\frac{\beta_2\bar{y}}{(b+\bar{y})},\ m_{12} = -r\bar{x}/K \\ \qquad -(1-u_2)\frac{\beta_2 b\bar{x}}{(b+\bar{y})^2}, m_{13} = -(1-u_1)\frac{\beta_1 a\bar{x}}{(b+\bar{v})^2},\ m_{22} = -(\alpha+\mu), \\ m_{32} = (1-u_3)c\alpha, m_{33} = -\gamma, n_{21} = (1-u_1)\frac{\beta_1\bar{v}}{(a+\bar{v})} + (1-u_2)\frac{\beta_2\bar{y}}{(b+\bar{y})}, \\ n_{22} = (1-u_2)\frac{\beta_2 b\bar{x}}{(b+\bar{y})^2}, n_{23} = (1-u_1)\frac{\beta_1 a\bar{x}}{(b+\bar{v})^2}. \end{cases} \tag{3.8}$$

The characteristic equation is then given by

$$|Y + Ze^{-\lambda\tau} - \lambda I| = 0,$$

and can be expressed as

$$\Phi(\lambda,\tau) = \lambda^3 + M_1\lambda^2 + M_2\lambda + M_3 + (N_1\lambda^2 + N_2\lambda + N_3)e^{-\lambda\tau} = 0, \tag{3.9}$$

where

$$\begin{cases} M_1 = -(m_{11}+m_{22}+m_{33}),\ M_2 = m_{11}m_{22} + m_{22}m_{33} + m_{33}m_{11},\ M_3 = -m_{11}m_{22}m_{33}, \\ N_1 = -n_{22}, N_2 = n_{22}(m_{11}+m_{33}) - m_{12}n_{21} - m_{32}n_{23},\ N_3 = n_{21}(m_{12}m_{33} - m_{13}m_{32}) \\ \qquad -m_{11}(m_{33}n_{22} - m_{32}n_{23}). \end{cases}$$

Theorem 3.3 *In the absence of delay, the disease-free steady state $E_1(x_0,0,0)$ is locally asymptotically stable if $\beta_2 < \beta_2^*$ and $c < c^*(\beta_2)$, where*

$$\beta_2^* = \frac{b(\alpha+\mu)}{(1-u_2)x_0},\ \ c^*(\beta_2) = \frac{(1-u_2)\gamma a}{(1-u_1)(1-u_3)\beta_1\alpha b}(\beta_2^* - \beta_2).$$

Proof The entries m_{ij} and n_{ij}, $i,j = 1,2,3$, corresponding to the equilibrium E_1 are

$$P_{ij} = m_{ij},\ Q_{ij} = n_{ij},\ i,j = 1,2,3.$$

For $\tau = 0$, the characteristic equation (3.9) corresponding to E_1 can be written as

$$\Phi(\lambda,0) = (\lambda - P_{11})[\lambda^2 - (P_{22}+P_{33}+Q_{22})\lambda + \{P_{33}(P_{22}+Q_{22}) - P_{32}Q_{23}\}] = 0. \tag{3.10}$$

One root of (3.10) is given by $\lambda = P_{11} = -\mu + r(1-2x_0/K) = -(\frac{s}{x_0} + \frac{rx_0}{K}) < 0$. The other two roots will have negative real parts if $P_{22}+P_{33}+Q_{22} < 0$ and $P_{33}(P_{22}+Q_{22}) - P_{32}Q_{23} > 0$. From (3.8), we have

$$P_{22}+P_{33}+Q_{22} = -\Big\{(\alpha+\mu) - \frac{(1-u_2)x_0}{b}\beta_2\Big\} - \gamma < 0, \text{ if } \beta_2 < \beta_2^*, \text{ where}$$
$$\beta_2^* = \frac{b(\alpha+\mu)}{(1-u_2)x_0}, \text{and}$$
$$P_{33}(P_{22}+Q_{22}) - P_{32}Q_{23} = \gamma\Big\{(\alpha+\mu) - \frac{(1-u_2)x_0}{b}\beta_2\Big\} - (1-u_1)(1-u_3)\frac{\beta_1\alpha x_0}{a}c > 0$$
$$\text{if } \beta_2 < \beta_2^* \text{ and } c < c^*(\beta_2), \text{ where } c^*(\beta_2) = \frac{(1-u_2)\gamma a}{(1-u_1)(1-u_3)\beta_1\alpha b}(\beta_2^* - \beta_2).$$

Therefore, E_1 is locally asymptotically stable in the absence of delay if $\beta_2 < \beta_2^*$ and $c < c^*(\beta_2)$.

Theorem 3.4 *The disease-free steady state E_1 is globally asymptotically stable for any $\tau > 0$ if $\beta_2 < \beta_2^*$ and $c < c^*(\beta_2)$, where $\beta_2^* = \frac{b(\alpha+\mu)}{(1-u_2)x_0}$ and $c^*(\beta_2) = \frac{(1-u_2)\gamma a}{(1-u_1)(1-u_3)\beta_1\alpha b}(\beta_2^* - \beta_2)$.*

Proof To prove the global stability, we define the following Lyapunov function

$$\begin{aligned} H(t) =& y(t) + \frac{(1-u_1)\beta_1 x_0}{\gamma a}v(t) + (1-u_2)\beta_2\int_{t-\tau}^{t}\frac{x(m)y(m)}{b+y(m)}dm + \\ & \frac{(1-u_1)\beta_1 x_0}{a}\int_{t-\tau}^{t} v(m)dm. \end{aligned} \tag{3.11}$$

Clearly, $H(t) > 0$ for $x(t,y(t),v(t)) > 0$ and $H(t) = 0$ if and only if $y(t) = v(t) = 0$.

The derivative of $H(t)$ along the solutions of (3.1) is

$$\begin{aligned}\dot{H}(t) =&\dot{y}(t)+\frac{(1-u_1)\beta_1 x_0}{\gamma a}\dot{v}(t)+(1-u_2)\beta_2\frac{x(t)y(t)}{b+y(t)}-(1-u_2)\beta_2\frac{x(t-\tau)y(t-\tau)}{b+y(t-\tau)}\\&+\frac{(1-u_1)\beta_1 x_0}{a}v(t)-\frac{(1-u_1)\beta_1 x_0}{a}v(t-\tau)\\=&(1-u_1)\frac{\beta_1 x(t-\tau)v(t-\tau)}{a+v(t-\tau)}+(1-u_2)\frac{\beta_2 x(t-\tau)y(t-\tau)}{b+y(t-\tau)}-(\alpha+\mu)y(t)\\&+\frac{(1-u_1)(1-u_3)c\alpha\beta_1 x_0}{\gamma a}y(t)-\frac{(1-u_1)\beta_1 x_0}{a}v(t)+(1-u_2)\beta_2\frac{x(t)y(t)}{b+y(t)}\\&-(1-u_2)\beta_2\frac{x(t-\tau)y(t-\tau)}{b+y(t-\tau)}+\frac{(1-u_1)\beta_1 x_0}{a}v(t)-\frac{(1-u_1)\beta_1 x_0}{a}v(t-\tau)\\=&\left[\frac{(1-u_1)(1-u_3)c\alpha\beta_1 x_0}{\gamma a}+(1-u_2)\beta_2\frac{x(t)}{b+y(t)}-(\alpha+\mu)\right]y(t)\\&+(1-u_1)\beta_1\left[\frac{x(t-\tau)}{a+v(t-\tau)}-\frac{x_0}{a}\right]v(t-\tau).\end{aligned}\tag{3.12}$$

From (3.5), we have $\lim_{t\to\infty} supx(t)\le x_0$ and hence $x(t-\tau)\le x_0$. Therefore,

$$(1-u_1)\beta_1\left[\frac{x(t-\tau)}{a+v(t-\tau)}-\frac{x_0}{a}\right]v(t-\tau)\le 0.$$

As all solutions of (3.1) are positive and $\frac{1}{b+y(t)}\le\frac{1}{b}$, one can write

$$\begin{aligned}&\left[\frac{(1-u_1)(1-u_3)c\alpha\beta_1 x_0}{\gamma a}+(1-u_2)\beta_2\frac{x(t)}{b+y(t)}-(\alpha+\mu)\right]y(t)\le\\&\left[\frac{(1-u_1)(1-u_3)c\alpha\beta_1 x_0}{\gamma a}+(1-u_2)\frac{\beta_2 x_0}{b}-(\alpha+\mu)\right]y(t)\le 0,\end{aligned}$$

provided $\beta_2<\beta_2^*$ with $c<c^*(\beta_2)$. Under this restriction, Eq. (3.12) gives

$$\dot{H}(t)\le 0.$$

On the contrary, if $\beta_2>\beta_2^*$ then $c^*(\beta_2)<0$. So, to make $\dot{H}(t)\le 0$, c must be negative, which is impossible. Therefore, $\dot{H}(t)\le 0$ whenever $\beta_2<\beta_2^*$ with $c<c^*(\beta_2)$.

Now, let $A=\{(x(t),y(t),v(t))\in M:\dot{H}(t)=0\}$ and T be the largest invariant set in A. By La Salle's invariance principle [65], all nonnegative solutions convergence to T. Again, $\dot{H}(t)=0$ if and only if $x(t)=x_0, y(t)=v(t)=0$. Therefore, the largest invariance set of A is $T=\{E_1\}$ and every solutions in Σ goes to E_1 when $\beta_2<\beta_2^*$ and $c<c^*(\beta_2)$. Hence E_1 is globally asymptotically stable whenever $\beta_2<\beta_2^*$ and $c<c^*(\beta_2)$.

Theorem 3.5 *Assume the conditions of Lemma 3.2 hold. In the absence of delay, the infected steady state E^* is locally asymptotically stable if $S_1>0$, $S_2>0$ and $S_1S_2-S_3>0$ and unstable if at least one of them is negative, where S_i $(i=1,2,3)$ are defined below.*

Proof First we define the entries of the Jacobian matrix for E^* as

$$J_{ij} = m_{ij},\ K_{ij} = n_{ij},\ i,j = 1,2,3.$$

In the absence of delay, the characteristic equation (3.9) can be written as

$$\Phi(\lambda,0) = \lambda^3 + S_1\lambda^2 + S_2\lambda + S_3 = 0, \tag{3.13}$$

where

$$\begin{cases} S_1 = M_1 + N_1 = -(J_{11} + J_{22} + J_{33} + K_{22}), \\ S_2 = M_2 + N_2 = J_{11}J_{22} + J_{22}J_{33} + J_{33}J_{11} + J_{11}K_{22} + J_{33}K_{22} - J_{12}K_{21} - J_{32}K_{23}, \\ S_3 = M_3 + N_3 = -J_{11}J_{22}J_{33} + J_{12}J_{33}K_{21} - J_{13}J_{32}K_{21} - J_{11}J_{33}K_{22} + J_{11}J_{32}K_{23}, \\ S_1S_2 - S_3 = -J_{11}^2[J_{22} + J_{33} + K_{22}] - J_{22}^2[J_{11} + J_{33}] - J_{33}^2[J_{11} + J_{22} + K_{22}] \\ \qquad\qquad - K_{22}^2[J_{11} + J_{33}] - 2J_{11}J_{22}J_{33} - 2K_{22}[J_{11}J_{22} + J_{22}J_{33} + J_{11}J_{33}] \\ \qquad\qquad + J_{12}K_{21}[J_{11} + J_{22} + K_{22}] + J_{32}K_{23}[J_{22} + J_{33} + K_{22}] + J_{13}J_{32}K_{21}. \end{cases}$$

By Routh-Hurwitz criterion, E^* is locally asymptotically stable if $S_1 > 0$, $S_2 > 0$ and $S_1S_2 - S_3 > 0$ and unstable if at least one of them is negative.

Theorem 3.6 *Assume that the conditions of Lemma 3.2 and Lemma 3.5 are satisfied. (i) If (3.17) has no positive roots, then E^* is stable for all $\tau \geq 0$. (ii) If (3.17) has k positive root, $k = 1,2,3$, then there exists k critical values τ_j^*, $1 \leq j \leq k$; $j \in \mathbb{N}$, of τ such that E^* will change its stability and Hopf bifurcation will occur at these critical values.*

Proof For Hopf bifurcation, we investigate whether the characteristic equation (3.9) has a pair of purely imaginary roots $\lambda = \pm i\omega$, $\omega \in \mathbb{R}^+ - \{0\}$ for some parametric conditions. For this, we put $\lambda = i\omega$ in (3.9) and obtain

$$\alpha_1 cos(\omega\tau) + \alpha_2 sin(\omega\tau) - \alpha_3 + i(\alpha_2 cos(\omega\tau) - \alpha_1 sin(\omega\tau) - \alpha_4) = 0,$$

where

$$\alpha_1 = N_3 - N_1\omega^2,\ \alpha_2 = N_2\omega,\ \alpha_3 = M_1\omega^2 - M_3,\ \alpha_4 = \omega^3 - M_2\omega. \tag{3.14}$$

Separating real and imaginary parts, we have

$$\begin{cases} \alpha_1 cos(\omega\tau) + \alpha_2 sin(\omega\tau) = \alpha_3, \\ \alpha_2 cos(\omega\tau) - \alpha_1 sin(\omega\tau) = \alpha_4. \end{cases} \tag{3.15}$$

After some manipulations, we obtain

$$H(\omega_1) = \omega^6 + F_1\omega^4 + F_2\omega^2 + F_3 = 0, \tag{3.16}$$

where $F_1 = M_1^2 - 2M_2 - N_1^2,\ F_2 = M_2^2 + 2N_1N_3 - 2M_1M_3 - N_2^2,\ F_3 = M_3^2 - N_3^2$.

Setting $y = \omega^2$, Eq. (3.16) reads

$$H(y) = y^3 + F_1y^2 + F_2y + F_3 = 0. \tag{3.17}$$

The cubic equation (3.17) can have maximum three positive roots. If this equation has no positive roots, then there will be no switching of stability.

Now suppose (3.17) has k positive roots, $k = 1,2,3$, given by $y = y_j,\ 1 \le j \le k;\ j \in \mathbb{N}$. Corresponding to these k positive roots, one have k positive values of ω, say $\omega = \omega_j^* = \sqrt{y_j}$, $1 \le j \le k;\ j \in \mathbb{N}$. Therefore, for each ω_j^*, the Eq. (3.9) will have a pair of imaginary roots $\lambda = \pm i\omega_j^*$, and switching of stability might occur through a Hopf bifurcation at $\tau = \tau_j^*$, $1 \le j \le k$; $j \in \mathbb{N}$, where

$$\tau_j^* = \frac{1}{\omega_j^*}\arccos\Big(\frac{\alpha_1\alpha_3 + \alpha_2\alpha_4}{\alpha_1^2 + \alpha_2^2}\Big),\ \ 1 \le j \le k; j \in \mathbb{N},\ k = 1,2,3. \tag{3.18}$$

Here $\alpha_1, \alpha_2, \alpha_3, \alpha_4$ are calculated from (3.14) with $\omega = \omega_j^*$.

To show that the transversality condition is also satisfied, we differentiate Eq. (3.9) with respect to τ to obtain

$$\begin{aligned}
&[3\lambda^2 + 2M_1\lambda + M_2 + e^{-\lambda\tau}(2N_1 + N_2) - \tau e^{-\lambda\tau}(N_1\lambda^2 + N_2\lambda + N_3)]\frac{d\lambda}{d\tau}\\
&- \lambda e^{-\lambda\tau}(N_1\lambda^2 + N_2\lambda + N_3) = 0.\\
&\Longrightarrow (\frac{d\lambda}{d\tau})^{-1} = \frac{3\lambda^2 + 2M_1\lambda + M_2 + e^{-\lambda\tau}(2N_1\lambda + N_2)}{\lambda e^{-\lambda\tau}(N_1\lambda^2 + N_2\lambda + N_3)} - \frac{\tau}{\lambda}\\
&\Longrightarrow (\frac{d\lambda}{d\tau})^{-1} = \frac{3\lambda^2 + 2M_1\lambda + M_2}{-\lambda(\lambda^3 + M_1\lambda^2 + M_2\lambda + M_3)} + \frac{2N_1\lambda + N_2}{\lambda(N_1\lambda^2 + N_2\lambda + N_3)} - \frac{\tau}{\lambda}
\end{aligned}$$

From (3.15), we have $\alpha_1^2 + \alpha_2^2 = \alpha_3^2 + \alpha_4^2$. Using this relation and (3.14), the value of $(\frac{d\lambda}{d\tau})^{-1}$ at $\tau = \tau_j^*$, $\lambda = i\omega_j^*$ is given by

$$\begin{aligned}
\left[\left(\frac{d\lambda}{d\tau}\right)^{-1}\right]_{\lambda = i\omega_j^*,\ \tau = \tau_j^*} =& \frac{\Big((M_2 - 3\omega_j^{*2}) + 2iM_1\omega_j^*\Big)\Big(-\alpha_4 - i\alpha_3\Big)}{\alpha_1^2 + \alpha_2^2}\\
&+ \frac{\Big(N_2 + 2iN_1\omega_j^*\Big)\Big(-\alpha_2 - i\alpha_1\Big)}{\alpha_1^2 + \alpha_2^2}.
\end{aligned}$$

Substituting $\omega_j^* = \sqrt{y_j}$, we have

$$\left[Re\left(\frac{d\lambda}{d\tau}\right)^{-1}\right]_{\lambda=i\omega_j^*,\ \tau=\tau_j^*} = \frac{3y_j^2 + F_1 y_j + F_2}{\alpha_1^2 + \alpha_2^2}$$
$$= \frac{H'(\omega_j^{*2})}{(N_3 - N_1\omega_j^{*2})^2 + N_2^2\omega_j^{*2}} \neq 0, \text{ if } H'(\omega_j^{*2}) \neq 0,$$
$$1 \leq j \leq k; j \in \mathbb{N},\ k = 1,2,3.$$

Thus, the transversality condition of Hopf bifurcation at $\tau = \tau_j^*$ is verified. The direction of Hopf bifurcation depends on the signs of the transversality condition. If the sign of the transversality condition is positive, then the stability of E^* switches from stable to unstable through a Hopf bifurcation in the forward direction. Conversely, the negative transversality condition indicates that the stability of E^* changes from unstable to stable through a Hopf bifurcation in the backward direction.

Table 3.1: Parameter descriptions and their values with references

Parameter	Description	Range of parameters	References	Default values
s	Constant input rate of $CD4^+T$ cells	0-10 cells mm^{-3} day^{-1}	[91, 93, 174, 175]	10
μ	Death rate of susceptible $CD4^+T$ cells	0.07-0.1 day^{-1}	[175, 176]	0.01
β_1	Cell-free disease transmission coefficient	0.000025-0.5 virons mm^{-3} day^{-1}	[91, 93]	0.4
β_2	Cell-to-cell disease transmission coefficient	0.00001-0.7 mm^{-3} infected cells day^{-1}	[99]	varies
r	Proliferation rate of $CD4^+T$ cells	0.03-3 day^{-1}	[91, 93]	2
K	Carrying capacity of $CD4^+T$ cells	600-1600 cells mm^{-3}	[91, 94]	1100
α	Lysis death rate of infected $CD4^+T$ cells	$0.2 - 0.5$ day^{-1}	[84, 91]	0.3
c	Virus replication factor	10-2500 virions cell^{-1}	[93, 174]	varies
γ	Removal rate of virus	2-3 day^{-1}	[82, 91, 175]	3
a	Half-saturation constant			1
b	Half-saturation constant			1
τ	intracellular delay	Estimated from analytical result		varies

3.3.2 Numerical results

Here we present various numerical results of the system with the help of ODE45 and DDE23 of MATLAB R2015a, considering the parameter values of Table 3.1. The control parameters are considered as constant ($u_1 = u_2 = u_3 = 0.5$) for all numerical results. We calculate the critical value of β_2 as $\beta_2^* == 5.6389 \times 10^{-4}$. The critical value $c^*(\beta_2)$ of c can be calculated for any given value of β_2. Considering $\beta_2 = 0.0005 < \beta_2^*$, we get $c^*(\beta_2) = 0.0032$. From Lemma 3.4, E_1 is globally asymptotically stable if $\beta_2 < \beta_2^*$ with $c = 0.003 < c^*(\beta_2)$ for all delay $\tau \geq 0$. Such global behaviour of the system is presented in Fig. 3.1.

To discuss the stability of E^*, we first investigate the existence of infected steady state E^* of the system (3.1). First condition of Lemma 3.2 states that E^* exists if either $\beta_2 < \beta_2^*$ with $c > c^*(\beta_2)$, or $\beta_2 > \beta_2^*$ with $c > 0$. The considered parameter set satisfies the stability

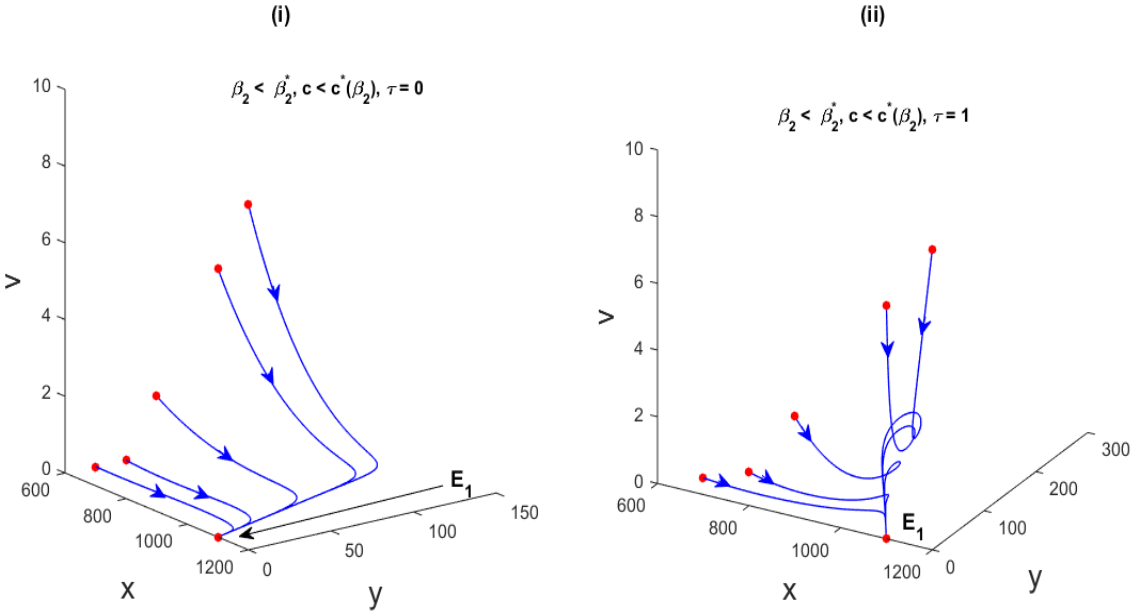

Figure 3.1: Time evolutions of the system (3.1) in the absence or presence of delay for $c = 0.003 < c^*(\beta_2) = 0.0032$ and $\beta_2 = 0.0005 < \beta_2^* = 5.6389 \times 10^{-4}$. Here $u_1 = u_2 = u_3 = 0.5$ and other parameters are in the Table 3.1. Figures (i) and (ii) show that E_1 is globally asymptotically stable for all delay $\tau \geq 0$.

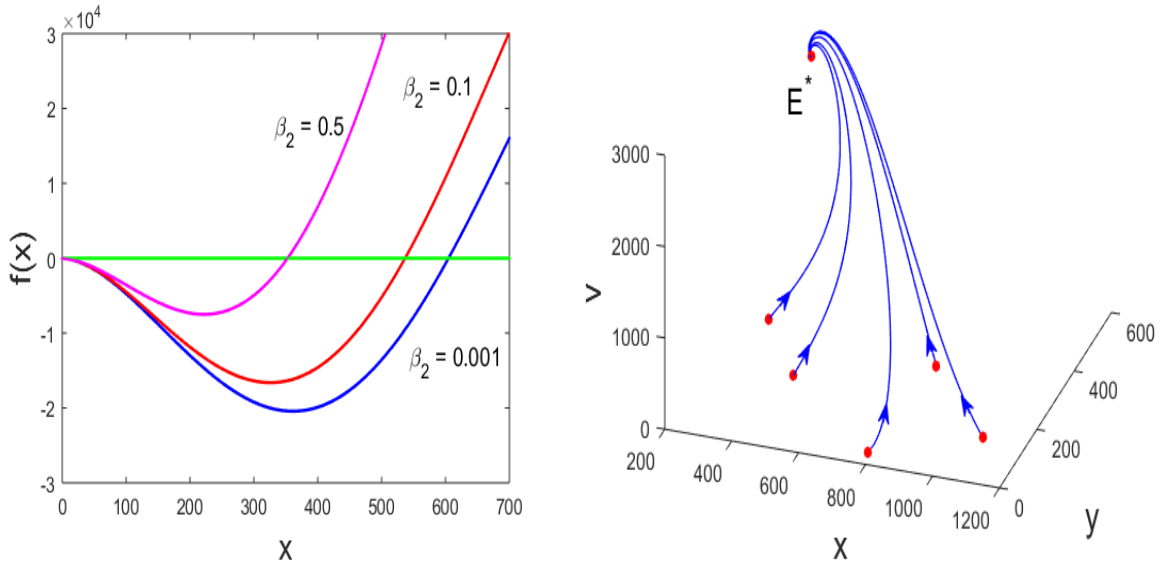

Figure 3.2: Left figure: This figure shows that the function $f(x)$ has a unique root for each value of $\beta_2 > \beta_2^*$ for fixed value of $c = 100$, implying the existence of a unique positive root of the equation (3.6) for each value of β_2. Right figure: The time evolution of the system in the absence of delay for $\beta_2 = 0.5 > \beta_2^* = 5.6389 \times 10^{-4}$ and $c = 100 > 0 > c^*(\beta_2)$. It shows that E^* is locally asymptotically stable. Other parameters are as in Fig. 3.1

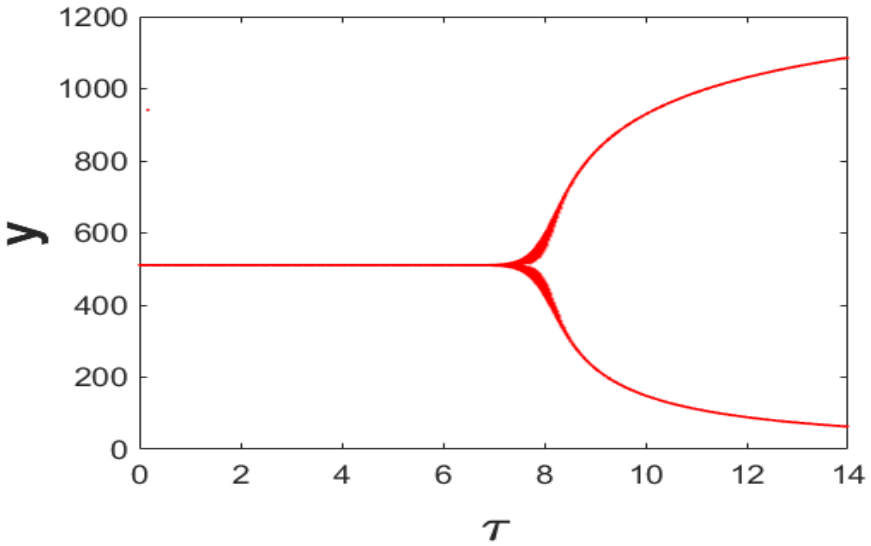

Figure 3.3: Bifurcation diagram of the infected CD4$^+$T cell population with respect to the intracellular delay τ. It demonstrates that y population switches its stability from stable to unstable at the Hopf bifurcation value $\tau = \tau^* = 8.1589$. Here $c = 100$ and $\beta_2 = 0.5$. Other parameters are as in Fig. 3.1

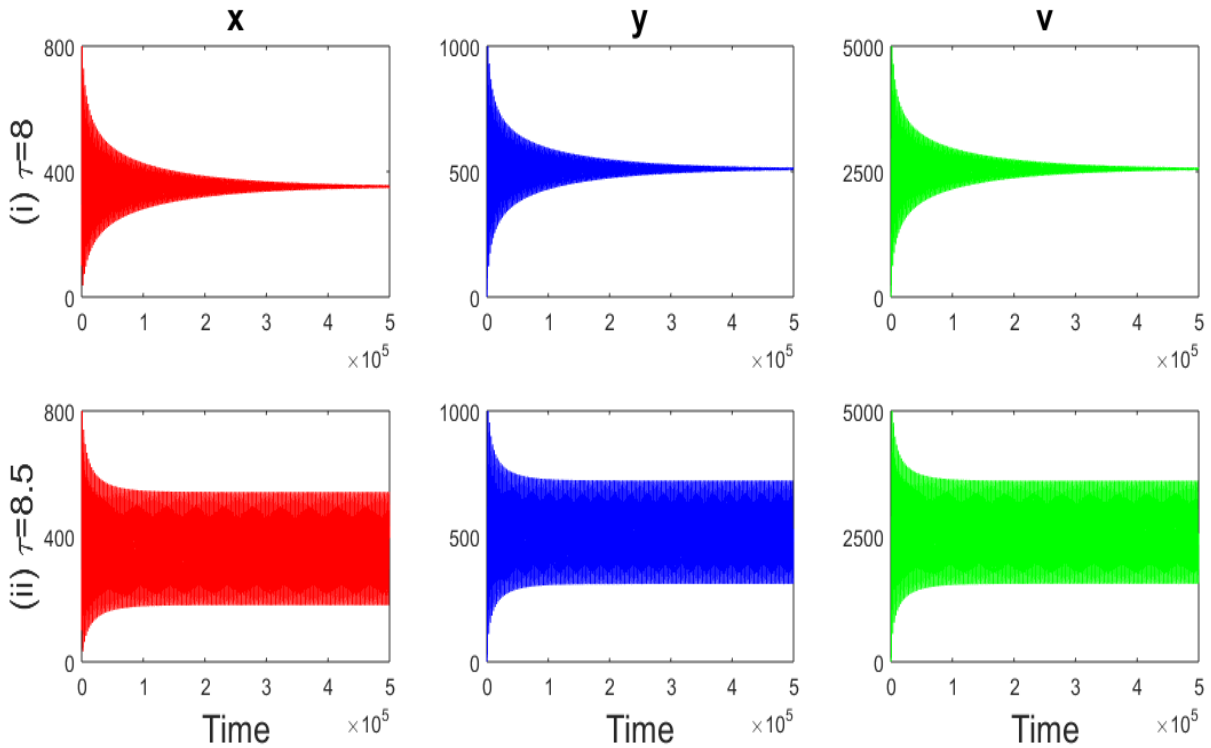

Figure 3.4: Upper row: The infected steady state E^* is stable for $\tau = 8 (< \tau^*)$. Lower row: The infected steady state E^* is unstable when $\tau = 8.5 (> \tau^*)$, where $\tau^* = 8.1589$. Here $c = 100$ and $\beta_2 = 0.5$. Other parameters are as in Fig. 3.1

condition of E^* with the existence condition $\beta_2 > \beta_2^*$. We took $c = 100$, $\beta = 0.5$ along with the other parameters as in the Table 3.1 for the simulations. The left diagram of Fig 3.2 shows that the function $f(x)$ (see (3.6)) crosses the horizontal line exactly once for each value of β_2, confirming the existence of a unique positive root $x = x^*$ of equation (3.6). Consequently, for unique x^*, we get a unique y^* and v^*. Hence a unique E^* exists for each $\beta_2 > \beta_2^*$ and any $c > 0$. In this case, the non-delayed system satisfies the stability condition for the parameter values in Table 3.1. In particular, for $c = 100$ and $\beta_2 = 0.5$, Fig. 3.2 (right figure) shows that the non-delayed system is locally asymptotically stable. However, for the delay-induced system, we find a critical value $\tau = \tau^* = 8.1589$ for the same set of parameter values. This indicates a Hopf bifurcation at $\tau = \tau^* = 8.1589$, where the delay-induced system changes its stability. The system is stable for $\tau < \tau^*$ and unstable for $\tau > \tau^*$ (see Fig. 3.3). The time evolutions presented in Fig. 3.4 show the stable and unstable behaviour of the system for two particular values of τ ($\tau = 8$ ($< \tau^*$) and $\tau = 8.5$ ($> \tau^*$)).

3.4 The Optimal Control problem

In this section, we consider that the controls u_i $(i = 1,2,3,)$ are time-dependent. The host cells $CD4^+T$ are white blood cells and fight against the infection. The HIV-1 virus kills these cells, causing a gradual depletion of $CD4^+T$ cells. Therefore, one of our objectives is to maximize the number of healthy $CD4^+T$ cells. The number of infected $CD4^+T$ cells increases through infection, which, in turn, increases the free virus particles and the cell-to-cell infection rate. So, our other target is to minimize the number of infected $CD4^+T$ cells and free virus using the control mechanisms. Therefore, we define the objective functional subject to the state (3.1) as:

$$J(u_1,u_2,u_3) = \int_0^{t_f} \left(A_1 x(t) - (A_2 y(t) + A_3 v(t) + \frac{B_1 u^2{}_1(t)}{2} + \frac{B_2 u^2{}_2(t)}{2} + \frac{B_3 u^2{}_3(t)}{2}) \right) dt. \tag{3.19}$$

In the integrand, the first positive term represents the benefit, and a negative sign represents the ensembled negative effects. Here $A_i > 0$, $i = 1,2,3$, are the weight constants which balance the size of the terms $x(t)$ and $y(t)$, respectively; B_1, B_2 and B_3 are positive weight constants which are employed to balance the deleterious side effects of the respective controls u_1, u_2 and u_3; and t_f is the terminal time.

Thus, our object is to find the optimal control triplet ($\hat{u_1}$, $\hat{u_2}$, $\hat{u_3}$)

$$J(\hat{u_1},\hat{u_2},\hat{u_3}) = \max_{(u_1,u_2,u_3)\in\Theta} J(u_1,u_2,u_3), \tag{3.20}$$

where, $\Theta = \{(u_1(t),u_2(t),u_3(t)) : u_i \text{ is measurable, } 0 \le u_i(t) \le 1, t \in [0,t_f],\ i = 1,2,3,\ t_f \text{ is the final time}\}$.

3.4.1 Existence of an optimal control triplet

Theorem 3.7 *There exists an optimal control triplet* $(\hat{u_1}, \hat{u_2}, \hat{u_3}) \in \Theta$ *with time-dependent control problem (3.1) that maximizes the objective functional* $J(u_1, u_2, u_3)$, *i.e.,* $J(\hat{u_1}, \hat{u_2}, \hat{u_3}) = \max_{(u_1,u_2,u_3)\in\Xi} J(u_1, u_2, u_3)$.

Proof To prove this Lemma, we use an existence result in Flaming and Rishel [71]. To apply this result, we check the following properties:

(a_1) The set of controls and corresponding state variables is nonempty.

(a_2) The control set Θ is convex and closed.

(a_3) The right hand side of the state system is continuous, bounded above by a sum of the bounded control and state, and can be written as a linear function of u_i with coefficients depending on the state and time.

(a_4) The integrand of the objective functional is concave on Θ.

(a_5) There exists constants $c_1,\ c_2 > 0$ and $b > 1$ such that the integrand of the objective functional is bounded above by $c_2 - c_1(|u_1(t)|^2 + |u_2(t)|^2 + |u_3(t)|^2)^{b/2}$.

In order to verify these properties, we use a result from Lukes [184] for the existence of solutions of (3.1) with bounded coefficients and (a_1) is satisfied. By the definition of Θ, (a_2) is satisfied. As our control system is linear in u_1, u_2 and u_3, the right-hand side of (3.1) satisfies (a_3) as the solutions are bounded. The integrand of the objective functional is concave for the control set Θ and hence a_4 is satisfied. For the last condition

$$\begin{aligned} A_1x - (A_2y + A_3v + \frac{B_1{u_1}^2}{2} + \frac{B_2{u_2}^2}{2} + \frac{B_3{u_3}^2}{2}) &\leq A_1x - (\frac{B_1{u_1}^2}{2} + \frac{B_2{u_2}^2}{2} + \frac{B_3{u_3}^2}{2}) \\ &\leq c_2 - c_1(|u_1|^2 + |u_2|^2 + |u_3|^2)^{\frac{b}{2}}, \end{aligned}$$

where c_2 depends on the upper bound of x, $b > 1$ and $c_1 > 0$ as $B_1, B_2, B_3 > 0$. Hence, we conclude that there exists an optimal control triplet.

3.4.2 Optimality system

Pontryagin's minimum principle [195] and state delay provides necessary conditions for an optimal control triplet $(\hat{u_1}, \hat{u_2}, \hat{u_3})$. This principle converts (3.1), (3.19) and (3.20) into a problem

which maximizes Hamiltonian, H,

$$\begin{aligned}
H(t;x,y,v;x_\tau,y_\tau,v_\tau;u_1,u_2,u_3;\lambda_1,\lambda_2,\lambda_3) = & \left(A_2y(t)+A_3v(t)+\frac{B_1{u_1}^2(t)}{2}+\frac{B_2{u_2}^2(t)}{2}\right.\\
&+\left.\frac{B_3{u_3}^2(t)}{2}-A_1x(t)\right)+\lambda_1\left(s-\mu x(t)+rx(t)\left(1-\frac{x(t)+y(t)}{K}\right)-(1-u_1(t))\frac{\beta_1x(t)v(t)}{a+v(t)}\right.\\
&\left.-(1-u_2(t))\frac{\beta_2x(t)y(t)}{b+y(t)}\right)+\lambda_2\left((1-u_1(t))\frac{\beta_1x(t-\tau)v(t-\tau)}{a+v(t-\tau)}\right.\\
&\left.+(1-u_2(t))\frac{\beta_2x(t-\tau)y(t-\tau)}{b+y(t-\tau)}-(\alpha+\mu)y(t)\right)\\
&+\lambda_3\left((1-u_3(t))c\alpha y(t)-\mu v(t)\right),
\end{aligned} \tag{3.21}$$

where $\lambda_i, i=1,2,3$ are co-state or adjoint variables. Applying Pontryagin's minimum principle with state delay [195], we obtain the following Lemma.

Theorem 3.8 *Suppose $(\hat{u_1},\hat{u_2},\hat{u_3})$ is an optimal control triplet of (3.19) subject to the system (3.1) and $(\hat{x},\hat{y},\hat{v})$ is the corresponding optimal solutions of (3.1), then there exists co-state or adjoint variables $\lambda_i,(i=1,2,3)$ such that the following conditions are satisfied with the system (3.1):*

i. co-state equation:

$$\begin{aligned}
\dot{\lambda}_1(t) = & A_1+\lambda_1(t)\left(\mu+(1-u_1(t))\frac{\beta_1v(t)}{a+v(t)}+(1-u_2(t))\frac{\beta_2y(t)}{b+y(t)}-r(1\right.\\
&\left.-\frac{2x(t)+y(t)}{K})\right)-\chi_{[0,t_f-\tau]}\lambda_2(t+\tau)\left((1-u_1(t+\tau))\frac{\beta_1v(t)}{a+v(t)}\right.\\
&\left.+(1-u_2(t+\tau))\frac{\beta_2y(t)}{b+y(t)}\right),\\
\dot{\lambda}_2(t) = & -A_2+\lambda_1(t)\left(\frac{rx(t)}{K}+(1-u_2(t))\frac{\beta_2bx(t)}{(b+y(t))^2}\right)+\lambda_2(t)(\alpha+\mu)\\
&-\lambda_3(t)(1-u_3(t))c\alpha-\chi_{[0,t_f-\tau]}\lambda_2(t+\tau)(1-u_2(t+\tau))\frac{\beta_2bx(t)}{(b+y(t))^2},\\
\dot{\lambda}_3(t) = & -A_3+\lambda_1(t)(1-u_1(t))\frac{\beta_1ax(t)}{(a+v(t))^2}+\lambda_3(t)\gamma\\
&-\chi_{[0,t_f-\tau]}\lambda_2(t+\tau)(1-u_1(t+\tau))\frac{\beta_1ax(t)}{(a+v(t))^2},
\end{aligned} \tag{3.22}$$

with transversality conditions $\lambda_i(t_f)=0, i=1,2,3.$

ii. optimality conditions:

$$H(\hat{x},\hat{y},\hat{v};\hat{u_1},\hat{u_2},\hat{u_3};\lambda_1,\lambda_2,\lambda_3)=H(\hat{x},\hat{y},\hat{v};u_1,u_2,u_3;\lambda_1,\lambda_2,\lambda_3),$$

which implies

$$\begin{aligned}
\hat{u_1}(t) =& min\left\{1, max\{0, \frac{\lambda_2(t)\frac{\beta_1\hat{x}(t-\tau)\hat{v}(t-\tau)}{a+\hat{v}(t-\tau)} - \lambda_1(t)\frac{\beta_1\hat{x}(t)\hat{v}(t)}{a+\hat{v}(t)}\}}{B_1}\right\},\\
\hat{u_2}(t) =& min\left\{1, max\{0, \frac{\lambda_2(t)\frac{\beta_2\hat{x}(t-\tau)\hat{y}(t-\tau)}{b+\hat{y}(t-\tau)} - \lambda_1(t)\frac{\beta_2\hat{x}(t)\hat{y}(t)}{b+\hat{y}(t)}\}}{B_2}\right\},\\
\hat{u_3}(t) =& min\left\{1, max\{0, \frac{\lambda_3(t)c\alpha\hat{y}(t)}{B_3}\}\right\}.
\end{aligned} \tag{3.23}$$

Proof By Pontryagin's minimum principle with state delay [195], the co-state equations and its transversality conditions can be obtained by

$$\begin{aligned}
\dot{\lambda_1}(t) =& -\frac{\partial H(t)}{\partial x} - \chi_{[0,t_f-\tau]}\frac{\partial H(t+\tau)}{\partial x_\tau}, \qquad \lambda_1(t_f) = 0,\\
\dot{\lambda_2}(t) =& -\frac{\partial H(t)}{\partial y} - \chi_{[0,t_f-\tau]}\frac{\partial H(t+\tau)}{\partial y_\tau}, \qquad \lambda_2(t_f) = 0,\\
\dot{\lambda_3}(t) =& -\frac{\partial H(t)}{\partial v} - \chi_{[0,t_f-\tau]}\frac{\partial H(t+\tau)}{\partial v_\tau}, \qquad \lambda_3(t_f) = 0,
\end{aligned} \tag{3.24}$$

where $\chi_{[0,t_f-\tau]}$ is the characteristic function defined as

$$\chi_{[0,t_f-\tau]} = \begin{cases} 1 \text{ if } t \in [0, t_f-\tau] \\ 0, \text{ otherwise.} \end{cases}$$

The optimal control triplet $\hat{u_1}, \hat{u_2}$ and $\hat{u_3}$ can be solved from the optimality conditions

$$\begin{aligned}
&\frac{\partial H(t)}{\partial u_1} = 0, \ at\ u_1(t) = \hat{u_1}(t);\ \frac{\partial H(t)}{\partial u_2} = 0, \ at\ u_2(t) = \hat{u_2}(t);\\
&\frac{\partial H(t)}{\partial u_3} = 0, \ at\ u_3(t) = \hat{u_3}(t).
\end{aligned} \tag{3.25}$$

On then obtain the following optimal system

$$
\begin{cases}
\dot{x}(t) = s - \mu x(t) + rx(t)\Big(1 - \frac{x(t)+y(t)}{K}\Big) - (1-u_1(t))\frac{\beta_1 x(t)v(t)}{a+v(t)} \\
\qquad - (1-u_2(t))\frac{\beta_2 x(t)y(t)}{b+y(t)}, \\
\dot{y}(t) = (1-u_1(t))\frac{\beta_1 x(t-\tau)v(t-\tau)}{a+v(t-\tau)} + (1-u_2(t))\frac{\beta_2 x(t-\tau)y(t-\tau)}{b+y(t-\tau)} - (\alpha+\mu)y(t), \\
\dot{v}(t) = (1-u_3(t))c\alpha y(t) - \gamma v(t), \\
\dot{\lambda}_1(t) = A_1 + \lambda_1(t)\Bigg(\mu + (1-u_1(t))\frac{\beta_1 v(t)}{a+v(t)} + (1-u_2(t))\frac{\beta_2 y(t)}{b+y(t)} - r(1 \\
\qquad - \frac{2x(t)+y(t)}{K})\Bigg) - \chi_{[0,t_f-\tau]}\lambda_2(t+\tau)\Bigg((1-u_1(t+\tau))\frac{\beta_1 v(t)}{a+v(t)} \\
\qquad + (1-u_2(t+\tau))\frac{\beta_2 y(t)}{b+y(t)}\Bigg), \\
\dot{\lambda}_2(t) = -A_2 + \lambda_1(t)\Bigg(\frac{rx(t)}{K} + (1-u_2(t))\frac{\beta_2 bx(t)}{(b+y(t))^2}\Bigg) + \lambda_2(t)(\alpha+\mu) \\
\qquad - \lambda_3(t)(1-u_3(t))c\alpha - \chi_{[0,t_f-\tau]}\lambda_2(t+\tau)(1-u_2(t+\tau))\frac{\beta_2 bx(t)}{(b+y(t))^2}, \\
\dot{\lambda}_3(t) = -A_3 + \lambda_1(t)(1-u_1(t))\frac{\beta_1 ax(t)}{(a+v(t))^2} + \lambda_3(t)\gamma \\
\qquad - \chi_{[0,t_f-\tau]}\lambda_2(t+\tau)(1-u_1(t+\tau))\frac{\beta_1 ax(t)}{(a+v(t))^2}, \\
\\
x(0) = x_0 > 0,\ y(0) = y_0 \geq 0,\ v(0) = v_0 \geq 0, \\
\lambda_i(t_f) = 0,\ i = 1,2,3, \\
\\
\text{where} \\
\hat{u_1}(t) = min\Bigg\{1, max\{0, \frac{\lambda_2(t)\frac{\beta_1 \hat{x}(t-\tau)\hat{v}(t-\tau)}{a+\hat{v}(t-\tau)} - \lambda_1(t)\frac{\beta_1 \hat{x}(t)\hat{v}(t)}{a+\hat{v}(t)}}{B_1}\}\Bigg\}, \\
\hat{u_2}(t) = min\Bigg\{1, max\{0, \frac{\lambda_2(t)\frac{\beta_2 \hat{x}(t-\tau)\hat{y}(t-\tau)}{b+\hat{y}(t-\tau)} - \lambda_1(t)\frac{\beta_2 \hat{x}(t)\hat{y}(t)}{b+\hat{y}(t)}}{B_2}\}\Bigg\}, \\
\hat{u_3}(t) = min\Bigg\{1, max\{0, \frac{\lambda_3(t)c\alpha\hat{y}(t)}{B_3}\}\Bigg\}.
\end{cases}
\tag{3.26}
$$

3.4.3 Numerical results

We solve the optimal system (3.26) numerically using combination of forward and backward difference approximation method [196] in MATLAB R2015a. The initial values of the state variables are considered as $x(0) = 500, y(0) = 100, v(0) = 100$ [116]. Since A_1 and A_2 are the weight parameters associated with $CD4^+T$ cells, we give the same weight value for these parameters. It is assumed that the allotted drugs/inhibitors' harmful effects are the same, allowing us to take the same weight value of the parameters B_1, B_2 and B_3. We consider both the mono-drug and multi-drug therapies and observe which therapy gives better control to viremia in the presence of intracellular delay τ.

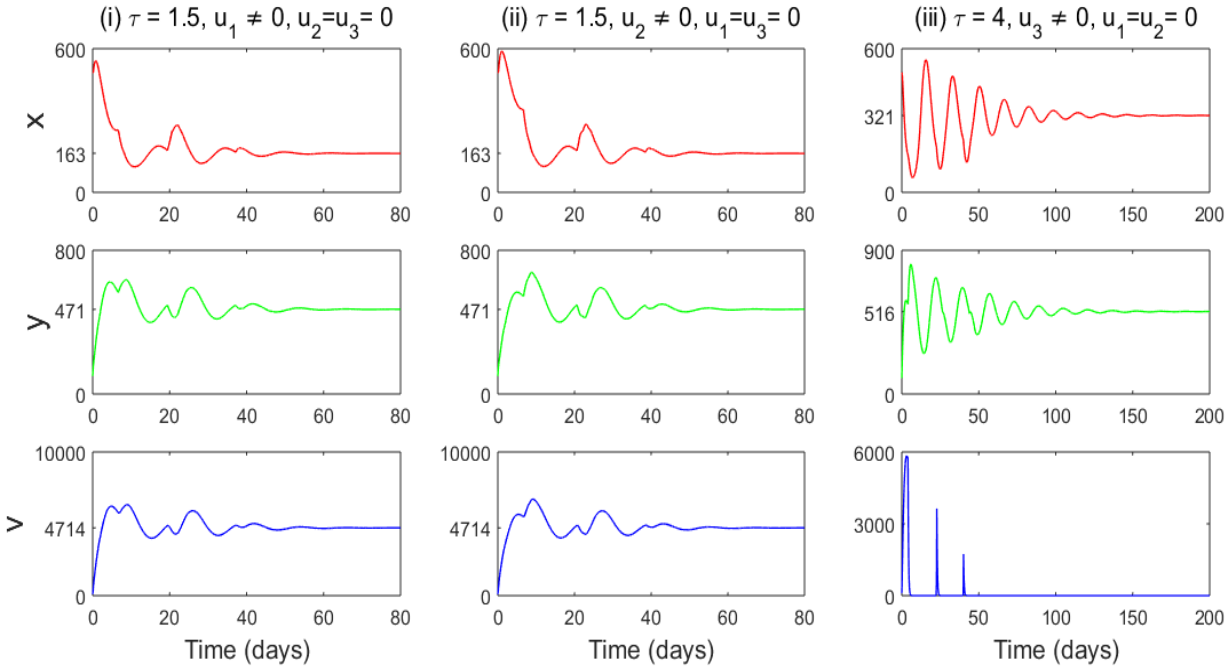

Figure 3.5: Time evolutions of susceptible CD4$^+$T cells (x), infected CD4$^+$T cells (y), and virus particles (v) for different mono-drug therapies in the presence of different delay τ. First two columns represent, respectively, the time variations corresponding u_1 blocker ($u_1 \neq 0, u_2 = u_3 = 0$) and u_2 blocker ($u_2 \neq 0, u_1 = u_3 = 0$) for $\tau = 1.5$. Third column indicate the same with u_3 blocker ($u_3 \neq 0, u_1 = u_2 = 0$) for $\tau = 4$. Here $A_1 = A_2 = A_3 = 10$, $B_1 = B_2 = B_3 = 0.1$. Other parameter values are as in Fig. 3.4.

3.4.3.1 Mono-drug therapy

Here we present the computational results to compare the efficacy of different inhibitors with mono-drug therapy protocol in the presence of different delays. The first two columns of Fig. 3.5 show that the healthy CD4$^+$T cell, infected CD4$^+$T cell and free virus counts become stable in a short time (about 60 days) when the mono-drug therapies $(u_1 \neq 0, u_2 = 0 = u_3)$ or $(u_2 \neq 0, u_1 = 0 = u_3)$ are administered with $\tau = 1.5$ but fluctuate if the length of delay is increased to $\tau = 2.5$ days (see the first two columns of Fig. 3.6). However, the mono-drug therapy $(u_3 \neq 0, u_1 = 0 = u_2)$ can tolerate longer delay. All populations remain stable even when the length of the delay is 4 day (see the third column of Fig. 3.5). Though the free virus counts, in this case, go very low, the infected CD4$^+$T cell count is higher. If the length of the delay is further increased (say $\tau = 4.5$), then the system becomes unstable with sustained oscillations (see the third column of Fig. 3.6).

3.4.3.2 Multi-drug therapy

As in the previous chapter, we apply different multi-drug therapies: (i) $u_1 \neq 0, u_2 \neq 0, u_3 = 0$, (ii) $u_1 = 0, u_2 \neq 0, u_3 \neq 0$, (iii) $u_1 \neq 0, u_2 = 0, u_3 \neq 0$ and (iv) $u_1 \neq 0, u_2 \neq 0, u_3 \neq 0$ to observe the viremia. The comparison results of all four multi-drug therapies are presented in

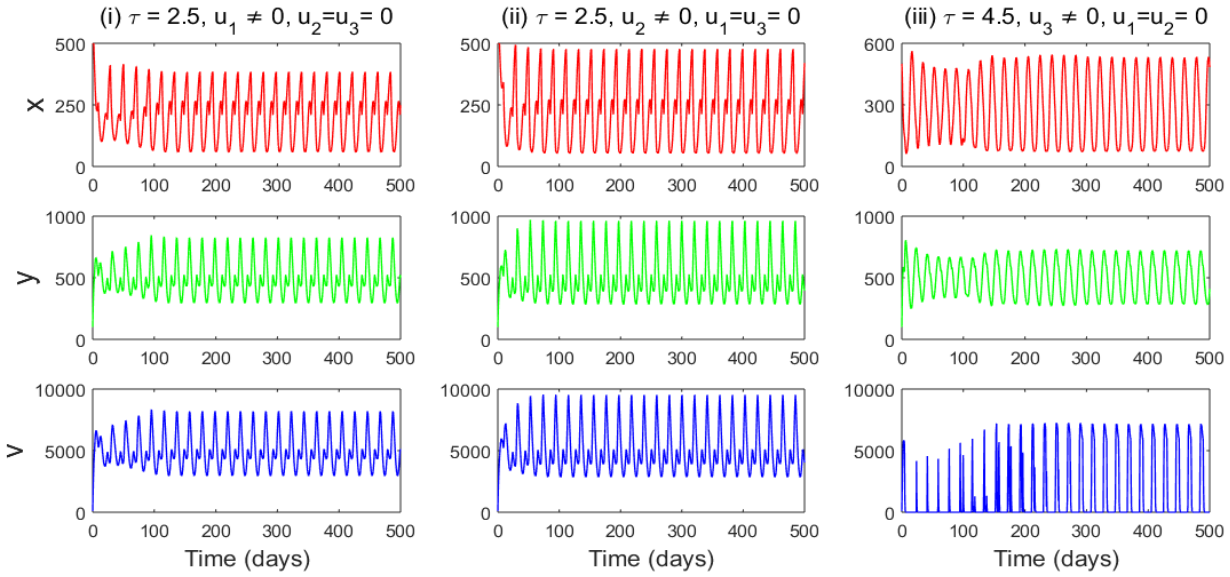

Figure 3.6: Time evolutions of susceptible CD4$^+$T cells (x), infected CD4$^+$T cells (y), and virus particles (v) for different mono-drug therapies in the presence of different delay τ. First two columns decipher the time variations corresponding to u_1 blocker ($u_1 \neq 0, u_2 = u_3 = 0$) and u_2 blocker ($u_2 \neq 0, u_1 = u_3 = 0$) for $\tau = 2.5$. Third column represent the same with u_3 blocker ($u_3 \neq 0, u_1 = u_2 = 0$) for $\tau = 4.5$. Parameter values are as in Fig. 3.5

Fig. 3.7. It shows that both the infected CD4$^+$T cell and the virus particle go to extinction in all cases except the third protocol, where $u_1 \neq 0, u_2 = 0, u_3 \neq 0$. In this latter case, the virus particle becomes extinct, but the infected CD4$^+$T cells persist, indicating that this multi-drug combination is ineffective in controlling the viremia. If we look at the control profiles of multi-drug therapies (i), (ii) and (iv) of Fig. 3.7, considering the cost and other deleterious side effects of antiretroviral drugs, multi-drug therapies ($u_1 \neq 0, u_2 \neq 0, u_3 = 0$), ($u_1 = 0, u_2 \neq 0, u_3 \neq 0$) would be better for removing HIV-1 infection compared to the ($u_1 \neq 0, u_2 \neq 0, u_3 \neq 0$) multi-drug therapy. The corresponding control variables are presented in the last row. It indicates that the multi-drug therapy ($u_2 \neq 0, u_3 \neq 0, u_1 = 0$) has a better profile compared to the therapy ($u_1 \neq 0, u_2 \neq 0, u_3 = 0$) because in the former case the inhibitor u_2 is no longer require after 23 days for controlling the infection, whereas in the former case both the controls are required to apply throughout the treatment period. The last control ($u_1 \neq 0, u_2 \neq 0, u_3 \neq 0$) is slightly better than the second control but its cost would be high as it considers all three inhibitors.

3.5 Discussion

We considered a multi-pathways in-host HIV-1 infection model with saturated infection rates and intracellular delay using three controls in this chapter. We analyzed it under two cases: the controls are constant or time-dependent. This study is an extension of our previous study presented in the last chapter. We considered here a saturated type incidence rate instead of a bilin-

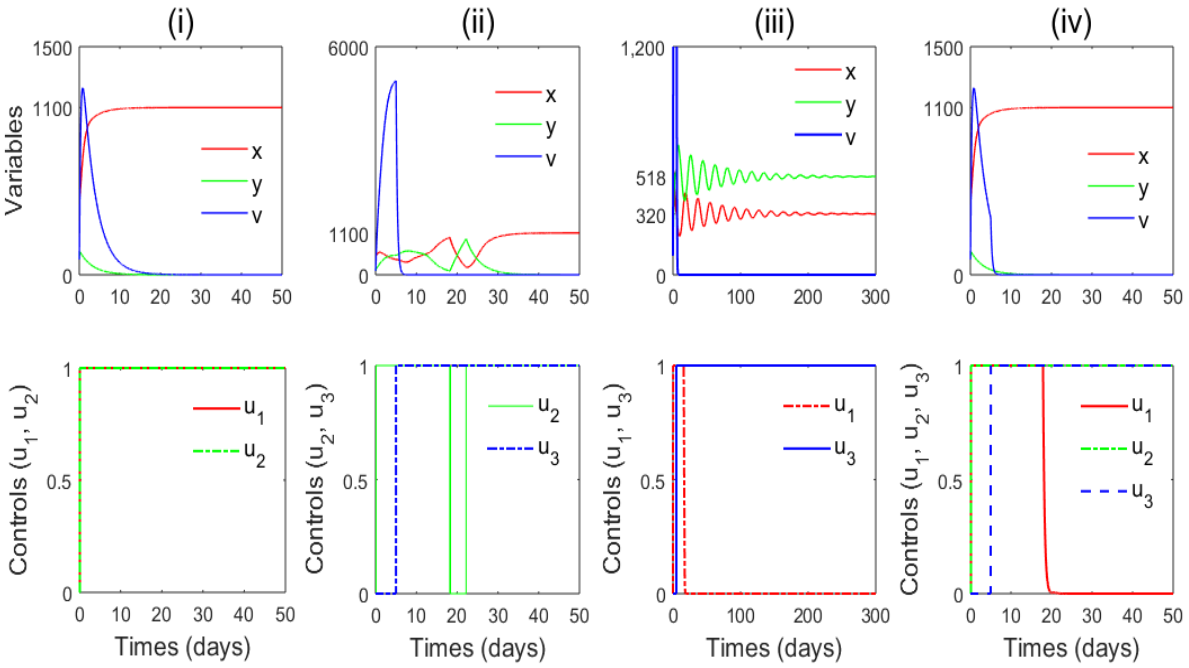

Figure 3.7: Upper row: Changes in the counts of susceptible CD4$^+$T cells (x), infected CD4$^+$T cells (y), and virus particles (v) for different multi-drug therapies with $\tau = 5$. Lower row: The corresponding optimal controls. The parameters are as in Fig. 3.5

ear type and incorporated the proliferation of susceptible CD4$^+$T cells. Further, an intracellular delay was considered in the infection transmission terms to make the model biologically more realistic. In the case of constant controls, we proved that the infection-free equilibrium of the system is locally and globally asymptotically stable for any delay if the parameters satisfy the restrictions $\beta_2 < \beta_2^*$. The delay may, however, affect the stability of the infected equilibrium through Hopf bifurcation. The infected equilibrium is locally asymptotically stable if the intracellular delay is shorter than some critical value. The stability, however, is lost if the delay becomes longer. In the case of time-dependent controls, we define a suitable objective functional to maximize the cell counts of healthy CD4$^+$T cells and minimize the infected CD4$^+$T cells and the virus particles. We derived the optimality conditions of our delay-induced control problem. We numerically observed and compared the results of different time-dependent control therapies. In the case of mono-drug treatment, no blocker can remove the infection for any delay, as infected CD4$^+$ T cells always remain present in the system. Interestingly, the mono-blocker, where $u_3 \neq 0$ but $u_1 = 0 = u_2$, can send the virus level to an undetectable stage, but the infected cells persist through cell-to-cell transmission. In the case of multi-drug therapy, the infection can be removed by all multi-drug therapies for any delay, except the combination of RTI and PI inhibitors. The result shows that a multi-drug therapy scheme that contains u_2 and u_3 blockers is a better option for treating HIV-1 infection. The result also indicates that the treatment duration depends on delay, i.e., if the delay is shorter, then the treatment period is also shorter.

4

Optimal drug therapy in a multi-pathways HIV-1 infection model with immune response delays[1]

4.1 The Model

A basic HIV in-host infection model considers the interaction between the host cells ($CD4^+T$) and virus particles without considering the role of cytotoxic T lymphocytes (CTL) or $CD8^+T$ cells, which on activated by $CD4^+T$ cells, kills the infected cells directly. Basic models also do not consider the infection spreading through cell-to-cell mode. Recently, some mathematical models have extended the basic model by considering the multi-mode dissemination of disease [129–132]. Acknowledging the controlling role of CTL cells, Lai and Zou [187] considered a four-dimensional multi-pathways in-host model. Since immune activation is not instantaneous but mediated by some time lag. Xu and Zhou [133] modified the model of Lai and Zou [187]

[1]The bulk of this chapter has been published in Trends in Biomathematics ed. By R. P. Mondaini, Springer Verlag, (2022). (Accepted).

taking into consideration the CTL activation delay and analyzed the model

$$\begin{aligned}
\dot{x}(t) &= s - dx(t) + rx(t)\left(1 - \frac{x(t)+\alpha y(t)}{K}\right) - \beta_1 x(t)v(t) - \beta_2 x(t)y(t),\\
\dot{y}(t) &= \beta_1 x(t)v(t) + \beta_2 x(t)y(t) - \sigma y(t) - d_1 y(t)z(t),\\
\dot{v}(t) &= c\sigma y(t) - d_2 v(t),\\
\dot{z}(t) &= py(t-\tau) - d_3 z(t).
\end{aligned} \tag{4.1}$$

Here $x(t), y(t), v(t)$ and $z(t)$ represent, respectively, the concentrations of susceptible CD4$^+$T cells (target cells), productively infected CD4$^+$T cells, free plasma virus and CTL cells at time t. Target cells are infected by free virus particle as well as infectious CD4$^+$T cells following mass action law with rate constants β_1 and β_2, respectively. The time required for the activation of CTL cells is represented by τ. Here s is the constant input rate, d is the death rate, r $(> d)$ is the proliferation rate, K is the maximum density of CD4$^+$T cells, and α is a limitation coefficient of infected cells. The parameters d_1, d_2, and d_3 represent, respectively, the killing rate of infected cells by CTL, clearance rate of virus particles, and clearance rate of CTL. The virus replication factor is represented by c, and p is the production rate of CTL. The model 4.1 was analyzed by Xu and Zou [133].

It is to be mentioned that an infected cell may die naturally or through cell-lysis [91, 197]. In model (4.1), both types of death have been represented by a single term $\sigma y(t)$ and the production rate of new virus particles has been represented by $c\sigma y(t)$, where c is the number of new viruses produced per cell lysis. This may cause an overestimation of free virus in the blood plasma because the free virus can be created only through cell lysis, whereas no virus protein can be released during normal cell death. Taking care of this fact, we split the total death rate (σ) of the infected cells into two parts: natural death, d, and death due to cell lysis, μ, (i.e., $\sigma = d + \mu$). Here all parameters are non-negative. We now introduce three blockers to reduce viremia. A control $u_1(t) \in [0,1]$ is applied to reduce the transmission of infection through cell-free mode. This control is mainly reverse transcriptase inhibitor (RTI) drugs that block the synthesis of viral DNA from HIV-1 RNA, thereby reducing viral infectivity. A second control $u_2(t) \in [0,1]$ is used to block the cellular mechanisms required for synapse formation, the primary mechanism of cell-to-cell transmission of HIV. We call it a synapse-forming inhibitor (SI). The third control $u_3(t) \in [0,1]$ is applied to prevent HIV-1 protease from cleaving the HIV-1 polyprotein into functional units, popularly known as protease inhibitor (PI). Introducing

these modifications, the model (4.1) reads

$$\begin{aligned}
\dot{x}(t) &= s - dx(t) + rx(t)\Big(1 - \frac{x(t)+\alpha y(t)}{K}\Big) - (1-u_1(t))\beta_1 x(t)v(t) \\
&\quad - (1-u_2(t))\beta_2 x(t)y(t), \\
\dot{y}(t) &= (1-u_1(t))\beta_1 x(t)v(t) + (1-u_2(t))\beta_2 x(t)y(t) - (d+\mu)y(t) - d_1 y(t)z(t), \\
\dot{v}(t) &= (1-u_3(t))c\mu y(t) - d_2 v(t), \\
\dot{z}(t) &= py(t-\tau) - d_3 z(t).
\end{aligned} \tag{4.2}$$

The initial conditions are taken as

$$\begin{aligned}
&x(\theta) = \phi_1(\theta) > 0, y(\theta) = \phi_2(\theta) > 0, v(\theta) = \phi_3(\theta) > 0, z(\theta) = \phi_4(\theta) > 0, \theta \in [-\tau, 0], \\
&\text{where } \phi = (\phi_1, \phi_2, \phi_3, \phi_4) \in C = C([-\tau, 0], \mathbb{R}^4_+) \text{ with} \\
&\phi_i(\theta) \geq 0 \ (\theta \in [-\tau, 0], i = 1,2,3,4), (\phi_1(0), \phi_2(0), \phi_3(0), \phi_4(0)) \in C.
\end{aligned} \tag{4.3}$$

The objectives are to (i) observe how far these blockers can control the viremia, (ii) know whether multi-drug therapy is beneficial over mono-drug therapy, considering toxicities of the antiviral drugs, (iii) explore how immune response delay affect the plasma viral load in the presence and absence of the blockers and (iv) have insights about the optimal dose of the blockers.

The chapter is arranged in the following sequence. In Section 4.2, we present some preliminary results. Section 4.3 represents the system analysis and its simulations when controls are constant. Section 4.4 deals with the optimal management of the system when controls are time-dependent. A comparison of different control schemes is presented here. The chapter ends with a discussion in Section 4.5.

4.2 Preliminary results

4.2.1 Existence and uniqueness of solution

Let $N = C([-\tau, 0], \mathbb{R}^4_+)$ be the Banach space of continuous real-valued functions from $[-\tau, 0]$ *to* $\mathbb{R}^4_+$ with sup-norm $\|\phi\| = sup_{-\tau \leq \theta \leq 0}\{|\phi_1(\theta)|, |\phi_2(\theta)|, |\phi_3(\theta)|, |\phi_4(\theta)|\}$. Following fundamental theory of functional differential equations [198], for any $\phi \in N$ and initial conditions (4.3), the system (4.2) has a unique solution

$$\Omega(t, \phi) = (x(t, \phi), y(t, \phi), v(t, \phi), z(t, \phi)).$$

One can easily prove the following lemma from [133].

Lemma 4.1 *Let $\Omega(t,\phi) = (x(t), y(t), v(t), z(t))$ be a solution of the system (4.2) with initial conditions (4.3). Then the solution is positively invariant provided $u_1(t) = u_2(t) = 1$ does not hold simultaneously and $u_3(t) \in [0,1)$. The solution is uniformly bounded on the region*

$$\Theta = \left\{ \begin{array}{c} \Omega(t,\phi) \in \mathbb{R}^4_+ \mid 0 < x(t) \leq x_0, 0 \leq y(t) \leq \frac{M}{\delta}, 0 \leq v(t) \leq \frac{(1-u_3)cd_1M}{\delta d_2}, \\ 0 \leq z(t) \leq \frac{pM}{\delta d_4} \end{array} \right\}, \tag{4.4}$$

where $x_0 = \frac{K}{2r}[(r-d) + \sqrt{(r-d)^2 + \frac{4rs}{K}}]$, $\delta = min\{d, (d+\mu)\}$, $M = s + \frac{rK}{4}$. Moreover, there exists $\Psi_0 > 0$ such that $\liminf_{t\to\infty} x(t) > \Psi_0$, i.e., $x(t)$ is uniformly bounded away from zero.

4.3 Model analysis with fixed controls

Control parameters $u_i, i = 1,2,3$, may be either constant or time-dependent. Here we analyze the model treating control parameters as constant and in the next section the controls are considered as time-dependent.

4.3.1 Basic reproduction number

A threshold quantity, R_0, called the basic reproduction number, is used to determine whether an infection will spread over time or it will be washed out. It is considered to be an essential threshold quantity for the elimination of infection. Typically, R_0 is defined by the expected number of secondary cases produced by an infected cell in a completely susceptible host population [199]. Using the next-generation matrix [180], one can easily prove the following proposition.

Lemma 4.2 *If R_0 be the basic reproduction number of the system (4.2) and R_{01}, R_{02} are the respective basic reproduction numbers corresponding to the cell-free infection mode (i.e., $\beta_2 = 0$) and cell-to-cell infection mode (i.e., $\beta_1 = 0$) then $R_0 = R_{01} + R_{02}$, where $R_0 = \frac{[(1-u_1)(1-u_3)c\mu\beta_1 + (1-u_2)\beta_2 d_2]x_0}{d_2(d+\mu)}$, $R_{01} = \frac{(1-u_1)(1-u_3)c\mu\beta_1 x_0}{d_2(d+\mu)}$, $R_{02} = \frac{(1-u_2)\beta_2 d_2 x_0}{d_2(d+\mu)}$ and $x_0 = \frac{K}{2r}[(r-d) + \sqrt{(r-d)^2 + \frac{4rs}{K}}]$ is the equilibrium density of CD4$^+$T cells in infection-free state.*

Proof The basic reproduction number is determined using the next generation matrix [180]. The Jacobian matrix J_{11} of the system (4.2) at $(x_0, 0, 0, 0)$ is

$$J_{11} = \begin{pmatrix} -d + r(1 - \frac{2x_0}{K}) & \frac{-r\alpha x_0}{K} - (1-u_2)\beta_2 x_0 & -(1-u_1)\beta_1 x_0 & 0 \\ 0 & (1-u_2)\beta_2 x_0 - (d+\mu) & (1-u_1)\beta_1 x_0 & 0 \\ 0 & (1-u_3)c\mu & -d_2 & 0 \\ 0 & p & 0 & -d_3 \end{pmatrix}.$$

The sub-matrix of J_{11} associated with the infectious compartments can be written as

$$J_{12} = \begin{pmatrix} (1-u_2)\beta_2 x_0 - (d+\mu) & (1-u_1)\beta_1 x_0 \\ (1-u_3)c\mu & -d_2 \end{pmatrix} = \begin{pmatrix} (1-u_2)\beta_2 x_0 & (1-u_1)\beta_1 x_0 \\ 0 & 0 \end{pmatrix} - \begin{pmatrix} (d+\mu) & 0 \\ -(1-u_3)c\mu & d_2 \end{pmatrix} = F - V.$$

Then the next generation matrix [180] is defined as

$$FV^{-1} = \frac{1}{d_2(d+\mu)} \begin{pmatrix} (1-u_1)(1-u_3)c\mu\beta_1 x_0 + (1-u_2)d_2\beta_2 x_0 & (1-u_1)(d+\mu)\beta_1 0_0 \\ 0 & 0 \end{pmatrix}.$$

The basic reproduction number R_0 is then obtained from the spectral radius [180] of the matrix FV^{-1} as

$$\begin{aligned} R_0 &= \frac{[(1-u_1)(1-u_3)c\mu\beta_1 + (1-u_2)\beta_2 d_2]x_0}{d_2(d+\mu)} \\ &= (1-u_1)\beta_1 x_0 \frac{1}{(d+\mu)}(1-u_3)c\mu\frac{1}{d_2} + (1-u_2)\beta_2 x_0 \frac{1}{(d+\mu)}. \end{aligned} \tag{4.5}$$

In the expression of R_0, the terms $(1-u_1)\beta_1$ and $(1-u_2)\beta_2$ indicate, respectively, the effective infection rate corresponding to the cell-free and cell-to-cell infection modes; x_0 is the equilibrium value of CD4$^+$T cells in the absence of infection; $\frac{1}{(d+\mu)}$ is the average life span of infected CD4$^+$T cells; $(1-u_3)c\mu$ is the number of virus produced from the infected CD4$^+$T cells and $\frac{1}{d_2}$ is the average life span of virus.
For cell-free infection mode (i.e., $\beta_2 = 0$), J_{11} can be rewritten as

$$J_{21} = \begin{pmatrix} -d + r(1-\frac{2x_0}{K}) & \frac{-r\alpha x_0}{K} & -(1-u_1)\beta_1 x_0 & 0 \\ 0 & -(d+\mu) & (1-u_1)\beta_1 x_0 & 0 \\ 0 & (1-u_3)c\mu & -d_2 & 0 \\ 0 & p & 0 & -d_3 \end{pmatrix}.$$

The sub-matrix of J_{21} associated with the infectious compartments can be written as

$$J_{22} = \begin{pmatrix} -d_1 & (1-u_1)\beta_1 x_0 \\ (1-u_3)Nd_1 & -d_2 \end{pmatrix} = \begin{pmatrix} 0 & (1-u_1)\beta_1 x_0 \\ 0 & 0 \end{pmatrix} - \begin{pmatrix} (d+\mu) & 0 \\ -(1-u_3)c\mu & d_2 \end{pmatrix} = F_1 - V_1.$$

One can then similarly compute the basic reproduction number in the case of cell-free infection mode as

$$R_{01} = \frac{(1-u_1)(1-u_3)c\mu\beta_1 x_0}{d_2(d+\mu)} = (1-u_1)\beta_1 x_0 \frac{1}{(d+\mu)}(1-u_3)c\mu\frac{1}{d_2}.$$

Similarly, the basic reproduction number R_{02} corresponding to the cell-to-cell infection mode (i.e., $\beta_1 = 0$) is

$$R_{02} = \frac{(1-u_2)d_2\beta_2 x_0}{d_2(d+\mu)}.$$

Thus, the basic reproduction number of the system is the sum of the basic reproduction numbers of two subsystems and is given by $R_0 = R_{01} + R_{02}$.

4.3.2 Equilibria of the system

It is easy to see that the system (4.2) has two equilibrium points. A disease-free equilibrium point $E_0 = (x_0, 0, 0, 0)$, where $x_0 = \frac{K}{2r}[(r-d) + \sqrt{(r-d)^2 + \frac{4rs}{K}}]$ and an infected equilibrium point $E^* = (x^*, y^*, v^*, z^*)$, where $x^* = \frac{1}{2A}(-2B + \sqrt{B^2 - 4As})$, $y^* = \frac{d_3(d+\mu)}{d_1 p}(\frac{x^* R_0}{x_0} - 1)$, $v^* = \frac{(1-u_3)c\mu y^*}{d_2}$, $z^* = \frac{py^*}{d_3}$. Here x^* is the positive root of the quadratic equation

$$Ax^{*2} - Bx^* - s = 0, \tag{4.6}$$

where $A = \frac{r}{K}(1 + \frac{\alpha d_3(d+\mu)R_0}{d_1 p x_0}) + \frac{d_3(d+\mu)^2 R_0^2}{d_1 p x_0^2}$ (> 0) and $B = (r-d) + \frac{r\alpha d_3(d+\mu)}{d_1 K p} + \frac{d_3(d+\mu)^2 R_0}{d_1 p x_0}$ (> 0). As $A > 0, B > 0$, Eqn. (4.6) always has a unique positive root. Note that y^* exists if and only if $R_0 > \frac{x_0}{x^*}$. Susceptible CD4$^+$T cells attains its maximum value x_0 in the absence of infection, giving $x_0 > x^*$. Hence, a sufficient condition for the existence of y^* is $R_0 > 1$. If y^* exists, then v^* exists if $0 \leq u_3 < 1$. Thus, there exists a unique infected equilibrium point E^* if

(i) $R_0 > 1$,

(ii) $u_1 = 1 = u_2$ does not hold simultaneously and

(iii) $u_3 \in [0, 1)$.

4.3.3 Stability of the equilibrium points

Consider the perturbations

$$X(t) = x(t) - \bar{x},\ Y(t) = y(t) - \bar{y},\ V(t) = v(t) - \bar{v},\ Z(t) = z(t) - \bar{z},$$

where $(\bar{x},\ \bar{y},\ \bar{v},\ \bar{z})$ is any arbitrary equilibrium point of the system (4.2). Then the linearzied system in the matrix form reads

$$\frac{dQ}{dt} = MQ(t) + NQ(t-\tau),$$

where

$$M = \begin{pmatrix} a_{11} & a_{12} & a_{13} & 0 \\ a_{21} & a_{22} & a_{23} & a_{24} \\ 0 & a_{32} & a_{33} & 0 \\ 0 & 0 & 0 & a_{44} \end{pmatrix},\ N = \begin{pmatrix} 0 & 0 & 0 & 0 \\ 0 & 0 & 0 & 0 \\ 0 & 0 & 0 & 0 \\ 0 & b_{42} & 0 & 0 \end{pmatrix},\ Q(t) = \begin{pmatrix} X(t) & Y(t) & V(t) & Z(t) \end{pmatrix}^T,$$

and the entries of the matrices M and N are

$$\begin{cases} a_{11} = -d + r\left(1 - \frac{2\bar{x}+\alpha\bar{y}}{K}\right) - (1-u_1)\beta_1\bar{v} - (1-u_2)\beta_2\bar{y},\ a_{12} = -\frac{r\alpha\bar{x}}{K} - (1-u_2)\beta_2\bar{x}, \\ a_{13} = -(1-u_1)\beta_1\bar{x}, a_{21} = (1-u_1)\beta_1\bar{v} + (1-u_2)\beta_2\bar{y}, \\ a_{22} = (1-u_2)\beta_2\bar{x} - (d+\mu) - d_1\bar{z}, a_{23} = (1-u_1)\beta_1\bar{x},\ a_{24} = -d_1\bar{y}, \\ a_{32} = (1-u_2)c\mu,\ a_{33} = -d_2,\ a_{44} = -d_3,\ b_{42} = p. \end{cases}$$

The corresponding characteristic equation is given by

$$\Phi(\lambda,\tau) = \det\left(\lambda I - M - e^{-\lambda\tau}N\right) = 0. \tag{4.7}$$

We have the following theorem for the stability of the infection-free equilibrium point.

Theorem 4.3 *The infection-free equilibrium point E_0 is locally and globally asymptotically stable for all delay $\tau \geq 0$ if $R_0 < 1$.*

Proof The characteristic equation in this case becomes

$$(\lambda + \frac{s}{x_0} + \frac{rx_0}{K})(\lambda + d_3)\left(\lambda^2 + (d_2 + (d+\mu) - (1-u_2)\beta_2 x_0)\lambda + d_2(d+\mu)(1-R_0)\right) = 0. \tag{4.8}$$

This equation has two negative real roots, $\lambda_1 = -(\frac{s}{x_0} + \frac{rx_0}{K})$ and $\lambda_2 = -d_3$. The other two are the roots of the equation

$$\lambda^2 + (d_2 + (d+\mu) - (1-u_2)\beta_2 x_0)\lambda + d_2(d+\mu)(1-R_0) = 0. \tag{4.9}$$

Thus, if $R_0 < 1$ then both roots of the equation (4.9) have negative real parts, implying that E_0 is locally asymptotically stable.

To prove the global stability of the disease-free equilibrium E_0, we use Fluctuation Lemma

[200]. The following result is true for a continuous and bounded function $f(t)$:

$$f^{\infty} = \limsup_{t\to\infty} f(t), \quad f_{\infty} = \liminf_{t\to\infty} f(t).$$

Since the solutions $x = x(t)$, $y = y(t)$, $v = v(t)$ and $z = z(t)$ of the system (4.2) are continuous and bounded,

$$0 < x_{\infty} \leq x^{\infty} < \infty,\ 0 \leq y_{\infty} \leq y^{\infty} < \infty,\ 0 \leq v_{\infty} \leq v^{\infty} < \infty,\ 0 \leq z_{\infty} \leq z^{\infty} < \infty.$$

From Lemma 4.1, $x = x(t)$ is bounded in $(0, x_0]$, for all $t \geq 0$. From Fluctuation Lemma [200], the last three equations of (4.2) can then be written as

$$\begin{aligned} (d+\mu)y^{\infty} &\leq (1-u_1)\beta_1 x_0 v^{\infty} + (1-u_2)\beta_2 x_0 y^{\infty}, \\ d_2 v^{\infty} &\leq (1-u_3)c\mu y^{\infty}, \\ d_3 z^{\infty} &\leq p y^{\infty}. \end{aligned} \tag{4.10}$$

First two inequalities of (4.10) lead to

$$y^{\infty}(1-R_0) \leq 0, \quad \text{where } R_0 \text{ is defined in (4.5).} \tag{4.11}$$

Now, suppose $R_0 < 1$, which is the local stability condition of E_0, then the inequality (4.11) gives $y^{\infty} \leq 0$. Since y^{∞} is the supremum of $y(t)$, then y^{∞} is nonnegative. Therefore, the possible value of y^{∞} is $y^{\infty} = 0$ provided $R_0 < 1$, and hence $\limsup_{t\to\infty} y(t) = 0$. If $y^{\infty} = 0$ and as $v(t), z(t)$ are nonnegative, from the last two inequalities of (4.10), we obtain $v^{\infty} = 0$ and $z^{\infty} = 0$. Therefore, $\limsup_{t\to\infty} v(t) = 0$ and $\limsup_{t\to\infty} z(t) = 0$. Following the Fluctuation Lemma [200], the first equation of system (4.2) yields

$$s - dx^{\infty} + rx^{\infty}\Big(1 - \frac{x^{\infty} + \alpha y}{K}\Big) - (1-u_1)\beta_1 x^{\infty} v - (1-u_2)\beta_2 x^{\infty} y = 0. \tag{4.12}$$

From Lemma 4.1, all solutions are nonnegative and if $R_0 < 1$, then $\limsup_{t\to\infty} y(t) = 0$ and henceforth $\limsup_{t\to\infty} v(t) = 0$, $\limsup_{t\to\infty} z(t) = 0$. Therefore, if $R_0 < 1$, the solution of $y(t)$ should be $y(t) = 0$ and hence $v(t) = 0$, $z(t) = 0$. The equation (4.12) then becomes

$$\begin{aligned} s - dx^{\infty} + rx^{\infty}\Big(1 - \frac{x^{\infty}}{K}\Big) &= 0 \\ (x^{\infty} - x_n)(x_0 - x^{\infty}) &= 0. \end{aligned}$$

This equation has two roots, $x_0 = \frac{K}{2r}[(r-d) + \sqrt{(r-d)^2 + \frac{4rs}{K}}] > 0$, which is the equilibrium density of CD4$^+$T cells in the infection-free state, and $x_n = \frac{K}{2r}[(r-d) - \sqrt{(r-d)^2 + \frac{4rs}{K}}]$ (< 0). Hence theorem is proven.

Below we prove the stability of the infected equilibrium point in two cases.

Theorem 4.4 *If E^* exists and $\tau = 0$, then the infected steady state E^* is locally asymptotically stable if and only if $a_1 > 0,\ (a_3+b_1) > 0,\ (a_4+b_2) > 0,\ a_1(a_2+b_0)(a_3+b_1) - (a_3+b_1)^2 - a_1^2(a_4+b_2) > 0$, where $a_i > 0, b_j > 0, i = 1,2,3,4, j = 0,1,2$, are given below.*

Proof The characteristic equation (4.7) at E^* is given by

$$\Phi(\lambda,\tau) = \lambda^4 + a_1\lambda^3 + a_2\lambda^2 + a_3\lambda + a_4 + (b_0\lambda^2 + b_1\lambda + b_2)e^{-\lambda\tau} = 0, \tag{4.13}$$

where

$$\begin{cases} a_1 = (\frac{s}{x^*} + \frac{rx^*}{K}) + d_2 + d_3 + \frac{(1-u_1)(1-u_3)c\mu\beta_1 x^*}{d_2}, \\ a_2 = (\frac{s}{x^*} + \frac{rx^*}{K})(d_2 + d_3 + \frac{(1-u_1)(1-u_3)c\mu\beta_1 x^*}{d_2}) + d_3(d_2 + \frac{(1-u_1)(1-u_3)c\mu\beta_1 x^*}{d_2}) \\ \quad + \frac{(d+\mu)y^*R_0}{x_0}(\frac{r\alpha x^*}{K} + (1-u_2)\beta_2 x^*), \\ a_3 = d_3(\frac{s}{x^*} + \frac{rx^*}{K})(d_2 + \frac{(1-u_1)(1-u_3)c\mu\beta_1 x^*}{d_2}) + \frac{(d+\mu)y^*R_0}{x_0}[(1-u_1)(1-u_3)c\mu\beta_1 x^* \\ \quad + (d_2+d_3)(\frac{r\alpha x^*}{K} + (1-u_2)\beta_2 x^*)], \\ a_4 = \frac{d_3(d+\mu)y^*R_0}{x_0}[\frac{d_2 r\alpha x^*}{K} + \frac{d_2(d+\mu)x^*R_0}{x_0}],\ b_0 = d_1 py^*,\ b_1 = d_1 py^*(d_2 + \frac{s}{x^*} + \frac{rx^*}{K}), \\ b_2 = d_1 d_2 py^*(\frac{s}{x^*} + \frac{rx^*}{K}). \end{cases}$$

Note that $a_i, b_j, i = 1,2,3,4, j = 0,1,2$ are all positive. At $\tau = 0$, the characteristic equation (4.13) then becomes

$$\Phi(\lambda,0) = \lambda^4 + a_1\lambda^3 + (a_2+b_0)\lambda^2 + (a_3+b_1)\lambda + (a_4+b_2) = 0,$$

According to Routh-Hurwitz criteria, E^* will be locally asymptotically stable if and only if the conditions mentioned in the theorem hold.

Theorem 4.5 *Assume that E^* is stable in the absence of delay and the conditions given in the Theorem (4.4) are satisfied. If (4.17) has at least one positive root following one of the conditions specified in (4.19), then there exists a critical value $\tau = \tau^*$, where τ^* is defined in (4.20), for which E^* is locally asymptotically stable if $\tau \in [0,\tau^*)$ and unstable for $\tau > \tau^*$. The switching of stability occurs through a Hopf bifurcation at $\tau = \tau^*$.*

Proof For $\tau > 0$, we first investigate whether the equation (4.13) has a pair of purely imaginary roots of the form $\lambda = \pm i\omega^*,\ \omega^* \in \mathbb{R}^+ - \{0\}$ for some parametric conditions. In such a case, putting $\lambda = i\omega^*$ in (4.13), one gets

$$(i\omega^*)^4 + a_1(i\omega^*)^3 + a_2(i\omega^*)^2 + a_3(i\omega^*) + a_4 + (b_0(i\omega^*)^2 + b_1(\omega^*) + b_2)e^{-(i\omega^*)\tau} = 0.$$

Separating real and imaginary parts, we have

$$\begin{cases} S_1 = S_3\cos(\omega^*\tau) - S_4\sin(\omega^*\tau), \\ S_2 = S_3\sin(\omega^*\tau) + S_4\cos(\omega^*\tau), \end{cases} \tag{4.14}$$

where,

$$\begin{aligned} &S_1 = (\omega^*)^4 - a_2(\omega^*)^2 + a_4,\ S_2 = a_1(\omega^*)^3 - a_3\omega^*, \\ &S_3 = b_0(\omega^*)^2 - b_2,\ S_4 = b_1\omega^*. \end{aligned} \tag{4.15}$$

Summing up the squares of the equations in (4.14), we get

$$S_1^2 + S_2^2 = S_3^2 + S_4^2 \tag{4.16}$$

Let $z = (\omega^*)^2$. Then (4.16) becomes

$$H(z) = z^4 + A_1 z^3 + A_2 z^2 + A_3 z + A_4 = 0, \tag{4.17}$$

where $A_1 = a_1^2 - 2a_2,\ A_2 = a_2^2 + 2a_4 - 2a_1a_3 - b_0^2,\ A_3 = a_3^2 - 2a_2a_4 - b_1^2 + 2b_0b_2,\ A_4 = a_4^2 - b_2^2$. Therefore, $\Phi(\lambda, \tau) = 0$ has a purely imaginary root $i\omega^*$ if $H(z) = 0$ has a positive real root. Differentiation of (4.17) yields

$$H'(z) = 4z^3 + 3A_1z^2 + 2A_2z + A_3.$$

Let $y = z + \frac{A_1}{4}$, so that $H'(z) = 0$ becomes

$$y^3 + n_1y^2 + n_2 = 0,$$

where $n_1 = \frac{A_2}{2} - \frac{3A_1^2}{16},\ n_2 = \frac{A_1^3}{32} - \frac{A_1A_2}{8} + \frac{A_3}{4}$. Define, $\Gamma = (\frac{n_2}{2})^2 + (\frac{n_1}{3})^3$, $\rho = \frac{-1+i\sqrt{3}}{2}$. We then get [133]

$$\begin{aligned} y_1 &= (-\frac{n_2}{2} + \sqrt{\Gamma})^{1/3} + (-\frac{n_2}{2} - \sqrt{\Gamma})^{1/3}, \\ y_2 &= (-\frac{n_2}{2} + \sqrt{\Gamma})^{1/3}\rho + (-\frac{n_2}{2} - \sqrt{\Gamma})^{1/3}\rho^2, \\ y_3 &= (-\frac{n_2}{2} + \sqrt{\Gamma})^{1/3}\rho^2 + (-\frac{n_2}{2} - \sqrt{\Gamma})^{1/3}\rho, \\ z_l &= y_l - \frac{A_1}{4},\ l = 1,2,3. \end{aligned} \tag{4.18}$$

Following [201], the existence of positive roots of the equation $H(z) = 0$ can then be asserted as

(i) If $A_4 < 0,$ then $H(z)$ has at least one positive root.

(ii) If $A_4 \geq 0$ and $\Gamma \geq 0,$ then $H(z) = 0$ has positive roots iff

$z_1 > 0$ and $H(z_1) < 0.$ (4.19)

(iii) If $A_4 > 0$ and $\Gamma < 0,$ then $H(z) = 0$ has positive roots

iff there exists at least one$z_* \in \{z_1, z_2, z_3\}$such that $z_* > 0$ and $H(z_*) \leq 0.$

Without loss of generality, we assume that $H(z)=0$ has four positive roots, say $z_k^*, k=1,2,3,4$. Let $\omega_k^*=\sqrt{z_k^*}$. From (4.14), one then finds

$$\cos(\omega_k^*\tau^*)=H_1=\frac{S_1S_3+S_2S_4}{S_3^2+S_4^2},$$
$$\sin(\omega_k^*\tau^*)=H_2=\frac{S_1S_3-S_2S_4}{S_3^2+S_4^2}.$$

Here S_1,S_2,S_3,S_4 are calculated form (4.15) with $\omega^*=\omega_k^*$. Define

$$\tau_j^{(k)}=\begin{cases}\frac{1}{\omega_k^*}[\arccos(H_1)+2\pi j], & H_2\geq 0,\\ \frac{1}{\omega_k^*}[2\pi-\arcsin(H_1)+2\pi j], & H_2<0,\end{cases}$$

where, $k=1,2,3,4$, $j=0,1,2,3,...$, and

$$\tau^*=\min_{1\leq k\leq 4, j\geq 0}\tau_j^{(k)}. \tag{4.20}$$

Let $\tilde{\omega}_k^*$ be the value of ω_k^* $(k=1,2,3,4)$ for which τ^* is obtained. Hence $\tilde{\omega}_k^*=\sqrt{z_0}$.

To show that the transversality condition of Hopf bifurcation at $\tau=\tau^*$ is also hold, we differentiate the characteristic equation (4.13) with respect to τ to obtain

$$(4\lambda^3+3a_1\lambda^2+2a_2\lambda+a_3)\frac{d\lambda}{d\tau}+(2b_0\lambda+b_1)e^{-\lambda\tau}\frac{d\lambda}{d\tau}-e^{-\lambda\tau}(b_0\lambda^2+b_1\lambda+b_2)(\lambda+\tau\frac{d\lambda}{d\tau})=0.$$

One then finds

$$\begin{aligned}\left(\frac{d\lambda}{d\tau}\right)^{-1}&=\frac{4\lambda^3+3a_1\lambda^2+2a_2\lambda+a_3}{-\lambda(b_0\lambda^2+b_1\lambda+b_2)}+\frac{2b_0\lambda+b_1}{\lambda(b_0\lambda^2+b_1\lambda+b_2)}-\frac{\tau}{\lambda}\\&=\frac{4\lambda^3+3a_1\lambda^2+2a_2\lambda+a_3}{-\lambda(\lambda^4+a_1\lambda^3+a_2\lambda^2+a_3\lambda+a_4)}+\frac{2b_0\lambda+b_1}{\lambda(b_0\lambda^2+b_1\lambda+b_2)}-\frac{\tau}{\lambda}.\end{aligned}$$

Using (4.16), the value of $\left(\frac{d\lambda}{d\tau}\right)^{-1}$ at $\tau=\tau^*$ and $\lambda=i\tilde{\omega}_0$ reads

$$\left[\left(\frac{d\lambda}{d\tau}\right)^{-1}\right]_{\lambda=i\hat{\omega}_k^*,\ \tau=\tau^*}=\frac{N_1N_2+N_4N_5}{\hat{\omega}_k^*N_3}+\frac{i\tau^*}{\hat{\omega}_k^*},$$

where $N_1=\left(4\hat{\omega}_k^{*3}-2a_2\hat{\omega}_k^*\right)+i\left(a_3-3a_1\hat{\omega}_k^{*2}\right)$, $N_2=\left(\hat{\omega}_k^{*4}-a_2\hat{\omega}_k^{*2}+a_4\right)+i\left(a_1\hat{\omega}_k^{*3}-a_3\hat{\omega}_k^*\right)$, $N_3=\left(b_2-b_0\hat{\omega}_k^{*2}\right)^2+\left(b_1\hat{\omega}_k^*\right)^2$, $N_4=2b_0\hat{\omega}_k^*-ib_1$, $N_5=\left(b_2-b_0\hat{\omega}_k^{*2}\right)-ib_1\hat{\omega}_k^*$.

Substituting $\hat{\omega}_k^* = \sqrt{\hat{z}_k^*}$, we then have

$$\left[Re\left(\frac{d\lambda}{d\tau}\right)^{-1}\right]_{\lambda=i\hat{\omega}_k^*,\ \tau=\tau^*} = \frac{4\hat{z}_k^{*3} + 3A_1\hat{z}_k^{*2} + 2A_2\hat{z}_k^* + A_3}{N_3}$$
$$= \frac{H'(\hat{z}_k^*)}{N_3} \neq 0, \text{ if } H'(\hat{z}_k^*) \neq 0,$$

where $H(z)$ is defined in (4.17) .

Therefore, the sign of $\left[Re\left(\frac{d\lambda}{d\tau}\right)^{-1}\right]_{\lambda=i\omega_0,\ \tau=\tau^*}$ is same as $H'(z_0)$. The direction of Hopf bifurcation depends on the sign of the transversality condition. If the value of the transversality condition is positive, then the stability of E^* will change from a stable to an unstable state through a Hopf bifurcation in the forward direction. In contrast, its negative value implies the change from an unstable state to a stable equilibrium through a Hopf bifurcation in the backward direction.

Table 4.1: Parameter descriptions and their values with references

Parameter	Description	Range of parameters	Default values	References
s	Constant input rate of CD4$^+$T cells	0-10 cells mm^{-3} day^{-1}	10	[91, 93, 175, 197]
d	Death rate of susceptible CD4$^+$T cells	0.07-0.1 day^{-1}	0.01	[133, 175, 197]
β_1	Cell-free disease transmission coefficient	0.000025-0.5 virons mm^{-3} day^{-1}	0.00025	[91, 93, 133, 197]
β_2	Cell-to-cell disease transmission coefficient	0.00001-0.7 mm^{-3} infected cells day^{-1}	varies	
r	Proliferation rate of CD4$^+$T cells	0.03-3 day^{-1}	0.1	[91, 93, 133, 197]
K	Maximum density of CD4$^+$T cells where proliferation stops	1500 mm^{-3}	1500	[91, 133, 197]
α	Limitation coefficient of infected cells imposed on the proliferation of CD4$^+$T cells	≥ 1	1.2	[133, 187]
d_1	Killing rate of infected cells by CTL	0.812 day^{-1}	0.812	[133, 202]
d_2	Clearance rate of virus particles	2.4-3 day^{-1}	2.4	[91, 133, 197]
d_3	Clearance rate of CTL	1.618 day^{-1}	1.618	[133, 202]
c	Virus replication factor	10-2500 virions cell^{-1}	varies	[93, 174]
p	Production rate of CTL	0.05 day^{-1}	0.05	[133, 203]
μ	Lysis death rate of infected CD4$^+$T cells	0.2-0.5 day^{-1}	0.4	[91, 197]

4.3.4 Simulation results

System (4.2) in the absence of delay and control has thirteen parameters. So the question is which parameters are essential and should be selected for further investigation. For this, we have performed a sensitivity analysis (see Fig.4.1) of the system parameters (see Table 4.1) using the Latin Hypercube sampling method. It shows that c and β_2 are the most sensitive parameters. So, we fix other parameter values and consider c and β_2 as the variable parameters for further study.

In Fig. 4.2, we have drawn the stability region of the disease-free equilibrium E_0 and the

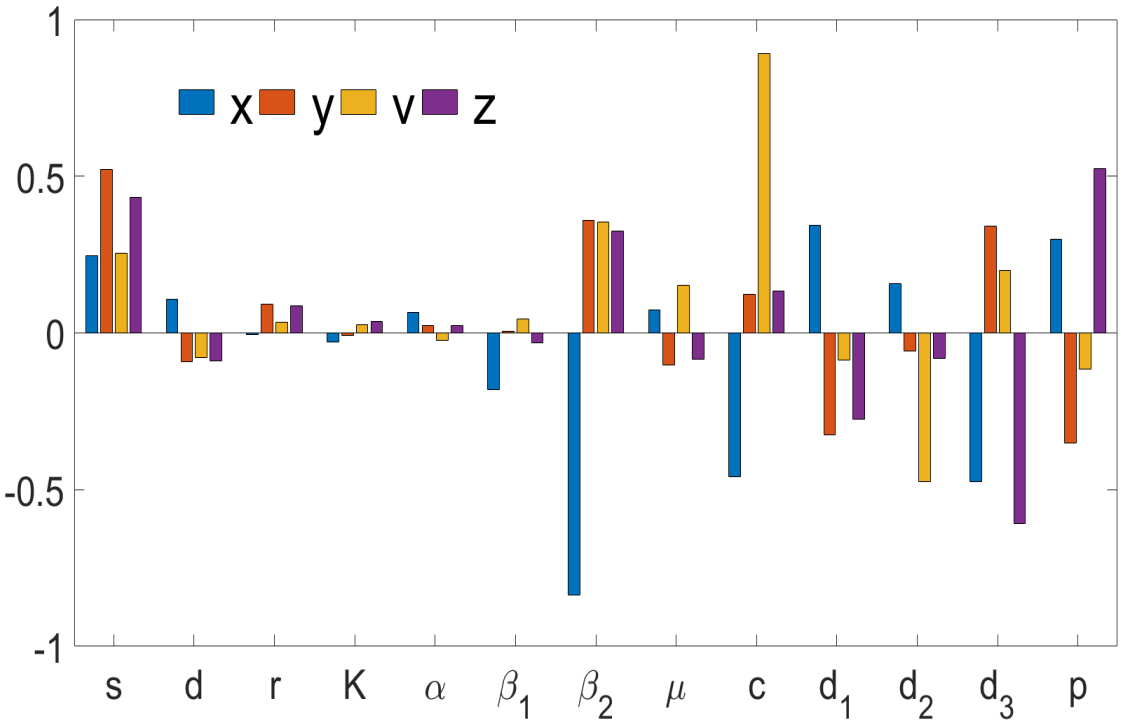

Figure 4.1: Sensitivity analysis of the parameters (see Table 4.1) following Latin hypercube sampling-partial ranked correlation coefficients ($p < 0.00001$). Here $u_1 = u_2 = u_3 = 0$.

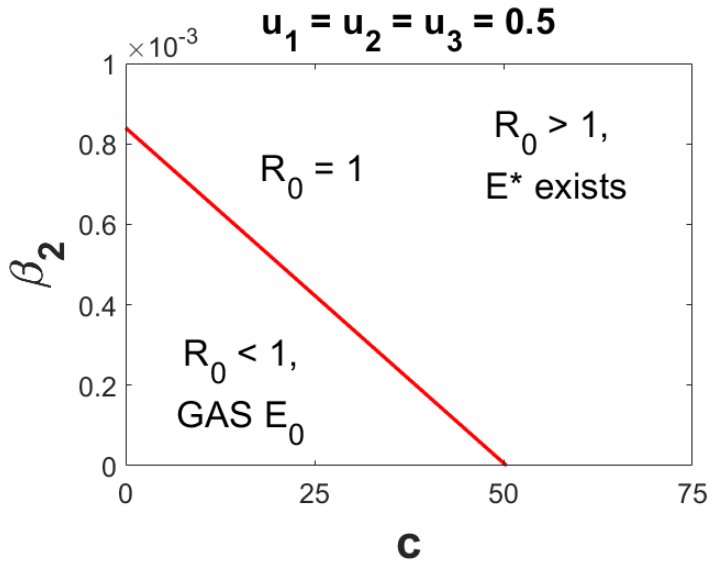

Figure 4.2: Stability region of the disease-free equilibrium E_0 and the existence region of the endemic equilibrium E^* in $c-\beta_2$ plane. Parameters are $s = 10, d = 0.02, \beta_1 = 0.00025, r = 0.03, K = 1500, \alpha = 1.2, \mu = 0.4, d_1 = 0.812, d_2 = 3, d_3 = 1.618, p = 0.05$ and$u_1 = u_2 = u_3 = 0.5$.

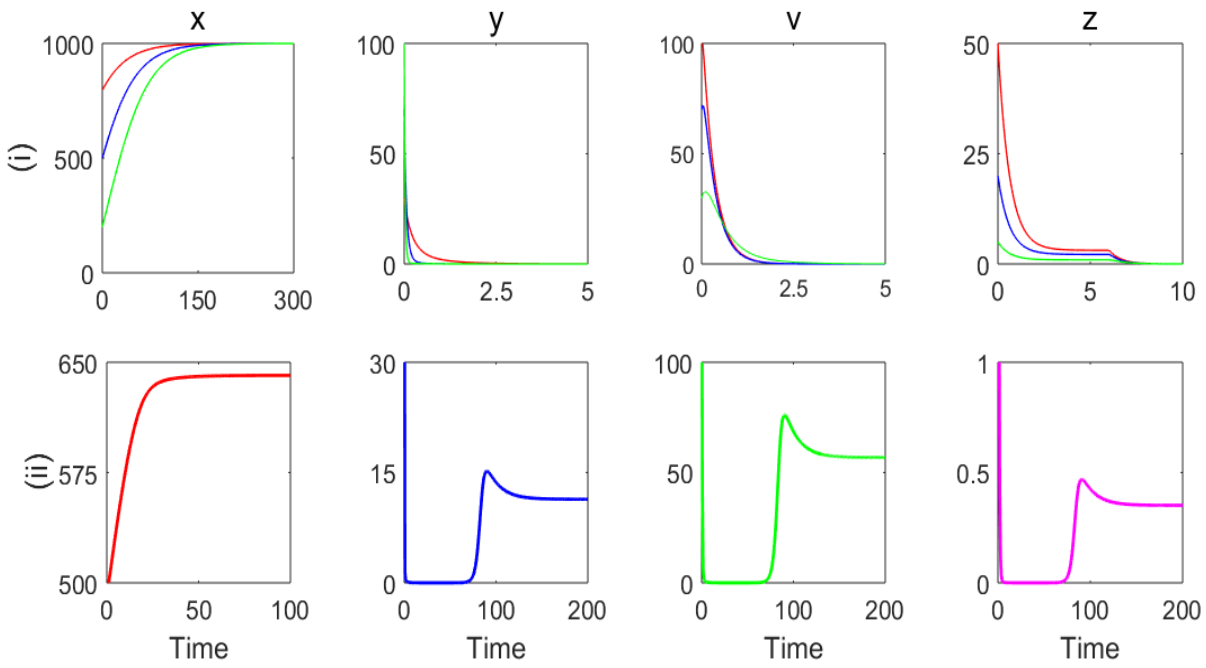

Figure 4.3: Upper row: Time evolutions of the non-delayed system show that the disease-free equilibrium E_0 is stable when parameters are selected from the lower region of Fig. 4.2 with $c = 4, \beta_2 = 0.0001$. Lower row: Figures show that the non-delayed system is locally asymptotically stable for $c = 75, \beta_2 = 0.001$. Other parameters are as in Fig. 4.2.

existence region of the infected equilibrium E^* in $c - \beta_2$ parameter plane when other parameters remain fixed with $u_1 = u_2 = u_3 = 0.5$. Time evolutions of the system (4.2) with constant controls (Fig. 4.3 (upper row)) show that the disease-free equilibrium E_0 is stable when the parameters are selected from the lower region of Fig. 4.2 $(c = 4, \beta_2 = 0.0001)$. In fact, the delay has no effect on the stability of E_0. The disease-free equilibrium is globally asymptotically stable for all $\tau \geq 0$ (figures not given). If $c = 75, \beta_2 = 0.001$ then the parameter values satisfy the stability conditions of the non-delayed system. Fig. 4.3 (lower row) shows that the non-delayed system is locally asymptotically stable. Figure 4.4 is the bifurcation diagram of the infected population with respect to the delay parameter, τ. It shows that the system is stable for $\tau < \tau^*$, unstable for $\tau > \tau^*$, and a Hopf bifurcation occurs at $\tau = \tau^* = 5.1051$ days. Time evolutions of the system populations for two particular values of τ $(\tau = 5$ and $\tau = 5.2)$ represent the stable and unstable behaviour of the system (see Fig. 4.5).

4.4 The Optimal Control Problem

In the previous section, we discussed the effect of constant control. Here we assume that the control parameters are time-dependent. Our objective here is to maximize the number of healthy $CD4^+T$ cells, CTLs, and minimize the number of infected $CD4^+T$ cells and virus particles using three controls. At the same time, we want to reduce the deleterious side effects

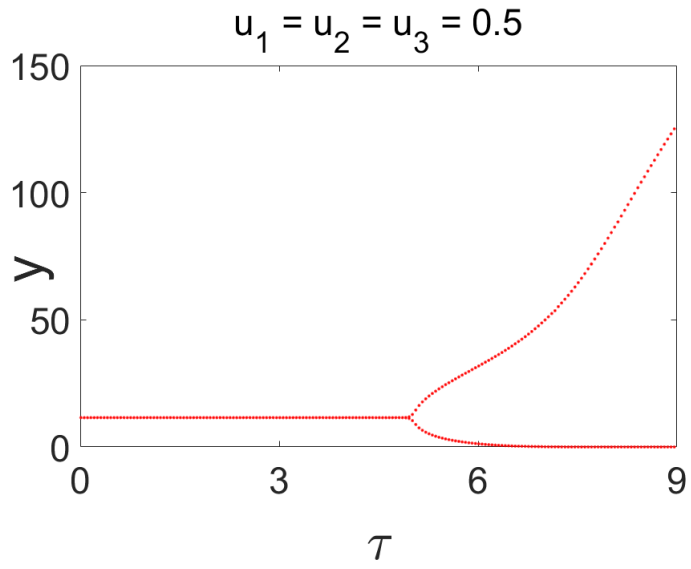

Figure 4.4: Bifurcation diagram of the infected CD4$^+$T cell population with respect to the delay, τ. The y population is stable for $\tau < \tau^*$ and unstable for $\tau > \tau^*$, where $\tau^* = 5.1051$ days. Here $u_1 = u_2 = u_3 = 0.5$, $c = 75, \beta_2 = 0.001$ and other parameters are as in Fig. 4.2.

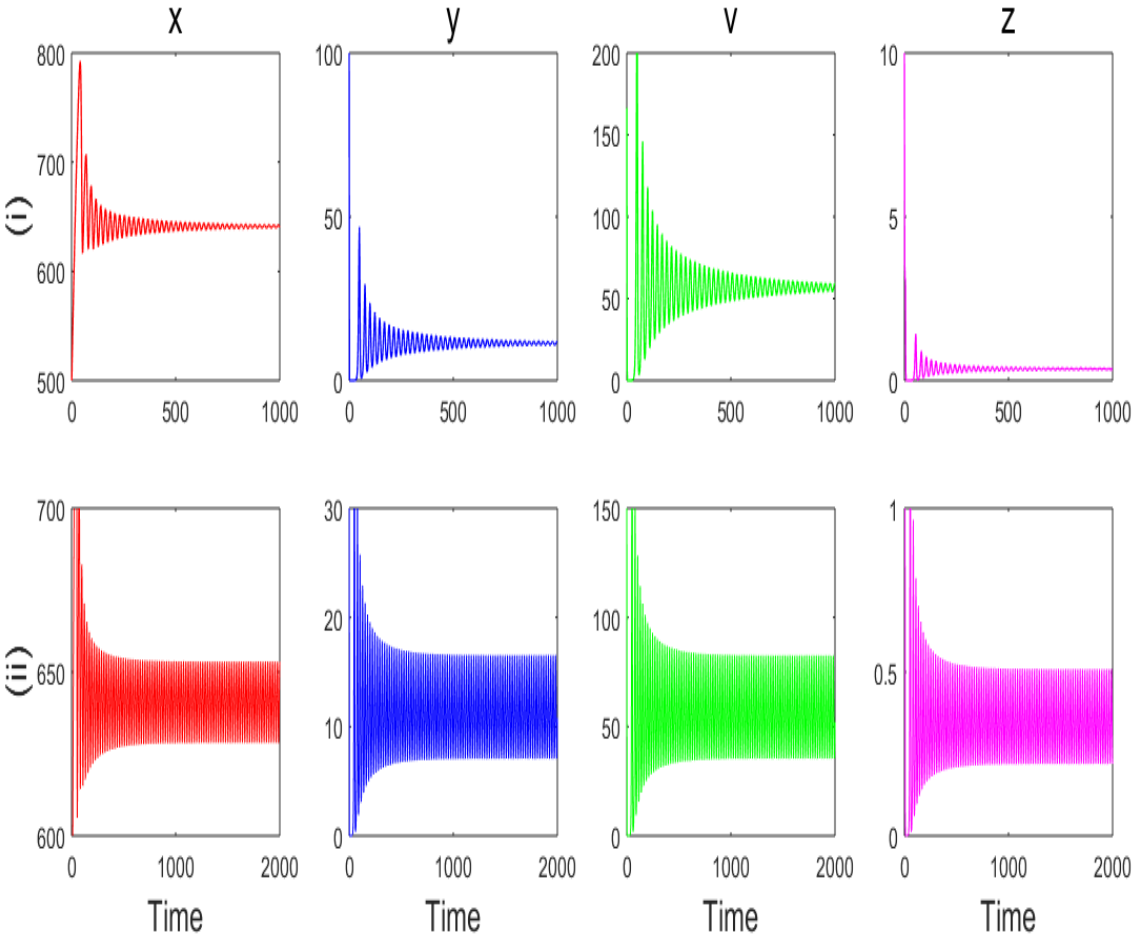

Figure 4.5: Upper row: The infected equilibrium E^* is stable when $\tau = 5 (< \tau^*)$. Lower row: The infected equilibrium E^* is unstable when $\tau = 5.2 (> \tau^*)$, where $\tau^* = 5.1051$. Here $u_1 = u_2 = u_3 = 0.5$ and $c = 75, \beta_2 = 0.001$. Other parameters are as in Fig. 4.4.

of the drugs. For this, we define the objective functional

$$J(u_1,u_2,u_3)=\int_0^{t_f}\left(A_1x(t)+A_2z(t)-\left(A_3y(t)+A_4v(t)+\frac{B_1u^2{}_1(t)}{2}+\frac{B_2u^2{}_2(t)}{2}+\frac{B_3u^2{}_3(t)}{2}\right)\right)dt \tag{4.21}$$

subject to the states (4.2). In the integrand, the first two terms represent the benefit and the next two terms indicate the deleterious effects. Here $A_i>0$, $i=1,2,3,4$, are the weight constants, which balance the size of the terms $x(t)$,$z(t)$,$y(t)$ and $v(t)$. Three square terms are the respective cost of $u_1(t),u_2(t)$ and $u_3(t)$, and B_1,B_2 and B_3 are the weight parameters employed relative to the cost implication of the controls u_1, u_2 and u_3. Here t_f is the final time, where treatment stops. Therefore, our object is to find the optimal control triplet ($\hat{u_1}$, $\hat{u_2}$, $\hat{u_3}$) such that

$$J(\hat{u_1},\hat{u_2},\hat{u_3})=\max_{(u_1,u_2,u_3)\in\Xi}J(u_1,u_2,u_3), \tag{4.22}$$

where, $\Xi=\{(u_1(t),u_2(t),u_3(t)):u_i\ measurable,0\le u_i(t)\le 1,t\in[0,t_f],i=1,2,3\}$.

4.4.1 Existence of an optimal control triplet

Theorem 4.6 *There exists an optimal control triplet $(\hat{u_1},\hat{u_2},\hat{u_3})\in\Xi$ with time dependent control problem (4.2) that maximizes the objective functional $J(u_1,u_2,u_3)$, i.e., $J(\hat{u_1},\hat{u_2},\hat{u_3})=\max_{(u_1,u_2,u_3)\in\Xi}J(u_1,u_2,u_3)$.*

Proof We use an existence result of Flaming and Rishel [71]. To apply this result, we check the following properties:

(a_1) The set of controls and the corresponding state variables is nonempty.

(a_2) The control set Ξ is convex and closed.

(a_3) The right hand side of the state system is continuous, bounded above by a sum of the bounded control and state, and can be written as a linear function of u_i with coefficients depending on the state and time.

(a_4) The integrand of the objective functional is concave on Ξ.

(a_5) There exists constants $c_1,\ c_2>0$ and $b>1$ such that the integrand of the objective functional is bounded above by $c_2-c_1(|u_1(t)|^2+|u_2(t)|^2+|u_3(t)|^2)^{b/2}$.

In order to verify these properties, we use a result from Lukes [184] for the existence of solutions of (4.2) with bounded coefficients and (a_1) is satisfied. By the definition of Ξ, (a_2) is satisfied. As our control system is linear in u_1,u_2 and u_3, the right-hand side of (4.2) satisfies

(a_3) as the solutions are bounded. The integrand of the objective functional is concave for the control set Ξ and hence a_4 is satisfied. For the last condition

$$\begin{aligned}
&A_1x+A_2z-\left(A_3y+A_4v+\frac{B_1{u^2}_1}{2}+\frac{B_2{u^2}_2}{2}+\frac{B_3{u^2}_3}{2}\right)\\
&\leq A_1x+A_2z-(\frac{B_1{u_1}^2}{2}+\frac{B_2{u_2}^2}{2}+\frac{B_3{u_3}^2}{2})\\
&\leq c_2-c_1(|u_1|^2+|u_2|^2+|u_3|^2)^{\frac{b}{2}},
\end{aligned}$$

where c_2 depends on the upper bound of x and z, $b>1$ and $c_1>0$ as $B_1,B_2,B_3>0$. Hence, we conclude that there exists an optimal control triplet.

Pontryagin's minimum principle [195] and the state delay provides a necessary condition for an optimal control triplet $(\hat{u_1},\hat{u_2},\hat{u_3})$. This principle converts (4.2), (4.21) and (4.22) into a problem which maximizes the Hamiltonian (H)

$$\begin{aligned}
&H(t;x,y,v,z;y_\tau;u_1,u_2,u_3;\lambda_1,\lambda_2,\lambda_3,\lambda_4)=A_3y(t)+A_4v(t)+\frac{B_1{u_1}^2(t)}{2}+\frac{B_2{u_2}^2(t)}{2}\\
&+\frac{B_3{u_3}^2(t)}{2}-A_1x(t)-A_2z(t)+\lambda_1\dot{x}(t)+\lambda_2\dot{y}(t)+\lambda_3\dot{v}(t)+\lambda_4\dot{z}(t),
\end{aligned}\tag{4.23}$$

where $\lambda_i, i=1,2,3,4$, are the co-state or adjoint variables. Applying Pontryagin's minimum principle with state delay [195], we obtain the following Proposition.

Theorem 4.7 *Suppose $(\hat{u}_1,\hat{u}_2,\hat{u}_3)$ is an optimal control triplet of (4.21) subject to the system (4.2) and $(\hat{x},\hat{y},\hat{v},\hat{z})$ is the corresponding optimal solutions of (4.2), then there exists co-state or adjoint variables $\lambda_i,(i=1,2,3,4)$ such that the following conditions are satisfied with the delay-induced controlled system (4.2).*

i. *Co-state equations:*

$$\begin{aligned}
\dot{\lambda}_1(t)=&\ A_1+\lambda_1(t)\Bigg(d+(1-\hat{u}_1(t))\beta_1\hat{v}(t)+(1-\hat{u}_2(t))\beta_2\hat{y}(t)\\
&-r(1-\frac{2\hat{x}(t)+\alpha\hat{y}(t)}{K})\Bigg)-\lambda_2(t)\Bigg((1-\hat{u}_1(t))\beta_1\hat{v}(t)+(1-\hat{u}_2(t))\beta_2\hat{y}(t)\Bigg),\\
\dot{\lambda}_2(t)=&-A_3+\lambda_1(t)\left(\frac{r\alpha\hat{x}(t)}{K}+(1-\hat{u}_2(t))\beta_2\hat{x}(t)\right)\\
&-\lambda_2(t)\Bigg((1-\hat{u}_2(t))\beta_2\hat{x}(t)-(d+\mu)-d_1\hat{z}(t)\Bigg)\\
&-\lambda_3(t)(1-\hat{u}_3(t))c\mu-\chi_{[0,t_f-\tau]}p\lambda_4(t+\tau),\\
\dot{\lambda}_3(t)=&-A_4+\lambda_1(t)(1-\hat{u}_1(t))\beta_1\hat{x}(t)-\lambda_2(t)(1-\hat{x}_1(t))\beta_1\hat{x}(t)+\lambda_3(t)d_2,\\
\dot{\lambda}_4(t)=&\ A_2+\lambda_2(t)d_1\hat{y}(t)+\lambda_4(t)d_3,
\end{aligned}\tag{4.24}$$

with the transversality conditions $\lambda_i(t_f) = 0, i = 1,2,3,4$, *and* $\chi_{[0,t_f-\tau]}$ *is the characteristic function [204, 205] defined by*

$$\chi_{[0,t_f-\tau]} = \begin{cases} 1 \text{ if } t \in [0,t_f-\tau], \\ 0 \text{ otherwise}. \end{cases}$$

ii. *Optimality conditions:*

$$H(\hat{x},\hat{y},\hat{v},\hat{z};\hat{u_1},\hat{u_2},\hat{u_3};\lambda_1,\lambda_2,\lambda_3,\lambda_4) = H(\hat{x},\hat{y},\hat{v},\hat{z};u_1,u_2,u_3;\lambda_1,\lambda_2,\lambda_3,\lambda_4),$$

which implies

$$\begin{aligned} \hat{u_1}(t) =& min\left\{1, max\{0, \frac{(\lambda_2(t)-\lambda_1(t))\beta_1\hat{x}(t)\hat{v}(t)}{B_1}\}\right\}, \\ \hat{u_2}(t) =& min\left\{1, max\{0, \frac{(\lambda_2(t)-\lambda_1(t))\beta_2\hat{x}(t)\hat{y}(t)}{B_2}\}\right\}, \\ \hat{u_3}(t) =& min\left\{1, max\{0, \frac{\lambda_3(t)c\mu\hat{y}(t)}{B_3}\}\right\}. \end{aligned} \tag{4.25}$$

Proof By Pontryagin's minimum principle with state delay [195], the co-state equations and its transversality conditions can be solved by

$$\begin{aligned} \dot{\lambda_1}(t) =& -\frac{\partial H(t)}{\partial x}, \qquad \lambda_1(t_f) = 0, \\ \dot{\lambda_2}(t) =& -\frac{\partial H(t)}{\partial y} - \chi_{[0,t_f-\tau]}\frac{\partial H(t+\tau)}{\partial y_\tau}, \qquad \lambda_2(t_f) = 0, \\ \dot{\lambda_3}(t) =& -\frac{\partial H(t)}{\partial v}, \qquad \lambda_3(t_f) = 0, \\ \dot{\lambda_4}(t) =& -\frac{\partial H(t)}{\partial z}, \qquad \lambda_4(t_f) = 0. \end{aligned} \tag{4.26}$$

The optimal control triplet $\hat{u_1}, \hat{u_2}$ and $\hat{u_3}$ are solved from the optimality conditions

$$\begin{aligned} &\frac{\partial H(t)}{\partial u_1} = 0, \text{ at } u_1(t) = \hat{u_1}(t); \ \frac{\partial H(t)}{\partial u_2} = 0, \text{ at } u_2(t) = \hat{u_2}(t); \\ &\frac{\partial H(t)}{\partial u_3} = 0, \text{ at } u_3(t) = \hat{u_3}(t) \end{aligned} \tag{4.27}$$

and we get

$$\begin{aligned} &\frac{\partial H(t)}{\partial u_1} = B_1u_1(t) + (\lambda_1(t)-\lambda_2(t))\beta_1x(t)v(t) = 0, \ \frac{\partial H(t)}{\partial u_2} = B_2u_2(t) + (\lambda_1(t) \\ &-\lambda_2(t))\beta_2x(t)y(t) = 0, \ \frac{\partial H(t)}{\partial u_3} = B_3u_3(t) - \lambda_3(t)c\mu y(t) = 0. \end{aligned} \tag{4.28}$$

We calculate $\hat{u_1}(t), \hat{u_2}(t)$ and $\hat{u_3}(t)$ from the bounds of Ξ in the form of (4.25).

Therefore, the optimal system associated with the system (4.2) is represented by

$$
\begin{cases}
\frac{d\hat{x}}{dt} = s - d\hat{x}(t) + r\hat{x}(t)(1 - \frac{\hat{x}(t)+\alpha\hat{y}(t)}{K}) - (1-\hat{u}_1(t))\beta_1\hat{x}(t)\hat{v}(t) \\
\qquad - (1-\hat{u}_2(t))\beta_2\hat{x}(t)\hat{y}(t), \\
\frac{d\hat{y}}{dt} = (1-\hat{u}_1(t))\beta_1\hat{x}(t)\hat{v}(t) + (1-\hat{u}_2(t))\beta_2\hat{x}(t)\hat{y}(t) - (d+\mu)\hat{y}(t) - d_1\hat{y}(t)\hat{z}(t), \\
\frac{d\hat{v}}{dt} = (1-\hat{u}_3(t))c\mu\hat{y}(t) - d_2\hat{v}(t), \\
\frac{d\hat{z}}{dt} = p\hat{y}(t-\tau) - d_3\hat{z}(t), \\
\frac{d\lambda_1}{dt} = -A_1 + \lambda_1(t)\Big(d + (1-\hat{u}_1(t))\beta_1\hat{v}(t) + (1-\hat{u}_2(t))\beta_2\hat{y}(t) \\
\qquad - r(1 - \frac{2\hat{x}(t)+\alpha\hat{y}(t)}{K})\Big) - \lambda_2(t)\Big((1-\hat{u}_1(t))\beta_1\hat{v}(t) + (1-\hat{u}_2(t))\beta_2\hat{y}(t)\Big), \\
\frac{d\lambda_2}{dt} = A_3 + \lambda_1(t)\Big(\frac{r\alpha\hat{x}(t)}{K} + (1-\hat{u}_2(t))\beta_2\hat{x}(t)\Big) - \lambda_2(t)\Big((1-\hat{u}_2(t))\beta_2\hat{x}(t) \\
\qquad - (d+\mu) - d_1\hat{z}(t)\Big) - \lambda_3(t)(1-\hat{u}_3(t))c\mu - p\lambda_4(t), \\
\frac{d\lambda_3}{dt} = A_4 + \lambda_1(t)(1-\hat{u}_1(t))\beta_1\hat{x}(t) - \lambda_2(t)(1-\hat{u}_1(t))\beta_1\hat{x}(t) + \lambda_3(t)d_2, \\
\frac{d\lambda_4}{dt} = \ -A_2 + \lambda_2(t)d_1\hat{y}(t) + \lambda_4(t)d_3, \\
x(0) = x_0 > 0,\ y(0) = y_0 > 0,\ v(0) = v_0 > 0,\ z(0) = z_0 > 0, \\
\lambda_i(t_f) = 0,\ i = 1,2,3,4, \\
\text{where} \\
\hat{u_1}(t) = min\Big\{1, max\{0, \frac{(\lambda_2(t)-\lambda_1(t))\beta_1\hat{x}(t)\hat{v}(t)}{B_1}\}\Big\}, \\
\hat{u_2}(t) = min\Big\{1, max\{0, \frac{(\lambda_2(t)-\lambda_1(t))\beta_2\hat{x}(t)\hat{y}(t)}{B_2}\}\Big\}, \\
\hat{u_3}(t) = min\Big\{1, max\{0, -\frac{\lambda_3(t)c\mu\hat{y}(t)}{B_3}\}\Big\}.
\end{cases}
\tag{4.29}
$$

4.4.2 Simulation results

Here we solve the optimal systems (4.29) numerically by combination of forward and backward difference approximation methods [196]. The treatment period is continued for 300 days and therefore the time interval is considered as $[0, t_f]$, where $t_f = 300$. The initial values of the state variables are taken as $x(0) = 500, y(0) = 100, v(0) = 100$ and $z(0) = 10$ [116]. Since the weight parameters A_1 and A_3 are associated with the CD4$^+$T cells, we assign the same values for them. Considering the same harmful effects of all the inhibitors, the same value for the weight parameters B_1, B_2, B_3 are considered. Other parameter values remain as in Table 4.1. We consider both the mono-drug and multi-drug therapies and compare their efficacies in controlling viremia under different delays.

4.4.2.1 Mono-drug therapy

Figure 4.6 represents various outcomes of mono-drug therapies for the system (4.29) with $\tau = 1$. The first column of this figure shows the counts of various immune cells and plasma viruses when the inhibitor u_1 is only administered (the case $(u_1 \neq 0, u_2 = 0, u_3 = 0)$). The last row of this figure gives the respective control profile. These figures show that no inhibitor can completely remove the infection, and infected cells persist in all three cases. However, in the case of blocker u_3, virus counts go below the detection level, though it exists in the other two cases, but infected CD4$^+$T cells (y) persist. It happens due to the cell-to-cell dissemination of infection. Observe that healthy CD4$^+$T cells count is relatively low in the mono-drug therapy $(u_1 = 0, u_2 \neq 0, u_3 = 0)$ compared to other two cases. Thus, u_2 is the worst mono-drug therapy. The respective control profiles indicate that all the controls should be applied with full efficacy for the entire treatment period, except for some occasional reduction in the u_1 control. This analysis shows that the mono-drug therapy with the blocker u_3 is relatively a better performer because its application can reduce the free virus particles, thereby reducing the chances of cell-free infection.

Figure 4.7 shows the time evolutions of the optimal system (4.29) for $\tau = 2$ days. These figures show that plasma concentrations of CD4$^+$T cells, CTls and virus particles oscillate in the case of $(u_1 \neq 0, u_2 = 0, u_3 = 0)$ and $(u_1 = 0, u_2 \neq 0, u_3 = 0)$, but they are stable in the case of mono-drug therapy $(u_1 = 0, u_2 = 0, u_3 \neq 0)$ with higher value of susceptible CD4$^+$T cells and lower value of infected CD4$^+$T cell counts. The free virus particles count (v) also remains below the detectable level in the latter case. The control profile (last row) also shows a significant difference for u_3 inhibitor compared to the other two controls, where oscillations are predominant. Similar simulation results are presented when the delay is further increased to $\tau = 2.5 > \tau^*$, where $\tau^* = 2.37$ days. These figures show that plasma concentrations of CD4$^+$T cells, CTls, and virus particles oscillate in all three control strategies. The control profile also oscillates in each case. Thus, a large immune activation delay causes significant changes in the plasma counts and the control profile. Therefore, no mono-drug therapy is capable of controlling the viremia in an HIV-1 infected individual if immune response delay is high.

4.4.2.2 Multi-drug therapy

In the case of a multi-drug therapy, we observed that infection can be removed (i.e., where $y = 0$) in three options. The multi-drug option $(u_1 \neq 0, u_2 = 0, u_3 \neq 0)$ cannot eliminate infection, implying that it is the worst combination, but in the other three cases, both the infected cells and virus particles are eliminated. It is to be noted that the control u_2 should be used while using multi-drug therapy to eliminate the infection. However, the control u_2 was not an efficient blocker when administered alone. Control profiles are all most same for three cases except the one $(u_1 \neq 0, u_2 = 0, u_3 \neq 0)$, where the infection persists. Considering the cost of drugs and its side effects, any of the multi-drug therapies $(u_1 \neq 0, u_2 \neq 0, u_3 = 0)$ or $(u_1 = 0, u_2 \neq 0, u_3 \neq 0)$

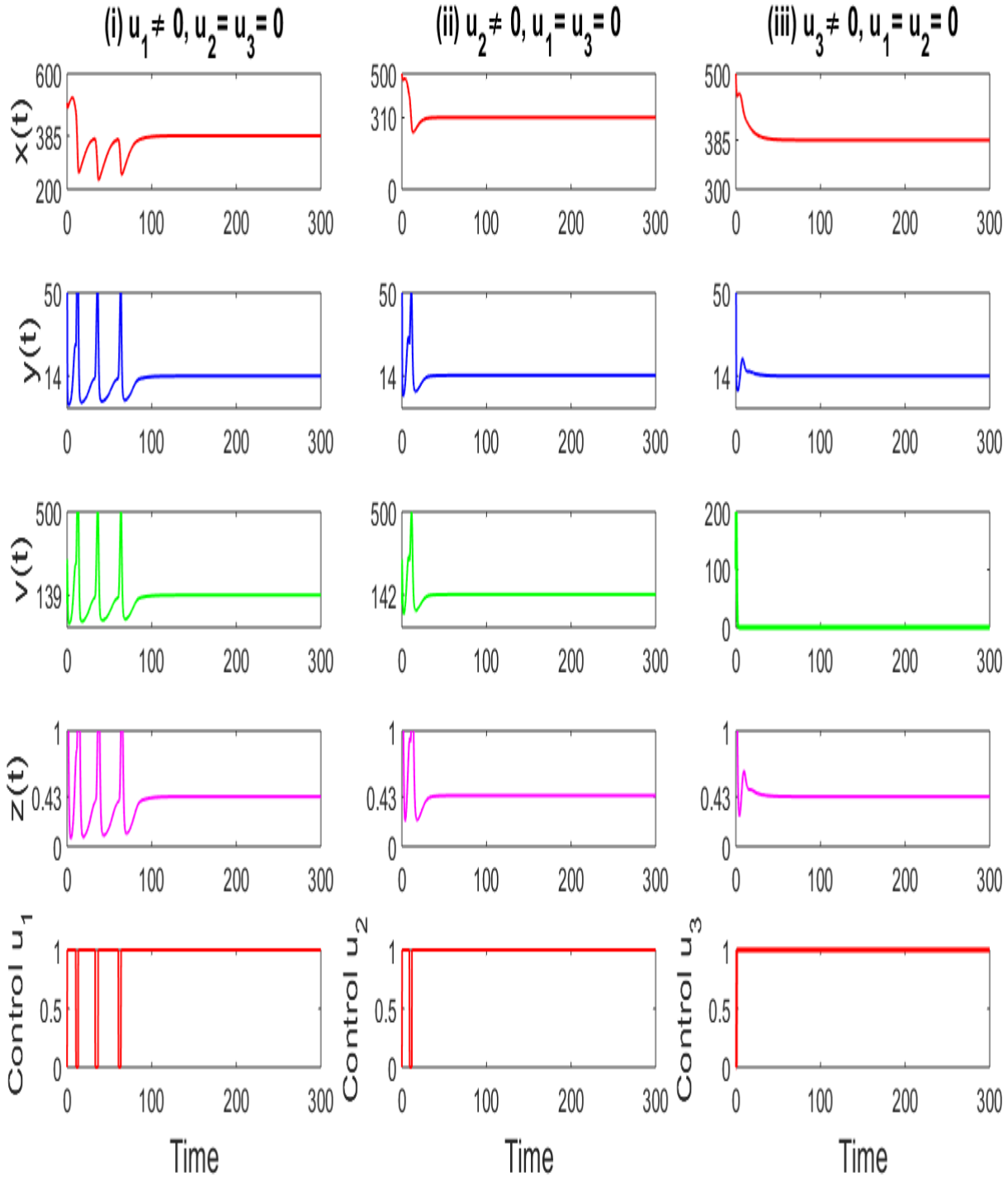

Figure 4.6: The time variations of susceptible CD4$^+$T cells, infected CD4$^+$T cells, virus particles and CTLs due to different mono-drug therapy with $\tau = 1$ day. The last row represents the optimal controls corresponding to each mono-drug therapy. Here $\tau = 1$ and other parameters are $s = 10, d = 0.02, \beta 1 = 0.00025, r = 0.03, K = 1500, \alpha = 1.2, \mu = 0.4, d_1 1 = 0.812, d_2 2 = 3, d_3 = 1.618; p = 0.05; c = 75, \beta_2 = 0.002, A_1 = A_3 = 5, A_2 = A_4 = 2$ and $B_1 = B_3 = B_3 = 0.1$.

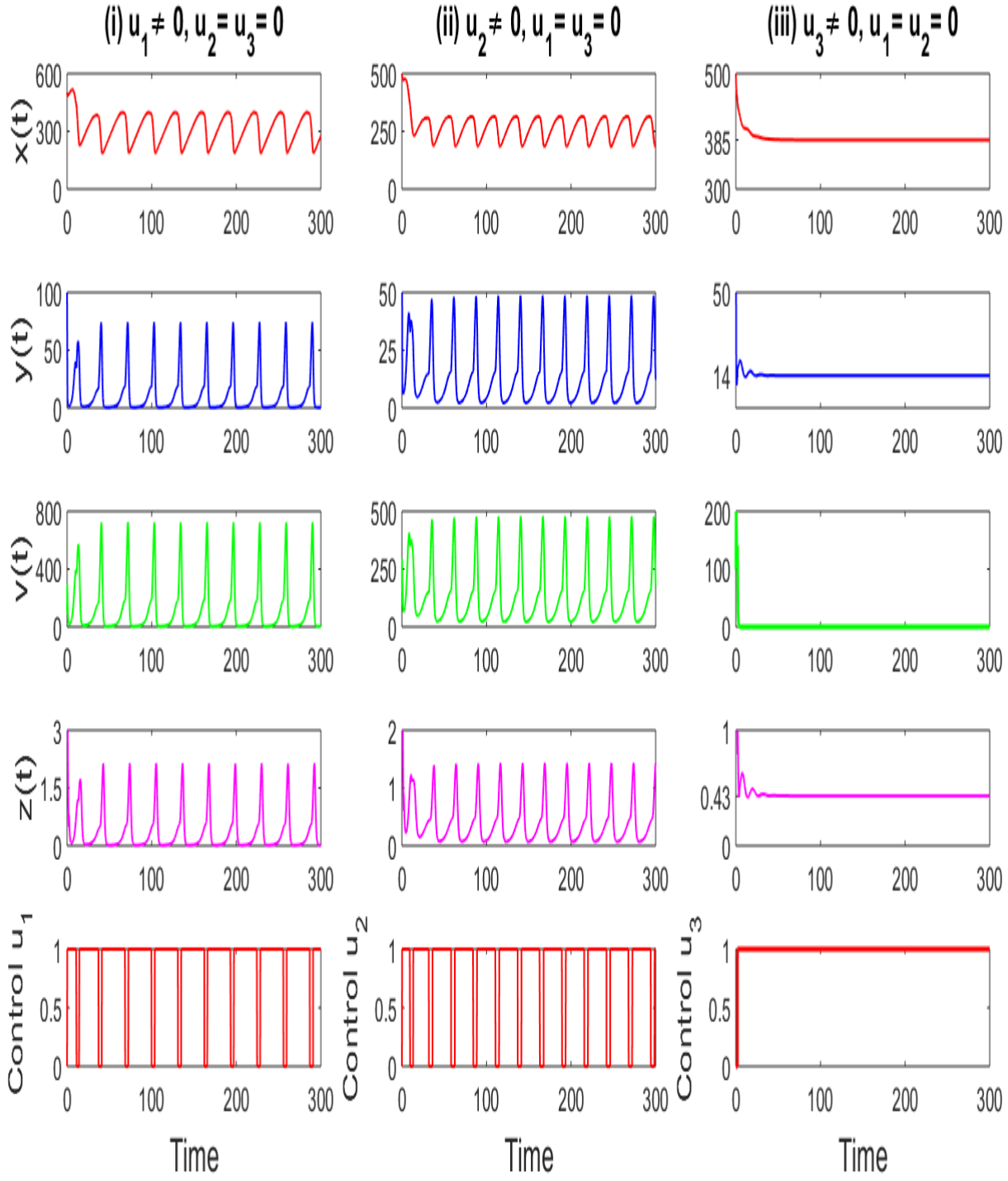

Figure 4.7: The time variations of susceptible CD4$^+$T cells, infected CD4$^+$T cells, virus particles and CTLs due to different mono-drug therapies with $\tau = 2$ days. The last row represents the control profiles corresponding to each mono-drug therapy. Here $\tau = 2$ and other parameters are as in Fig. 4.6.

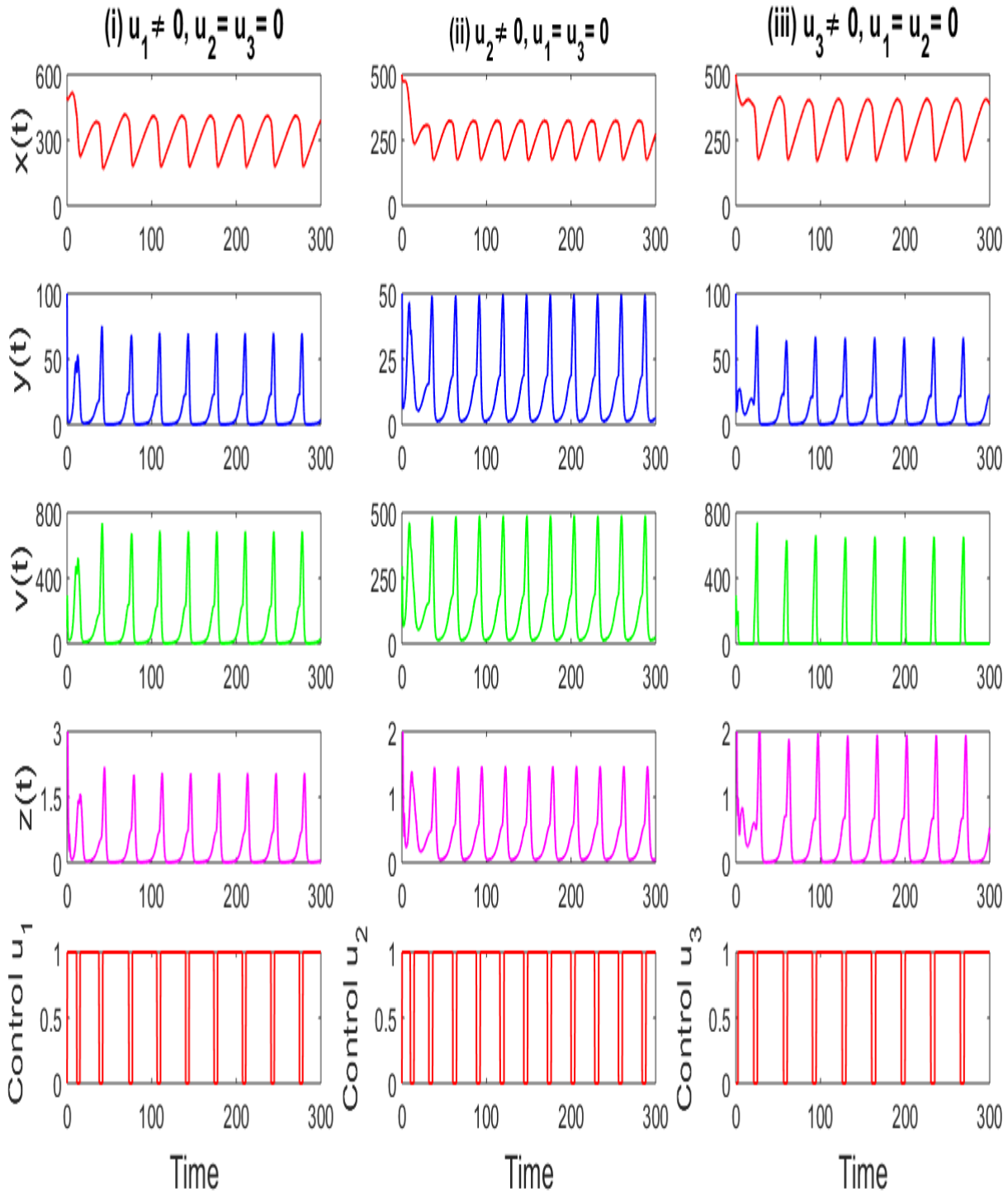

Figure 4.8: Concentrations of susceptible CD4$^+$T cells, infected CD4$^+$T cells, virus particles and CTLs with respect to time under different mono-drug therapies with $\tau = 2.5$ days. The last row represents the control profiles corresponding to each mono-drug therapy. Here $\tau = 2.5$ and other parameters are as in Fig. 4.6.

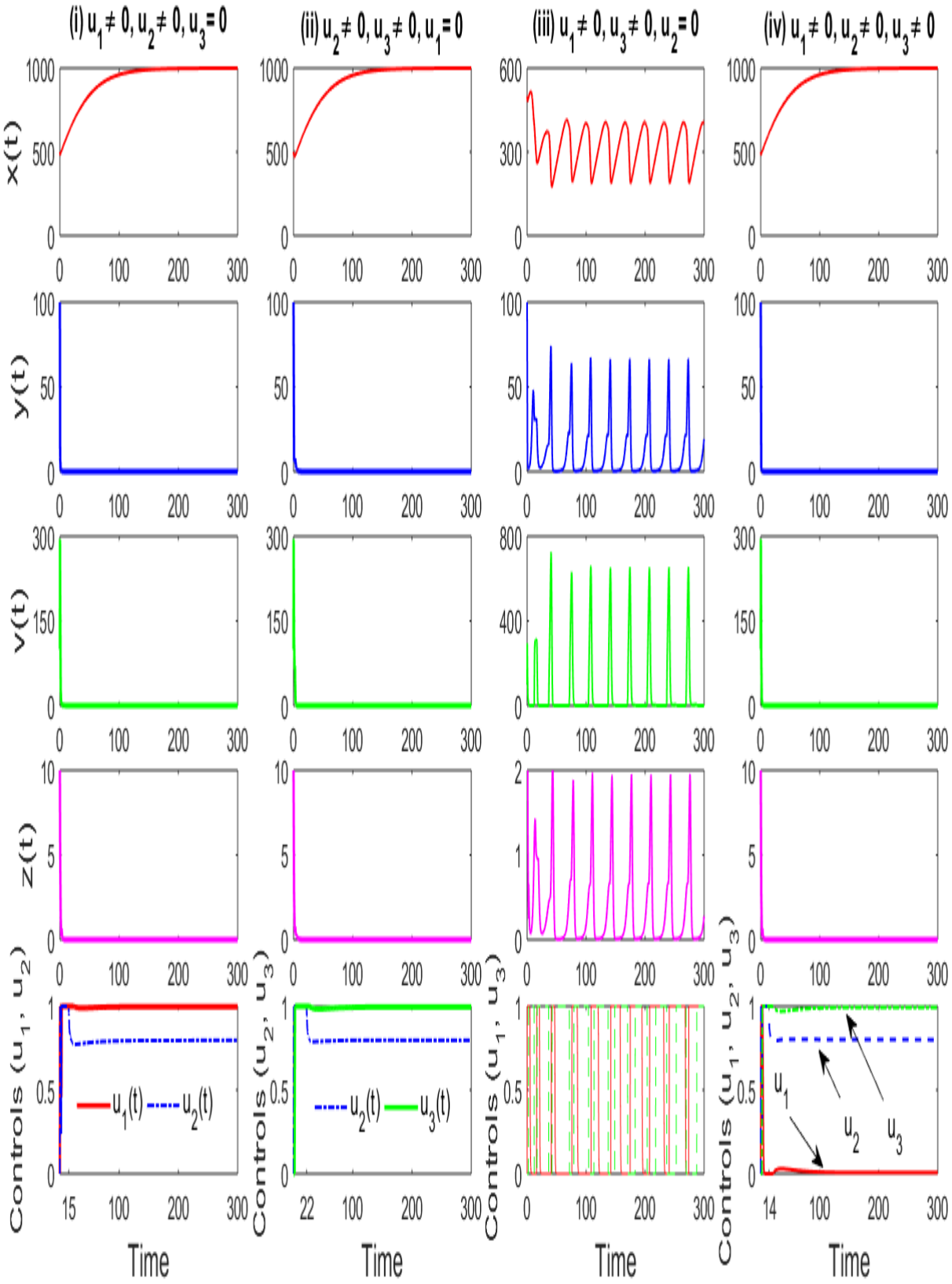

Figure 4.9: The time variations of susceptible CD4$^+$T cells, infected CD4$^+$T cells, virus particles and CTLs due to different mono-drug therapies with $\tau = 2.5$ days. The last row represents the control profiles corresponding to each mono-drug therapy. Here $\tau = 2.5$ and other parameters are as in Fig. 4.6.

may be used instead of ($u_1 \neq 0, u_2 \neq 0, u_3 \neq 0$).

4.5 Discussion

Recent experimental studies show that cell-to-cell disease transmission mode is a more efficient and faster mode of disease transmission than the cell-free mode in the case of in-host HIV-1 infection [97, 98, 101]. This paper has studied a multi-pathways HIV-1 infection model with immune activation delay. The model is further modified with three different blockers that may be used in controlling the viremia. An RTI control ($u_1(t)$) is used to inhibit the synthesis of viral DNA from HIV-1 RNA to inhibit the viral infectivity. A synapse-forming inhibitor ($u_2(t)$) is used to block the cellular mechanisms required for synapse formation. The third control, a protease inhibitor ($u_3(t)$) is applied to stop the process of free virus formation. We first prove that solutions of our system remain positive for all future time assuming positive initial values. It is also shown that the solutions are uniformly bounded. The analytical results are presented in two phases. In the first phase, we assume that the considered controls are time-independent constant controls. In the second phase, we relaxed this assumption and considered the controls as time-dependent. Applying the next-generation matrix, we calculated the basic reproduction number (R_0) of the system with constant controls and showed the disease-free equilibrium is locally and globally asymptotically stable if $R_0 < 1$. The infected steady state, if it exists, is locally asymptotically stable under some parametric restrictions. Delay may, however, cause instability in the system. There exists some critical value (τ^*) of the delay parameter below which the system is stable and above which it is unstable. The stability switching occurs through a Hopf bifurcation.

If the controls are time-dependent variables, then we defined an objective functional to maximize the healthy CD4$^+$T cells & CTL cells and minimize the infected CD4$^+$T cells & virus particles. We derived the necessary conditions for optimal infection control by applying Pontryagin's minimum principle. It is analytically shown that an optimal control triplet exists that maximizes the objective functional. We have demonstrated the effect of different control measures with mono-drug and multi-drug therapies with different delays using extensive simulation results. It is shown that removing infection is not possible, and the infected cells persist in all three mono-drug protocols, using any mono-drug therapy. However, in the case of blocker u_3, virus counts (v) go below the detection level, but infected CD4$^+$T cells (y) persist. This, however, does not happen in the other two controls, where both the infected cells and virus particles survive. Infected CD4$^+$T cells persist, but the non-zero virus count may be possible due to the presence of cell-to-cell dissemination of infection and the use of blocker u_3. Such a result has not been shown in any previous study. It is observable that CD4$^+$T cells count in this case is low compared to the other two cases. Thus, u_2 is the worst mono-drug therapy, and u_3 is better. However, when immune response delay increases, then plasma concentrations of CD4$^+$T cells, CTls, and virus particles oscillate in all three mono-control strategies, showing

uncontrolled behavior. The control profile also oscillates in each case. In the case of a multi-drug therapy, we observed that infection could be removed in three options, where control u_2 is present. The multi-drug option ($u_1 \neq 0, u_3 \neq 0, u_2 = 0$), where u_2 is absent, is the worst one. Our study thus shows that immune response delay significantly affects the system dynamics. If CTL's response is quicker, then $CD4^+T$ cells count may remain stable but fails to do so if response time increases.

5

Mitigating the transmission of infection and death due to SARS-CoV-2 through non-pharmaceutical interventions and repurposing drugs[1]

5.1 Introduction

Susceptible individuals get an infection from COVID-19 infected individuals through direct contact or inhaling the droplets caused due to coughing and sneezing by an infected person or through objects in the immediate environment around the infected person. Though some vaccines are under use, the non-pharmaceutical interventions (NPIs) like individual hygiene, cough etiquette, safe distancing, and lockdown (partial or total) are still the easiest ways to contain this highly contagious disease. Such NPIs have been proven effective in slowing down community transmission and reducing the epidemic load.

Mathematical models and computation techniques may play an important role in understanding this epidemic and may help a lot in policymaking. In fact, policymakers have been increasingly relying on mathematical projections and taking various important decisions to curb the disease in more systematic and effective ways.

[1]The bulk of this chapter has been published in ISA Transactions, doi.org/10.1016/j.isatra.2020.09.015, (2020).

In this chapter, we have proposed a minimal epidemic model to capture the dynamics of observed data of detecting, recovered and death cases of any Covid-19 affected country. The model is then extended to include three control strategies to mitigate the transmission of Covid-19 and to reduce its related deaths. Human-to-human transmission of infection depends mainly on two things: the number of per capita daily contacts between susceptible and infectives, and the probability of disease transmission per effective contact [206]. As mentioned before, per capita daily contacts may be significantly reduced through lockdown, while the probability of virus transmission can be reduced by using face masks and other good hygiene practices. We, therefore, used these nonpharmaceutical interventions as two control measures. The third control is used to reduce the death rate of severely infected Covid-19 patients using repurposing drugs. The proposed epidemic model is then analyzed to determine the criteria for persistence and extinction of the disease. It is shown that repurposing drugs is very useful in saving lives and increasing the recovery rate. Through a case study, it is shown that India can significantly improve the overall Covid-19 epidemic burden through the combined use of NPIs and repurposing drugs and it is true for any other country. India can save lives of 4794 corona infected patients in the next one month (August 28 to September 26) if the repurposing drug has efficacy 0.3.

The rest of the chapter is organized as follows. In Section 5.2, we present the mathematical model to be analyzed. Different mathematical results that determine the dynamics of the system are given in Section 5.3. A case study with Indian Covid-19 epidemic data is presented in Section 5.4. Various results are demonstrated there in relation to the proposed model. The paper ends with a discussion in Section 5.5.

5.2 Model construction

We consider five compartments, viz. susceptible (S), latent (E), home isolated (I_h), hospitalized (I_c) and recovered (R) classes, to classify the human population of a coronavirus-affected country based on their health status. Thus, $N(t) = S(t) + E(t) + I_h(t) + I_c(t) + R(t)$ represents the total population of the country at any time t. As SARS-CoV-2 is a novel virus, every individual is assumed to be susceptible to this virus. After getting an infection, an individual joins the latent class, E. Latent individuals are detected through real-time polymerase chain reaction (RT-PCR) test and advised for home isolation. Some infected individuals under home isolation state (I_h) may develop complicacy and are shifted to hospital for necessary treatment. Such critically infected individuals are denoted by I_c. Critically ill Covid-19 patients join the class R after recovery or succumb to infection. It is further assumed that individuals join S class through birth at a rate G. The average per capita daily contacts of an infected individual is assumed to be n and the probability of disease transmission through contact between an infected individual and a susceptible individual is p. A common practice while writing the incidence term is to express the product of n and p as a single term, called the disease transmission coef-

ficient or the force of infection [206]. We, however, express it explicitly because different NPIs affect differently on these parameters. Individuals of E class are identified as covid positive at a rate of δ and immediately join I_h class. A proportion ω of I_h class develops complicacy and are transferred to I_c class for the treatment. The parameters v_1, v_2 and m_1, m_2 are the recovery and death rates of I_h and I_c classes, respectively. There are reports that covid patients die in transit due to lack of hospital beds, unavailability of ambulance [207–209] . We, therefore, assume that some individuals of I_h class may also succumb to infection before they are shifted to I_c class. It is, however, true that most of the members in mildly infected class (I_h) recover from the infection. Therefore, it would be justified to assume that $v_1 >> v_2$ and $m_1 << m_2$. The natural death rate of susceptible individuals is assumed to be σ, giving $\frac{1}{\sigma}$ as the average life expectancy of the common people, and considered in all compartments. We also consider a death class V to represent the virulence of the disease (Covid-19 related death). Note that the individuals of the death class are not included to represent the total population. The dimension of the proposed model was kept low, though this simplified representation reflects the usual coronavirus infection management protocol followed in many countries including India. With these assumptions, we propose the following model for Covid-19 epidemic:

$$\begin{aligned}
\frac{dS}{dt} &= G - \sigma S - \frac{npSI_h}{N} - \frac{npSI_c}{N}, \\
\frac{dE}{dt} &= \frac{npSI_h}{N} + \frac{npSI_c}{N}, -\delta E - \sigma E, \\
\frac{dI_h}{dt} &= \delta E - (\omega + v_1 + m_1 + \sigma) I_h, \\
\frac{dI_c}{dt} &= \omega I_h - (v_2 + m_2 + \sigma) I_c, \\
\frac{dR}{dt} &= v_1 I_h + v_2 I_c - \sigma R, \\
\frac{dV}{dt} &= m_1 I_h + m_2 I_c.
\end{aligned} \tag{5.1}$$

Those who are critically ill are assumed, for simplicity, to be unable to spread the infection further. This assumption may be too strict but simplifies the model to

$$\begin{aligned}
\frac{dS}{dt} &= G - \sigma S - \frac{npSI_h}{N}, \\
\frac{dE}{dt} &= \frac{npSI_h}{N} - \delta E - \sigma E, \\
\frac{dI_h}{dt} &= \delta E - (\omega + v_1 + m_1 + \sigma) I_h, \\
\frac{dI_c}{dt} &= \omega I_h - (v_2 + m_2 + \sigma) I_c, \\
\frac{dR}{dt} &= v_1 I_h + v_2 I_c - \sigma R, \\
\frac{dV}{dt} &= m_1 I_h + m_2 I_c.
\end{aligned} \tag{5.2}$$

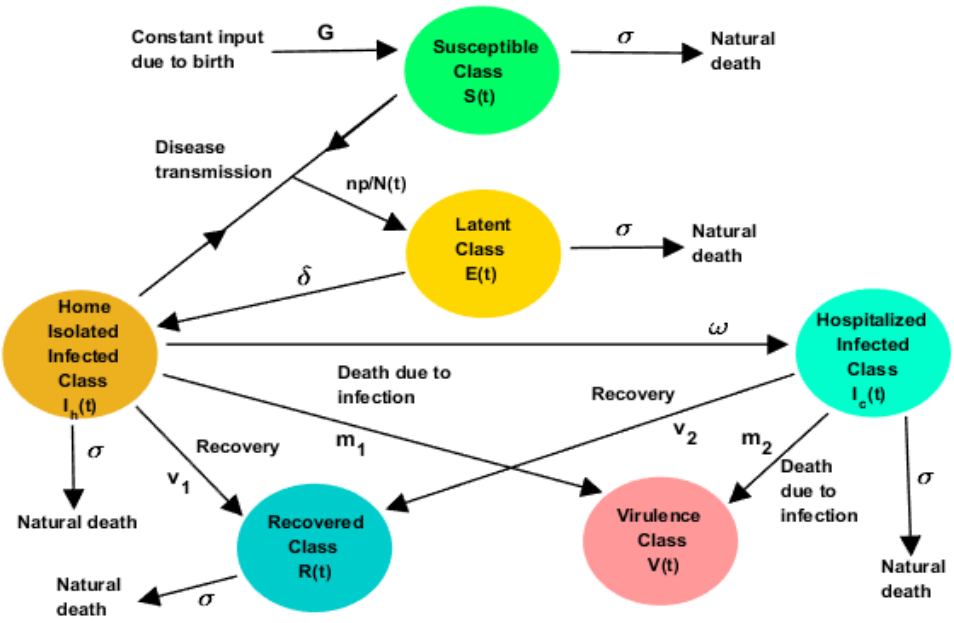

Figure 5.1: Schematic diagram of the disease progression mechanism considered in the system (5.2).

A schematic representation of the system (5.2) is given in Fig. 5.1.

Table 5.1: Variables and parameter with their definitions

Variable	Description	Default value
$S(t)$	Susceptible human population at time t	-
$E(t)$	Latent individuals at time t	-
$I_h(t)$	Home isolated infected individuals at time t	-
$I_c(t)$	Hospitalized infected individuals at time t	-
$R(t)$	Recovered individuals at time t	-
$V(t)$	Virulence class individuals at time t	-
Parameter	**Description**	**Default value**
G	Constant input of susceptible individuals through birth	To be estimated
σ	Natural death rate	To be estimated
n	Average per capita daily contact	To be estimated
p	Probability of disease transmission per contact	To be estimated
δ	Leaving rate from E class	To be estimated
ω	Transfer rate from I_h class to I_c class	To be estimated
v_1	Recovery rate of I_h class	To be estimated
m_1	Death rate of I_h class	To be estimated
v_2	Recovery rate of I_c class	To be estimated
m_2	Death rate of I_c class	To be estimated
u_i $(i = 1,2,3)$	Control parameter	0 to 1

We now introduce three constant controls u_i $(i = 1,2,3),\ 0 \leq u_i \leq 1$ to the above epidemic model. The control u_1 is introduced to reduce the daily number of contacts due to lockdown (complete or partial). A second control u_2 is introduced to diminish the probability of transmission due to using a face mask and maintaining social distance, individual hygiene, cough etiquette, etc. Thus, $(1-u_1)$ and $(1-u_2)$ are the effective daily number of contacts and transmission probability in the presence of the control measures u_1 and u_2. The third and most interesting control u_3 is applied to reduce the death rate and increase the recovery rate by using various repurposing drugs and convalescent plasma therapy. As the effect of the application of repurposing drugs, a fraction of infected people, who earlier succumbed to infection, now recovers and joins R class; while the remaining fraction is the member of the disease-related death class, V. In fact, without the repurposing drugs, infected individuals will die at a rate m_2 and there will be no extra recovery or a reduction in the death class. Introducing these controls, the system (5.2) reads

$$\begin{aligned}
\frac{dS}{dt} &= G - \sigma S - \frac{\{n(1-u_1)\}\{p(1-u_2)\}SI_h}{N},\\
\frac{dE}{dt} &= \frac{\{n(1-u_1)\}\{p(1-u_2)\}SI_h}{N} - \delta E - \sigma E,\\
\frac{dI_h}{dt} &= \delta E - (\omega + v_1 + m_1 + \sigma)I_h,\\
\frac{dI_c}{dt} &= \omega I_h - [v_2 + m_2\{u_3 + (1-u_3)\} + \sigma]I_c,\\
\frac{dR}{dt} &= v_1 I_h + v_2 I_c + m_2 u_3 I_c - \sigma R,\\
\frac{dV}{dt} &= m_1 I_h + m_2(1-u_3)I_c.
\end{aligned} \tag{5.3}$$

The models (5.2) and (5.3) will be analyzed with the initial conditions

$$\begin{aligned}
&S(0) = S_0 > 0,\ E(0) = E_0 \geq 0,\ I_h(0) = I_{h0} \geq 0,\\
&I_c(0) = I_{c0} \geq 0,\ R(0) = R_0 \geq 0,\ V(0) = V_0 \geq 0.
\end{aligned} \tag{5.4}$$

It is to be noted that different sub-cases may be deduced from the model (5.3) depending on the mitigation measures. For example, an epidemic model of Covid-19 can be deduced for the pre-lockdown period, when there was no control measure, by setting $u_1 = u_2 = u_3 = 0$. The model (5.3) has to be modified with $u_3 = 0$ if repurposing drugs are not used. A subsystem can be deduced with $u_1 = 0$ but $u_2, u_3 \neq 0$ if there is no lockdown but individual hygiene care and repurposing drugs are present. In the presence of all types of control measures, the variables u_1, u_2, u_3 will have non-zero values. This model, therefore, can capture various lockdown and unlock stages applied in relation to Covid-19 pandemic as well as the recently approved treatment strategy with repurposing drugs.

5.3 Mathematical results

We here present the analysis technique of the model and give the stability results of different equilibrium points of the system. First, from biological view point, we show that all solutions of the system (5.3) are positive and bounded.

5.3.1 Positivity and boundedness of the solutions

In the sequel, we will use the following well known lemma [210].

Lemma 5.1 *Consider a system $\dot{X} = F(X)$, where $F(X) = [F_1(X), F_2(X), ..., F_n(X)]$, $X \in \mathbb{R}^n_+$, with initial condition $X(0) = X_0 \in \mathbb{R}^n_+$. If for $X_i = 0,\ i = 1,2,...,n,\ F_i(X)|_{X_i=0} \geq 0$, then any solution of $\dot{X} = F(X)$ with given initial condition, say, $X(t) = X(t;X_0)$ will remain positive, i.e., $X(t) \in \mathbb{R}^n_+$, $\forall t > 0$.*

Lemma 5.2 *For initial condition (5.4), solutions of the system (5.3) are positively invariant provided $u_i(t) \in [0,1)$. Moreover, all solutions are uniformly bounded in Γ, where*

$$\Gamma = \left\{ \begin{array}{l} (S(t),E(t),I_h(t),I_c(t),R(t)) \in \mathbb{R}^5_+ \mid \\ 0 < S(t)+E(t)+I_h(t)+I_c(t)+R(t) \leq \dfrac{G}{\sigma} \end{array} \right\}. \tag{5.5}$$

Proof Define $X(t) = (S(t),E(t),I_h(t),I_c(t),R(t))$. It can be easily seen from (5.3) that

$$\left(\frac{dS}{dt}\right)_{X=0} = G > 0, \left(\frac{dE}{dt}\right)_{X=0} = \left(\frac{dI_h}{dt}\right)_{X=0} = \left(\frac{dI_c}{dt}\right)_{X=0} = \left(\frac{dR}{dt}\right)_{X=0} = 0.$$

Lemma 5.1 then gives that all solutions of the system (5.3) starting with the initial condition (5.4) are positive. Again,

$$\begin{aligned} &\frac{dS}{dt}|_{S=0} = G > 0,\ \frac{dE}{dt}|_{E=0} = \frac{n(1-u_1)p(1-u_2)SI_h}{N} > 0, \\ &\frac{dI_h}{dt}|_{I_h=0} = \delta E > 0,\ \frac{dI_c}{dt}|_{I_c=0} = \omega I_h > 0, \\ &\frac{dR}{dt}|_{R=0} = v_1 I_h + v_2 I_c + m_2 u_3 I_c > 0. \end{aligned}$$

Thus, following [211] , $\mathbb{R}^5_+$ is invariant. Therefore, all solutions of the system (5.3) with initial condition (5.4) are positively invariant. To show the boundedness of the solutions of (5.3), we define

$$W(t) = S(t)+E(t)+I_h(t)+I_c(t)+R(t).$$

Then we have

$$\frac{dW(t)}{dt} + \sigma W(t) \leq G - (1-u_3)m_2 I_c \leq G$$
$$\Rightarrow \lim_{t\to\infty} W(t) = \lim_{t\to\infty} [S(t) + E(t) + I_h(t) + I_c(t) + R(t)] \leq \frac{G}{\sigma}.$$

Hence all the solutions of the system (5.3) are positively invariant and ultimately bounded in the region Γ defined in (5.5).

5.3.2 Basic reproduction number

The basic reproduction number (R_0) is one of the most important metrics in epidemic theory. It quantifies the condition of disease progression or extinction in a population. More precisely, a disease will grow over time if $R_0 > 1$, otherwise it will die out. Here we evaluate the basic reproduction number of the system (5.3) with the help of next-generation matrix [212]. One can see that the population settles at $S = \frac{G}{\sigma}$ in the absence of infection. The infection subsystem of (5.3), which describes the production of new infections and changes in the state capable of creating new infections, is given by

$$\begin{aligned}
\frac{dE}{dt} &= \frac{n(1-u_1)p(1-u_2)SI_h}{N} - \delta E - \sigma E, \\
\frac{dI_h}{dt} &= \delta E - (\omega + v_1 + m_1 + \delta) I_h, \\
\frac{dI_c}{dt} &= \omega I_h - [v_2 + m_2 + \sigma] I_c,
\end{aligned} \tag{5.6}$$

The transmission matrix and transition matrix associated with this infection subsystem (5.6) in a completely susceptible scenario (when $S = \frac{G}{\sigma}$) are given by T and Σ, respectively, where

$$T = \begin{pmatrix} 0 & n(1-u_1)p(1-u_2) & 0 \\ 0 & 0 & 0 \\ 0 & 0 & 0 \end{pmatrix}$$
$$\text{and } \Sigma = \begin{pmatrix} -(\sigma+\delta) & 0 & 0 \\ \delta & -(\omega + v_1 + m_1 + \sigma) & 0 \\ 0 & \omega & -(v_2 + m_2 + \sigma) \end{pmatrix}.$$

Then the spectral radius of the matrix $-T\Sigma^{-1}$ gives the basic reproduction number of the system (5.3) and is defined by

$$R_0 = \rho(-T\Sigma^{-1}) = \frac{n(1-u_1)p(1-u_2)\delta}{(\delta+\sigma)(\omega + v_1 + m_1 + \sigma)}, \tag{5.7}$$

whenever $u_i \in [0,1),\ i = 1,2$. It is straightforward to see that the value of R_0 is higher when there is no control. It is to be noted that whenever $u_1 = 1$ or $u_2 = 1$ then the incidence term becomes zero and all subsequent state variables tend to zero as time becomes large, implying that the system becomes infection-free. Therefore, there is no question of the basic reproduction number if $u_i = 1, i = 1,2$.

5.3.3 Existence and stability of the equilibria

To determine the asymptotic behavior of the system (5.3), we find that it has two equilibrium points: (i) the disease-free equilibrium, $E_1(\bar{S},0,0,0,0)$, where $\bar{S} = \frac{G}{\sigma}$, and (ii) the endemic equilibrium $E^*(S^*,E^*,I_h^*,I_c^*,R^*)$. The equilibrium components of E^* can be computed as

$$S^* = \frac{G}{\sigma+\phi^*},\ E^* = \frac{G\phi^*}{(\sigma+\delta)(\sigma+\phi^*)},\ I_u^* = \frac{\delta G\phi^*}{k_1(\sigma+\delta)(\sigma+\phi^*)},$$
$$I_c^* = \frac{\omega G\phi^*}{k_1k_2(\sigma+\delta)(\sigma+\phi^*)},\ R^* = \frac{v_1I_u^* + v_2I_d^* + m_2u_3I_d^*}{\sigma},$$

where

$$\phi^* = \frac{n(1-u_1)p(1-u_2)I_u^*}{N^*}, \tag{5.8}$$

$N^* = S^* + E^* + I_h^* + I_c^* + R^*$, $k_1 = \omega + v_1 + m_1 + \sigma$ and $k_2 = v_2 + m_2 + \sigma$.
Then the Eq. (5.8) can be reexpressed as

$$\begin{aligned}&\left[G + \frac{\delta G}{k_1(\sigma+\delta)} + \frac{\omega G}{k_1k_2(\sigma+\delta)} + \frac{v_1\delta G}{k_1\sigma(\sigma+\delta)} + \frac{\omega G(v_2+m_2u_3)}{\sigma k_1k_2(\sigma+\delta)}\right]\phi^* \\ =&\left[\frac{n(1-u_1)p(1-u_2)\delta}{(\omega+v_1+m_1+\sigma)(\sigma+\delta)} - 1\right]G \\ =&(R_0-1)G,\end{aligned}$$

where R_0 is given by (5.7) with $u_i \in [0,1),\ i = 1,\ 2$. Clearly, there exists a unique interior equilibrium E^* of the system (5.3) whenever $R_0 > 1$.

We give below the stability results of these equilibrium points.

Theorem 5.3 *The disease-free equilibrium E_1 of the system (5.3) is globally asymptotically stable if $R_0 \leq 1$.*

Proof Consider the Lyapunov function

$$U_1 = \frac{\delta}{(\sigma+\delta)(\omega+v_1+m_1+\sigma)}E + \frac{1}{\omega+v_1+m_1+\sigma}I_h.$$

Differentiation of U_1 along the solutions of (5.3) gives

$$\begin{aligned}\dot{U}_1 &= \frac{\delta}{(\sigma+\delta)(\omega+v_1+m_1+\sigma)}\dot{E} + \frac{1}{\omega+v_1+m_1+\sigma}\dot{I}_h \\ &= \frac{\delta}{(\sigma+\delta)(\omega+v_1+m_1+\sigma)}\left[\frac{n(1-u_1)p(1-u_2)SI_h}{N} - \delta E - \sigma E\right] \\ &+ \frac{1}{\omega+v_1+m_1+\sigma}[\delta E - (\omega+v_1+m_1+\delta)I_h].\end{aligned}$$

Noting that $S(t) \leq S(t)+E(t)+I_h(t)+I_c(t)+R(t) = N(t)$ for all $t \geq 0$,

$$\begin{aligned}\dot{U}_1 \leq & \frac{\delta}{(\sigma+\delta)(\omega+v_1+m_1+\sigma)}[n(1-u_1)p(1-u_2)I_h - \delta E - \sigma E] \\ &+ \frac{1}{\omega+v_1+m_1+\sigma}[\delta E - (\omega+v_1+m_1+\delta)I_h] \\ &\leq [R_0 - 1]I_h.\end{aligned}$$

Thus, $\dot{U}_1 \leq 0$ if $R_0 \leq 1$. The equality sign occurrs at the disease free equilibrium, E_1. Therefore, using LaSalle's invariance principle [65], one obtains $(E(t), I_h(t)) \to 0$ as $t \to \infty$. It gives that $\limsup_{t\to\infty} I_h(t) = 0$. Therefore, for any sufficiently small $\varepsilon > 0$, there exists a positive constant $M > 0$ such that $\limsup_{t\to\infty} I_h(t) \leq \varepsilon$ for all $t > M$. From (5.3), one can have for $t > M$,

$$\frac{dI_c}{dt} \leq \omega\varepsilon - [v_2+m_2+\sigma]I_c \Rightarrow \limsup_{t\to\infty} I_c(t) \leq \frac{\omega\varepsilon}{v_2+m_2+\sigma}.$$

Letting $\varepsilon \to 0$, we obtain $\limsup_{t\to\infty} I_c(t) \leq 0$. Again, using the fact that $\liminf_{t\to\infty} I_h(t) = 0$, one gets $\liminf_{t\to\infty} I_c(t) \geq 0$. Thus, we finally get $\lim_{t\to\infty} I_c(t) = 0$. In a similar manner, one can show that $\lim_{t\to\infty} R(t) = 0$ and $\lim_{t\to\infty} S(t) = \frac{G}{\sigma}$. Therefore, all solutions of the system (5.3) with initial conditions in Γ eventually converge to the disease-free equilibrium E_1 if $R_0 \leq 1$. Hence the theorem is proven.

Theorem 5.4 *The endemic equilibrium E^* of the system (5.3) is locally asymptotically stable whenever it exists, i.e., if $R_0 > 1$.*

Proof The proof is based on the line of [213]. The variational matrix of the system (5.3) evaluated at E_1 is given by

$$A' = \begin{pmatrix} -\sigma & 0 & -n(1-u_1)p(1-u_2) & 0 & 0 \\ 0 & -(\delta+\sigma) & n(1-u_1)p(1-u_2) & 0 & 0 \\ 0 & \delta & -(\omega+v_1+m_1+\sigma) & 0 & 0 \\ 0 & 0 & \omega & -(v_2+m_2u_3+\sigma) & 0 \\ 0 & 0 & v_1 & v_2+\theta m_2u_3 & -\sigma \end{pmatrix}.$$

We consider the average per capita daily contacts of an undetected infectious individual, n,

as the bifurcating parameter and apply the central manifold theorem to determine the local stability of E^*. The critical value $n = n^*$ for which $R_0 = 1$ holds is

$$n^* = \frac{(\delta+\sigma)(\omega+v_1+m_1+\sigma)}{p\delta(1-u_1)(1-u_2)},\ u_i \in [0,1),\ i = 1,2.$$

Now let at $n = n^*$, the Jacobian matrix $J_{E_1}|_{n=n^*}$ has a right eigenvector $u = (x_1,x_2,x_3,x_4,x_5)^T$ corresponding to the zero eigenvalue, where

$$x_1 = -\frac{\sigma+\delta}{\sigma}x_2,\ x_2 = x_2,\ x_3 = \frac{x_2\delta}{\omega+v_1+m_1+\sigma}, x_4 = \frac{\omega x_2}{(\omega+v_1+m_1+\sigma)(v_2+m_2+\sigma)},$$
$$x_5 = \frac{x_2\delta}{(\omega+v_1+m_1+\sigma)\sigma}\left[v_1+\left\{\frac{v_2+m_2u_3}{v_2+m_2+\sigma}\right\}\right].$$

Similarly, a left eigenvector corresponding to the zero eigenvalue of the Jacobian matrix $J_{E_1}|_{n=n^*}$ is $w = (w_1,w_2,w_3,w_4,w_5)$, where

$$w_1 = 0,\ w_2 = w_2,\ w_3 = \frac{(\sigma+\delta)w_2}{\delta},\ w_4 = w_5 = 0.$$

With the transformations $S = y_1, E = y_2, I_h = y_3, I_c = y_4, R = y_5$, the system (5.3) can be expressed as

$$\frac{dy_i}{dt} = g_i(y_i),$$

where $g_i \in \mathbb{C}^2(\mathbb{R}^5 \times \mathbb{R})$, $i = 1,..,5$. Then the second order partial derivatives of g_i at E_1 are evaluated as

$$\frac{\partial^2 g_2}{\partial y_3 \partial y_2} = -\frac{n(1-u_1)p(1-u_2)\sigma}{G},\ \frac{\partial^2 g_2}{\partial y_4 \partial y_2} = 0,\ \frac{\partial^2 g_2}{\partial y_3 \partial y_3} = -\frac{2n(1-u_1)p(1-u_2)\sigma}{G},$$
$$\frac{\partial^2 g_2}{\partial y_4 \partial y_3} = -\frac{n(1-u_1)p(1-u_2)\sigma}{G},\ \frac{\partial^2 g_2}{\partial y_3 \partial y_4} = -\frac{n(1-u_1)p(1-u_2)\sigma}{G},\ \frac{\partial^2 g_2}{\partial y_4 \partial y_4} = 0,$$
$$\frac{\partial^2 g_2}{\partial y_3 \partial y_5} = -\frac{n(1-u_1)p(1-u_2)\sigma}{G},\ \frac{\partial^2 g_2}{\partial y_4 \partial y_5} = 0.$$

The signs of the quantities α and β evaluated at $n = n^*$ determine the local stability of the system [213], where

$$\alpha = \Sigma_{k,m,n=1}^{5} w_k x_m x_n \frac{\partial^2 g_k(0,0)}{\partial y_m \partial y_n} \text{ and } \beta = \Sigma_{k,i=1}^{5} w_k x_i \frac{\partial^2 g_k(0,0)}{\partial y_i \partial n}.$$

Following the Remark 1 of Theorem 4.1 given in [213], a transcritical bifurcation will occur at $R_0 = 1$ if $\alpha < 0$ and $\beta > 0$ at $n = n^*$. Substituting all the values of the second order partial derivative evaluate at E_1 with $n = n^*$, we then have

$$\alpha = -\frac{w_2 n(1-u_1)p(1-u_2)\sigma}{G}[x_3^2 + x_2x_3 + 2x_3x_4 + x_3x_5] < 0$$

and

$$\beta = w_2 x_3 p(1-u_1)(1-u_2) > 0,$$

implying a transcritical bifurcation at $R_0 = 1$. Thus, whenever the endemic equilibrium exists, i.e., when $R_0 > 1$, it becomes locally asymptotically stable. Hence the theorem is proven.

5.4 Simulation results: Indian case study

India is the third worst-hit country of the world by the Covid-19 pandemic with a tally of 33,84,576 confirmed cases and 61,695 casualties as of August 27, 2020 (https://covid19india.org). The first confirmed case in the country was reported on January 30 when a student, who returned to home state Kerela from Wuhan, was tested positive. India observed 68 days nationwide lockdown starting from March 25 to May 31, 2020, to restrict the transmission of the coronavirus. Though this lockdown allowed the healthcare providers to take necessary preparations for combating the coronavirus by improving the health care infrastructures, India remained unsuccessful to prevent the spread of infection. Phase wise unlocking process in India started from June 1 [214]. During the first phase of unlocking (June 1-30), religious places, hotels and restaurants were allowed to reopen maintaining the self-distancing protocol. The second phase started from July 1 and to be continued till July 31. During this period more activities in a calibrated manner were allowed. People's daily life, however, was not normal [215]. Regular domestic and international flights, local transportation, both short-and long-distance train services remain cancelled. All educational institutions, shopping malls, community halls are completely closed since March 25. Night curfew has been continuing since the first day of unlocking.

5.4.1 Data collection

The data for India was collected from the online freely available repository Covid19India.Org (https://www.covid19india.org/). In this website, day-wise data, as well as the cumulative data of corona cases in India and its all states/ union territories are given. We here considered the time series data of confirmed, recovered and deceased cases of India for the study period 1^{st} March to 27^{th} August 2020, but did not consider the state-wise data.

5.4.2 Parameter estimations and curve fitting

Study period data was divided into three time windows: 1^{st} March to 24^{th} March (before lockdown period), 25^{th} March to 31^{st} May (lockdown period) and 1^{st} June to 27^{th} August (unlock period). The value of the constant input G to the susceptible class through birth is assumed to be equal to the per day new birth 77575 [216]. It is to be mentioned that no immigration or emigration was considered due to international travel restriction. Average life expectancy

of an Indian is 66.8 years [216], giving the value $\sigma = \frac{1}{365\times 66.8} = 4.1 \times 10^{-5}$. During parameter estimation, it was taken into account that $\nu_1 >> \nu_2$ and $m_1 << m_2$. The leaving rate of E class is measured by the parameter δ, which is a test-dependent parameter. Covid test in India increased significantly during the later stage compared to the early stage of the epidemic. Accordingly, the value of δ should be lower in the pre-lockdown stage and higher in the post-lockdown period. Further, the effective daily contact $n(1-u_1)$ should be the lowest during the complete lockdown period. On the contrary, the probability (p) of disease transmission per contact is expected to be the highest at the initial stage of the epidemic because people were less aware of the importance of individual hygiene in the disease transmission. In the subsequent time, people became more concern about the infection and therefore the effective probability ($p(1-u_2)$) decreased. The population of India as of January 1, 2020 is considered as the initial value of susceptible population ($S(0)$), which is 1387297452 [216]. The controls were assumed to be zero during the pre-lockdown period and only two controls (u_1, u_2) were assumed to have non-zero values in the lockdown period as well as unlock period. Therefore, the third control was not used during the study period, but it was used for future prediction. The solution curve of the model system (5.3) was then fitted with the actual data. In this process, the fminsearch optimization toolbox of Matlab and nonlinear least-square technique were used [217]. We implemented the fminsearch optimization technique in the way described in [218] and have taken the nonlinear least-square method for MATLAB from mathworks repository [219]. The parameter values that best fit the epidemic data with the solution of the controlled system for different time periods are given in Table 5.2.

Table 5.2: Estimated parameter values for India

Time period	n	Effective daily contact $n(1-u_1)$	p	Effective probability $p(1-u_2)$	δ	ω	ν_1	ν_2	m_1	m_2	u_1	u_2
1^{st} March-24^{th} March	2.2199	2.2199	0.3070	0.3070	0.4038	0.3505	0.0134	0.0011	0.00001	0.00571	0	0
25^{th} March-31^{th} May	3.0875	2.1612	0.3070	0.2763	0.4438	0.3415	0.1554	0.0043	0.00001	0.00145	0.3	0.1
1^{st} June-27^{th} August	3.7599	3.1959	0.3003	0.1952	0.6238	0.4205	0.1374	0.0058	0.00001	0.0002	0.15	0.35

In Fig. 5.2, we have presented the curve fitting of the model for the before lockdown period (1^{st} March to 24^{th} March). It can be observed that fitting is relatively poor for the recovered and deceased classes. The main reason is that there were many inaccuracies in the initial data. In many cases, there were under-reporting of the actual facts, and comorbidities among COVID-19 deaths were also excluded. Such problems related to data, however, resolved later on by the health authority.

In Fig. 5.4, the actual data between 25^{th} March to 31^{st} May (lockdown period) and the data of the simulated results of the controlled system (5.3) with fixed values of $u_1 = 0.3$, $u_2 = 0.1$ and $u_3 = 0$ are shown. A similar figure for the time period 1^{st} June to 27^{th} August (unlock

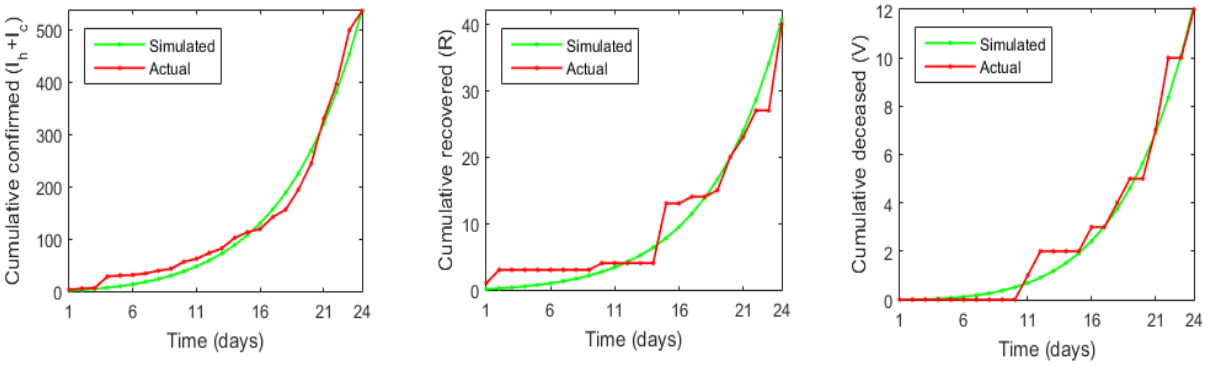

Figure 5.2: Actual cumulative values (red colour) of confirmed, recovered and death cases in India for the study period March 1 to March 24, 2020 (pre-lockdown period) are fitted by the solution (green colour) of the system (5.3) with $u_1 = u_2 = u_3 = 0$.

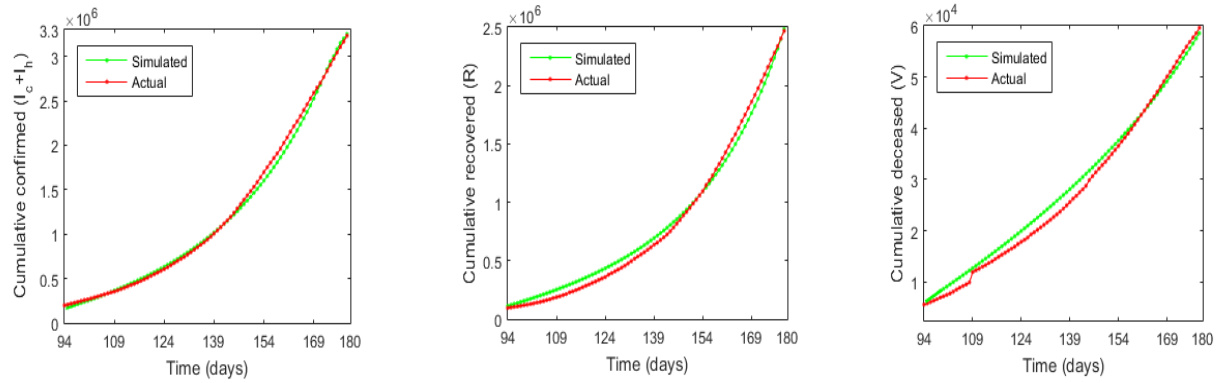

Figure 5.3: Actual cumulative values (red colour) of confirmed, recovered and death cases in India for the study period 1^{st} June to 27^{th} August, 2020 (unlock period) are fitted by the solution (green colour) of the system (5.3) with fixed controls $u_1 = 0.15$, $u_2 = 0.35$ and $u_3 = 0$.

period) with fixed control $u_1 = 0.15$, $u_2 = 0.35$ and $u_3 = 0$ are presented. These curves show good fitting of actual and simulated data.

5.4.3 Effect of repurposing drugs

Here we explore the effect of repurposing drugs in treating covid-19 patients. Clinical results show that at least one-third of critically ill covid patients can survive by administrating the repurposing drug dexamethasone [143, 144]. Different countries have given approval of such life-saving drugs. The Government of India gave approval of using flavipiravir on July 23 [220] for the treatment of Covid-19 patients. Some states of India are supposed to get the first batch of coronavirus drug remdesivir for the use of covid patients very soon [221]. In addition, the life of some covid patients can be saved by applying convalescent plasma therapy also [150]. We here used three different values of the control parameter u_3 with the parameter values of the unlock period and demonstrated how repurposing drugs can reduce the epidemic burden. In Fig. 5.5, the green colour curve represents the cumulative values of the confirmed, recovered

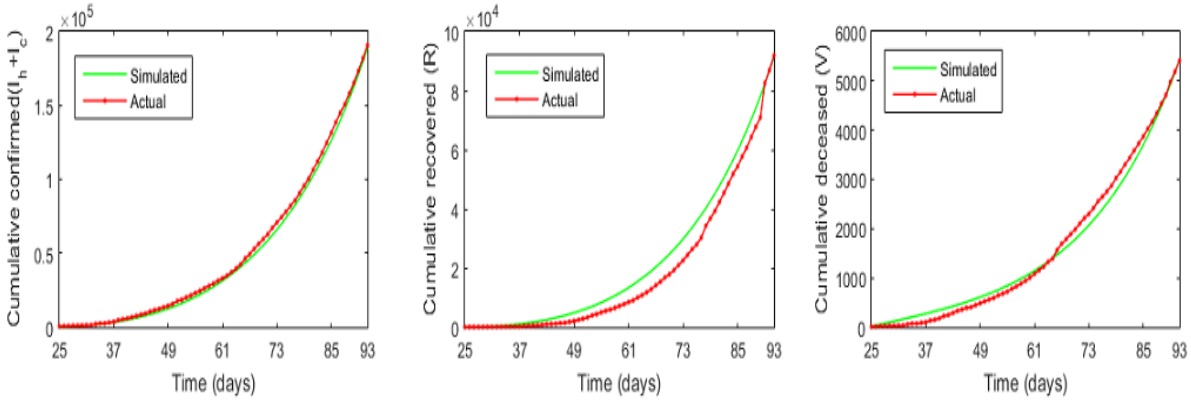

Figure 5.4: Actual cumulative data (red colour) of confirmed, recovered and death cases in India for the study period March 25 to May 31, 2020 (lockdown period) are fitted by the solution (green colour) of the system (5.3) with fixed controls $u_1 = 0.3$, $u_2 = 0.1$ and $u_3 = 0$.

and death cases in the next one month if the repurposing drugs are not used. The other three curves in these figures represent similar cumulative numbers if these drugs are used. The right figure shows that the number of deaths after one month will be 97243 if no repurposing drug is used (i.e., $u_3 = 0$). This number would be 92449 if the repurposing drugs are used with controlling efficacy $u_3 = 0.3$. Thus, 4794 deaths can be avoided in the next one month (August 28 to September 26, 2020) when u_3 takes value 0.3. This number will be 2353 and 7303 corresponding to the drug efficacies $u_3 = 0.2$ and $u_3 = 0.4$, respectively.

5.5 Discussion

In this work, we have proposed a mathematical model that divides the population of a covid-infected country into five disjoint classes depending on the health status of its subjects and then compared the outcomes of different controlling strategies as well as various treatment options currently available. Use of repurposing drugs in the mathematical model to study the Covid-19 epidemic burden is unique and has not been considered in earlier studies.

Basic reproduction of an epidemic model usually delineates the stability and existence of a disease-free state from its endemic state. More precisely, if the basic reproduction number R_0 is greater than unity then an epidemic can grow, epidemic dies out in the opposite case. We determined the basic reproduction number of our system by next-generation matrix and it showed that the classical properties of the basic reproduction number remained intact for Covid-19 epidemic. In the case of India, the basic reproduction number significantly reduced during the lockdown period, however, it remained almost the same during the unlock period (Fig. 5.6(a)). To contain the epidemic, the value of R_0 has to be brought down below 1 through NPIs in the absence of vaccine. It is worth mentioning that the value of the nonpharmaceutical control parameters must be significantly high in this case. Fig. 5.6(b) shows that any combination of the control parameters u_1 and u_2 that lies above the curve $R_0 = 1$ for the unlock parameters can

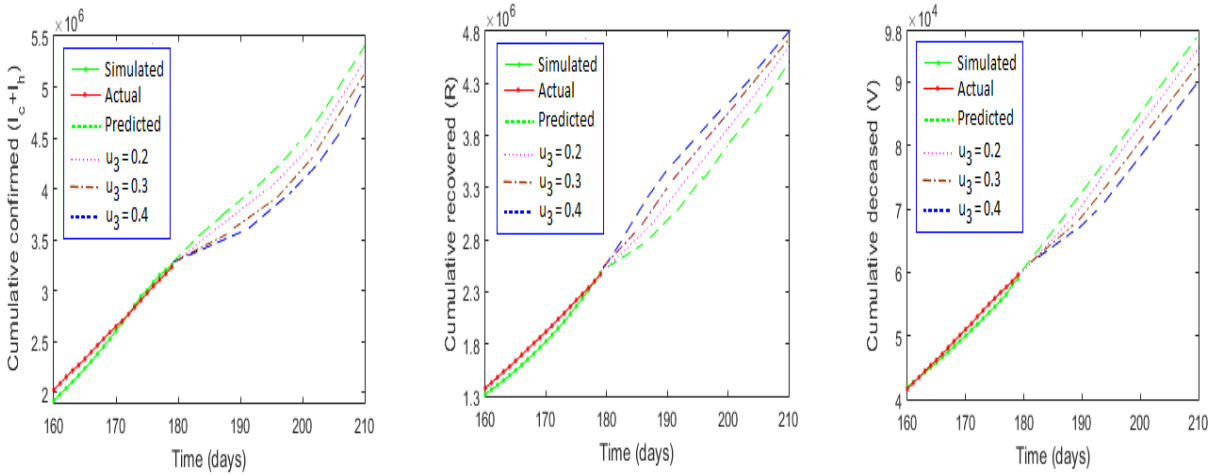

Figure 5.5: Predicted cumulative Covid-19 confirmed, recovered and death cases in India for the next one month (August 28 to September 26, 2020) for different values of the control u_3. Here 180 days implies August 27, 2020, and 210 days implies September 26, 2020. The predicted results with $u_3 = 0$ is represented by the green dashed line in each figure. The red, brown and blue colours represent the same for $u_3 = 0.2$, $u_3 = 0.3$ and $u_3 = 0.4$, respectively. The cumulative number of deaths as of September 26 when $u_3 = 0$ are 97,243 and the same for $u_3 = 0.3$ are 92.449, implying 4,794 fewer deaths in one month. Parameters are as in Table 5.2 (unlock period).

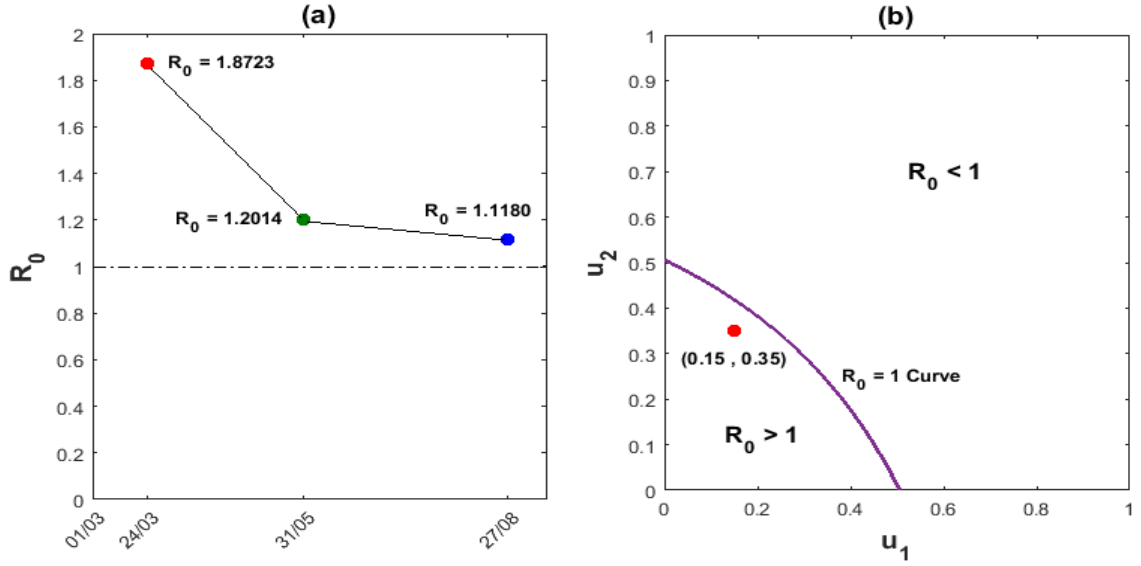

Figure 5.6: (a) Variation in the basic reproduction number, R_0, of the Covid-19 epidemic in India for the study period March 1 to August 27, 2020. It shows that R_0 decreases from its value 1.8723 as of March 24 to 1.1180 as of August 27. March 24 is the lockdown starting date and May 31 is the lockdown ending date for India. The daily positive cases will decline from its current value once R_0 goes below the dashed line $R_0 = 1$. (b) The curve $R_0 = 1$ separates the infection-free state ($R_0 < 1$) from the endemic state ($R_0 > 1$) in the plane of control parameters u_1, u_2. The present estimated values of u_1 and u_2 are marked with a red dot. Parameters are as in the Table 5.2 with unlock case.

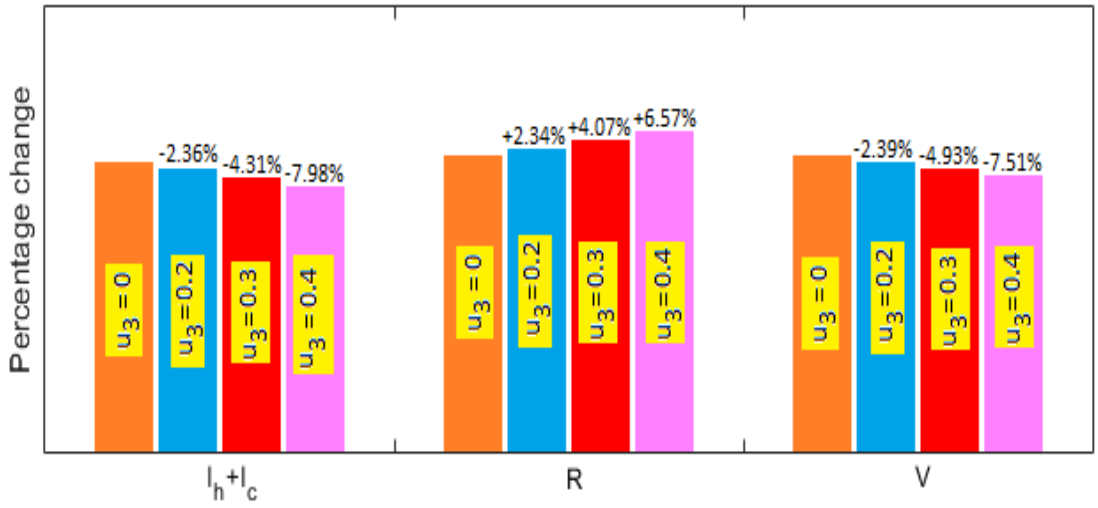

Figure 5.7: Percentage change in the projected numbers of positive, recovered and death cases as of September 26 due to the use of repurposing drug therapy with different control efficacies. The change is calculated with their corresponding values of August 27. It shows that the use of repurposing drugs will reduce the projected deaths by 2.39%, 4.93% and 7.51% when u_3 takes values 0.2, 0.3 and 0.4, respectively. Similar changes may be observed in the cumulative infected cases ($I_h + I_c$). An increase in the recovery class (R) is also observed and the percentage change is indicated by a positive sign.

eliminate SARS-CoV-2 virus from the system. India tried hard to prevent the transmission of coronavirus by implementing NPIs. People have become more aware of this deadly virus and following the statutory instructions more sincerely than before. Some state governments even have imposed punitive measures for flouting covid controlling norms [222–224]. Community involvement may certainly help to push the point $(u_1, u_2) = (0.15, 0.35)$ in the region $R_0 > 1$ to the region $R_0 < 1$, resulting in the elimination of infection.

Some repurposing drugs have brought new hopes for critically ill Covid-19 patients. It can significantly reduce the covid related deaths and increase the recovery number. Our simulation results show that recovery can be increased by 6.57%, and death & positive cases can be reduced, respectively, by 7.51% & 7.98% (corresponding to the control parameter $u_3 = 0.4$) within a month by using repurposing drugs. This study shows that containment of coronavirus by NPIs only is a hard task for India but definitely not impossible. The use of repurposing drugs is very successful in saving lives and reducing the number of infectives. The combined use of NPIs and repurposing drugs may significantly improve the overall Covid-19 epidemic burden. It is to be mentioned that we have used fixed control in our study, one can, however, consider these controls as time-varying in finding optimal control strategies to reach out to the target. In this case, the objective should be to minimize the number of individuals to all infection-related classes, the decease related deaths and the related cost. To get rid of this Covid-19 pandemic, we have to be united and fight together to eliminate the infection from each corner of the world

until an effective vaccine appears and peoples are immunized. We have to keep in mind that the disease started spreading from a market of Wuhan and eventually spread throughout the globe. In combating the global epidemics, collaboration among industry, academia, and public health entities are essential [225].

6

Conclusions and future directions

A mathematical model is critical to understanding the host-pathogen interactions. In this thesis, we theoretically studied the effect of different control mechanisms of infection spreading of the Human Immunodeficiency Virus within the host body and the dissemination SARS-CoV-2 virus in a community. In the case of the within-host HIV-1 model, we considered three blockers on a hypothetical HIV-1 infected subject and then studied its effect when administered either individually or in combination. We first considered a three-dimensional HIV-1 model where the infection spreads through cell-free and cell-to-cell modes. Three controls, viz. the reverse transcriptase inhibitor (RTI), synapse forming inhibitor (SFI) and protease inhibitor (PI), were incorporated to reduce the transmission of infection through various mechanisms. The applied controls were assumed to be either constant or time-dependent.

In the case of constant control, we proved the local and global stabilities of the disease-free and infected steady states. We have defined a suitable optimal control problem in the case of time-dependent control. An objective function is characterized based on maximizing the healthy $CD4^+T$ cell count and minimizing the count of infected $CD4^+T$ cells along with other systemic costs of drug therapy. Using Pontryagin's Maximum Principle, we gave a set of necessary conditions for optimal control. We investigated and compared the effect of different mono-and multi-drug therapies through numerical simulations. In the case of mono blockers, the results show that the drug which blocks cell-to-cell dissemination of infection is a better option for treating an HIV-1 infected individual. On the other hand, in the case of multi-blockers, a combined drug that contains cell-to-cell blockers and protease inhibitors controls the infection efficiently.

Delay is an inherent part of cellular and biochemical mechanisms. The immune cell $CD8^+T$ is activated by the antigen-presenting cells, and the activated $CD8^+T$ cells then kill the infected $CD4^+T$ cells to protect against further infection. However, the activation and subsequent killing of infected $CD4^+T$ cells are not instantaneous. We considered such immune activation delay in an HIV-1 infection model and studied the role of different blockers. It is shown that the stability of the infected equilibrium may be lost through Hopf bifurcation if the immune response delay is longer. We defined a suitable objective function in the time-dependent controls to maximize the cell counts of healthy $CD4^+T$ cells and CTLs and derive the optimality of our delay-induced control problem. We demonstrated that removing infection is not possible using any mono-drug therapy. It is also shown that the SFI blocker that inhibits synapse formation during cell-to-cell disease transmission should be used while using multi-drug therapy to clear the infection. However, this SFI control is not an efficient blocker in the mono-drug treatment protocol. Our study reveals that if CTL's response is quicker, CD4+T cell count may remain stable but become unstable if response time increases.

Mathematical models are vital in understanding the progress of an epidemic. Using different mathematical results, one can project the epidemic burden for a shorter period and estimate the effect of various control measures. Different non-pharmaceutical interventions are effective in preventing the SARS-CoV-2 virus spread, while some repurposing drugs may reduce the death rate of severely infected Covid-19 patients. It is particularly beneficial when there is no specific drug or vaccine to curb the spread of the novel coronavirus. We proposed and studied a five-compartment epidemic model incorporating the effect of repurposing drugs along with non-pharmaceutical intervention strategies. It is shown that the disease elimination & persistence are dependent on the basic reproduction number of the epidemic model. A case study with the Indian Covid-19 epidemic data was presented to visualize and illustrate the effects of such controls. We demonstrated that India significantly improved the overall Covid-19 epidemic burden by using NPIs and repurposing drugs.

It is worth mentioning that there are many avenues for improving the models considered in this thesis. Epidemic models contain several rate parameters. These parameters are usually assumed to be constant. However, the parameters, like the force of infection, recovery rate, and virus reproduction rate per cell lysis, are not constant but fluctuate around their average value. One should consider a noise-induced system to capture the inherent randomness of this biological phenomenon. In this case, the considered rate parameter of the deterministic system is replaced by its average value plus an error term. The error term is represented by multiplicative white noise. One can then incorporate the effect of different inhibitors and find the optimal dose of the inhibitors.

Earlier COVID models did not consider the effect of vaccination. Consequently, such models can no longer be used to determine the course of the epidemic in the presence of covid vaccine. Studies show that vaccine-induced immunity is significantly reduced after six to eight months post-vaccination, and the vaccinated people are subject to reinfection. Theoretical stud-

ies to understand the course of the coronavirus performed by analyzing the deterministic models are insufficient to reflect the random fluctuations observed in the positive case count, infection time, recovery time, etc. There is uncertainty regarding the rate of immunity loss among the vaccinated population. Therefore, considering such uncertainties/fluctuations in the SARS-CoV-2 epidemic models with vaccine-induced immunity loss is essential. One can then find the optimal vaccination rate to control the epidemic.

References

[1] AL Costa, MA Pires, RL Resque, and SSMS Almeida. Mathematical modeling of the infec-tious diseases: key concepts and applications. *Journal of Infectious Diseases and Epidemiology*, 7:209, 2021.

[2] Michael S Gottlieb. *Current topics in AIDS*, volume 2. John Wiley & Sons Incorporated, 1990.

[3] Centers for Disease Control (CDC et al. Immunodeficiency among female sexual partners of males with acquired immune deficiency syndrome (aids)-new york. *MMWR. Morbidity and Mortality Weekly Report*, 31(52):697–698, 1983.

[4] Centers for Disease Control (CDC et al. Pneumocystis carinii pneumonia among persons with hemophilia a. *MMWR. Morbidity and Mortality Weekly Report*, 31(27):365–367, 1982.

[5] KennethB Hymes, JeffreyB Greene, Aaron Marcus, DanielC William, Tony Cheung, NeilS Prose, Harold Ballard, and LindaJ Laubenstein. Kaposi's sarcoma in homosexual men—a report of eight cases. *The Lancet*, 318(8247):598–600, 1981.

[6] Michael S Gottlieb, Robert Schroff, Howard M Schanker, Joel D Weisman, Peng Thim Fan, Robert A Wolf, and Andrew Saxon. Pneumocystis carinii pneumonia and mucosal candidiasis in previously healthy homosexual men: evidence of a new acquired cellular immunodeficiency. *New England Journal of Medicine*, 305(24):1425–1431, 1981.

[7] Centers for Disease Control et al. Kaposi's sarcoma and pneumocystis pneumonia among homosexual men-new york city and california. *MMWR*, 30:305–308, 1981.

[8] Henry Masur, Mary Ann Michelis, Jeffrey B Greene, Ida Onorato, Robert A Vande Stouwe, Robert S Holzman, Gary Wormser, Lee Brettman, Michael Lange, Henry W Murray, et al. An outbreak of community-acquired pneumocystis carinii pneumonia: initial manifestation of cellular immune dysfunction. *New England Journal of Medicine*, 305(24):1431–1438, 1981.

[9] AIDS Gov. "a timeline of aids," washington, dc: Us department of health and human services, 2011.

[10] Centers for Disease Control (CDC et al. Opportunistic infections and kaposi's sarcoma among haitians in the united states. *MMWR. Morbidity and Mortality Weekly Report*, 31(26):353–361, 1982.

[11] JJRCAC Vilaseca, JM Arnau, R Bacardi, C Mieras, A Serrano, and C Navarro. Kaposi's sarcoma and toxoplasma gondii brain abscess in a spanish homosexual. *The Lancet*, 319(8271):572, 1982.

[12] John Coffin, Ashley Haase, Jay A Levy, Luc Montagnier, Steven Oroszlan, Natalie Teich, Howard Temin, Kumao Toyoshima, Harold Varmus, Peter Vogt, et al. Human immunodeficiency viruses. *Science*, 232(4751):697–697, 1986.

[13] Peter B Gilbert, Ian W McKeague, Geoffrey Eisen, Christopher Mullins, Aissatou Guéye-NDiaye, Souleymane Mboup, and Phyllis J Kanki. Comparison of hiv-1 and hiv-2 infectivity from a prospective cohort study in senegal. *Statistics in Medicine*, 22(4):573–593, 2003.

[14] Jacqueline D Reeves and Robert W Doms. Human immunodeficiency virus type 2. *Journal of General Virology*, 83(6):1253–1265, 2002.

[15] JM Coffin and JA Levy. Structure and classification of retroviruses. the retroviridae. Plenum Press, NY, 1992.

[16] Susan L McGovern, Emilia Caselli, Nikolaus Grigorieff, and Brian K Shoichet. A common mechanism underlying promiscuous inhibitors from virtual and high-throughput screening. *Journal of Medicinal Chemistry*, 45(8):1712–1722, 2002.

[17] Patricia L Earl, Robert W Doms, and Bernard Moss. Oligomeric structure of the human immunodeficiency virus type 1 envelope glycoprotein. *Proceedings of the National Academy of Sciences*, 87(2):648–652, 1990.

[18] Brian Thomas Foley, Bette Tina Marie Korber, Thomas Kenneth Leitner, Cristian Apetrei, Beatrice Hahn, Ilene Mizrachi, James Mullins, Andrew Rambaut, and Steven Wolinsky. Hiv sequence compendium 2018. Technical report, Los Alamos National Lab.(LANL), Los Alamos, NM (United States), 2018.

[19] David C Chan and Peter S Kim. Hiv entry and its inhibition. *Cell*, 93(5):681–684, 1998.

[20] Richard Wyatt and Joseph Sodroski. The hiv-1 envelope glycoproteins: fusogens, antigens, and immunogens. *Science*, 280(5371):1884–1888, 1998.

[21] James Arthos, Claudia Cicala, Elena Martinelli, Katilyn Macleod, Donald Van Ryk, Danlan Wei, Zhen Xiao, Timothy D Veenstra, Thomas P Conrad, Richard A Lempicki, et al. Hiv-1 envelope protein binds to and signals through integrin $\alpha 4\beta 7$, the gut mucosal homing receptor for peripheral t cells. *Nature Immunology*, 9(3):301–309, 2008.

[22] Yong-Hui Zheng, Nika Lovsin, and B Matija Peterlin. Newly identified host factors modulate hiv replication. *Immunology Letters*, 97(2):225–234, 2005.

[23] Anthony S Fauci and H Clifford Lane. Human immunodeficiency virus (hiv) disease: Aids and related disorders. *Harrisons Principles of Internal Medicine*, 2:1852–1912, 2001.

[24] James O Kahn and Bruce D Walker. Acute human immunodeficiency virus type 1 infection. *New England Journal of Medicine*, 339(1):33–39, 1998.

[25] Eric S Daar, Susan Little, Jacqui Pitt, Joanne Santangelo, Pauline Ho, Nina Harawa, Peter Kerndt, Janis V Giorgi, Jiexin Bai, Paula Gaut, et al. Diagnosis of primary hiv-1 infection. *Annals of Internal Medicine*, 134(1):25–29, 2001.

[26] Ruth L Berkelman, William L Heyward, Jeanette K Stehr-Green, and James W Curran. Epidemiology of human immunodeficiency virus infection and acquired immunodeficiency syndrome. *The American Journal of Medicine*, 86(6):761–770, 1989.

[27] HIV What Are. Aids?: hiv. gov; 2017 [cited 2018 10/09]. *Avail-able from: https://www. hiv. gov/hiv-basics/overview/about-hiv-and-aids/what-are-hiv-and-aids*.

[28] Bennett Mandell. Dolan (2010). hiv/aids. retrieved from www. wikipedia com on 16th july 2016 hospital, tanzania. *MPH Thesis submitted to the*.

[29] Karol Sestak. Chronic diarrhea and aids: insights into studies with non-human primates. *Current HIV Research*, 3(3):199–205, 2005.

[30] Martin Vogel, Carolynne Schwarze-Zander, Jan-Christian Wasmuth, Ulrich Spengler, Tilman Sauerbruch, and Jürgen Kurt Rockstroh. The treatment of patients with hiv. *Deutsches Ärzteblatt International*, 107(28-29):507, 2010.

[31] ED Murray, EA Buttner, and BH Price. Depression and psychosis in neurological practice. *Daroff R, Fenichel G, Jankovic J, Mazziotta J. Bradley's Neurology in Clinical Practice.(6th ed.). Philadelphia, PA: Elsevier/Saunders*, 2012.

[32] Joint United Nations Programme on HIV/AIDS et al. Global hiv & aids statistics—fact sheet. *UNAIDS: Geneva, Switzerland*, 2021.

[33] Geeta Pandey. The woman who discovered india's first hiv cases. *BBC News*, 30, 2016.

[34] National Aids Control Organisation. Annual report:hiv facts & figures. `http://naco.gov.in/surveillance-epidemiology-0`, 2019.

[35] Richard D Moore and Richard E Chaisson. Natural history of hiv infection in the_era of combination antiretroviral therapy. *AIDS*, 13(14):1933–1942, 1999.

[36] World Health Organization. *Consolidated guidelines on HIV prevention, testing, treatment, service delivery and monitoring: recommendations for a public health approach*. World Health Organization, 2021.

[37] Jeremy Page, Drew Hinshaw, and Betsy McKay. In hunt for covid-19 origin, patient zero points to second wuhan market–the man with the first confirmed infection of the new coronavirus told the who team that his parents had shopped there. *The Wall Street Journal*, 2021.

[38] Donald G McNeil Jr. Wuhan coronavirus looks increasingly like a pandemic, experts say. *The New York Times. Cited February*, 4, 2020.

[39] Dan Fox. What you need to know about the wuhan coronavirus. *Nature*, 10, 2020.

[40] World Health Organization et al. Novel coronavirus (2019-ncov): situation report, 11. 2020.

[41] World Health Organization et al. Naming the coronavirus disease (covid-19) and the virus that causes it. *Brazilian Journal of Implantology and Health Sciences*, 2(3), 2020.

[42] The species severe acute respiratory syndrome-related coronavirus: classifying 2019-ncov and naming it sars-cov-2. *Nature Microbiology*, 5(4):536–544, 2020.

[43] Na Zhu, Dingyu Zhang, Wenling Wang, Xingwang Li, Bo Yang, Jingdong Song, Xiang Zhao, Baoying Huang, Weifeng Shi, Roujian Lu, et al. A novel coronavirus from patients with pneumonia in china, 2019. *New England Journal of Medicine*, 2020.

[44] Nanshan Chen, Min Zhou, Xuan Dong, Jieming Qu, Fengyun Gong, Yang Han, Yang Qiu, Jingli Wang, Ying Liu, Yuan Wei, et al. Epidemiological and clinical characteristics of 99 cases of 2019 novel coronavirus pneumonia in wuhan, china: a descriptive study. *The Lancet*, 395(10223):507–513, 2020.

[45] Philip V'kovski, Annika Kratzel, Silvio Steiner, Hanspeter Stalder, and Volker Thiel. Coronavirus biology and replication: implications for sars-cov-2. *Nature Reviews Microbiology*, 19(3):155–170, 2021.

[46] Canrong Wu, Yang Liu, Yueying Yang, Peng Zhang, Wu Zhong, Yali Wang, Qiqi Wang, Yang Xu, Mingxue Li, Xingzhou Li, et al. Analysis of therapeutic targets for sars-cov-2

and discovery of potential drugs by computational methods. *Acta Pharmaceutica Sinica B*, 10(5):766–788, 2020.

[47] Cody B Jackson, Michael Farzan, Bing Chen, and Hyeryun Choe. Mechanisms of sars-cov-2 entry into cells. *Nature reviews Molecular Cell Biology*, 23(1):3–20, 2022.

[48] Jeffrey K Aronson. Coronaviruses–a general introduction. *Centre for Evidence-Based Medicine, Nuffield Department of Primary Care Health Sciences, University of Oxford*, 2020.

[49] Chia C Wang, Kimberly A Prather, Josué Sznitman, Jose L Jimenez, Seema S Lakdawala, Zeynep Tufekci, and Linsey C Marr. Airborne transmission of respiratory viruses. *Science*, 373(6558):eabd9149, 2021.

[50] Trisha Greenhalgh, Jose L Jimenez, Kimberly A Prather, Zeynep Tufekci, David Fisman, and Robert Schooley. Ten scientific reasons in support of airborne transmission of sars-cov-2. *The Lancet*, 397(10285):1603–1605, 2021.

[51] Shelly L Miller, William W Nazaroff, Jose L Jimenez, Atze Boerstra, Giorgio Buonanno, Stephanie J Dancer, Jarek Kurnitski, Linsey C Marr, Lidia Morawska, and Catherine Noakes. Transmission of sars-cov-2 by inhalation of respiratory aerosol in the skagit valley chorale superspreading event. *Indoor AIR*, 31(2):314–323, 2021.

[52] CDC Coronavirus. symptoms of coronavirus. centers for disease control and prevention. 2020, 2021.

[53] CDC. Coronavirus disease 2019 (covid-19)–symptoms. centers for disease control and prevention. 2020.

[54] JHU CSSE. Covid19/csse_covid_19_data/csse_covid_19_time_series at master· cssegisanddata. *COVID-19· GitHub*, 2019.

[55] World Health Organization et al. Laboratory testing for coronavirus disease 2019 (covid-19) in suspected human cases: interim guidance, 2 march 2020. Technical report, World Health Organization, 2020.

[56] Reed AC Siemieniuk, Jessica J Bartoszko, Long Ge, Dena Zeraatkar, Ariel Izcovich, Elena Kum, Hector Pardo-Hernandez, Anila Qasim, Juan Pablo Díaz Martinez, Bram Rochwerg, et al. Drug treatments for covid-19: living systematic review and network meta-analysis. *BMJ*, 370, 2020.

[57] Yvette N Lamb. Nirmatrelvir plus ritonavir: first approval. *Drugs*, pages 1–7, 2022.

[58] Kara Rogers. Covid-19 vaccine. `http://www.britannica.com/science/COVID-19-vaccine`, 11 May 2022.

[59] Dan Vergano. Covid-19 vaccines work way better than we had ever expected. scientists are still figuring out why. *BuzzFeed News*, 2021.

[60] Smriti Mallapaty, Ewen Callaway, Max Kozlov, Heidi Ledford, John Pickrell, Richard Van Noorden, et al. How covid vaccines shaped 2021 in eight powerful charts. *Nature*, 600(7890):580–583, 2021.

[61] MA Andrews, Binu Areekal, KR Rajesh, Jijith Krishnan, R Suryakala, Biju Krishnan, CP Muraly, and PV Santhosh. First confirmed case of covid-19 infection in india: A case report. *The Indian journal of Medical Research*, 151(5):490, 2020.

[62] Shepley L Ross. *Differential equations*. John Wiley & Sons, 2007.

[63] Lawrence Perko. *Differential equations and dynamical systems*, volume 7. Springer Science & Business Media, 2013.

[64] Linda JS Allen. *Introduction to mathematical biology*. Pearson/Prentice Hall, 2007.

[65] Joseph P La Salle. *The stability of dynamical systems*. SIAM, 1976.

[66] I Michael Ross. *A primer on Pontryagin's principle in optimal control*. Collegiate Publishers, 2015.

[67] VG Boltyanskiy, RV Gamkrelidze, YEF MISHCHENKO, and LS Pontryagin. Mathematical theory of optimal processes. 1962.

[68] Frank H Clarke. *Optimization and Nonsmooth Analysis*. SIAM, 1990.

[69] Rachael Miller Neilan and Suzanne Lenhart. An introduction to optimal control with an application in disease modeling. In *Modeling Paradigms and Analysis of Disease Trasmission Models*, pages 67–81, 2010.

[70] Suzanne Lenhart and John T Workman. *Optimal control applied to biological models*. Chapman and Hall/CRC, 2007.

[71] Wendell H Fleming and Raymond W Rishel. *Deterministic and stochastic optimal control*, volume 1. Springer Science & Business Media, 2012.

[72] Morton I Kamien and Nancy Lou Schwartz. *Dynamic optimization: the calculus of variations and optimal control in economics and management*. courier corporation, 2012.

[73] Jack Macki and Aaron Strauss. *Introduction to optimal control theory*. Springer Science & Business Media, 2012.

[74] AoF Filippov. On certain questions in the theory of optimal control. *Journal of the Society for Industrial and Applied Mathematics, Series A: Control*, 1(1):76–84, 1962.

[75] JT Betts. Practical methods for optimal control using nonlinear programming, ser. *Advances in Design and Control. Philadelphia, PA: Society for Industrial and Applied Mathematics (SIAM)*, 3, 2001.

[76] Dominik Wodarz and David N Levy. Human immunodeficiency virus evolution towards reduced replicative fitness in vivo and the development of aids. *Proceedings of the Royal Society B: Biological Sciences*, 274(1624):2481–2491, 2007.

[77] Alan S Perelson. Modeling the interaction of the immune system with hiv. In *Mathematical and statistical approaches to AIDS epidemiology*, pages 350–370. Springer, 1989.

[78] Alan S Perelson, Denise E Kirschner, and Rob De Boer. Dynamics of hiv infection of cd4+ t cells. *Mathematical Biosciences*, 114(1):81–125, 1993.

[79] David D Ho, Avidan U Neumann, Alan S Perelson, Wen Chen, John M Leonard, and Martin Markowitz. Rapid turnover of plasma virions and cd4 lymphocytes in hiv-1 infection. *Nature*, 373(6510):123–126, 1995.

[80] Xiping Wei, Sajal K Ghosh, Maria E Taylor, Victoria A Johnson, Emilio A Emini, Paul Deutsch, Jeffrey D Lifson, Sebastian Bonhoeffer, Martin A Nowak, Beatrice H Hahn, et al. Viral dynamics in human immunodeficiency virus type 1 infection. *Nature*, 373(6510):117–122, 1995.

[81] D Kirschner, A Perelson, et al. A model for the immune system response to hiv: Azt treatment studies. *Mathematical Population Dynamics: Analysis of Heterogeneity*, 1:295–310, 1995.

[82] Alan S Perelson, Avidan U Neumann, Martin Markowitz, John M Leonard, and David D Ho. Hiv-1 dynamics in vivo: virion clearance rate, infected cell life-span, and viral generation time. *Science*, 271(5255):1582–1586, 1996.

[83] Martin A Nowak and Charles RM Bangham. Population dynamics of immune responses to persistent viruses. *Science*, 272(5258):74–79, 1996.

[84] Denise Kirschner and Glenn F Webb. A model for treatment strategy in the chemotherapy of aids. *Bulletin of Mathematical Biology*, 58(2):367–390, 1996.

[85] Denise E Kirschner and GF Webb. Understanding drug resistance for monotherapy treatment of hiv infection. *Bulletin of Mathematical Biology*, 59(4):763–785, 1997.

[86] Sebastian Bonhoeffer, John M Coffin, and Martin A Nowak. Human immunodeficiency virus drug therapy and virus load. *Journal of Virology*, 71(4):3275–3278, 1997.

[87] Sebastian Bonhoeffer, Robert M May, George M Shaw, and Martin A Nowak. Virus dynamics and drug therapy. *Proceedings of the National Academy of Sciences*, 94(13):6971–6976, 1997.

[88] Denise Kirschner, Suzanne Lenhart, and Steve Serbin. Optimal control of the chemotherapy of hiv. *Journal of Mathematical Biology*, 35(7):775–792, 1997.

[89] Rob J De Boer and Alan S Perelson. Target cell limited and immune control models of hiv infection: a comparison. *Journal of Theoretical Biology*, 190(3):201–214, 1998.

[90] Alan S Perelson and Patrick W Nelson. Mathematical analysis of hiv-1 dynamics in vivo. *SIAM Review*, 41(1):3–44, 1999.

[91] Rebecca V Culshaw and Shigui Ruan. A delay-differential equation model of hiv infection of cd4+ t-cells. *Mathematical Biosciences*, 165(1):27–39, 2000.

[92] Alan S Perelson. Modelling viral and immune system dynamics. *Nature Reviews Immunology*, 2(1):28–36, 2002.

[93] Hal L Smith and Patrick De Leenheer. Virus dynamics: a global analysis. *SIAM Journal on Applied Mathematics*, 63(4):1313–1327, 2003.

[94] Liancheng Wang and Michael Y Li. Mathematical analysis of the global dynamics of a model for hiv infection of cd4+ t cells. *Mathematical Biosciences*, 200(1):44–57, 2006.

[95] Alan S Perelson and Ruy M Ribeiro. Modeling the within-host dynamics of hiv infection. *BMC Biology*, 11(1):1–10, 2013.

[96] Muhammad Sohaib et al. Mathematical modeling and numerical simulation of hiv infection model. *Results in Applied Mathematics*, 7:100118, 2020.

[97] Wolfgang Hübner, Gregory P McNerney, Ping Chen, Benjamin M Dale, Ronald E Gordon, Frank YS Chuang, Xiao-Dong Li, David M Asmuth, Thomas Huser, and Benjamin K Chen. Quantitative 3d video microscopy of hiv transfer across t cell virological synapses. *Science*, 323(5922):1743–1747, 2009.

[98] Peng Zhong, Luis M Agosto, James B Munro, and Walther Mothes. Cell-to-cell transmission of viruses. *Current Opinion in Virology*, 3(1):44–50, 2013.

[99] Shingo Iwami, Junko S Takeuchi, Shinji Nakaoka, Fabrizio Mammano, François Clavel, Hisashi Inaba, Tomoko Kobayashi, Naoko Misawa, Kazuyuki Aihara, Yoshio Koyanagi, et al. Cell-to-cell infection by hiv contributes over half of virus infection. *Elife*, 4:e08150, 2015.

[100] Peng Zhong, Luis M Agosto, Anna Ilinskaya, Batsukh Dorjbal, Rosaline Truong, David Derse, Pradeep D Uchil, Gisela Heidecker, and Walther Mothes. Cell-to-cell transmission can overcome multiple donor and target cell barriers imposed on cell-free hiv. *PloS One*, 8(1):e53138, 2013.

[101] Ping Chen, Wolfgang Hübner, Matthew A Spinelli, and Benjamin K Chen. Predominant mode of human immunodeficiency virus transfer between t cells is mediated by sustained env-dependent neutralization-resistant virological synapses. *Journal of Virology*, 81(22):12582–12595, 2007.

[102] Luis M Agosto, Peng Zhong, James Munro, and Walther Mothes. Highly active antiretroviral therapies are effective against hiv-1 cell-to-cell transmission. *PLoS Pathogens*, 10(2):e1003982, 2014.

[103] Armando Del Portillo, Joseph Tripodi, Vesna Najfeld, Dominik Wodarz, David N Levy, and Benjamin K Chen. Multiploid inheritance of hiv-1 during cell-to-cell infection. *Journal of Virology*, 85(14):7169–7176, 2011.

[104] Marion Sourisseau, Nathalie Sol-Foulon, Françoise Porrot, Fabien Blanchet, and Olivier Schwartz. Inefficient human immunodeficiency virus replication in mobile lymphocytes. *Journal of Virology*, 81(2):1000–1012, 2007.

[105] DS Dimitrov, RL Willey, H Sato, L-Ji Chang, R Blumenthal, and MA Martin. Quantitation of human immunodeficiency virus type 1 infection kinetics. *Journal of Virology*, 67(4):2182–2190, 1993.

[106] Hironori Sato, Jan Orensteint, Dimiter Dimitrov, and Malcolm Martin. Cell-to-cell spread of hiv-1 occurs within minutes and may not involve the participation of virus particles. *Virology*, 186(2):712–724, 1992.

[107] Martin A Nowak, Sebastian Bonhoeffer, George M Shaw, and Robert M May. Anti-viral drug treatment: dynamics of resistance in free virus and infected cell populations. *Journal of Theoretical Biology*, 184(2):203–217, 1997.

[108] Yinggao Zhou, Yiting Liang, and Jianhong Wu. An optimal strategy for hiv multitherapy. *Journal of Computational and Applied Mathematics*, 263:326–337, 2014.

[109] Libin Rong and Alan S Perelson. Modeling hiv persistence, the latent reservoir, and viral blips. *Journal of Theoretical Biology*, 260(2):308–331, 2009.

[110] Jose Orellana. Optimal control for hiv multitherapy enhancement. 2009.

[111] K Renee Fister, Suzanne Lenhart, and Joseph Scott McNally. Optimizing chemotherapy in an hiv model. 1998.

[112] Hem Raj Joshi. Optimal control of an hiv immunology model. *Optimal Control Applications and Methods*, 23(4):199–213, 2002.

[113] Dominik Wodarz and Martin A Nowak. Mathematical models of hiv pathogenesis and treatment. *BioEssays*, 24(12):1178–1187, 2002.

[114] Shohel Ahmed, Sumaiya Rahman, and Md Kamrujjaman. Optimal treatment strategies to control acute hiv infection. *Infectious Disease Modelling*, 6:1202–1219, 2021.

[115] Jaouad Danane and Karam Allali. Optimal control of an hiv model with ctl cells and latently infected cells. *Numerical Algebra, Control & Optimization*, 10(2):207, 2020.

[116] Purity Ngina, Rachel Waema Mbogo, and Livingstone S Luboobi. Modelling optimal control of in-host hiv dynamics using different control strategies. *Computational and Mathematical Methods in Medicine*, 2018, 2018.

[117] Amel Rahmoun, Bedreddine Ainseba, and Djamila Benmerzouk. Optimal control applied on an hiv-1 within-host model. *Mathematical Methods in the Applied Sciences*, 39(8):2118–2135, 2016.

[118] Karam Allali, Sanaa Harroudi, and Delfim FM Torres. Analysis and optimal control of an intracellular delayed hiv model with ctl immune response. *arXiv preprint arXiv:1801.10048*, 2018.

[119] Amine Hamdache, Smahane Saadi, and Ilias Elmouki. Free terminal time optimal control problem for the treatment of hiv infection. *An International Journal of Optimization and Control: Theories & Applications (IJOCTA)*, 6(1):33–51, 2016.

[120] JM Carr, H Hocking, Peng Li, and CJ Burrell. Rapid and efficient cell-to-cell transmission of human immunodeficiency virus infection from monocyte-derived macrophages to peripheral blood lymphocytes. *Virology*, 265(2):319–329, 1999.

[121] Christopher JA Duncan, Rebecca A Russell, and Quentin J Sattentau. High multiplicity hiv-1 cell-to-cell transmission from macrophages to cd4+ t cells limits antiretroviral efficacy. *AIDS (London, England)*, 27(14):2201, 2013.

[122] Marc Permanyer, Ester Ballana, Alba Ruiz, Roger Badia, Eva Riveira-Munoz, Encarna Gonzalo, Bonaventura Clotet, and José A Esté. Antiretroviral agents effectively block hiv replication after cell-to-cell transfer. *Journal of Virology*, 86(16):8773–8780, 2012.

[123] Alex Sigal, Jocelyn T Kim, Alejandro B Balazs, Erez Dekel, Avi Mayo, Ron Milo, and David Baltimore. Cell-to-cell spread of hiv permits ongoing replication despite antiretroviral therapy. *Nature*, 477(7362):95–98, 2011.

[124] Najmeh Akbari and Rasoul Asheghi. Optimal control of an hiv infection model with logistic growth, celluar and homural immune response, cure rate and cell-to-cell spread. *Boundary Value Problems*, 2022(1):1–12, 2022.

[125] Yu Liu, Xiaolin Lin, and Jianquan Li. Analysis and control of a delayed hiv infection model with cell-to-cell transmission and cytotoxic t lymphocyte immune response. *Mathematical Methods in the Applied Sciences*, 44(7):5767–5786, 2021.

[126] Suxia Zhang, Fei Li, and Xiaxia Xu. Dynamics and control strategy for a delayed viral infection model. *Journal of Biological Dynamics*, 16(1):44–63, 2022.

[127] Chunyang Qin, Xia Wang, and Libin Rong. An age-structured model of hiv latent infection with two transmission routes: analysis and optimal control. *Complexity*, 2020, 2020.

[128] Ting Guo and Zhipeng Qiu. The effects of ctl immune response on hiv infection model with potent therapy, latently infected cells and cell-to-cell viral transmission. *Mathematical Biosciences and Engineering*, 16(6):6822–6841, 2019.

[129] Chenwei Song, Rui Xu, and Ning Bai. Dynamics of a within-host virus infection model with multiple pathways: Stability switch and global stability. *International Journal of Bifurcation and Chaos*, 31(13):2150195, 2021.

[130] Debadatta Adak and Nandadulal Bairagi. Analysis and computation of multi-pathways and multi-delays hiv-1 infection model. *Applied Mathematical Modelling*, 54:517–536, 2018.

[131] Xiulan Lai and Xingfu Zou. Modeling hiv-1 virus dynamics with both virus-to-cell infection and cell-to-cell transmission. *SIAM Journal on Applied Mathematics*, 74(3):898–917, 2014.

[132] Yu Yang, Lan Zou, and Shigui Ruan. Global dynamics of a delayed within-host viral infection model with both virus-to-cell and cell-to-cell transmissions. *Mathematical Biosciences*, 270:183–191, 2015.

[133] Jinhu Xu and Yicang Zhou. Bifurcation analysis of hiv-1 infection model with cell-to-cell transmission and immune response delay. *Mathematical Biosciences & Engineering*, 13(2):343, 2016.

[134] Albert W Wu, Cheryl Connors, and George S Everly Jr. Covid-19: peer support and crisis communication strategies to promote institutional resilience, 2020.

[135] World Health Organization. Novel coronavirus global research and innovation forum: Towards a research roadmap. `https://www.who.int/blueprint/`

priority-diseases/key-action/Overview_of_SoA_and_outlinekey_knowledge_gaps.pdf?ua=1, 2019.

[136] Leonardo Setti, Fabrizio Passarini, Gianluigi De Gennaro, Pierluigi Barbieri, Maria Grazia Perrone, Massimo Borelli, Jolanda Palmisani, Alessia Di Gilio, Prisco Piscitelli, and Alessandro Miani. Airborne transmission route of covid-19: why 2 meters/6 feet of inter-personal distance could not be enough, 2020.

[137] Derek K Chu, Elie A Akl, Stephanie Duda, Karla Solo, Sally Yaacoub, Holger J Schünemann, Amena El-harakeh, Antonio Bognanni, Tamara Lotfi, Mark Loeb, et al. Physical distancing, face masks, and eye protection to prevent person-to-person transmission of sars-cov-2 and covid-19: a systematic review and meta-analysis. *The Lancet*, 395(10242):1973–1987, 2020.

[138] Jeremy Howard, Austin Huang, Zhiyuan Li, Zeynep Tufekci, Vladimir Zdimal, Helene-Mari van der Westhuizen, Arne von Delft, Amy Price, Lex Fridman, Lei-Han Tang, et al. Face masks against covid-19: an evidence review. 2020.

[139] Kanta Subbarao and Siddhartha Mahanty. Respiratory virus infections: understanding covid-19. *Immunity*, 52(6):905–909, 2020.

[140] Annelies Wilder-Smith, Calvin J Chiew, and Vernon J Lee. Can we contain the covid-19 outbreak with the same measures as for sars? *The Lancet Infectious Diseases*, 20(5):e102–e107, 2020.

[141] Sara Momtazmanesh, Hans D Ochs, Lucina Q Uddin, Matjaz Perc, John M Routes, Duarte Nuno Vieira, Waleed Al-Herz, Safa Baris, Carolina Prando, Laszlo Rosivall, et al. All together to fight covid-19. *The American Journal of Tropical Medicine and Hygiene*, 102(6):1181, 2020.

[142] Mrudula Phadke and Sujata Saunik. Covid-19 treatment by repurposing drugs until the vaccine is in sight. *Drug Development Research*, 81(5):541–543, 2020.

[143] World health Organization. Dexamethasone and covid-19. https://www.who.int/news-room/q-a-detail/q-a-dexamethasone-and-covid-19.

[144] National Institutes of Health. Dexamethasone: Coronavirus disease covid-19. covid-19 treat guidel 2020. retrieved 12 july 2020.

[145] Jonathan Grein, Norio Ohmagari, Daniel Shin, George Diaz, Erika Asperges, Antonella Castagna, Torsten Feldt, Gary Green, Margaret L Green, François-Xavier Lescure, et al. Compassionate use of remdesivir for patients with severe covid-19. *New England Journal of Medicine*, 382(24):2327–2336, 2020.

[146] Jason D Goldman, David CB Lye, David S Hui, Kristen M Marks, Raffaele Bruno, Rocio Montejano, Christoph D Spinner, Massimo Galli, Mi-Young Ahn, Ronald G Nahass, et al. Remdesivir for 5 or 10 days in patients with severe covid-19. *New England Journal of Medicine*, 383(19):1827–1837, 2020.

[147] Brandi N Williamson, Friederike Feldmann, Benjamin Schwarz, Kimberly Meade-White, Danielle P Porter, Jonathan Schulz, Neeltje Van Doremalen, Ian Leighton, Claude Kwe Yinda, Lizzette Pérez-Pérez, et al. Clinical benefit of remdesivir in rhesus macaques infected with sars-cov-2. *Nature*, 585(7824):273–276, 2020.

[148] First COVID-19 treatment recommended for eu authorisation (press release). European medicines agency (ema); 2020, retrieved 25 june 2020.

[149] Trump administration secures new supplies of remdesivir for the united states" (press release). United states department of health & human services (hhs); 2020, retrieved 3 july 2020.

[150] Long Chen, Jing Xiong, Lei Bao, and Yuan Shi. Convalescent plasma as a potential therapy for covid-19. *The Lancet Infectious Diseases*, 20(4):398–400, 2020.

[151] Anne Catherine Cunningham, Hui Poh Goh, and David Koh. Treatment of covid-19: old tricks for new challenges, 2020.

[152] Duccio Fanelli and Francesco Piazza. Analysis and forecast of covid-19 spreading in china, italy and france. *Chaos, Solitons & Fractals*, 134:109761, 2020.

[153] Faïçal Ndaïrou, Iván Area, Juan J Nieto, and Delfim FM Torres. Mathematical modeling of covid-19 transmission dynamics with a case study of wuhan. *Chaos, Solitons & Fractals*, 135:109846, 2020.

[154] Kaustuv Chatterjee, Kaushik Chatterjee, Arun Kumar, and Subramanian Shankar. Healthcare impact of covid-19 epidemic in india: A stochastic mathematical model. *Medical Journal Armed Forces India*, 76(2):147–155, 2020.

[155] Chayu Yang and Jin Wang. A mathematical model for the novel coronavirus epidemic in wuhan, china. *Mathematical Biosciences and Engineering: MBE*, 17(3):2708, 2020.

[156] Milan Batista. Estimation of the final size of the second phase of coronavirus epidemic by the logistic model. *medrxiv*, 2020.

[157] Igor Nesteruk. Estimations of the coronavirus epidemic dynamics in south korea with the use of sir model. *Preprint.] ResearchGate*, 2020.

[158] Abhijit Paul, Samrat Chatterjee, and Nandadulal Bairagi. Prediction on covid-19 epidemic for different countries: Focusing on south asia under various precautionary measures. *Medrxiv*, 2020.

[159] Matjaž Perc, Nina Gorišek Miksić, Mitja Slavinec, and Andraž Stožer. Forecasting covid-19. *Frontiers in Physics*, 8:127, 2020.

[160] Abhijit Paul, Samrat Chatterjee, and Nandadulal Bairagi. Covid-19 transmission dynamics during the unlock phase and significance of testing. *medRxiv*, 2020.

[161] Yaqing Fang, Yiting Nie, and Marshare Penny. Transmission dynamics of the covid-19 outbreak and effectiveness of government interventions: A data-driven analysis. *Journal of Medical Virology*, 92(6):645–659, 2020.

[162] Steffen E Eikenberry, Marina Mancuso, Enahoro Iboi, Tin Phan, Keenan Eikenberry, Yang Kuang, Eric Kostelich, and Abba B Gumel. To mask or not to mask: Modeling the potential for face mask use by the general public to curtail the covid-19 pandemic. *Infectious Disease Modelling*, 5:293–308, 2020.

[163] Andrei Korobeinikov. Global properties of basic virus dynamics models. *Bulletin of Mathematical Biology*, 66(4):879–883, 2004.

[164] Martin A Nowak, Sebastian Bonhoeffer, Andrew M Hill, Richard Boehme, Howard C Thomas, and Hugh McDade. Viral dynamics in hepatitis b virus infection. *Proceedings of the National Academy of Sciences*, 93(9):4398–4402, 1996.

[165] Rui Xu. Global stability of an hiv-1 infection model with saturation infection and intracellular delay. *Journal of Mathematical Analysis and Applications*, 375(1):75–81, 2011.

[166] Dan Li and Wanbiao Ma. Asymptotic properties of a hiv-1 infection model with time delay. *Journal of Mathematical Analysis and Applications*, 335(1):683–691, 2007.

[167] Nandadulal Bairagi and Debadatta Adak. Global analysis of hiv-1 dynamics with hill type infection rate and intracellular delay. *Applied Mathematical Modelling*, 38(21-22):5047–5066, 2014.

[168] Nandadulal Bairagi and Debadatta Adak. Dynamics of cytotoxic t-lymphocytes and helper cells in human immunodeficiency virus infection with hill-type infection rate and sigmoidal ctl expansion. *Chaos, Solitons & Fractals*, 103:52–67, 2017.

[169] AV Herz, Sebastian Bonhoeffer, Roy M Anderson, Robert M May, and Martin A Nowak. Viral dynamics in vivo: limitations on estimates of intracellular delay and virus decay. *Proceedings of the National Academy of Sciences*, 93(14):7247–7251, 1996.

[170] Michael Y Li and Hongying Shu. Global dynamics of an in-host viral model with intracellular delay. *Bulletin of Mathematical Biology*, 72(6):1492–1505, 2010.

[171] Patrick W Nelson and Alan S Perelson. Mathematical analysis of delay differential equation models of hiv-1 infection. *Mathematical Biosciences*, 179(1):73–94, 2002.

[172] Rebecca V Culshaw, Shigui Ruan, and Glenn Webb. A mathematical model of cell-to-cell spread of hiv-1 that includes a time delay. *Journal of Mathematical Biology*, 46(5):425–444, 2003.

[173] Xianwei Guan and Rui Xu. Cell-free infection and cell-cell transmission hiv-1 dynamics model with cure rate. *Commun. Math. Biol. Neurosci.*, 2016:Article–ID, 2016.

[174] Narendra M Dixit and Alan S Perelson. Complex patterns of viral load decay under antiretroviral therapy: influence of pharmacokinetics and intracellular delay. *Journal of Theoretical Biology*, 226(1):95–109, 2004.

[175] Patrick W Nelson, James D Murray, and Alan S Perelson. A model of hiv-1 pathogenesis that includes an intracellular delay. *Mathematical Biosciences*, 163(2):201–215, 2000.

[176] Rebecca V Culshaw, Shigui Ruan, and Raymond J Spiteri. Optimal hiv treatment by maximising immune response. *Journal of Mathematical Biology*, 48(5):545–562, 2004.

[177] Andrew N Phillips. Reduction of hiv concentration during acute infection: independence from a specific immune response. *Science*, 271(5248):497–499, 1996.

[178] Vangipuram Lakshmikantham, Srinivasa Leela, and Anatoly A Martynyuk. *Stability Analysis of Nonlinear Systems*. Springer, 1989.

[179] Sally M Blower and Hadi Dowlatabadi. Sensitivity and uncertainty analysis of complex models of disease transmission: an hiv model, as an example. *International Statistical Review/Revue Internationale de Statistique*, pages 229–243, 1994.

[180] Pauline Van den Driessche and James Watmough. Reproduction numbers and subthreshold endemic equilibria for compartmental models of disease transmission. *Mathematical Biosciences*, 180(1-2):29–48, 2002.

[181] Abid Ali Lashari and Gul Zaman. Optimal control of a vector borne disease with horizontal transmission. *Nonlinear Analysis: Real World Applications*, 13(1):203–212, 2012.

[182] Brian M Adams, Harvey T Banks, Hee-Dae Kwon, and Hien T Tran. Dynamic multidrug therapies for hiv: Optimal and sti control approaches. *Mathematical Biosciences & Engineering*, 1(2):223, 2004.

[183] JAM Felippe De Souza, Marco Antonio Leonel Caetano, and Takashi Yoneyama. Optimal control theory applied to the anti-viral treatment of aids. In *Proceedings of the 39th IEEE conference on decision and control (Cat. No. 00CH37187)*, volume 5, pages 4839–4844. IEEE, 2000.

[184] Dahlard L Lukes and LUKES DL. Differential equations: classical to controlled. 1982.

[185] LS Pontryagin, VG Boltyanskii, RV Gamkrelidze, and EF Mishchenko. The maximum principle. *The Mathematical Theory of Optimal Processes. New York: John Wiley and Sons*, 1962.

[186] Anuj Kumar, Prashant K Srivastava, and Yasuhiro Takeuchi. Modeling the role of information and limited optimal treatment on disease prevalence. *Journal of Theoretical Biology*, 414:103–119, 2017.

[187] Xiulan Lai and Xingfu Zou. Modeling cell-to-cell spread of hiv-1 with logistic target cell growth. *Journal of Mathematical Analysis and Applications*, 426(1):563–584, 2015.

[188] Péter Érdi and János Tóth. *Mathematical models of chemical reactions: theory and applications of deterministic and stochastic models*. 1989.

[189] Dongmei Xiao and Shigui Ruan. Global analysis of an epidemic model with nonmonotone incidence rate. *Mathematical Biosciences*, 208(2):419–429, 2007.

[190] Norman MacDonald and N MacDonald. *Biological Delay Systems: Linear Stability Theory*. Cambridge University Press, 2008.

[191] John L Spouge, Richard I Shrager, and Dimiter S Dimitrov. Hiv-1 infection kinetics in tissue cultures. *Mathematical Biosciences*, 138(1):1–22, 1996.

[192] Debadatta Adak and Nandadulal Bairagi. Bifurcation analysis of a multidelayed hiv model in presence of immune response and understanding of in-host viral dynamics. *Mathematical Methods in the Applied Sciences*, 42(12):4256–4272, 2019.

[193] JACK K Hale and WZ Huang. Global geometry of the stable regions for two delay differential equations. *Journal of Mathematical Analysis and Applications*, 178(2):344–362, 1993.

[194] D Kirschner, A Perelson, and R Deboer. The dynamics of hiv infection of cd4+t cells. *Mathematical Biosciences*, 114(1):81–125, 1993.

[195] Laurenz Göllmann, Daniela Kern, and Helmut Maurer. Optimal control problems with delays in state and control variables subject to mixed control–state constraints. *Optimal Control Applications and Methods*, 30(4):341–365, 2009.

[196] Khalid Hattaf and Noura Yousfi. Optimal control of a delayed hiv infection model with immune response using an efficient numerical method. *International Scholarly Research Notices*, 2012, 2012.

[197] Yan Wang, Yicang Zhou, Jianhong Wu, and Jane Heffernan. Oscillatory viral dynamics in a delayed hiv pathogenesis model. *Mathematical Biosciences*, 219(2):104–112, 2009.

[198] Jack K Hale and Sjoerd M Verduyn Lunel. *Introduction to functional differential equations*, volume 99. Springer Science & Business Media, 2013.

[199] Odo Diekmann, Johan Andre Peter Heesterbeek, and Johan AJ Metz. On the definition and the computation of the basic reproduction ratio r 0 in models for infectious diseases in heterogeneous populations. *Journal of Mathematical Biology*, 28(4):365–382, 1990.

[200] Warren M Hirsch, Herman Hanisch, and Jean-Pierre Gabriel. Differential equation models of some parasitic infections: methods for the study of asymptotic behavior. *Communications on Pure and Applied Mathematics*, 38(6):733–753, 1985.

[201] Xiuling Li and Junjie Wei. On the zeros of a fourth degree exponential polynomial with applications to a neural network model with delays. *Chaos, Solitons & Fractals*, 26(2):519–526, 2005.

[202] MS Ciupe, BL Bivort, DM Bortz, and PW Nelson. Estimating kinetic parameters from hiv primary infection data through the eyes of three different mathematical models. *Mathematical Biosciences*, 200(1):1–27, 2006.

[203] Kasia A Pawelek, Shengqiang Liu, Faranak Pahlevani, and Libin Rong. A model of hiv-1 infection with two time delays: mathematical analysis and comparison with patient data. *Mathematical Biosciences*, 235(1):98–109, 2012.

[204] Laurenz Göllmann and Helmut Maurer. Theory and applications of optimal control problems with multiple time-delays. *Journal of Industrial & Management Optimization*, 10(2):413, 2014.

[205] Fathalla A Rihan and Bassel F Rihan. Numerical modelling of biological systems with memory using delay differential equations. *Applied Mathematics & Information Sciences*, 9(3):1645, 2015.

[206] Marc Lipsitch, Ted Cohen, Ben Cooper, James M Robins, Stefan Ma, Lyn James, Gowri Gopalakrishna, Suok Kai Chew, Chorh Chuan Tan, Matthew H Samore, et al. Transmission dynamics and control of severe acute respiratory syndrome. *Science*, 300(5627):1966–1970, 2003.

[207] Indian Express. Many covid-19 patients dying in transit as private hospitals deny admission in telangana. https://www.newindianexpress.com/states/telangana/2020/jul/01/many-covid-19-patients-dying-intransit-as-private-hospitals-deny-/admission-in-telangana-2163617.html.

[208] Hindustan Times. Serious lapses in ambulance service, bed availability in pune hospitals. https://www.hindustantimes.com/pune-news/seriouslapses-in-ambulance-service-bed-availability-patients-say/story-AA3Cmca9IyEcpizOXxMpCP.html.

[209] Indian Express. Mumbai hospitals run out of beds for critical covid patients. https://indianexpress.com/article/cities/mumbai/mumbai-hospitalsrun-out-of-beds-for-critical-covid-patients-6407221.

[210] Mitio Nagumo. Über die lage der integralkurven gewöhnlicher differentialgleichungen. *Proceedings of the Physico-Mathematical Society of Japan. 3rd Series*, 24:551–559, 1942.

[211] Xia Yang, Lansun Chen, and Jufang Chen. Permanence and positive periodic solution for the single-species nonautonomous delay diffusive models. *Computers & Mathematics with Applications*, 32(4):109–116, 1996.

[212] Odo Diekmann, JAP Heesterbeek, and Michael G Roberts. The construction of next-generation matrices for compartmental epidemic models. *Journal of the Royal Society Interface*, 7(47):873–885, 2010.

[213] Carlos Castillo-Chavez and Baojun Song. Dynamical models of tuberculosis and their applications. *Mathematical Biosciences & Engineering*, 1(2):361, 2004.

[214] Ministry of Home Affairs Government of India. Press release. https://www.mha.gov.in/sites/default/files/MHAOrderDt-30052020.

[215] Ministry of Home Affairs Government of India. Press release. https://www.mha.gov.in/sites/default/files/MHAOrder-29062020.

[216] India Population. India population countrymeters. https://countrymeters.info/en/India, (accessed July 27, 2020) 2020.

[217] Michael Y Li. *An introduction to mathematical modeling of infectious diseases*, volume 2. Springer, 2018.

[218] César Pérez López. Optimization techniques via the optimization toolbox. In *MATLAB Optimization Techniques*, pages 85–108. Springer, 2014.

[219] MathWorks. Least-squares fitting. https://in.mathworks.com/help/curvefit/least-squares-fitting.html, (Accessed on August 27, 2020) 2020.

[220] Press Information Bureau Government of IndiaPress release. Cost effective process technology of favipiravir developed by csir used by m/s cipla ltd. for scale up & the repurposed drug expected to be launched soon. https://pib.gov.in/PressReleseDetailm.aspx?PRID=1640742, 2020.

[221] By Indiacom News Desk. Coronavirus drug: Delhi, maharashtra to get first batch of remdesivir for 'restricted' use. https://www.india.com/news/india/coronavirus-drug-delhi-maharashtra-toget-first-batch-of-remdesivir/-for-restricted-use-4067358, (Published: June 25 2020) 2020.

[222] Hindutan Times. Rs 500 fine for flouting quarantine norms, not wearing mask and consumption of tobacco in public. https://www.hindustantimes.com/cities/rs-500-fine-for-flouting-quarantinenorms-not-weaing-mask-and/-consumption-of-tobacco-in-public/story-XWaenEDjMOjyzqdqgfxocJ.html, 2020.

[223] CNBCTV19. Coronavirus in mumbai: Bmc imposes rs 1, 000 fine for not wearing masks. https://www.cnbctv18.com/healthcare/coronavirusin-mumbai-bmc-imposes-rs-1000-fine-for-not-wearing-masks/-6225921.htm, 2020.

[224] Times of India. Pmc fines 300 citizens for not wearing masks. https://timesofindia.indiatimes.com/city/pune/pmc-fines-300-citizens-fornot-wearing-masks/articleshow/76804098.cms, 2020.

[225] Dirk Helbing, Dirk Brockmann, Thomas Chadefaux, Karsten Donnay, Ulf Blanke, Olivia Woolley-Meza, Mehdi Moussaid, Anders Johansson, Jens Krause, Sebastian Schutte, et al. Saving human lives: What complexity science and information systems can contribute. *Journal of Statistical Physics*, 158(3):735–781, 2015.

List of publications related to thesis

Published

1. **Chittaranjan Mondal**, Debadatta Adak and Nandadulal Bairagi, Optimal control in a multi-pathways HIV-1 infection model: a comparison between mono-drug and multi-drug therapies, *International Journal of Control*, 94(8), 2047-2064, 2019. (I.F.: 2.102)
2. **Chittaranjan Mondal**, Debadatta Adak, Abhijit Majumder and Nandadulal Bairagi, Mitigating the transmission of infection and death due to SARS-CoV-2 through non-pharmaceutical interventions and repurposing drugs, *ISA transactions*, DOI: org/10.1016/j.isatra.2020.09.015, 2020. (I.F.: 5.911)
3. **Chittaranjan Mondal**, Debadatta Adak and Nandadulal Bairagi, Optimal drug therapy in a multi-pathways HIV-1 infection model with immune response delay, *Trends in Biomathematics*, ed. By R. P. Mondaini, Springer Verlag Switzerland, DOI: doi.org/10.1007/978-3-031-12515-7-6, (2022).

Communicated

1. **Chittaranjan Mondal** and Nandadulal Bairagi,Optimal control in a multi-pathways in-host HIV infection model with saturated incidence, intracellular delay and self-proliferation of the host cells.